O. Elarras

The competitiveness of weathering steel-concrete composite bridges in the Dutch market

Master thesis

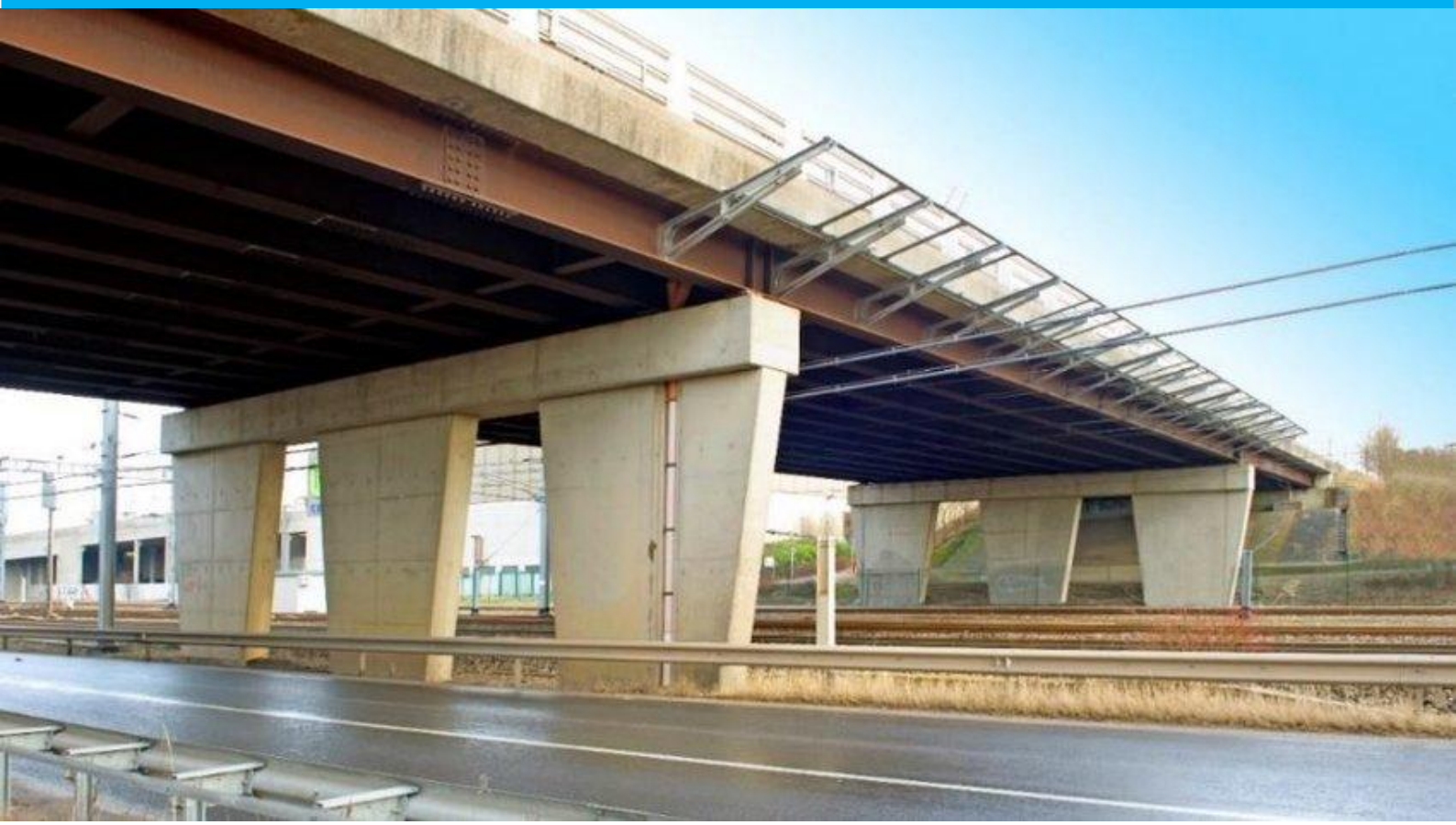

Figure 1 Composite weathering steel-concrete bridge with hot rolled sections (Rademacher, 2019)

TU Delft

The competitiveness of weathering steel-concrete composite bridges in the Dutch market

Master document

By

Oussama Elarras

in partial fulfilment of the requirements for the degree of

Master of Science
in Civil Engineering

at the Delft University of Technology in collaboration with Rijkswaterstaat,
to be defended publicly on Friday December 15, 2025 at 14:30 AM.

Supervisor:	Dr. ir. F. Kavoura	TU Delft
Thesis committee:	Dr. ir. M. Pavlovic,	TU Delft
	Prof. Dr. H.M. Jonkers,	TU Delft
	E.Thie, M.SC. , RC	Rijkswaterstaat

This thesis is confidential and cannot be made public until December 15, 2025.

An electronic version of this thesis is available at http://repository.tudelft.nl/.

TU Delft

Preface

This thesis was prepared in partial fulfilment of the requirements for the Master of Science in Civil Engineering at Delft University of Technology, in collaboration with Rijkswaterstaat. It investigates the structural feasibility, sustainability, and cost-effectiveness of weathering steel–concrete composite bridges in the Netherlands.

I sincerely thank my supervisor, Dr. ir. F. Kavoura, and my thesis committee, Dr. ir. M. Pavlovic, Prof. Dr. H.M. Jonkers, and E. Thie, M.Sc., for their guidance and feedback. I am also grateful to Rijkswaterstaat for access to data and practical insights.

Oussama Elarras

Delft, November 2025

Abstract

In the coming decades, Rijkswaterstaat faces the challenge of replacing and renovating a large number of Dutch highway bridges built in the 1950's and 1960's. These structures must be renewed in a sustainable, cost-efficient manner while minimizing traffic disruption. The objective is to retain the existing substructure and replace only the superstructure of the bridges, which are in need of replacement. This study investigates the competitiveness of weathering steel concrete composite bridges in the Netherlands, for small-span bridges (15–30 m). Hereby the following bridge variants will be considered for determining the competitiveness:

- Variant 1: Existing full reinforced concrete superstructure
- Variant 2: conventional painted steel–concrete composite superstructure
- Variant 3 : weathering steel–concrete composite superstructure

The research is structured into four phases: (1) a literature review on material behavior, corrosion performance, and durability of unpainted weathering steel under Dutch environmental conditions; (2) structural verification using a real bridge case study to assess Eurocode compliance; (3) a sustainability assessment using Life Cycle Assessment (LCA) and Environmental Cost Indicator (MKI) values for life-cycle stages A1–A5; and (4) an economic evaluation of construction, maintenance, and lifecycle costs.

The literature review highlighted that weathering steel offers substantial maintenance and sustainability advantages but faces environmental constraints in the Netherlands due to high humidity (≥76%) and frequent de-icing salt exposure. The standard Dutch vertical clearance of approximately 4.5 m is below the 6.1 m recommended in international guidelines (ASTM and ECCS) to prevent chloride spray contamination. Effective use of weathering steel thus requires sacrificial thicknesses, optimized detailing, and preventive maintenance to ensure long-term durability. Mechanically, weathering steel behaves comparably to conventional painted steel.

Structural verifications confirmed that variant 2 and variant 3 satisfy Eurocode requirements for bending moment, shear force, and deflection, considering different configurations of the superstructure. Accounting for a 1 mm sacrificial thickness in weathering steel reduces bending moment resistance by 3.5–6%, a small but measurable effect.

The sustainability assessment showed that Variant 3 achieved the lowest environmental impact for A1–A5 stages. The use of low-carbon XCarb® steel reduced total MKI by 50–55% compared to conventional NMD steel in Variant 2, and the elimination of paint provided an additional ~9% reduction. Variant 2 performed better than Variant 1, but worse than Variant 3, while Variant 1 (full concrete) had the highest MKI.

Life-cycle cost analysis indicated up to 30% savings over 100 years for Variant 3 compared to variant 2, mainly due to reduced maintenance and minimized traffic disruptions. Structural mass comparisons showed that Variants 2 and 3 are 53–56% lighter than Variant 1, reducing loads on existing abutments and facilitating replacement while preserving substructures.

Overall, weathering steel–concrete composite bridges are technically feasible, sustainable advantageous, and economically competitive for small-span superstructure replacement in the Netherlands. These findings support the potential of integrating weathering steel into Rijkswaterstaat's sustainable bridge renewal strategy, offering a robust pathway toward low-maintenance, low-impact, and long-lasting infrastructure.

Content

List of figures

List of tables

I Research framework

1 Introduction

1.1 Background & relevance

Rijkswaterstaat is currently devising a plan to undertake replacements and renovations of a significant number of bridges constructed in the 1950s and 1960s due to the substantial increase in heavy traffic. The overarching goal of this initiative is to ensure the safety of traffic users for the foreseeable future. These efforts must meet Rijkswaterstaat's stringent standards while minimizing disruptions to road accessibility (Rijkswaterstaat, n.d.).

Efforts are being made to renew these existing bridges, integrating innovation and sustainability, while also aiming to reduce costs as much as possible, given that the total maintenance expenses currently exceed the available budget (Rijkswaterstaat, n.d.). Consequently, there is a concerted effort to explore the feasibility of smart and sustainable design techniques.

In the Netherlands, small-span bridges (15 to 30 meters) are typically built using precast concrete elements. However, concrete production is widely recognized as one of the most polluting processes in terms of CO_2 emissions. Therefore, adopting a more sustainable design approach for these bridges would be a significant step in reducing CO_2 emissions in the bridge construction sector. One promising alternative is the use of a composite system consisting of weathering steel beams and a concrete deck, a solution already seen as sustainable and effective in countries like the UK, Japan and USA.

Weathering steel offers key sustainability benefits over conventional steel. It forms a protective oxide layer that eliminates the need for painting, reducing both maintenance requirements and the associated CO2 emissions. Additionally, the use of this composite system decreases the overall weight of the structure, which reduces the demand for materials and leverages the more sustainable properties of steel when compared to concrete-heavy bridge designs. This makes it a more resource-efficient and sustainable option for future bridge construction.

Despite these advantages, the adoption of weathering steel-concrete composite bridges in the Netherlands is still limited. Currently, the only known example is the Avenhornbrug, built in the 1970s, which is now undergoing inspection and reassessment. The findings from this reassessment may provide valuable insights into the broader potential of this design approach within the country. However, beyond the Avenhornbrug, there is a notable lack of comprehensive data on critical aspects such as structural feasibility, construction and maintenance costs, CO_2 emissions, material efficiency, construction speed, and reusability in the Dutch context. Addressing this research gap is essential for understanding the full potential of weathering steel-concrete composite bridges as a sustainable solution for the Netherlands.

1.2 Research objective

This research examines the competitiveness of weathering steel-concrete composite bridges in the Dutch market, focusing on 15-30 meter spans. The renovation strategy aims to minimize construction time and costs by preserving the substructure and replacing only the superstructure with minimal substructure modifications when necessary. Additionally, this study aims to assess and compare the competitiveness of weathering steel-concrete bridges/viaducts with conventional steel-concrete bridges and frequently utilized prefabricated box beam bridges in the Netherlands, covering structural performance, costs, and sustainability metrics of these structure types.

This study specifically targets the Dutch construction industry and assesses the feasibility of integrating weathering steel-concrete composite bridges/viaducts. It seeks to offer insights tailored to the distinctive conditions prevailing in the Netherlands. These unique circumstances are characterized by the flat terrain, soft soil conditions, dense population, sea climate and stringent limitations on highway disruptions during construction activities. The research will draw upon online found literature and literature provided by Rijkswaterstaat to inform its findings.

1.3 Research questions

In this chapter the main research question will be introduced and the sub questions that will be used to answer the main research question.

Main research question

To what extent do weathering steel–concrete composite bridges demonstrate competitiveness within the Dutch market for replacing aged concrete superstructures, in terms of sustainability, structural feasibility, and cost?

Sub questions

1. How does the structural performance of weathering steel-concrete composite bridges/viaducts, as per the Eurocode standards, compare to that of conventional steel-concrete composite bridges, considering the unique circumstances in the Netherlands?

2. What is the sustainability impact of weathering steel-concrete composite bridges compared to conventional steel-concrete composite bridges in the Dutch context?

3. What are the economic benefits/disadvantages of weathering steel-concrete composite bridges, compared to conventional steel-concrete bridges and concrete box beam bridges?

1.4 Research methodology

This research consists of four distinct phases, designed to systematically address the research question and provide a comprehensive analysis of the feasibility of weathering steel-concrete composite bridges in the Dutch market. A visualization of the methodology is given in Figure 2.

1.4.1 Phase 1: Literature Review

A literature review will be conducted to compile existing knowledge on weathering steel-concrete composite bridges. The focus will be on understanding the material properties of weathering steel, specifically in the context of bridge applications. This phase will establish a foundation for the subsequent structural and sustainability analyses by addressing key characteristics such as durability, corrosion resistance, and long-term performance under typical environmental conditions in the Netherlands.

1.4.2 Phase 2: Structural Analysis

The second phase involves the structural analysis of a self-designed composite superstructure based on a real-world case study of an existing concrete bridge in the Netherlands that requires replacement. The selected bridge will be used as a reference to design a new composite superstructure, which will be analyzed to determine its dimensions and structural feasibility. In this phase, different structural designs of the superstructure will be explored by varying key parameters such as:

- Centre-to-centre distance between the (weathering) steel beams
- Profile
- Steel grade

The resulting cross-sectional dimensions from these variations will serve as a basis for the subsequent sustainability and cost analyses.

1.4.3 Phase 3: Sustainability Assessment

Using the dimensions established in Phase 2 and insights from the literature review in Phase 1, a sustainability analysis will be carried out to evaluate the sustainability impact of constructing the proposed weathering steel-concrete composite bridge. This assessment will utilize a Life Cycle Assessment (LCA) methodology to quantify the sustainability costs. The results will then be compared to those of conventional steel-concrete and concrete-only bridges, highlighting the relative sustainability benefits or drawbacks.

1.4.4 Phase 4: Cost Analysis

The final phase focuses on evaluating the economic feasibility of building weathering steel-concrete composite bridges in the Netherlands. The costs will be estimated based on the components used in the different variants.

1.4.5 Integration and Final Evaluation

In the discussion, conclusion, and recommendation sections, the results from all four phases will be synthesized to provide a holistic evaluation of the feasibility of weathering steel-concrete composite bridges in the Netherlands. The limitations of the study, as well as the assumptions made during each phase, will be critically addressed to ensure that the findings are well-grounded and relevant for practical implementation in the Dutch infrastructure market.

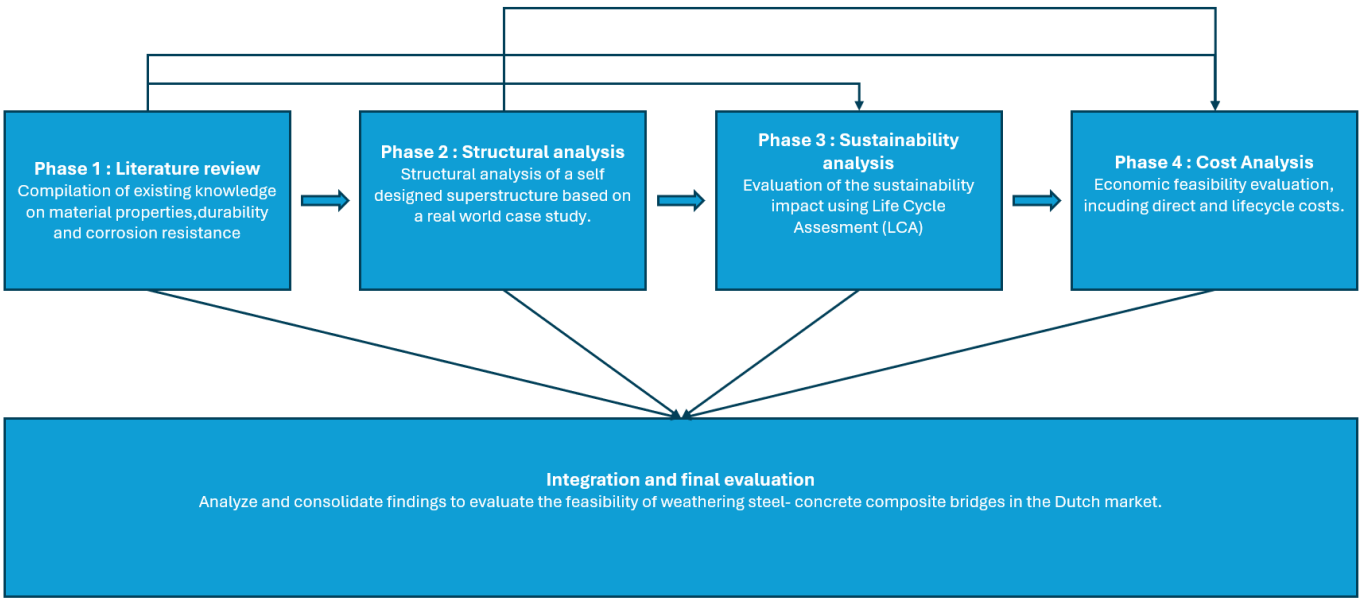

Figure 2 Methodology diagram

II Study phase

2 Literature review

2.1 Introduction

The literature review will focus on three key areas: the structural performance of weathering steel, the sustainability impact of weathering steel-concrete composite bridges, and the associated cost considerations.

Structural Performance: Understanding the material characteristics of weathering steel and its performance compared to conventional steel is essential. Key aspects include the corrosion risks and fatigue performance of weathering steel, which are important for assessing its suitability. Relevant design guidelines, such as Eurocodes and the ROK, will also be reviewed to ensure compliance in the design process. The reassessment of the Avenhorn bridge will be considered, for understanding how these type of bridges behave in the Dutch context.

Sustainability Impact: Comparing the sustainability impact of different superstructures using Life Cycle Assessment (LCA) is crucial. This will involve identifying key indicators and life cycle elements while defining system boundaries. Analyzing environmental product declarations from suppliers and the sustainability of production processes will provide valuable insights into the long-term benefits of using weathering steel-concrete composites.

Cost Considerations: The research will examine cost comparisons between different superstructures, focusing on initial investment, maintenance, and long-term operational efficiency. Understanding how sustainable solutions can influence lifecycle costs, including potential savings from reduced maintenance and extended service life, will be important in guiding material selection.

2.2 Structural Performance of weathering steel bridges

2.2.1 Introduction to weathering steel

Weathering steel-concrete composite bridges are widely used in North America, UK, Australia , New Zealand and Japan (Highways England, 2019). In the US over 50% of the steel highway bridges that have been constructed since 2017 are constructed with weathering steel. In Japan 80% of the newly built steel bridges were built with weathering steel in the period of 1994 to 2019 (Yu Zhang, 2019). In these countries several guidelines have been written applicable for these countries. The European Convention for Constructional Steelwork (ECCS) has recently released a new European Design guide for the Use of weathering Steel in bridge construction in 2021, which will be applicable for the Netherlands (Ungermann & Hatke, 2021).

Weathering steel is a high strength low alloy structural steel that can be left uncoated in suitable environments. This is due to the formation of an adherent protective rust “patina” which increases the thickness of the plate and minimizes further corrosion. This causes weathering steel to have an increased atmospheric corrosion resistance compared to conventional steel, see Figure 3. To make weathering steel, alloys such as copper, chromium, silicone and in some cases phosphorus are added. These added alloys do not influence the structural capability of the steel, the structural strength, ductility, toughness and weldability remain the same (Hicks, El Sarraf, & Mandeno, 2017).

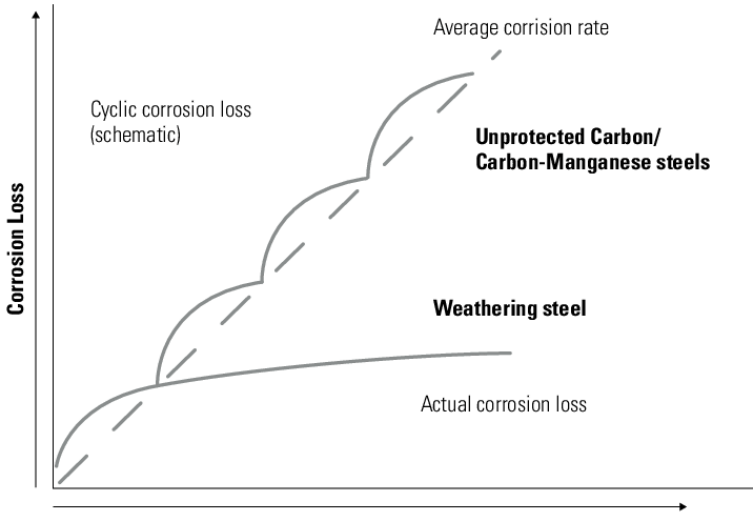

Figure 3 Corrosion loss over time for weathering steel and unprotected conventional steel (Hicks, El Sarraf, & Mandeno, 2017)

For conventional steel a corrosion protection layer should be added to have the desired corrosion resistance. The self-forming protective layer of weathering steel makes it an attractive material for bridge construction, as it requires minimal maintenance over time. In contrast, conventional steel has high maintenance costs due to the need for regular renewal of protective coatings throughout the structure's lifespan.

It is important to approach the performance of weathering steel in extreme environments, such as those with high pollution and elevated chloride concentrations, with caution, as these conditions may present challenges compared to conventional corrosion-protected steel (NSC, 2024). Therefore, assessing the corrosion risk for each specific location where the bridge will be constructed is essential. This assessment is conducted using corrosion classes (Highways England, 2019), which are based on the expected corrosion rates for various locations.

The Netherlands has a significant coastline, with many bridges located nearby. This proximity increases the risk of chloride contamination. Additionally, the Dutch climate requires the use of de-icing salt on all highways, affecting bridge design considerations. These factors influence the expected corrosion classes for new bridges.

As design recommendations in the reference guide for uncoated weathering steel components it is stated that prolonged exposure to wetness and/or high levels of chloride without the opportunity to dry needs to be prevented. The following environmental factors can accelerate bridge corrosion:

1. High humidity from climate or nearby water and vegetation.
2. Roadway and marine salts that slow drying and speed up corrosion.
3. Pollution trapping moisture.

When designing and detailing the structure these three mentioned conditions should be prevented, nevertheless there are locations where this cannot be prevented and therefore UWS will be an disadvantageous solution (American Institute of steel construction, 2022).

2.2.2 Environmental analysis of Unpainted Weathering Steel (UWS) in the Netherlands

When considering to use weathering steel components the macro- and micro – environments should be analyzed according to the ECCS guidelines for weathering steel (Ungermann & Hatke, 2021) . The macro- environment considers the general geographical location of the bridge while the micro-environment considers the local, site specific characteristics of this location. Regarding these environments it is stated if the use of UWS is recommended on a certain location. First, when neither the macro -and micro- environment are severe it is

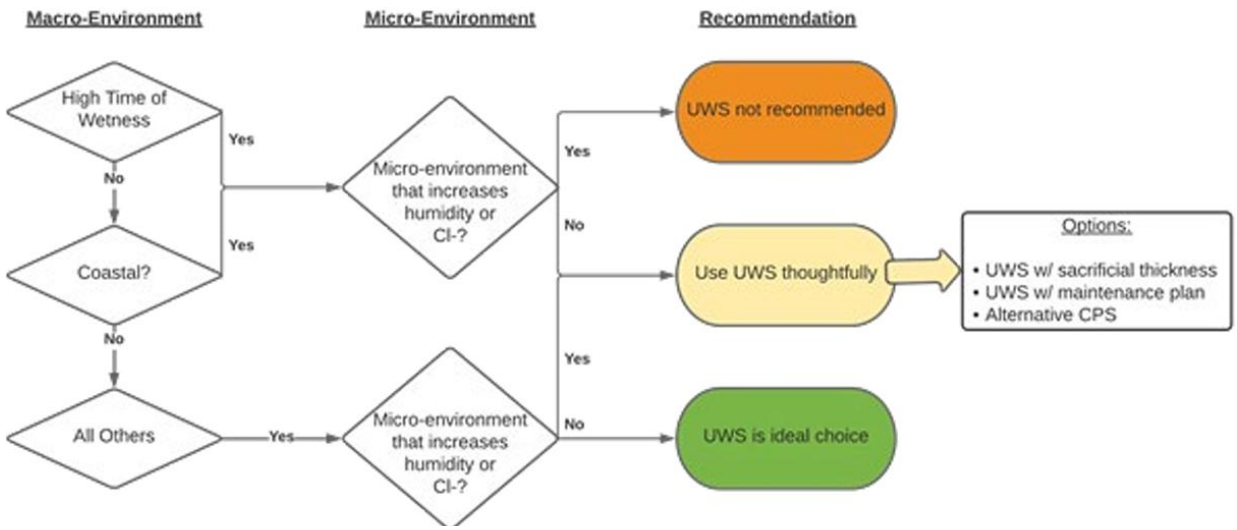

Figure 4 General concept micro- and macro- environment (American Institute of steel construction, 2022)

stated that UWS can be seen as the ideal solution. Second, when either the macro-or micro-environment contains features that increase the humidity or chloride exposure at site, the use of UWS should be done thoughtfully. This means the consideration of sacrificial thickness and/or a maintenance plan should be taken into account when designing the structure. This Maintenance plan could consist of activities such as washing of the structure or painting the structure in the future if this will be inevitable. Third, when both the macro- and micro- environments contains features that increase the humidity or chloride exposure at site, it is recommended to not make use of UWS (American Institute of steel construction, 2022). In Figure 4 a visualization of these steps are given.

From research performed in the USA it was made clear that a distance of more than 3.2 km from the coast should be respected, to have a sufficient structural performance. Regarding the humidity, it was mentioned that an average humidity of more than 76 percent for a period of eight or more months could be seen as concerning. In Table 1 the average monthly humidity of each province in 2023 are given. From these results it can be concluded that each location in the Netherlands has an average relative humidity for 8 months or more which is higher than 76%. Which makes the whole Netherlands to be seen as a concern area regarding the Macro-Environment and therefore the use of UWS should be done thoughtfully as has been stated in Figure 4.

Table 1 Average monthly relative humidity (Weerplaza, 2023)

	Zeeland	Noord-brabant	Limburg	Zuid-holland	Gelderland	Noord-holland	Flevoland	overrijsel	Friesland	Drenthe	Groningen	Utrecht
Jan	86%	87%	87%	87%	89%	87%	89%	88%	89%	89%	89%	86%
Feb	82%	81%	80%	82%	83%	83%	84%	82%	84%	84%	84%	81%
Mar	79%	74%	73%	77%	76%	78%	78%	75%	80%	78%	79%	75%
Apr	74%	69%	69%	74%	71%	75%	74%	71%	77%	74%	75%	71%
Mai	75%	70%	70%	74%	72%	75%	74%	72%	77%	74%	76%	72%
Jun	76%	71%	71%	75%	73%	77%	76%	73%	79%	77%	78%	73%
Jul	75%	71%	70%	75%	74%	77%	77%	73%	78%	77%	77%	74%
Aug	76%	74%	73%	77%	76%	78%	79%	75%	79%	78%	79%	77%
Sep	78%	79%	78%	81%	81%	82%	83%	81%	82%	83%	83%	81%
Oct	83%	84%	83%	85%	86%	85%	87%	85%	86%	87%	86%	85%
Nov	85%	87%	87%	88%	90%	88%	90%	88%	89%	90%	89%	87%
Dec	87%	88%	87%	89%	90%	88%	90%	88%	90%	90%	90%	88%

2.2.2.1 Corrosion classification

When the surfaces of metals is wetted, metals can suffer atmospheric corrosion. The nature and the rate of the corrosion attack depends upon the properties of the pollutant factor and the duration of pollution. In the NEN-EN-ISO 9223 the atmospheric corrosivity classification is described, this classification 6 categories of corrosivity have been described as can be seen in Table 2.

Table 2 Corrosivity categories of the atmosphere according to NEN-EN-ISO-9223

Category	Corrosivity
C1	Very low
C2	Low
C3	Medium
C4	High
C5	Very high
Cx	Extreme

The corrosion classification is tested on different criteria before placed in a certain corrosivity category, the air pollution in the region, the salt concentration, distance to the coast are examples of factors that are being considered when classifying. The global corrosion classes used in the Benelux are visualized in Figure 8.

The rate of corrosion also depends on the surroundings where the structure is placed, for example if it is close to the coast, city of a steel fabric are all factors that could influence the corrosion rate. From Figure 7 it can be observed that the coastal region of the Netherlands is classified as Category 5, which means a very high corrosivity risk in this region. Going more inwards the corrosivity risk decreases.

The chloride concentration in the Netherlands has been measured at certain locations from 2008 to 2010, from these measurements a model has been made to determine the chloride concentration over the whole Netherlands. The result of the made model can be seen in Figure 7. It can be observed that the high chloride concentration locations are in line with the C5 classification location in Figure 8. This is in line with the expectations since the chloride concentration has a significant influence on the corrosion risk of the structure.

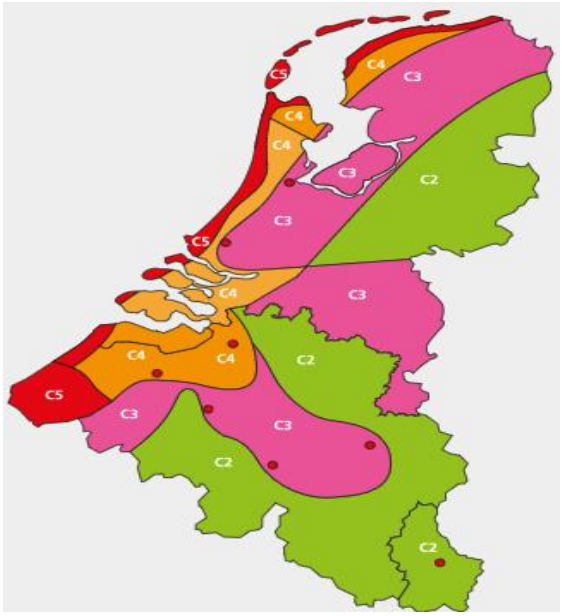

Figure 8 Global corrosion classes Benelux (Joostdevree, sd)

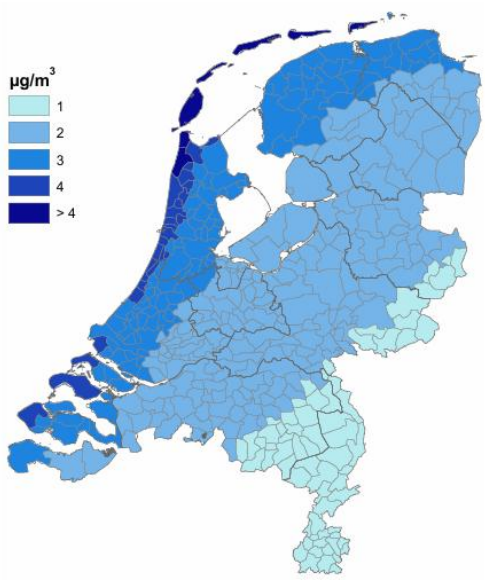

Figure 7 Division of the mean chloride concentration in the Netherlands (National Institute for public health and the Environment, 2012)

As mentioned before when considering to make use of UWS the macro and the Micro-Environment should be considered. From the Macro-environmental analysis of the Netherlands it was clear that the overall characteristics are undesirable for UWS. Therefore to get a recommendation to make use of UWS the micro-conditions should be kept beneficial (American Institute of steel construction, 2022).

To control the micro-environmental conditions it is essential to perform a site evaluation. The topography should be evaluated so the structure will not be exposed for an excessive period to wetness. Regarding vegetations two situations should be considered. First, Natural topography that causes dense vegetation in/or nearby the UWS has to be prevented. Second, Vegetations, and or shelters that obstacles the sunlight from reaching the UWS should also be prevented (American Institute of steel construction, 2022).

Highway crossings which pass a roadway which is heavily treated with deicing salts cause a more severe micro-environment relative to their macro-environment. This happens due to the collection of airborne salt-laden on the superstructure. Hereby the amount and type of deicing salt has a mayor influence on the structure. Also the clearance between the roadway and the UWS component of the superstructure will influence the environment. It is stated that micro-environmental effects of deicing agent use only occurs in the typical situations when the average annual snowfall exceeds 51 cm.

The use of brine deicing solutions should be done consciously, since it is observed that locations with a high percentage of used brines have an accelerated corrosion. If one of the mentioned conditions is met, it is recommended to thoughtfully make use of the UWS, hereby a sacrificial thickness and/or a maintenance plan should be considered when designing the structure (American Institute of steel construction, 2022).

The vertical clearance between roads which are heavily treated with deicing salt and the superstructure should have a minimum clearance of 6.1 m according to the American reference guidelines. This with the idea that the vaporized deicing salt will not reach the bottom part of the superstructure. When the micro-environment is classified as “extreme deicing environment” and the vertical clearance is less the mentioned threshold it is recommended to make use of a sacrificial thickness and/or an maintenance plan. Considering the European guidelines a formula is given where the length of the retaining walls influence the minimal allowable clearance (Ungermann & Hatke, 2021):

$$H > min.\ (4.3 + L/25\ ;\ 7.5\ m)$$

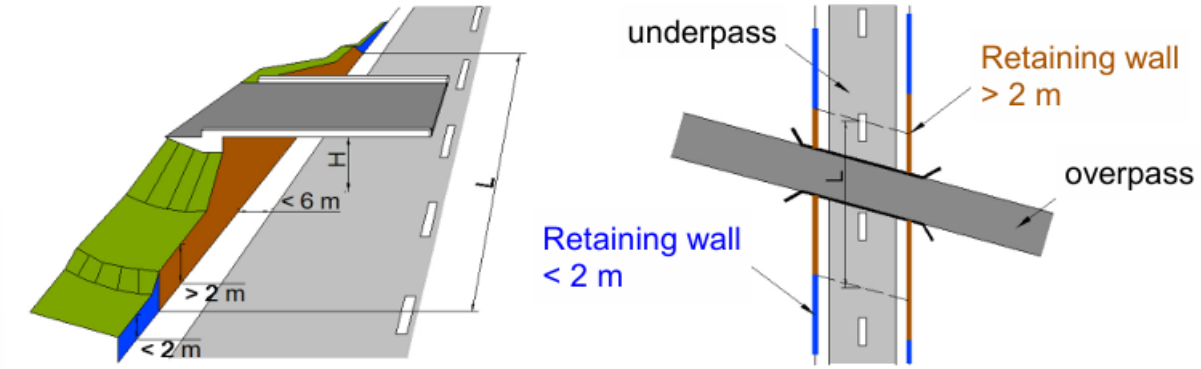

Figure 9 Length to be considered for formula 1 (Ungermann & Hatke, 2021)

Regarding the horizontal clearance , there should be a minimal clearance of 9.2m between the edge of the travelled way and the nearest substructure unit.

In the Netherlands, bridges crossing highways typically have a vertical clearance of approximately 4.5 m. As this value is significantly lower than the 6.1 m minimum recommended in the American guidelines for regions exposed to deicing salts, additional measures are required when applying weathering steel in the Dutch context. These measures should include the provision of a sacrificial thickness and/or the implementation of a well-defined maintenance plan to ensure adequate durability and corrosion protection under these conditions.

2.2.2.2 *Sacrificial thickness*

In the areas where it is expected that the corrosivity will be high it is recommended to make use of a sacrificial thickness. This is a more economical solution than painting the structure after significant corrosion has been observed. It is recommended to apply the sacrificial thickness only for the horizontal placed elements. For the case of open sections it is seen that the bottom flange is in need of a sacrificial layer. To prevent any increase of thickness of other elements thoughtful detailing should be performed by the responsible structural engineer. A typical sacrificial thickness for the normal service life of a structure is 1/16 inch = 1.6 mm . This is the total increase in thickness on both sides of the plate (American Institute of steel construction, 2022).

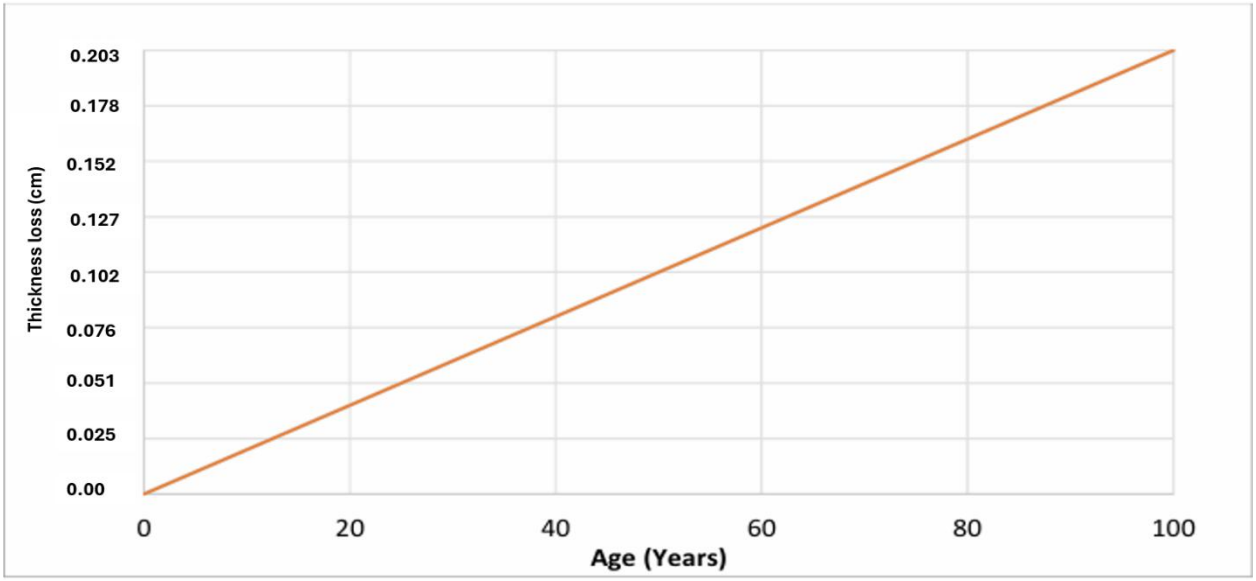

Figure 10 Estimated upper-bound section loss for fully exposed UWS plates in high corrosive environments (American Institute of steel construction, 2022).

The UWS elements that are used for a highway crossings are preferably used in combination with a reinforced-concrete deck. When properly detailed, this will ensure a water tight connection that prevents the UWS of having a high Time of wetness.

Regarding the composite structure the upper part of the weathering steel beams will be fully protected by the concrete deck. The bottom flange of the weathering steel beam will be fully exposed to the atmospheric corrosion, while working as a protection layer on the web and upper flange of the element.

When designing the bottom flange of the UWS beams it is essential to opt for a flange thickness maximization. This should be done so the width of the flange is kept as small as possible. A bigger width of the flange will cause the structure to have a bigger area where the moist can be collected, which will have a negative effect on the corrosion resistance of the UWS component.

Also when applying rather an flange thickness transition instead of a flange width transition it will be possible to predict the drainage path of any water that may travel along the length of the top sides of the bottom flanges.

Figure 11 Example of flange thickness transitions (American Institute of steel construction, 2022).

Regarding the use of bolted connections in the UWS-concrete superstructure, it is essential to make use of specific weathering steel fasteners. Some appropriate combinations of bolts, nuts and washes that can be used are listed in Table 3.

Table 3 Fasteners to be used for UWS (American Institute of steel construction, 2022)

Bolts	Nuts	Washers
ASTM F3125 Grade A325 Type 3	ASTM A563 Grade DH3 or C3	ASTM F436/F436M Type 3
ASTM F3125 Grade A490 Type 3	ASTM A563 Grade DH3	ASTM F436/F436M Type 3

During the life time of the weathering steel it is expected that some loss of material will occur. To account for this loss an allowable loss of thickness is defined for each corrosivity category. The typical inland corrosivity category inland Europe is C2 to C3 according to EN ISO 9223. In the ECCS the allowable loss of thickness in the Netherlands is not defined, therefore it has been chosen to use the values given for Belgium and the ECCS recommendation as reference values for the Netherlands, these allowable thickness losses are given in Table 4.

Table 4 Allowance for the loss of thickness for a design life of 100 years

Country/guidelines	Allowance for the loss of thickness related to corrosion classification in EN ISO 9223				
	C1	C2	C3	C4	C5
Belgium	-	0.11-0.8 [mm]	0.53-1.2 [mm]	1.05-1.5 [mm]	Not allowed
ECCS recommendation for bridges	Not applicable	0.8 [mm]	1.0 [mm]	1.5 [mm]	Not allowed

2.2.2.3 Design considerations for sacrificial thickness

The global analysis can be performed on the cross-section-areas and second moments of the area based on either the design thickness after deduction of the allowable loss thickness or the original thickness provided. Regarding the detailed design , the strength and stress calculations should be based on the net size after deduction of a uniform thickness allowance.

2.2.2.4 Detailing

When detailing the structure it is essential to prevent continuous wetness or damp of the structure. The natural drying process should be respected on all parts of the structure by avoiding moisture accumulation and adequate ventilation and drainage of the water. Structures consisting of pockets, crevices or faying surfaces should be prevented, since these structures stimulate accumulation of water. For good ventilation it is also recommended to have an adequate center to center distance between the beams.

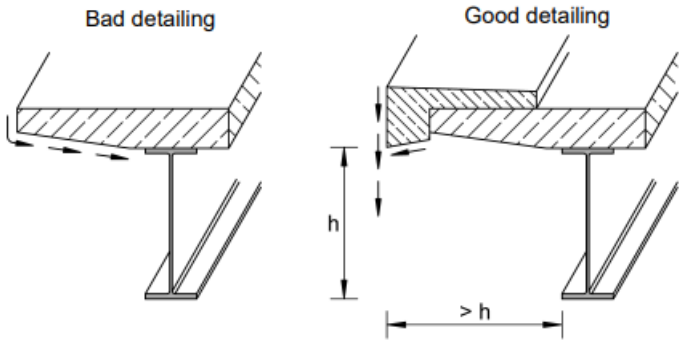

Figure 12 Drip details at the caps or edges of concrete decks and overhang (Ungermann & Hatke, 2021)

In composite weathering steel bridges with concrete decks, drip features should be placed along the deck edges or caps. Ideally, the deck should extend beyond the steel girder by a distance at least equal to the girder's depth so that rainwater does not fall directly onto the steel surface, as can be seen in Figure 12. The same recommendation applies to the concrete deck caps used in these bridge types. (Ungermann & Hatke, 2021).

2.2.3 Reassessment Avenhornbrug

To have a better understanding of the feasibility of making use of weathering steel-concrete bridges in the Netherlands it has been chosen to make use of the reassessment of the only weathering steel bridge built in the Netherlands, namely the Avenhornbrug. The Avenhornbrug was built in 1975, the bridges run from North to South and consists of two separate dual-carriageways of the A7 national highway. The Avenhorn bridge is located in the C4 region as can be seen in Figure 14.

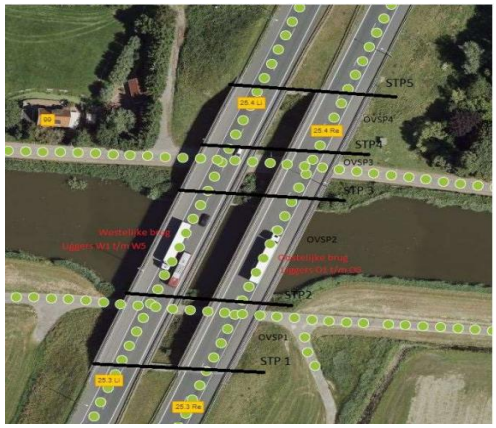

Figure 13 Top view Avenhornbridge (Jong, 2024).

From this reassessment interesting parameters will be the thickness loss of the weathering steel beam over the now passing 50 years would be of high interest value. This measured thickness loss can be compared with the theoretical thickness loss. From this comparison it will be possible to check if the current theoretical thickness loss is to conservative, to overestimating or just right.

From the inspections it was clear that due to bad detailing of the water transportations systems of the bridge some parts of the weathering steel beam were highly exposed to salinized water. It would be highly interesting to compare the thickness of this beam with the thickness of the weathering steel beam where proper detailing has taken place (Verhoef, 2021).

After a periodical inspection it was clear that the bridge was in need of a more thorough inspection and a reassessment was needed. This constructional inspection is while writing this thesis ongoing and therefore only the current concept state of this study will be used for enhancing the literature review.

Figure 14 Location of the Avenhorn Bridge (yellow dot) 2 km from the coast (Joostdevree, sd)

Figure 15 Visualization Avenhornbrug

2.2.3.1 General thickness loss

The first report that will be considered is the strain measurements installation report. Over here the installation location of the measurement tools will be considered and the thickness measurements of the weathering steel beams at different locations (Jong, 2024).

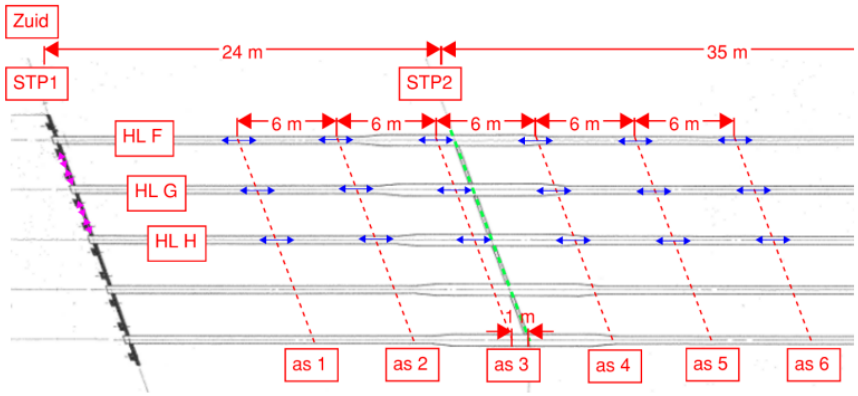

Figure 16 sensor locations (Jong, 2024).

In Figure 16 the new sensor locations of the main beams are given. On each sensor location the plate thickness has been measured. These measurement results will be compared with the original plate thicknesses to see how the corrosion process has evolved over time. These results are given in Table 5 . From these results we can see a clear thickness decrease difference between the top flange and the bottom flange of the weathering steel beams. As expected the bottom flanges have a higher

thickness loss since these flanges are the first in contact with evaporating water from the river passing beneath the bridge. The highest thickness loss could be found at HL H-as2-bot with a thickness loss of 4.8 mm.

Figure 17 visualization of the overall patina formation on the beams

Table 5 Thickness evolution at each sensor location

Sensornaam	Ingemeten plaatdikte [mm]	Plaatdikte archieftekening [mm]	Verschil [mm]
HLF-as1-top	19.8	20	-0.2
HLF-as1-bot	28.5	30	-1.5
HLF-as2-top	19.9	20	-0.1
HLF-as2-bot	28.6	30	-1.4
HLF-as3-STP2-top	24	25	-1
HLF-as3-STP2-bot	39.5	40	-0.5
HLF-as4-top	24.6	25	-0.4
HLF-as4-bot	38.6	40	-1.4
HLF-as5-top	24.4	25	-0.6
HLF-as5-bot	37.8	40	-2.2
HLF-as6-top	24.4	25	-0.6
HLF-as6-bot	38.6	40	-1.4
HLG-as1-top	19.6	20	-0.4
HLG-as1-bot	28.6	30	-1.4
HLG-as2-top	19.6	20	-0.4
HLG-as2-bot	29	30	-1
HLG-as3-STP2-top	24.1	25	-0.9
HLG-as3-STP2-bot	39.3	40	-0.7
HLG-as4-top	24.4	25	-0.6
HLG-as4-bot	38.7	40	-1.3
HLG-as5-top	24.5	25	-0.5
HLG-as5-bot	39.6	40	-0.4
HLG-as6-top	24.7	25	-0.3
HLG-as6-bot	39.4	40	-0.6
HLH-as1-top	19.8	20	-0.2
HLH-as1-bot	28.8	30	-1.2
HLH-as2-top	20.1	20	0.1
HLH-as2-bot	25.2	30	-4.8
HLH-as3-STP2-top	24.1	25	-0.9
HLH-as3-STP2-bot	38.9	40	-1.1
HLH-as4-top	24.2	25	-0.8
HLH-as4-bot	38.6	40	-1.4
HLH-as5-top	24.5	25	-0.5
HLH-as5-bot	38.9	40	-1.1
HLH-as6-top	24.2	25	-0.8
HLH-as6-bot	38.5	40	-1.5
DDF-G-mid-BLH	8.9	10	-1.1
DDF-G-mid-BV	15.7	16	-0.3
DDF-G-mid-OLH	15.5	16	-0.5
DDF-G-mid-OV	15.3	16	-0.7
DDF-G-HL-BLH	9.1	10	-0.9
DDF-G-HL-BV	15.9	16	-0.1
DDF-G-HL-OLH	15.8	16	-0.2
DDF-G-HL-OV	15.4	16	-0.6
DDG-H-mid-BLH	9	10	-1
DDG-H-mid-BV	15.8	16	-0.2
DDG-H-mid-OLH	15.7	16	-0.3
DDG-H-mid-OV	15.6	16	-0.4
DDG-H-HL-BLH	9.2	10	-0.8
DDG-H-HL-BV	15.7	16	-0.3
DDG-H-HL-OLH	15.9	16	-0.1
DDG-H-HL-OV	16	16	0

2.2.3.2 Local thickness loss

The second report that will be considered is the “Viaduct Beemsteruitweg A7-Steel thickness measurements”. From previous performed inspections it was clear that some locations were suffering of severe corrosion. Therefore it had been chosen to further inspect and quantify the material decrease at these locations. From this following report it could be concluded that two types of advices were given. The first advice considers all the weathering steel main beams, and all this beams are showing an undesirable situation with a limited risk. The beams are in general in an advanced stage of corrosion. The second advice was given regarding the support 1, at the southern end close to the abutment. This location is considered as a high risk location with undesired situations considered at four beams. In all cases corrosion with heavy material decrease at the end stage of the beams has been observed.

Figure 18 Local significant thickness losses

2.2.3.3 Conclusion reassessment

From the given reports at the most recent state it was clear that the thickness loss could be classified in two types. First the general thickness loss of the structure could be observed, this thickness loss is overall in line with the expectation of the structure and has also been assessed as sufficiently small according to thickness loss tolerance written in EN10029.

The Avenhornbrug lays woth a distance of 8 km from the sea, when comparing its location with the corrosion class map of Figure 5, it can be observed that this area lays under Corrosion class 4. According to Table 4 a maximum corrosion-loss for a 100 years lifespan of a weathering steel bridge should be within 1.05 mm and 1.5 mm. Considering the general thickness losses from Table 5, all the thickness losses fall within this range. However this bridge has a current lifespan of 50 years and already some thickness losses of 1.5 mm are observed, this show the cautioness that should be taken in the evaluation of this bridge in the future.

Second observed situation, is at certain location where significant thickness loss has been observed. These locations are almost all close to a connection of the structure. The cause of the significant thickness loss is due to inadequate detailing of the structure at these locations.

2.2.4 Expansion and deck joints

In this report a case study will be considered where a simply supported superstructure will be considered. At the supports it will be inevitable to have deck joints. Due to water accumulation and high chloride concentrations due to the seepage of de-icing salt, corrosion at the abutments could happen when detailed inadequately. Therefore special attention should be given to the prevention of leakage at these locations. This can be realized by providing a drainage systems, see Figure 19. These drainage systems should be designed on such a way that the run-off water from the superstructure should not be permitted to run down the visible external surfaces of the sub structure (Ungermann & Hatke, 2021).

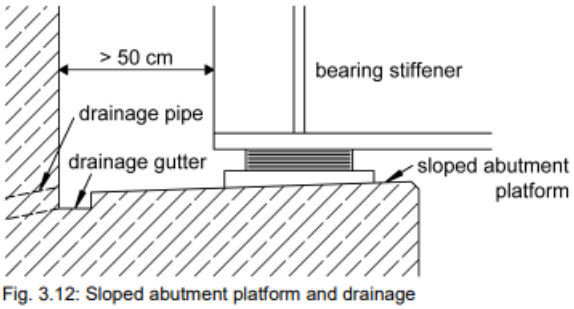

Fig. 3.12: Sloped abutment platform and drainage

Figure 19 Example of adequate detailing at the abutments (Ungermann & Hatke, 2021)

2.2.5 Welded connections

From a structural strength perspective, the requirements for welding weathering steel are largely the same as for conventional steel, except for the need to allow additional thickness in fillet welds. A critical design rule is that all welds should be made continuous around the entire joint. This prevents water from penetrating the interface between components, which would otherwise create a crevice prone to corrosion.

Because weathering steel typically has a higher carbon equivalent than many other high-strength steels, a greater level of preheating is usually required during welding. The need for careful electrode selection and the likelihood of mandatory preheating often make site welding less attractive than using bolted connections. When welding is performed, the surrounding surface generally requires grinding or grit blasting afterwards. This treatment can cause the affected area to weather differently from the rest of the structure, which is a minor aesthetic drawback that should be considered(Ungermann & Hatke, 2021).

2.2.6 Bolted connections

For bolted joints, it is good practice to use preloaded bolts so that the connected parts remain tightly clamped together, minimizing the risk of crevice corrosion. The bolt assemblies should have corrosion-resistance characteristics similar to those of the connected weathering steel components. Preloadable high-strength bolts manufactured from weathering steel are available in countries such as the UK, the USA, and Japan. In the UK, type HRC assemblies conforming to EN 14399-10 in property class 10.9/10 are available and correspond to ASTM F3125 type 3. Stainless steel preloaded bolts are also a viable option and do not pose bimetallic corrosion concerns (Ungermann & Hatke, 2021).

Although bolted joints naturally create crevices, no durability issues are expected if the contact surfaces are kept firmly pressed together. This requires good dimensional tolerances and appropriately preloaded bolts. Very thick plates should not be connected using bolts of small diameter. The minimum distance from any bolt center to a free edge, whether in the direction of force or perpendicular to it, should be the lesser of 8 times the thickness of the thinnest connected plate (8*t) or 125 mm. Similarly, bolt spacing along lines near the edges of plates or sections should not exceed 14*t or 175 mm (Ungermann & Hatke, 2021).

Current design codes do not impose specific corrosion allowances for bolt sizing. In a well-detailed bolted connection, the bolt shank is considered to be effectively shielded from direct exposure, and no additional corrosion allowance is required (Ungermann & Hatke, 2021).

2.2.7 Removal of rust stains

On a well-designed and drained bridge rust staining should not occur, nevertheless some extra care should be taken since the possibility it will happen is always there. The sensitivity of a material to dirt and staining is mainly dependent on its surface conditions. Concrete half-joint connections will be used, concrete is known to be prone to severe staining and difficult to clean. Therefore, this should be taken into consideration when detailing the connections (Ungermann & Hatke, 2021).

Figure 20 Extreme example of rust strains (shutterstock, 2021)

2.3 Fatigue performance of weathering steel bridges

A concern of weathering steel that should be taken into account is that the fatigue resistance may be less than conventional steel, as can be seen in the degradation process of Figure 22. This is due to the fact that corrosion causes pits from which fatigue cracks might initiate earlier. It is stated that especially in welded details of weathering steel connections that the fatigue life reduces significantly compared to conventional steel (Ungermann & Hatke, 2021).

The fatigue resistance of steel structures is determined by making use of the nominal stress interval expected on the relevant detail of the structure. In the NEN-EN 1993-1-9 the procedure to determine the fatigue resistance has been worked out. The given detail categories are linked to the nominal stress interval. The lower the detail category the lower the lower the allowable nominal stress interval will be the lower the fatigue resistance will be if the number of cyclic N remains the same. In Figure 21 S-N curve is given from NEN-EN 1993-1-9 which is used to determine the detail categories. The detail categories are again linked to the construction detail of the element to be checked. In table 8.1. of NEN-EN 1993-1-9 several construction details are given which can be linked to the detail category which can be used again to determine the fatigue resistance on the relevant detail.

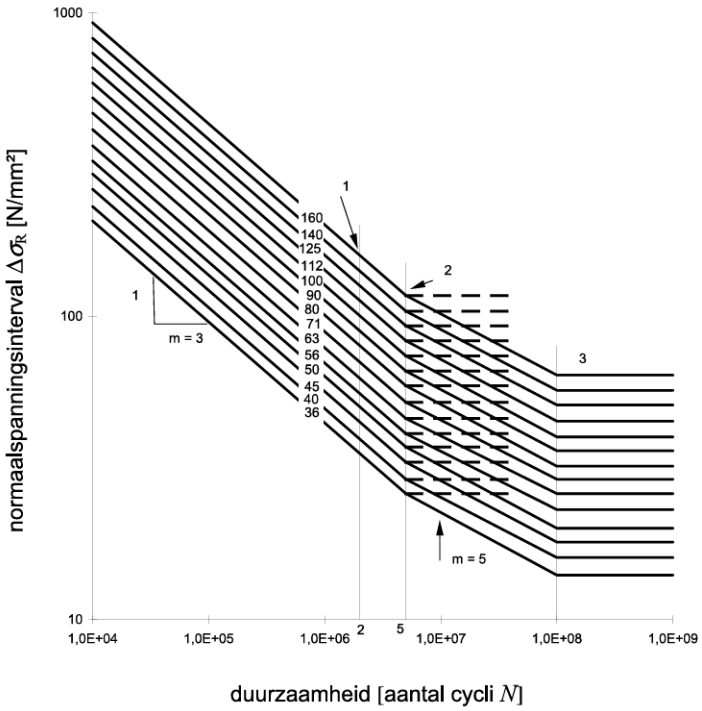

Figure 21 S-N curve form NEN-EN 1993-1-9

After the weathering process has occurred, plain weathering steel, will have a slightly lower fatigue strength than plain uncorroded steel. For this reason according to EN 1993-1-9, the next lower detail category should be used for plain products made of weathering steel. This only concerns the detail categories 160 for hot rolled and extruded products as well as 140 or 125 for sheared or thermally cut plates (Ungermann & Hatke, 2021).

For the hot rolled section detail class 160 should be considered for the flanges. Nevertheless it is stated in table 8.1 that weathering steel should be classified to the first following lower category. Therefore it has been chosen to make use of the detail category 140 for the flanges.

Regarding the web of the structure detail category 100 of table 8.1 should be used for conventional steel, for weathering steel detail category 112 will be used. However m= 5 will be taken into account and $\Delta\tau = \frac{VS(t)}{It}$ wil be used for the shear interval calculations.

For the studs, critical zone 1 will be considered This is in line with detail category 80 according to EN 1993-1-9 table 8.4 detail 9 will be used. However since the studs will be considered to be made of weathering steel detail category 71 will be considered for the studs.

In bridge structures, fatigue cracking typically begins at locations where the geometry changes abruptly or where stress concentrations occur, most commonly at welded or bolted joints. These discontinuities produce a far greater decrease in fatigue strength than the surface corrosion pits that may form on weathering steel. Evidence indicates that when the relevant detail is classified as category 112 or lower according to Eurocode 3-1-9, using weathering steel does not shorten the fatigue life. Even for details in category 125, no reduction is necessary, as the weld itself governs the fatigue performance(Ungermann & Hatke, 2021).

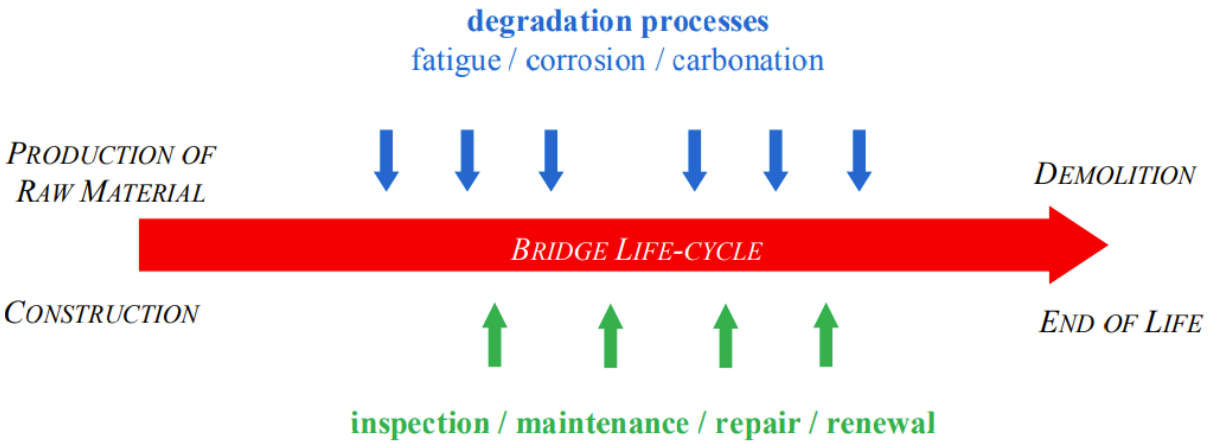

Figure 22 schematic representation of the life cycle of a bridge

In conventional painted steel structures fatigue cracks are often detected by visual checks, these cracks are made visible due to the colour contras between the paint and the rust stain in the vicinity of the crack. This visualisation detection of cracks will be hard to be performed in weathering steel bridges. Due to the corrosive pattern that will be formed in the bridge the cracks will be hard to be detected, this property of weathering steel elements should be taken into account in the maintenance plan of the bridge. A more effective fatigue crack detection method will be the use of magnetic particle inspection methods. This method can be seen as a effective method, however preparation of the suspected area is needed before it will be able to apply this method. Recent investigations have shown that the use of EMAT (Electro Magnetic Accoustic Transducer) is an effective method to detect cracks on steel structures with a protective oxide layer.

Figure 23 Fatigue cracks on conventional painted steel bridge (Center of advanced infrastructure and transportation, sd)

2.3.1 Conclusion Fatigue analysis

For a simply supported (Weathering) steel–concrete composite superstructure, the fatigue limit state is unlikely to govern overall member sizing. Although Eurocode provisions (EN 1993-1-9 and EN 1993-2) require a fatigue assessment, fatigue effects generally become critical only at detail-sensitive locations such as welded connections, butt and transverse welds, or shear connectors which are more relevant for continuous spans than for short, simply supported bridges. Practical design guidance and worked examples show that for typical road traffic loading and reasonable span lengths, the governing design checks are usually the ultimate and serviceability limit states (ULS/SLS), assuming adequate detailing and fabrication quality in accordance with EN 1090.

This conclusion holds for conventional span lengths, typical Dutch traffic conditions, and standard bridge details. Only in cases of unusually long spans, highly repetitive heavy axle loads, or non-standard details would a detailed fatigue assessment potentially influence design dimensions.

Given the overall aim of this thesis to evaluate the competitiveness and sustainability of weathering steel–concrete composite bridges performing a full fatigue calculation would not significantly contribute to answering the research questions, as fatigue has negligible influence on the governing dimensions and therefore minimal impact on comparative sustainability or economic outcomes. Consequently, the fatigue limit state will not be considered further in this thesis as its influence is deemed non-additive.

2.4 Costs analysis of weathering steel bridges

Weathering steel-concrete composite bridges are being used in the USA for more than 50 years for highway crossings. From their experience in the application of these type of bridges it can be stated that the Uncoated weathering steel component has a favorable and cost-effective performance in many environments. If it is even assumed that there are no significant changes in the environment, and when regular inspections are performed and any local problem areas are treated accordingly, it is stated that UWS bridges can have a service life of more than 100 years (American Institute of steel construction, 2022).

When comparing the material costs of weathering steel components it can be observed that the material costs are 2 to 6% higher compared to conventional steel components. Nevertheless when including the traditional three-coat paint options for conventional steel and the fact that the weathering steel component does not need any coating. It can be observed that the initial costs for UWS are approximately 10 % less than for the production of an conventional steel component (American Institute of steel construction, 2022).

When comparing the life-cycle costs of UWS components compared to convention steel components, it can be observed that for the UWS components costs are avoided regarding the materials used for painting process, labor, equipment and maintenance off traffic. It is estimated that this well lead to a cost reduction during the life-cycle of the component of up to 30% when compared to conventional painted steel (American Institute of steel construction, 2022).

2.5 Sustainability Analysis

In this paragraph the information will be gathered to be used to perform the sustainability analysis of the three variants. The sustainability impact of the three variants will be determined by calculating the Environmental costs of the three variants. These costs can be determined by making use of the EPD of the different components used in each variant. In this chapter the EPD's will be discussed on how these EPD's are made and also how these EPD's are used to calculate the Environmental cost of each variant.

2.5.1 Introduction to Life cycle analysis (LCA) and Environmental product declarations (EPD's)

In the past, bridges were primarily designed with safety and cost considerations in mind. To minimize expenses, the use of cheap and readily available materials was encouraged. As a result, many bridges were constructed using concrete as the primary material. The production of these concrete structures relied heavily on raw materials and cement, a process responsible for 7-8% of global carbon dioxide emissions (Sullivan & Olson, 2022).

Today, it is crucial to consider not only the safety and cost of bridge designs but also their sustainability impact. Factors such as emissions over the structure's lifespan, the use of raw materials, and the broader environmental and health effects associated with the bridge should all be integrated into the design process. By accounting for and quantifying these factors early in the design phase, it becomes possible to create bridges that are both functional and sustainable.

The quantification of the sustainability impact of a bridge design can be achieved through a Life Cycle Assessment (LCA). This method evaluates the environmental impact of a bridge across its entire lifecycle, from material extraction and construction to operation, maintenance, and eventual demolition. LCA provides valuable insights into the potential environmental impacts, allowing designers to make informed decisions about material choices, energy use, and long-term sustainability, ultimately ensuring that bridges are not only structurally sound but also environmentally responsible.

As stated in the ISO LCA standards the LCA framework consists of four phases (Du, 2015):

- *Goal and scope definition*: defining the objectives, the product system and the expected outcome of the study
- *Inventory analysis*: quantification of all the emissions related to the product system based on the functional unit of the product.
- *Impact assessment*: Transforming the inventory results into the environmental impact categories
- *Interpretation:* Explaining the results with the goal of the study through the whole analysis procedure.

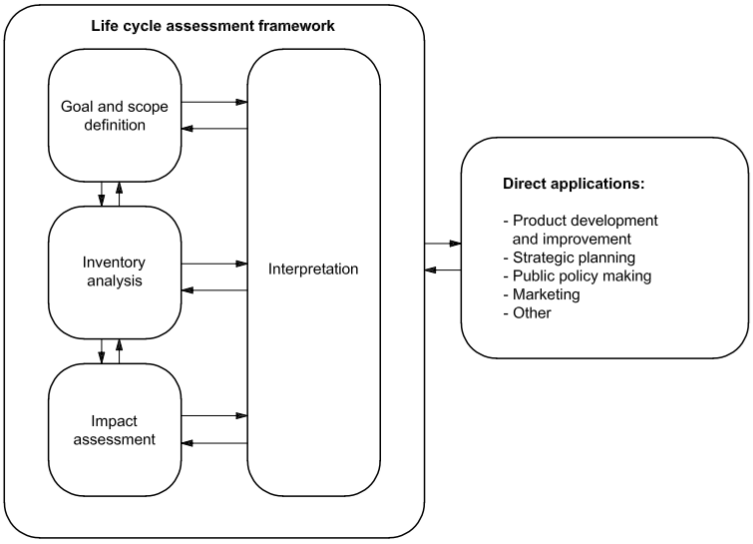

Figure 24 Stages of an LCA (NEN-EN-ISO 14040:2006, 2006)

LCA for bridges

For the performance of a LCA for a bridge it is essential to determine the life cycle stages involved in the realization of bridges. The life cycle of bridges can be divided into four main stages:

- Material manufacturing stage
- Construction stage
- Use and maintenance stage
- End Of Life stage

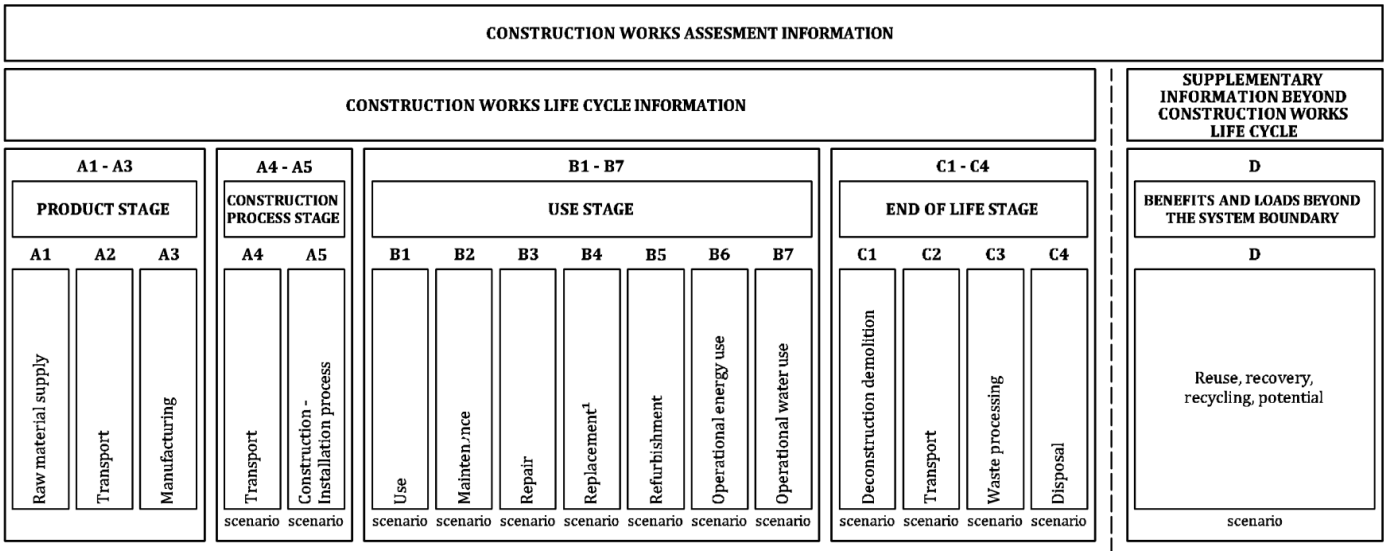

Figure 25 Construction works assessment information (NEN-EN 15804+A2, 2019)

The life cycle assessment (LCA) conducted forms the basis of the Environmental Product Declaration (EPD). The EPD reports the calculated environmental impacts for each category in the LCA, making it easier to compare the sustainability performance of different products and to select the most appropriate option when designing the bridge's superstructure.

According to the standard NEN-EN 15804:2012+A2:2019 the following definition is given to an EPD :

"*An EPD according to this standard provides quantified environmental information for a construction product or service on a harmonized and scientific basis. It also provides information on health related emissions to indoor air, soil and water during the use stage of the building. The purpose of an EPD in the construction sector is to provide the basis for assessing buildings and other construction works, and identifying those, which cause less stress to the environment.*"

To ensure a clear, fair, and justified comparison between different products , EPDs must always be determined on the basis of an LCA that follows the official determination method. Without this, results can be misleading and lead to distorted outcomes.

In the Dutch context, this is safeguarded by the Nationale Milieudatabase (NMD), managed by Stichting NMD. The NMD contains product data in the form of environmental declarations, structured according to the *Bepalingsmethode,* as can be seen in Figure 26 . This method ensures that all calculations are transparent, reproducible, and consistent, providing a reliable basis for assessing the environmental performance of construction works.

The NMD determination method for safeguarding the reliability of the performed LCA is based on the following categories:

Category 1 (brand-specific, verified)
Manufacturer-/product-specific data, independently verified according to the NMD Assessment Protocol. Highest level of specificity and reliability.

Category 2 (non-brand-specific, verified)
Generic (brandless) data, also independently verified, with indication of representativeness (e.g., Dutch market or group of producers) and participating parties.

Category 3 (non-brand-specific, not verified)
Generic data owned and managed by Stichting NMD, used as a fallback. Not verified; an uplift factor is applied to avoid underestimating impacts and to stimulate submission of higher-quality data. Underlying data are publicly available.

Category 3a (external energy carriers, not verified)
Non-brand-specific data for externally supplied energy (electricity, gas, heat, fuels) and forfaitary material-related impacts. Owned and managed by Stichting NMD; no uplift factor is applied. Underlying data are publicly available.

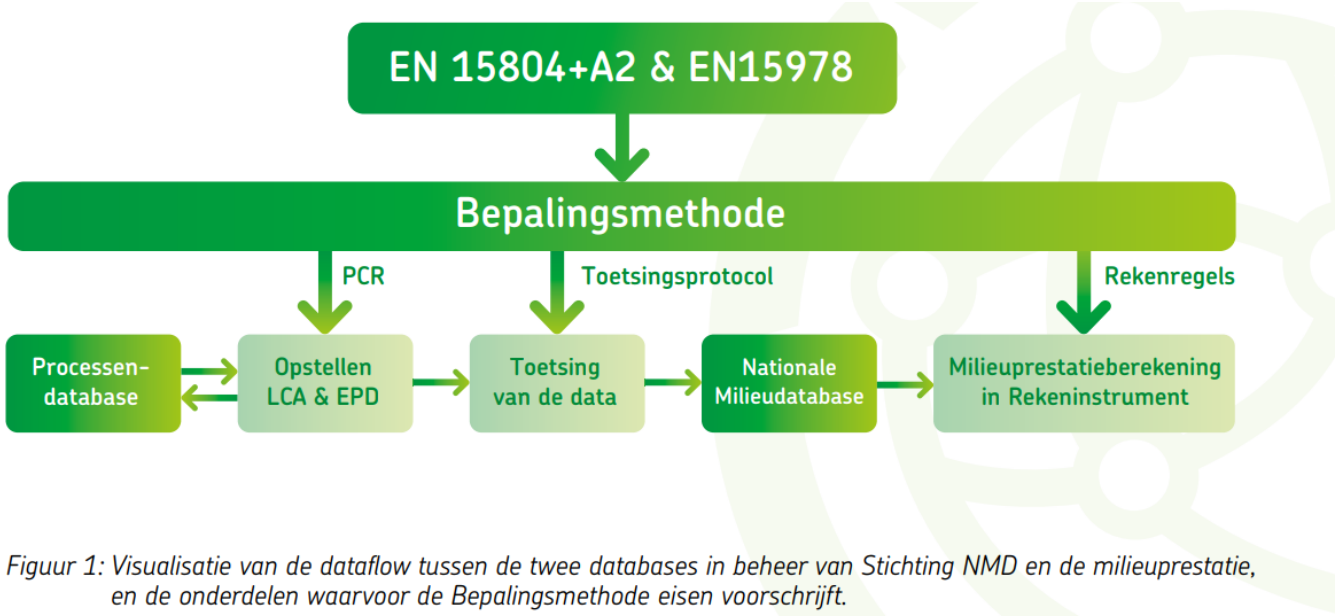

Figuur 1: Visualisatie van de dataflow tussen de twee databases in beheer van Stichting NMD en de milieuprestatie, en de onderdelen waarvoor de Bepalingsmethode eisen voorschrijft.

Figure 26 Visualization of the dataflow for safeguarding the reliability of the calculated EPDs acoording to the determination method (NationaalMilieudatabase, sd)

2.5.2 Environmental Cost indicator

For the determination of the Environmental cost of a product, the government determined shadow costs per impact category that can be used. Currently two sets of shadow costs are available, the A1 set according to the EN15804+A1 and the new extended set A2 based on the EN 15804+A2. The A1 set consists of 11 impact categories while the extended set A2 consists of 19 impact categories as can be seen in Table 6 and .

Table 6 A1 set of shadowcosts according to EN 15804+A1

Milieu-impactcategorie	Equivalent eenheid	Weegfactor (€ / kg equivalent)
Uitputting abiotische grondstoffen (exclusief fossiele energiedragers) – ADP	Sb eq	0.16
Uitputting fossiele energiedragers – ADP	Sb eq	0.16
Klimaatverandering – GWP 100 j.	CO2 eq	0.05
Aantasting ozonlaag – ODP	CFK-11 eq	30
Fotochemische oxidantvorming – POCP	C2H4 eq	2
Verzuring – AP	SO2 eq	4
Vermesting – EP	PO4 eq	9
Humane toxiciteit – HTP	1,4-DCB eq	0.09
Zoetwater aquatische ecotoxiciteit – FAETP	1,4-DCB eq	0.03
Mariene aquatische ecotoxiciteit – MAETP	1,4-DCB eq	0.0001
Terrestrische ecotoxiciteit – TETP	1,4-DCB eq	0.06

Table 7 A2 set of shadowcosts according to EN 15804+A2

Environmental impact categorie	Unit equivalent:	Weighing factor (€/unit equivalent)
GWP (Global Warming Potential) – total	kg CO2-eq	0,116
GWP – fossil	kg CO2-eq	0,116
GWP – biogenic	kg CO2-eq	0,116
GWP – LULUC (Land us and land use change)	kg CO2-eq	0,116
Ozone layer depletion potential	kg CFK11-eq	32
Acidification potential	Mol H+-eq.	0,39
EP (Eutrophication potential)-freshwater	kg P-eq	1,96
EP-marine water	kg N-eq	3,28
EP-terrestrial	Mol N-eq.	0,36
POCP ("smog")	kg NMVOC-eq.	1,22
ADP (Abiotic Depletion Potential)-minerals & metals	kg Sb-eq	0,3
ADP-fossil resources	MJ, net cal. val.	0,00033
Water use	m3 water, world eq. deprived	0,00506
PM (Respiratory inorganics - particulate matter)	kg disease incidence	549750
IR (Ionising radiation)	kg kBq U235-eq	0,049
ETP-FW (Ecotoxicity freshwater)	CTUe	0,00013
HTP-c (Cancer human health effects)	CTUh	1096368
HTP-nc (Non-cancer human health effects)	CTUh	147588
SQP (Land use related impacts. soil quality)	Pt/m2.jaar	0,000087

For this research it has been chosen to make use of the shadow costs according to the set A1. This has been chosen since for the A2 set insufficient literature could be found for the different components of the different variants. Especially for concrete superstructures the readily available information about the sustainability impact that is determined is also based on the A1 set. To have a reliable comparison of the different variants it is therefore essential to make use of the A1 based shadow costs for the (weathering) steel concrete composite variants. The comparison between the variants will be based on the environmental impact only.

2.5.3 Sustainability impact Variant 1 concrete superstructure

The first variant that will be considered is the existing concrete superstructure according to the given case study. For the determination of the Environmental cost of this variant the literature given by Rijkswaterstaat will be used. At Rijkswaterstaat a research has been performed to determine the sustainability impact of concrete bridges based on the span length and the bridge type. There will be made a distinguish between concrete plated superstructures and concrete girder superstructures. From the available data about these bridges in Rijkswaterstaat, the graphs in Figure 27 have been made. The environmental costs of these superstructures are calculated based on the A1 set for shadow costs regarding the sustainability impact. The impact is based on the girder system, including the concrete compressive layer, the pavementing and the edge detail of the superstructure (Thie, 2025).

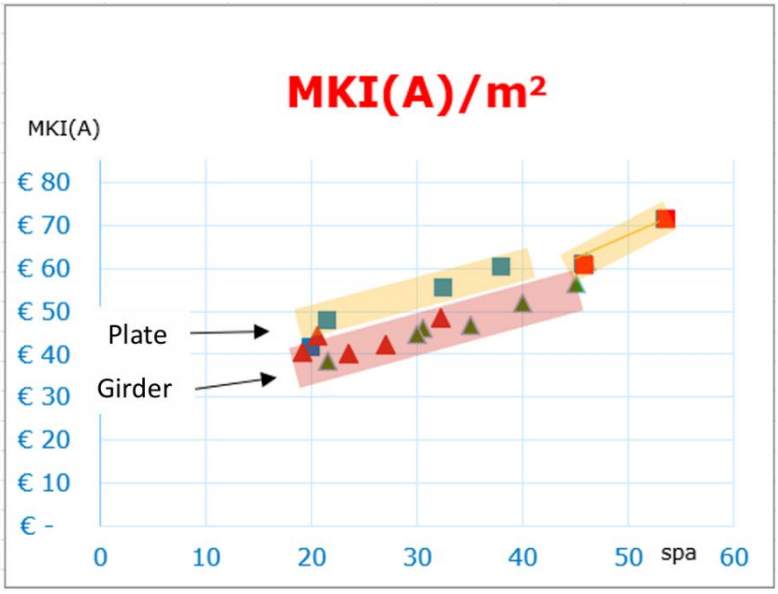

Figure 27 Environmental cost of concrete supertructers per area (Thie, 2025)

To ensure a consistent and comparable sustainability assessment, only the upfront life-cycle stages A1 to A5 are considered in these results. These stages include raw material extraction, production, transport to site, and the construction process. This approach is aligned with current Rijkswaterstaat practice and reflects the fact that 80–90% of the environmental impact of small concrete bridges occurs before the operational phase (Thie, 2025). The use and maintenance stage (B-modules) and End-of-Life stage (C-modules) are therefore excluded from the environmental cost calculation for this variant, as their relative contribution to the total impact is limited and highly project-specific (Thie, 2025).

2.5.4 Sustainability impact Variant 2 conventional steel concrete composite superstructure

This variant consists of 2 mayor components conventional steel beams and reinforced in-situ poured concrete. For the determination of the sustainability impact of this variant EPD's will be used found on the NMD Database and from EPD's found of companies which are operating in the Netherlands.

2.5.4.1 Conventional steel component

For the conventional steel components the EPD'S of the companies Arcelor Mittal and SSAB will be used and also the calculation made by the NMD for construction steel profiles (HEA/HEB/HEM/IPE/UNP) for bridging solutions.

2.5.4.1.1 Conventional steel beams from Arcelor Mittal

ArcelorMittal operates two major steel production facilities in Europe: one in Luxembourg and one in Spain. The Spanish plant produces plated steel products using the conventional blast furnace route, after which the plates are processed into structural profiles. In contrast, the Luxembourg facility manufactures hot-rolled steel profile sections using a 100% electric arc furnace (EAF) powered entirely by renewable energy. This plant uses 100% scrap (X-scrap) as the raw material for steel grades up to S355. Although ArcelorMittal indicates that higher grades such as S460 can also be produced through this route, Dutch regulations currently prohibit on-site welding of these grades. As a result, repairs or modifications during the service life may lead to non-conformities.

For this study, two Environmental Product Declarations (EPDs) from ArcelorMittal are used:

1. The conventional plated steel EPD
2. The XCarb® recycled and renewably produced steel sections EPD

The conventional plated steel EPD reports results for modules A1–A3, C3 and D, and provides values for only 6 of the 11 EN 15804+A1 impact categories, as can be seen in Table 8 . Because the downstream construction modules A4–A5 are missing, this dataset does not allow for a complete MKI (Milieu Kosten Indicator) calculation and therefore cannot be fully compared with the concrete dataset, which includes A1–A5 and all required categories.

In contrast, the XCarb® EPD is based on the EAF process using 100% scrap and renewable electricity and reports all relevant lifecycle stages, including A1–A5, C1–C4 and D, as can be seen in Table 9. Importantly, this EPD also provides all 11 A1-set impact categories, making it complete for MKI calculation. As a result, the XCarb® dataset allows for a full and consistent comparison with the concrete superstructure variant.

Meanwhile, the concrete superstructure data from Rijkswaterstaat also provide all 11 A1-set impact categories and cover modules A1–A5. This means that the XCarb® and concrete datasets are directly comparable on a full MKI basis, whereas the conventional plated steel dataset remains incomplete and cannot be included in a full MKI comparison.

Table 8 Environmental impact of steel profiles made of plates by Arcelor Mittal based on the indicator A1 (ArcelorMittal Europe, 2025)

Parameter	Unit	A1-A3	C3	D	weight factor	Costs A1-A3/ tonne	Costs D/ tonne	Total costs/ tonne
Global warming potential	kg CO2-Eq.	2.60E+03	1.99E+00	-1.80E+03	5.00E-02	1.30E+02	-9.00E+01	€ 40.10
Depletion potential of the stratospheric ozone layer	kg CFC11-Eq.	1.21E-12	4.48E-14	1.12E-11	3.00E+01	3.63E-11	3.36E-10	€ 0.00
Acidification potential of land and water	kg SO2-Eq.	4.76E+00	6.28E-03	-4.21E+00	4.00E+00	1.90E+01	-1.68E+01	€ 2.23
Eutrophication potential	kg PO4-Eq.	4.58E-01	7.23E-04	-3.59E-01	9.00E+00	4.12E+00	-3.23E+00	€ 0.90
Formation potential of tropospheric ozone photochemi	kg Ethene-Eq.	8.93E-02	4.70E-04	-5.47E-02	2.00E+00	1.79E-01	-1.09E-01	€ 0.07
Abiotic depletion potential for non-fossil resources	kg Sb-Eq.	8.08E-05	4.95E-07	4.27E-05	1.60E-01	1.29E-05	6.83E-06	€ 0.00
Abiotic depletion potential for fossil resources	MJ	2.35E+04	2.28E+01	-1.43E+04	0.00E+00	0.00E+00	0.00E+00	€ -
						€ 153.34	**€ -110.18**	**€ 43.29**

Table 9 Environmental impact of hot rolled sections made of 100% X scarp and based on the EAF process by Arcellor Mittal based on the indicator A1 (ArcellorMittal, 2023)

Indicator	Unit	A1-A5	B	C1	C2	C3	C4	D	Weught factor	Total Costs A1-A5/tonne	Costs D/ tonne	Total costs/ tonne
ADPE	kg Sb eq.	1.83E-03	0	1.99E-06	1.80E-05	5.56E-06	1.37E-07	2.33E-05	**0.16**	2.92E-04	3.73E-06	3.00E-04
ADPF	MJ	7.03E+03	0	6.54E+01	1.02E+02	1.83E+01	1.66E+00	1.57E+03	**0**	0.00E+00	0.00E+00	0.00E+00
GWP	kg CO2 eq.	4.63E+02	0	4.72E+00	6.67E+00	1.36E+00	6.55E-02	1.87E+02	**0.05**	2.32E+01	9.35E+00	3.31E+01
ODP	kg CFC11 eq.	4.82E-05	0	7.98E-07	1.21E-06	6.70E-08	1.75E-08	7.45E-06	**30**	1.45E-03	2.24E-04	1.73E-03
POCP	kg ethene eq.	1.58E-01	0	7.69E-04	8.47E-04	1.42E-04	1.73E-05	1.23E-01	**2**	3.16E-01	2.46E-01	5.66E-01
AP	kg SO2 eq.	1.47E+00	0	3.49E-02	1.84E-02	2.96E-03	4.04E-04	5.29E-01	**4**	5.87E+00	2.12E+00	8.21E+00
EP	kg (PO4)3- eq.	1.76E-01	0	7.36E-03	2.27E-03	5.93E-04	6.59E-05	8.15E-02	**9**	1.58E+00	7.34E-01	2.41E+00
HTP	kg DCB eq.	2.68E+02	0	1.52E+00	2.58E+00	1.99E-01	2.29E-02	1.01E+02	**0.09**	2.41E+01	9.09E+00	3.36E+01
FAETP	kg DCB eq.	7.28E+00	0	2.51E-02	7.74E-02	5.25E-03	6.16E-04	-2.44E+00	**0.03**	2.18E-01	-7.32E-02	1.48E-01
MAETP	kg DCB eq.	2.60E+04	0	8.63E+01	2.90E+02	2.11E+01	2.21E+00	-5.69E+03	**0.0001**	2.60E+00	-5.69E-01	2.07E+00
TETP	kg DCB eq.	1.78E+00	0	1.66E-03	8.41E-03	7.11E-03	1.14E-04	-7.03E+00	**0.06**	1.07E-01	-4.22E-01	-3.14E-01
ECI	Euro	5.84E+01	0	5.95E-01	7.01E-01	1.08E-01	7.96E-03	2.06E+01	**0**	0.00E+00	0.00E+00	0.00E+00
ADPF	kg Sb eq.	3.27E+00	0	3.11E-02	4.83E-02	1.02E-02	8.06E-04	1.32E+00	**0.16**	5.23E-01	2.11E-01	7.49E-01
										€ 58.44	**€ 20.68**	**€ 80.54**

The comparison of the two ArcelorMittal EPDs demonstrates that XCarb® recycled and renewably produced steel significantly outperforms conventional plated steel in terms of environmental impact, as shown in Table 8 and Table 9. The plated steel exhibits a total A1–A3 environmental cost of €153.34, whereas XCarb® steel, assessed across the full A1–A5 range, has a markedly lower total cost of €58.44, emphasizing the clear environmental advantage of the EAF route using 100% scrap and renewable electricity.

Although the plated steel benefits from a substantial recycling credit in Module D (–€110.18), due to the EPD's assumption of a 98% recycling rate and the associated avoided emissions from primary steel production, this credit does not offset the higher production impacts (ArcelorMittal Europe, 2025).

In contrast, Module D for XCarb® steel provides no benefit (€20.68) because its end-of-life scrap (880 kg recycled + 110 kg reused) is less than the 1,150 kg of scrap used in production, resulting in a small net load rather than an avoided production credit (ArcellorMittal, 2023).

Overall, when considering the available indicators, included lifecycle modules, and total A1–A5 environmental costs, the XCarb® dataset delivers a substantially lower environmental burden and therefore represents the more sustainable option despite its smaller Module D benefit.

2.5.4.1.2 Conventional steel beams from SSAB

SSAB operates two main production sites in the Nordics Raahe in Finland and Oxelösund in Sweden where hot-rolled steel plates are manufactured primarily from iron ore. Around 20% of scrap steel is also used to lower the environmental impact and improve material efficiency. SSAB continuously optimizes raw material and energy use, achieving some of the world's most efficient blast furnace operations in terms of CO_2 emissions. In addition, by-products and process dust are largely recycled, replacing virgin materials and further enhancing sustainability. In Table 10 the results of the environmental impact analysis are given for the SSAB produced products (SSAB, 2020).

The SSAB steel EPD shows a mixed environmental performance across the available indicators, but its overall result is strongly influenced by the high global warming potential in A1–A3 and the large recycling credit in Module D. As shown in Table 10, the total environmental cost for SSAB steel in modules A1–A3 amounts to €167.48 per tonne, with GWP contributing the largest share (€135.50 per tonne). Module D, however, provides a substantial credit of –€89.05 per tonne, largely due to avoided burdens from scrap recovery, most notably in GWP (–€74.00), resulting in a net total of €78.73 per tonne. A recycling rate of 95% has been assumed used to calculate the amount of net-scrap to be credited in Module D, which results in the high score for module D.It must be noted that the SSAB EPD reports only 6 of the 11 required EN 15804 impact categories and includes only the A1–A3 production stages, making it incomplete for a full MKI calculation and limiting its comparability with datasets such as XCarb® and concrete that include all indicators and the full A1–A5 range.

Table 10 Environmental impact of hot rolled sections made of around 20% of scrap based on the blast furnace process based on the indicator A1 (SSAB, 2020)

Parameter	Acronyms	Unit	Total A1–A3	C3	C4	D	weight factor	Costs A1-A3/ tonne	Costs D/ tonne	Total costs/ tonne
Global warming potential	GWP	kg CO2 eq	2710	2.49	0.744	-1480	0.05	€ 135.50	€ -74.00	€ 61.66
Eutrophication potential	EP	kg PO4 eq	0.63	0.0042	0.0005	-0.217	9	€ 5.67	€ -1.95	€ 3.76
Acidification potential	AP	kg SO2 eq	6.25	0.0176	0.0044	-2.93	4	€ 25.00	€ -11.72	€ 13.37
Photo-oxidant formation potential	POCP	kg ethene eq	0.651	0.002	0.0003	-0.686	2	€ 1.30	€ -1.37	-€ 0.07
Ozone layer depletion potential	ODP	kg CFC-11 eq	1.18E-09	8E-15	4E-15	3E-06	30	€ 0.00	€ 0.00	€ 0.00
Abiotic depletion potential: fossil	ADP-fossil	MJ, net calorifi	26600	48.3	10.4	-14400	0	€ -	€ -	€ -
Abiotic depletion potential: elements	ADP-elements	kg Sb eq	0.0211	3E-06	7E-08	-0.005	0.16	€ 0.00	€ -0.00	€ 0.00
								€ 167.48	**€ -89.05**	**€ 78.73**

2.5.4.1.3 Conventional steel profiles (HEA/HEB/HEM/IPE/UNP)for bridging solutions in the Netherlands based on the NMD

Steel structural profiles (HEA, HEB, HEM, IPE, UNP) are produced from hot-rolled structural steel and are represented in the National Environmental Database (NMD) under declaration #nmd_90901, published on 16 June 2022 and updated on 14 August 2025 (NationaalMilieudatabase, sd). This environmental declaration, issued by Stichting Nationale Milieudatabase, reports environmental costs of €0.21 per kilogram for a lifespan

of 100 years (excluding additive of €0.07 per kg). The data used are Category 3 generic datasets, based on average European production and transport distances of approximately 470 km. Installation is assumed to involve lifting and welding equipment, while corrosion is considered negligible due to common surface protection, which is not included in this declaration.

Table 11 Environmental impact of hot rolled sections determined by the NMD based on average european production based on the indicator A1

Impactcategorie	unit	Fase A Productie & Bouw	Fase B Gebruik	Fase C Sloop & Verwerking	Module D Buiten levenscyclus	Weegset (€/eenheid)	costs A1-A5 / tonne	costs D / tonne	Total costs / tonne
Uitputting van abiotische grondstoffen, ex. fossiele	kg antimoon	3.53E-05	-	2.05E-06	-2.96E-08	1.60E-01	€ 0.01	€ -0.00	€ 0.01
Uitputting van fossiele	kg antimoon	8.36E-03	-	2.61E-03	-2.53E-04	1.60E-01	€ 1.34	€ -0.04	€ 1.72
Klimaatverandering	kg CO2	1.19E+00	-	3.93E-01	-4.09E-02	5.00E-02	€ 59.55	€ -2.05	€ 77.17
Ozonlaagaantasting	kg CFK-11	1.37E-07	-	6.70E-08	-1.43E-09	3.00E+01	€ 0.00	€ -0.00	€ 0.01
Fotochemische oxidantvorming	kg ethyleen	8.18E-04	-	3.58E-04	-8.89E-05	2.00E+00	€ 1.64	€ -0.18	€ 2.17
Verzuring	kg SO2	6.00E-03	-	2.82E-03	-1.38E-04	4.00E+00	€ 24.00	€ -0.55	€ 34.71
Vermesting	kg PO4	1.19E-03	-	6.12E-04	-1.64E-05	9.00E+00	€ 10.72	€ -0.15	€ 16.08
Humaan-toxicologische effecten	kg 1,4-	6.17E-01	-	1.67E-01	-2.56E-02	9.00E-02	€ 55.53	€ -2.30	€ 68.25
Ecotoxicologische effecten, aquatisch (zoetwater)	kg 1,4-dichloorbenzeen	3.82E-02	-	2.56E-03	3.17E-04	3.00E-02	€ 1.14	€ 0.01	€ 1.23
Ecotoxicologische effecten, aquatisch (zoutwater)	kg 1,4-dichloorbenzeen	5.06E+01	-	9.45E+00	2.65E-01	1.00E-04	€ 5.06	€ 0.03	€ 6.03
Ecotoxicologische effecten,	kg 1,4-	7.30E-02	-	4.62E-04	2.14E-03	6.00E-02	€ 4.38	€ 0.13	€ 4.54
			-				**€ 163.37**	**€ -5.10**	**€ 211.91**

The NMD dataset for hot-rolled steel sections is fully comparable with both XCarb® and the concrete dataset because it reports all 11 EN 15804 impact categories and covers the complete A1–A5 and C–D lifecycle. As shown in Table 11, its A1–A5 environmental cost is €163.37 per tonne, which is substantially higher than both the XCarb® steel (€58.44) and the concrete variant. Module D provides only a small credit (–€5.10 per tonne), which is far lower than the strong recycling credit reported for SSAB (–€89.05 per tonne). As a result, the NMD steel ends up with the highest net environmental cost among the assessed steel options, reflecting the higher impacts of its conventional production route despite its methodological completeness.

2.5.4.2 Painting of the steel component

For conventional steel an extra zinc layer is needed for the protection of the steel against corrosion. Two types of MKI calculations will be used the first one will be done by making use of the EPD found on the NMD and the second one is by making use the made calculation nota by Rijkswaterstaat to determine the environmental impact of painting of steel structures.

The environmental declaration #nmd_94250 for the construction product *Constructieprofiel, zink conservering, staal* was published on 22 February 2024 and last updated on 14 August 2025 in the National Environmental Database (NMD) (NationaalMilieudatabase, sd). Issued by Stichting Nationale Milieudatabase, this Category 3 declaration reports environmental costs of €7.255 per kilogram for a 100-year lifespan. The product represents a steel construction profile with a zinc coating applied for corrosion protection, typically used in civil engineering applications. The declaration accounts for variable coating thicknesses ranging from 10 µm to 900 µm, with a standard thickness of 314 µm, corresponding to approximately 1.8 kg of zinc per square metre of steel surface.

The environmental assessment of zinc-painted steel sections, based on the NMD dataset, is methodologically complete, covering all 11 EN 15804 impact categories and considering all lifecycle phases (A1–A5, B, C) as well as Module D. The use phase (B) contributes the highest share of the environmental burden (€2.65/m^2), followed by the production and construction phase (A1–A5) at €2.03/m^2, while the end-of-life phase (C) adds €0.93/m^2. Module D provides only a minimal credit of –€0.03/m^2, indicating limited avoided impacts through recycling. Overall, the total net environmental cost of €5.57/m^2 reflects the significant impacts of zinc coating across multiple categories, with both production and use phases driving the majority of the environmental burden, while the recycling benefits remain small.

Table 12 Environmental impact of zinc painting of steel sections based on the NMD for indicator A1 (NationaalMilieudatabase, sd)

Impactcategorie	Fase A (Productie & Bouw)	Fase B (Gebruik)	Fase C (Sloop & verwerking)	Module D (Buiten levenscyclus)	Weegset (€/eenheid)	Total costs (€/m2)	sum/m2
Uitputting van abiotische grondstoffen, ex. kg antimon	0.1195	0.00007758	0.00003162	-0.0000002	0.16	€ 0.02	€ 0.02
Uitputting van fossiele energiedragers kg antimon	0.09479	0.1107	0.04493	-0.001705	0.16	€ 0.04	€ 0.04
Klimaatverandering kg CO2	12.15	20.1	11.58	-0.2763	0.05	€ 2.18	€ 2.18
Ozonlaagaantasting kg CFK-11	9.636E-07	0.000001958	0.000001038	-9.623E-09	30	€ 0.00	€ 0.00
Fotochemische oxidantvorming (smog) kg ethyleen	0.1396	0.2962	0.004756	-0.0006003	2	€ 0.88	€ 0.88
Verzuring kg SO2	0.06395	0.06839	0.02661	-0.0009344	4	€ 0.63	€ 0.63
Vermesting kg PO4	0.00944	0.01422	0.005702	-0.0001109	9	€ 0.26	€ 0.26
Humaan-toxicologische effecten kg 1,4-dichloorbenzeen	7.514	6.174	1.552	-0.1726	0.09	€ 1.36	€ 1.36
Ecotoxicologische effecten, aquatisch (zoet) kg 1,4-dichloorbenzeen	0.6827	0.9446	0.1693	0.002142	0.03	€ 0.05	€ 0.05
Ecotoxicologische effecten, aquatisch (zout) kg 1,4-dichloorbenzeen	661.2	461.6	298.3	1.79	0.0001	€ 0.14	€ 0.14
Ecotoxicologische effecten, terrestrisch kg 1,4-dichloorbenzeen	0.1163	0.01212	0.004947	0.01443	0.06	€ 0.01	€ 0.01
Netto MKI (€)	**€ 2.03**	**€ 2.65**	**€ 0.93**	**€ -0.03**	-	**€ 5.57**	**€ 5.57**

In the LCA of the corrosion protection used for steel members is stated that the painting should have a lifespan of at least 25 years. For a structure which will have a lifespan of 100 years and will be subjected to atmospheric corrosion at least two small maintenance moments and one more thorough maintenance moment will be taken int account in the LCA. Eventually the MKI and the lifespan of the structure will be combined to a MKI per m^2 per lifespan (Rijkswaterstaat, 2022).

For structures placed in atmospheric locations, different types of corrosion protection can be used, including painting systems, hot-dip galvanizing, thermal spraying, duplex systems with galvanizing and painting, or thermal spraying with painting. For fatigue-prone structures, such as traffic bridges, only the painting system is allowed, as it is the only protection that permits nondestructive inspection of fatigue-critical parts. While it is technically possible to apply the painting system only to fatigue-prone areas and another system elsewhere, the efficiency of such a hybrid approach is disputable (Rijkswaterstaat, 2022)

The environmental assessment of the painting system, based on the generic LCA underlying the Rijkswaterstaat matrices, is methodologically complete, including all relevant impact categories and considering the full expected lifespan of the structure (100 years) through scheduled maintenance (Rijkswaterstaat, 2022). The reported MKI of €3.35/m^2 , as can be seen in Table 13, includes the production phase (A1–A3) and the use/maintenance phase (B), covering two small maintenance events and one major maintenance over the lifespan. End-of-life impacts (C) and Module D credits are not included. Overall, the MKI highlights that production and maintenance dominate the environmental burden, while the coating system ensures a long service life, enabling the calculation of a MKI per m^2 per lifespan to support sustainable decision-making.

Table 13 properties of the painting system :Wet paint, including maintenance (Rijkswaterstaat, 2022)

Painting system ***including 2 small maintenances and one big maintenance***	
Lifespan (according to LCA)	100 years
MKI[euros/m^2]	3.35
MKI per year[euros/m^2/year][Lifespan =25-40 year]	0.044-0.071
MKI per year[euros/m^2/year][Lifespan =100 year]	0.035

2.5.4.3 *Reinforced Concrete component*

For the concrete component of the composite bridges, the environmental assessment is based on the NMD Environmental Product Declaration #nmd_201627 for Betonmortel C35/45 (CEM IIIB), which reports a total MKI of €27.66 per m^3 over a 100-year service life. The assessment is methodologically complete, including all relevant impact categories and accounting for the full production and construction phase (A1–A5), the use phase (B), and end-of-life disposal and recycling contributions (C and Module D). As shown in Table 14, the production phase dominates the environmental burden (€24.34/m^3), while the use phase is not quantified, and Module C and D provide a small net credit (–€1.34/m^3). Overall, the concrete component exhibits a substantial environmental impact over its service life, driven primarily by its production, and the MKI per cubic meter provides a clear basis for comparison with other structural materials such as reinforced steel or painted steel profiles.

Table 14 Environmental impact of *Concrete C35/45 (o.b.v. CEM IIIB), 2438.7 kg/m* based on the NMD for indicator A1

Impactcategorie	Fase A Productie- & Bouw	Fase B Gebruik	Fase C Sloop- en verwerking	Module D Buiten levenscyclus	Weegset (€/eenheid)	Total costs (€/m3)
Uitputting van abiotische grondstoffen , ex... (kg antimoon)	0.002457	-	0.0004775	-0.0005301	0.16	€ 0.00
Uitputting van fossiele energiedragers (kg antimoon)	1.115	-	0.2959	-0.07018	0.16	€ 0.21
Klimaatverandering (kg CO2)	220.2	-	41.82	-10.39	0.05	€ 12.58
Ozonlaagaantasting (kg CFX-11)	0.00001756	-	0.000007139	-0.000000906	30	€ 0.00
Fotochemische oxidantvorming (smog) (kg ethyleen)	0.1308	-	0.01887	-0.00768	2	€ 0.28
Verzuring (kg SO2)	0.9501	-	0.1794	-0.05903	4	€ 4.28
Vermesting (kg PO4)	0.1423	-	0.03685	-0.009619	9	€ 1.53
Humaan-toxicologische effecten (kg 1,4-dichloorbenzeen)	79.99	-	14.47	-4.81	0.09	€ 8.07
Ecotoxologische effecten, aquatisch (zoet...) (kg 1,4-dichloorbenzeen)	1.233	-	0.3452	-0.07461	0.03	€ 0.05
Ecotoxologische effecten, aquatisch (zout...) (kg 1,4-dichloorbenzeen)	5281	-	1209	-309.9	0.0001	€ 0.62
Ecotoxologische effecten, terrestrisch (kg 1,4-dichloorbenzeen)	0.6321	-	0.09934	-0.02502	0.06	€ 0.04
Netto MKI (€)	**€ 24.34**	**-**	**€ 4.66**	**-€ 1.34**	**-**	**€ 27.66**

For the reinforcement steel used in the study, environmental impacts are assessed based on Holterman B500B steel, sourced primarily from recycled European steel and processed at facilities in Hooge Zwaluwe and Markelo. The LCA focuses on the production of prefabricated reinforcement elements widely used in structural applications such as bridge girders, retaining walls, and floor slabs. The reported total environmental cost amounts to €119.70 per tonne , as can be seen in Table 15,with the vast majority arising from the production phases A1–A3 (€114.20/tonne, approximately 95%). It must be noted that this assessment does not include the full A1–A5 lifecycle, and Module D credits are not considered, so recycling and end-of-life benefits are omitted. Phases C2–C4 contribute only marginally to the total. Overall, while Holterman reinforcement steel benefits from using recycled inputs, the environmental burden is dominated by production, and the limited scope of the LCA means it is not fully comparable with datasets that report all lifecycle stages, such as the NMD concrete or XCarb® steel datasets.

Table 15 Environmental Impact reinforcement steel made by Holterman based on indicator A1

Fase	Total costs/tonne	Bijdarage(%)
A1	€ 106.60	89
A2	€ 2.90	2
A3	€ 4.70	4
C2	€ 0.80	1
C3	€ 4.70	4
C4	€ 0.04	0.03
Module D	€ -	0
totaal	**€ 119.70**	100

For reinforcement steel, the NMD dataset #nmd_45791 provides a comprehensive environmental assessment for typical use in concrete structures, including loose bars and prefabricated meshes, commonly applied in civil engineering works such as viaducts and foundations. The reported total environmental cost is €146.85 per tonne ,excluding supplements for a 100-year lifespan, as can be seen in Table 16. This assessment includes all relevant life cycle phases: production (A1–A5), use/maintenance (B), end-of-life (C), and accounts for beyond-life-cycle credits (Module D). Production (A1-A5) dominates the environmental impact, particularly in terms of climate change, human toxicity, and fossil fuel depletion, with a total costs of €163.03 per tonne. While the use and end-of-life phases contribute only marginally to the total. Module D provides a small credit due to material recovery. Compared to the Holterman LCA, this dataset covers the full lifecycle and Module D, making it more methodologically complete and fully comparable to other NMD-based materials such as the concrete superstructure or painted steel profiles.

Table 16 Environmental Impact reinforcement steel based on the NMD based on indicator A1

Impactcategorie	Eenheid	Fase A Productie & Bouw	Fase B Gebruik	Fase C Sloop & Verwerking	Module D Buiten levenscyclus	Weegset (€/eenheid)	Total costs/tonne
Uitputting van abiotische grondstoffen, ex. fossiele energiedragers	kg antimoon	9.69E-03	-	1.39E-03	-1.27E-04	1.60E-01	€ 0.00
Uitputting van fossiele energiedragers	kg antimoon	8.98E+00	-	1.91E-01	-1.08E+00	1.60E-01	€ 1.29
Klimaatverandering	kg CO2	1.22E+03	-	2.82E+01	-1.75E+02	5.00E-02	€ 53.64
Ozonlaagaantasting	kg CFK-11	9.18E-05	-	3.88E-06	-6.10E-06	3.00E+01	€ 0.00
Fotochemische oxidantvorming (smog)	kg ethyleen	1.32E+00	-	2.37E-02	-3.81E-01	2.00E+00	€ 1.92
Verzuring	kg SO2	4.85E+00	-	2.47E-01	-5.93E-01	4.00E+00	€ 18.01
Vermesting	kg PO4	6.98E-01	-	3.28E-02	-7.04E-02	9.00E+00	€ 5.94
Humaan-toxicologische effecten	kg 1,4-dichloorbenzeen	7.05E+02	-	2.93E+01	-1.10E+02	9.00E-02	€ 56.26
Ecotoxicologische effecten, aquatisch (zoetwater)	kg 1,4-dichloorbenzeen	2.29E+01	-	5.69E-01	1.36E+00	3.00E-02	€ 0.74
Ecotoxicologische effecten, aquatisch (zoutwater)	kg 1,4-dichloorbenzeen	4.83E+04	-	2.40E+03	1.14E+03	1.00E-04	€ 5.18
Ecotoxicologische effecten, terrestrisch	kg 1,4-dichloorbenzeen	5.48E+01	-	9.36E-02	9.15E+00	6.00E-02	€ 3.85
Netto MKI (€)		**€ 163.03**	-	**€ 5.67**	**-€ 21.85**	-	**€ 146.85**

2.5.5 Sustainability impact Variant 3 weathering steel concrete composite superstructure

This variant consists of two main components: weathering steel beams and in-situ poured reinforced concrete. The concrete component is identical to that used in Variant 2; therefore, the previously determined environmental impact from Variant 2 can also be applied here.

For the weathering steel component, only one manufacturer in Luxembourg produces weathering steel suitable for this application, ArcelorMittal, as previously mentioned. According to ArcelorMittal, the same Environmental Product Declarations (EPDs) used for conventional structural steel also apply to weathering steel. Therefore, the sustainability impact of the weathering steel can be assessed using the same EPD data as applied in Variant 2, see paragraph 2.5.4. The main advantage of weathering steel lies in its elimination of the need for surface painting or coating, which represents a significant reduction in environmental impact compared to conventionally painted steel structures.

2.5.6 Conclusion sustainability analysis

Overall, the environmental assessment is based on lifecycle stages A1–A5, because Variant 1, the fully concrete superstructure, considers these stages and all 11 EN 15804 impact categories. To ensure a consistent and fully comparable analysis, all other variants are evaluated on the same basis. This approach captures the major environmental impacts, as A1–A5 are the dominant contributors in the superstructure.

For Variant 1, conventional reinforced concrete is assessed, covering A1–A5 and all impact categories. This ensures that the main environmental burdens from production are captured, providing a robust baseline for comparison.

For Variant 2, XCarb® recycled steel is selected for the structural beams because it significantly reduces production impacts compared to conventional steel and is fully covered across all 11 impact categories, including all A1–A5 stages. Secondly also the EPD for NMD profile steel will also be considered, since this is also a methodologic complete EPD and shows the general burden of steel profiles in the Dutch context. NMD zinc-painted steel is used for corrosion protection, providing a methodologically complete assessment, and NMD concrete and NMD reinforcement steel are included. Only A1–A5 stages are considered to maintain full comparability across all variants.

Module D credits for the steel components show high variability: XCarb® steel has a modest credit of €20.68/t because its end-of-life scrap (880 kg recycled + 110 kg reused) is less than the 1,150 kg used in production, resulting in a small net load. SSAB steel has –€89.05/t, plated steel –€110.18/t due to high recycling rates (95–98%) and avoided primary steel production, and NMD steel –€5.10/t. This wide variation highlights that Module D credits should always be carefully reviewed, as differences in assumptions can give a distorted picture of environmental performance. The comparison of all Module D values for the steel profiles is given in Figure 28.

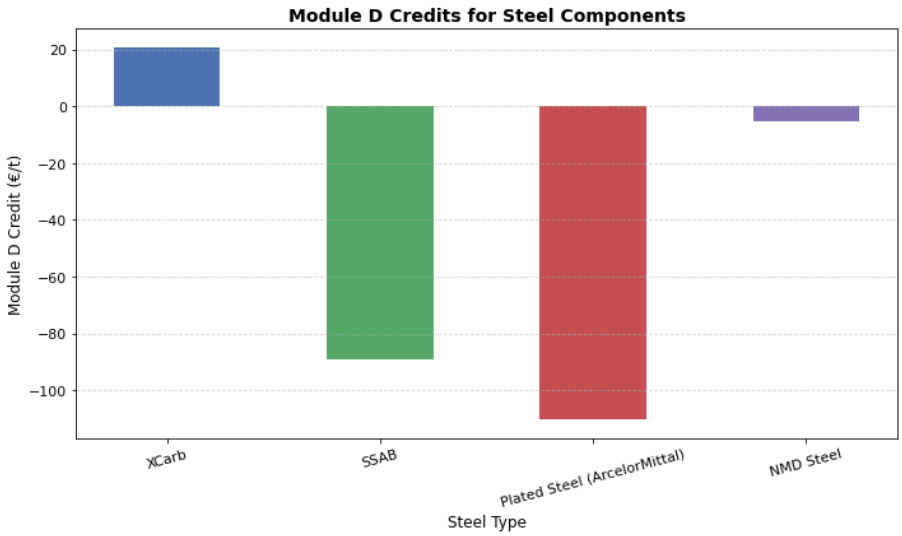

Figure 28 Module D components for the steel components

XCarb® clearly shows the lowest A1–A5 environmental cost (€58.44/t), outperforming all other steel options, and provides a substantial sustainability advantage.

Variant 3 is identical to Variant 2 in terms of materials XCarb® steel/NMD steel, NMD concrete, and NMD reinforcement steel, but excludes painting due to the use of weathering steel. This eliminates coating-related impacts, providing an additional sustainability benefit while remaining directly comparable on an A1–A5 basis.

II Structural analysis

3 Methodology of structural analysis

For the structural analysis, a specific methodology will be applied to determine the cross-sectional dimensions of the superstructure. These dimensions will be established for a case study provided by Rijkswaterstaat. The structural analysis consists of two main parts: Modelling Sequences and Design Calculations. The objective is to design different variants of the bridge deck by varying key parameters. See Figure 29 for the schematical breakdown of this chapter.

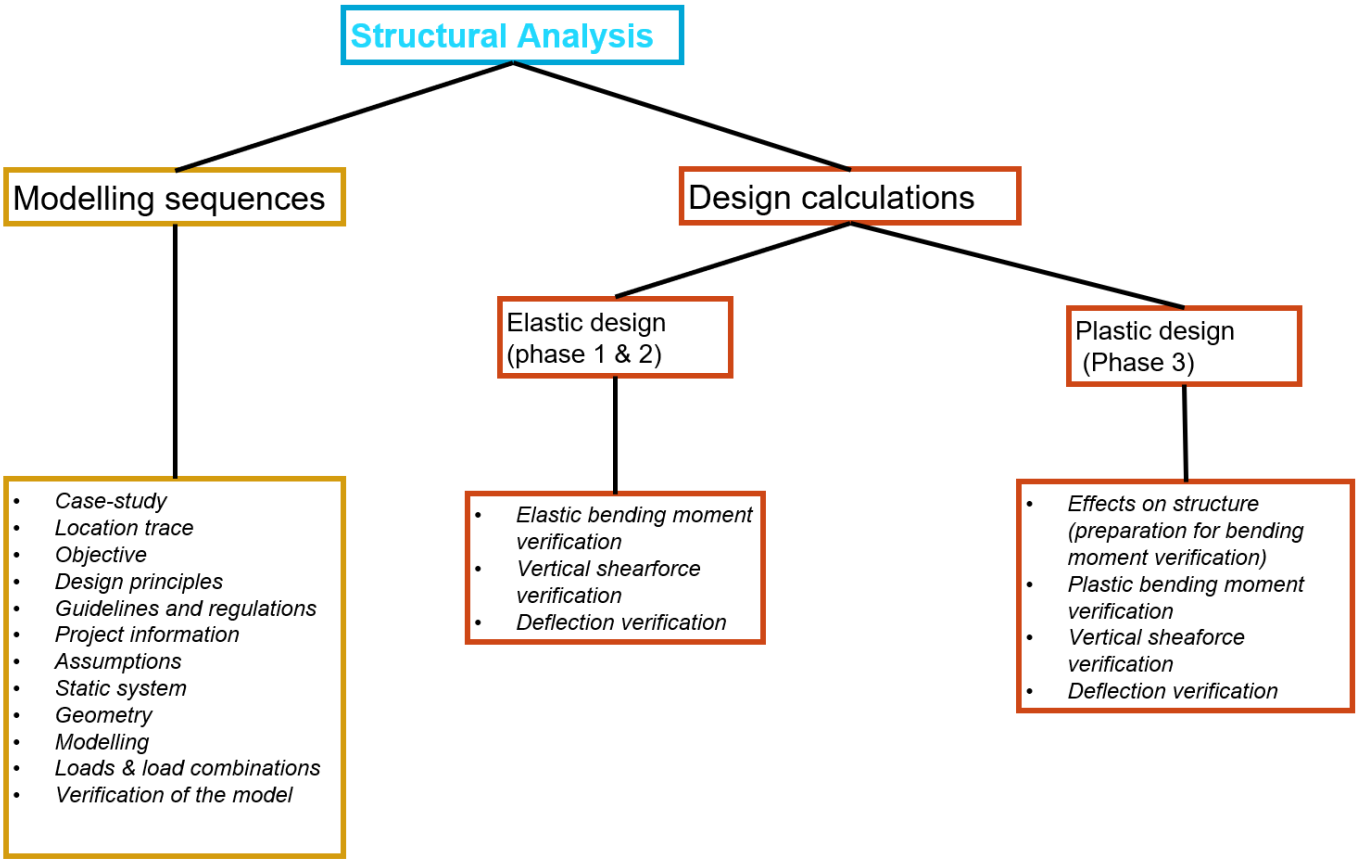

Figure 29 Structure of Structural analysis

In the Modelling Sequences, the case study will be introduced, and all assumptions, boundary conditions, and regulations used in the structural analysis will be discussed. The aim of this section is to clearly define the design and modelling parameters.

In the Design Calculations, the bridge's design resistances will be determined in accordance with the relevant Eurocodes. These resistances will be verified against the acting effects at the governing locations, identified through an RFEM model that complies with the applicable Eurocode standards.

The main objective of the structural analysis is to determine the cross-sectional dimensions of both the composite weathering steel–concrete bridge and the conventional steel–concrete bridge for the given case study. Several variants will be analyzed, differing in the centre-to-centre spacing of the (weathering) steel beams, the selected steel profiles, and the (weathering) steel grades used for the beams.

4 Modelling sequences

4.1 Description case-study

The Leenderheide junction, located in the south of the Netherlands, consists of four interconnected junctions. Originally constructed in 1975, these structures feature bridge decks made of inverted reinforced concrete T-beams topped with a concrete compression layer. The decks are connected to the abutments using half-joint connections. In 2009, a reassessment of the bridges confirmed that the bridge decks still met all safety requirements. However, the half-joint connections showed signs of concrete deterioration, primarily due to water infiltration.

Currently, a weight restriction is in place on the bridge, prohibiting heavy traffic. To extend the service life of the structure, it has been decided to strengthen the half-joint connections and investigate the feasibility to implement a more sustainable, lightweight superstructure. As part of this strategy, the feasibility of a weathering steel–concrete composite superstructure is being investigated.

This case study focuses on an existing bridge in need of renovation. The goal is to develop a solution that extends the lifespan of the structure. Since half-joint connections are common in the Netherlands, the insights gained from this master's thesis may also be applicable to other bridges with similar structural characteristics across the country.

4.2 Location Trace

Leenderheide is a village in the south of the Netherlands, close to the borders with Belgium as can be seen in Figure 31. In Figure 30 the trace is given, where the 4 junctions are situated.

Figure 31 Location Leenderheide junction

Figure 30 Trace Leenderheide junctions

4.3 Objective

The objective of this chapter is to define the constrains and boundary conditions which should be taken into account when designing the superstructure of the Leenderheide junction. Also a first model in RFEM is made of the superstructure consisting of composite (weathering) steel beams and a concrete deck. The first iteration of the dimensions of the weathering steel beams and the concrete deck will be performed by making use of the dimensions which were given as output on the Acrobi software given by ArcelorMittal, see the calculations performed in ANNEX A Acrobi calculations.

4.4 Design principles

4.4.1 Design demands Rijkswaterstaat

Within Rijkswaterstaat, the primary objective is to preserve the integrity of the substructure while replacing the superstructure. In the Netherlands, it is common to utilize bridges for crossing highways or rivers, due to the predominant flat surface of the Netherlands this results in embankments with abutments, as illustrated in Figure 32. Preserving this substructure is imperative to minimize disruption and costs. Therefore, the design of the composite weathering steel-concrete superstructure should ensure that its height is equal to or smaller than that of the existing structures. Opting for a smaller height would be more advantageous from a sustainability perspective, requiring only minimal elevation adjustments to the substructure. Conversely, if the new structure's height exceeds that of the existing one, the entire embankment would need to be elevated, which is less preferable.

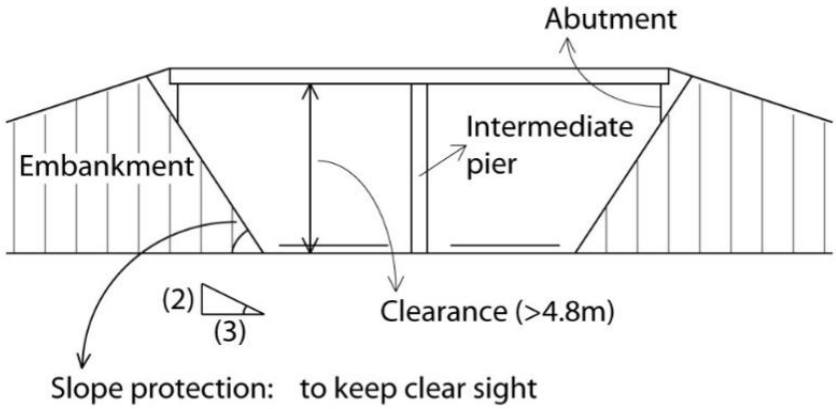

Figure 32 Example road crossing

4.4.2 Project main-boundaries

- The design should be conducted for a nominal design lifetime of 100 years.
- The structure has been classified to be in line with CC3.
- Only the deck of the Leenderheide junction will be considered in the final design. The existing abutment and support of the decks that will be designed are assumed to satisfy all the safety and durability guidelines.

Table 17 Durability classes

Part	Durability class
upper	XD3, XC4,XF4
Side	XD3, XC4,XF4
below	XD3, XC4,XF4

XD3 Wisselend nat en droog
XC4 Wisselend nat en droog
XF4 Verzadigd met water, met dooizouten of zeewater

Table 18 Minimum coverage

Minimum coverage [mm]	
Construction class	**XD3**
S3	40

4.5 Guidelines and regulations

The design of the proposed weathering steel–concrete composite superstructure was carried out in accordance with the Eurocodes and supplementary national and international guidelines. Eurocode 0 defines the fundamental principles for structural safety and load combinations, while Eurocode 1 specifies the actions on the structure, including permanent and traffic loads relevant for bridge design.

Eurocode 2 was applied solely to determine the strain effects due to creep in the concrete deck. Eurocode 3 provides the rules for the design and verification of the steel components. Eurocode 4 serves as the primary code for the design of the composite superstructure, defining the interaction between steel and concrete and the relevant verification methods. The ROK 2021 guidelines complement these Eurocodes by providing Dutch-specific boundary conditions and design requirements for civil structures.

In addition, several special guidelines and standards were consulted: EN 1337 for bridge bearings, EN 1090 for fabrication and execution of steel structures, EN ISO 5817 and EN ISO 15613 for welding quality and procedures, and EN ISO 12944-3 for corrosion protection. The ECCS European Design Guide for the Use of Weathering Steel in Bridge Construction (2021) and the Uncoated Weathering Steel Reference Guide (2022) provided additional guidance specific to the material properties, detailing, and durability performance of weathering steel in bridge applications.

Table 19 Guidelines and Regulations according to Eurocode

Eurocode 0 - Grondslagen		
NEN-EN 1990	Grondslagen van constructief ontwerp	2021
NEN-EN 1990/NB	Grondslagen van constructief ontwerp	2019
NEN-EN 1990-2	Beoordeling van bestaande constructies	2024

Eurocode 1- Belastingen		
NEN-EN 1991-1-2	Deel 1-1: Algemene belastingen	2021
NEN-EN 1991-1-2/NB	Deel 1-1: Algemene belastingen	2019
NEN-EN 1991-2	Deel 2: verkeersbelasting op bruggen	2021
NEN-EN 1991-2/NB	Deel 2: verkeersbelasting op bruggen	2019
Eurocode 2- Betonconstructies		
NEN-EN 1992-2	Deel 2: Ontwerp en berekening van betonconstructies-betonnen bruggen-regels voor ontwerp, berekening en detaillering	2011
NEN-EN 1991-2/NB	Deel 2: Ontwerp en berekening van betonconstructies-betonnen bruggen-regels voor ontwerp, berekening en detaillering	2016
Eurocode 3- Staalconstructies		
NEN-EN 1993-1-11	Deel 1-11: op trek belaste componenten	2011
NEN-EN 1993-1-11	Deel 1-11: op trek belaste componenten	2024
NEN-EN 1993-1-5	Plaatconstructies	
NEN-EN 1993-1-8	Verbindingen	
NEN-EN 1993-1-9	Vermoeiing	
NEN-EN 1993-1-10	Materiaaltaaiheid en eigenschappen over de dikte	
Eurocode 4- Staal-betonconstructies		
NEN-EN 1994-2	Deel 2: Algemene regels en regels voor bruggen	2024
NEN-EN 1994-2	Deel 2: Algemene regels en regels voor bruggen	2011

Table 20 Guidelines and regulations according to ROK

ROK		
ROK_v2.0	Richtlijnen ontwerp Kunstwerken	2021

Table 21 Special guidelines and regulations

Special guidelines and regulations	
EN 1337	Bearings
EN1090	Fabrication
EN 1990	Basis of structural design
EN ISO 5817	Welds
EN ISO 12944-3	Corrosion protection
EN ISO 15613	Welding
ECCS 2nd edition	European design guide for the use of weathering steel in bridge construction 2021
Uncoated Weathering Steel Reference Guide-USA	Uncoated Weathering Steel Reference Guide-USA 2022

4.6 Available project information

- Reassesment junctions Leenderheide 26-nov 2009 (Stroo, 2009)
- Reassesment junctions knooppunt Leenderheide 26-nov 2009, bijlage 6 (Stroo, 2009)
- As-built drawings Leenderheide, 1975

4.7 Assumptions

- All 4 decks of the junctions are in need of replacement. However for the calculation the governing deck is taken to be considered. This is the deck where the highest load should be considered at the edge of the deck. As can be seen in Figure 35. This is the deck without a guiding system. Since this deck will be loaded at the edge of the structure.
- No dynamic effects will be considered
- Only the superstructure will be considered
- Fatigue will not be considered (see 2.3.1 for explanation)
- Cross-beams are not included, as the transverse stiffness of the simply supported composite structure is assumed to be sufficient.

4.8 Static system to be considered

The statical system that will be considered is given in Figure 33. From this static system only the part from K5-k6 will be applicable for the design of the superstructure. Since the existing abutment will be kept and if needed reinforced. The connection between the abutment and the superstructure is a half-joint connection as can be seen in Figure 34 the superstructure will be placed on both sides on the half-joint connection and is free in moving in x and y direction, therefore it can be schematized as a simply supported structure. As can be seen in Figure 33, in the existing recalculations of the bridge the superstructure is also schematized as a simply supported structure.

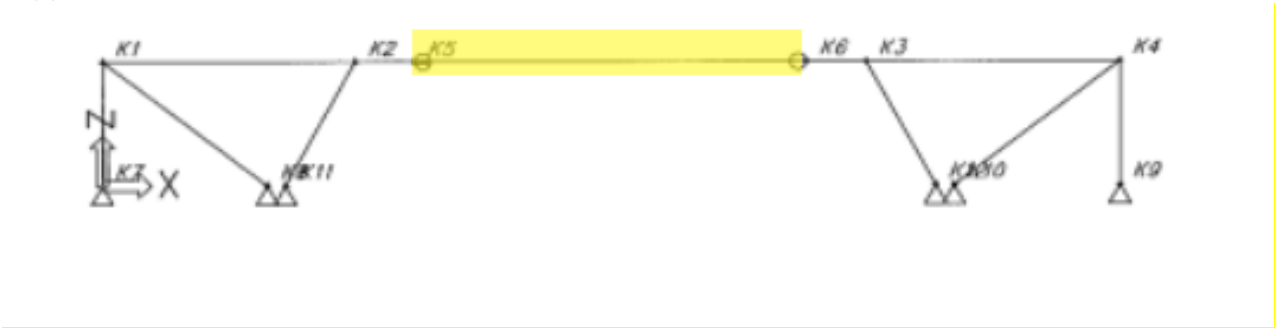

Figure 33 Static system to be considered

4.9 Geometry existing structure

In this paragraph the geometry is given of the existing structure. The objective will be to design a composite weathering steel-concrete superstructure which fits in the existing structure. The span length of the structure should be 21.5m and the width should be 14.4m. The superstructure will be placed on the existing half-joint connection, with an available height of 960 mm. The ideal situation will be if the composite structure will have a height which is smaller or equal than the available height. In Table 22 the assumed weight of the total structure is determined, considering the total area of the deck = 14.4 [m] * 21.5 [m] = 310 m^2, a total weight of 1.3 t/m^2 can be calculated.

Table 22 Assumption of the weight of the existing bridge according to the cross section drawing.

Component	Quantity	Dimensions (mm)	Length (m)	Volume (m^3)	Unit Weight (kN/m^3)	Weight (kN)	Weight (t)
RZ 800×980 Inverted T-Beams	14 pcs	Overall depth: **980 mm** Flange width: **800 mm** Web thickness: **120 mm** Flange thickness**: 200 mm**	21.5	≈ 9.9	25	2376	**242 t**
Reinforced Concrete Deck	1 pc	14.4 × 21.5 × 0.20 m	—	61.9	25	1548	**158 t**
TOTAL STRUCTURE	—	—	—	**≈ 71.8**	—	**3924 kN**	**≈ 400 t**

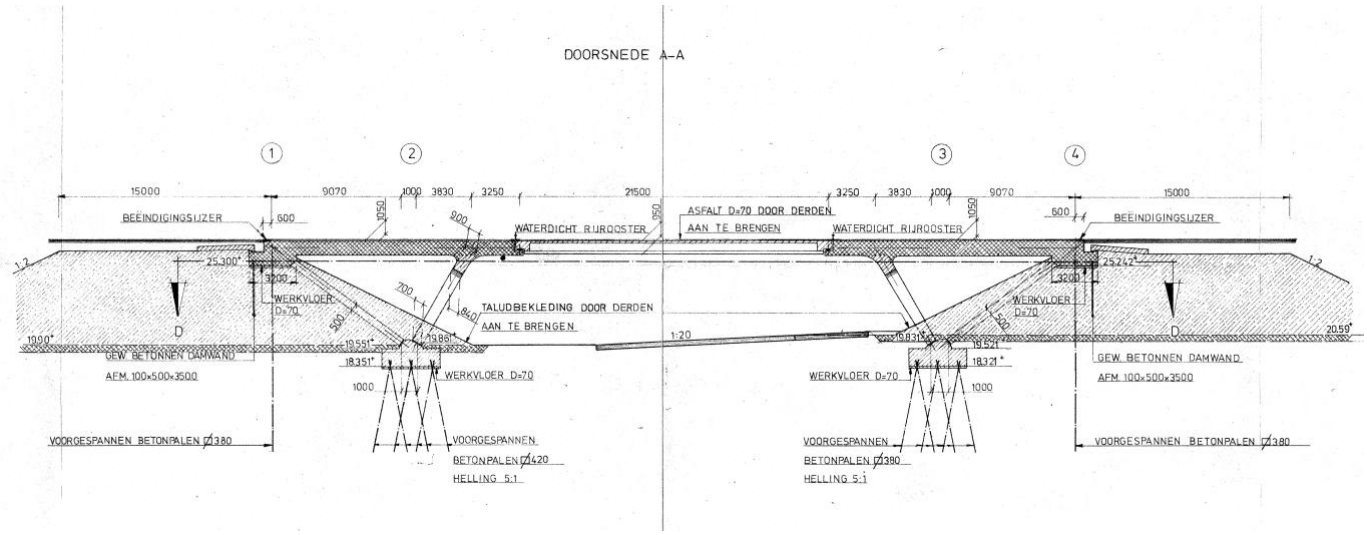

Figure 34 side view Leenderheide bridge

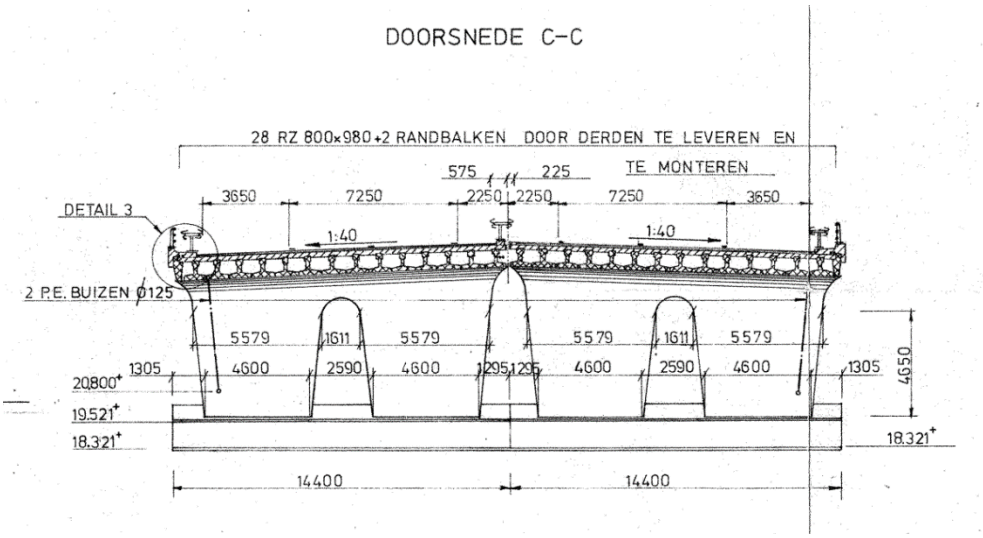

Figure 35 Cross-section Leenderheide bridge

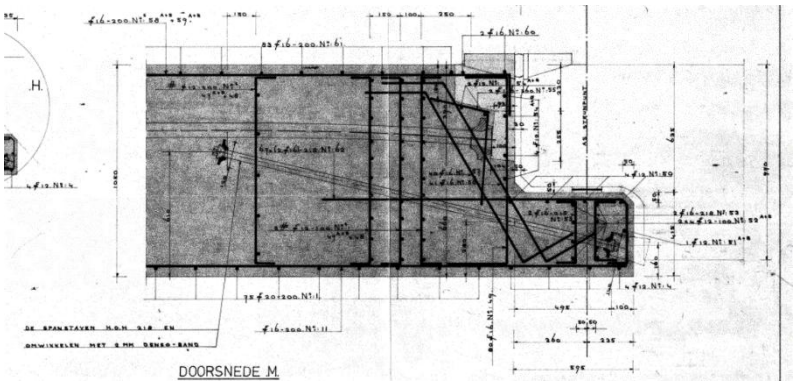

Figure 36 Half-joint connection Leenderheide bridge

4.10 Modelling

4.10.1 Modelling assumptions

- The global stability of the structure will be considered
- The internal stresses and deformations will be determined using a linear elastic analysis in RFEM.
- A 3D structural model will be created, consisting of 2D surface (shell) elements and 1D beam elements.
- The steel beams will be modelled as beam elements capable of carrying axial, shear, bending, and torsional forces.
- The concrete layer will be modelled as a surface element representing both membrane and bending behavior.
- The connection between the beams and the concrete surface will be assumed to be fully composite (fully connected).
- Material behavior will be assumed to be homogeneous, isotropic, and linearly elastic for both steel and concrete.
- Geometric imperfections and nonlinear effects (such as cracking of concrete or yielding of steel) will be neglected.
- Supports will be assumed to be idealized (pinned, fixed, or roller) as defined at the beam ends or nodes.
- The mesh density will be chosen sufficiently fine to ensure numerical convergence without excessive computational effort. A mesh size of 0.05 [m] x 0.05 [m] is taken for the elements, with a maximum distance of 0.001 [m] for integration between the nodes.

4.10.2 Lay out of the model

As mentioned in the assumptions above, only linear elastic behavior is considered in the model.
The concrete layer is modelled using surface elements. In RFEM, surface elements represent 2D plate or shell components that can carry in-plane forces (membrane action) and out-of-plane bending moments. This allows them to simulate the stiffness and deformation behavior of slab-like structures such as concrete surfaces.

The steel beams are modelled using member (beam) elements. In RFEM, member elements are

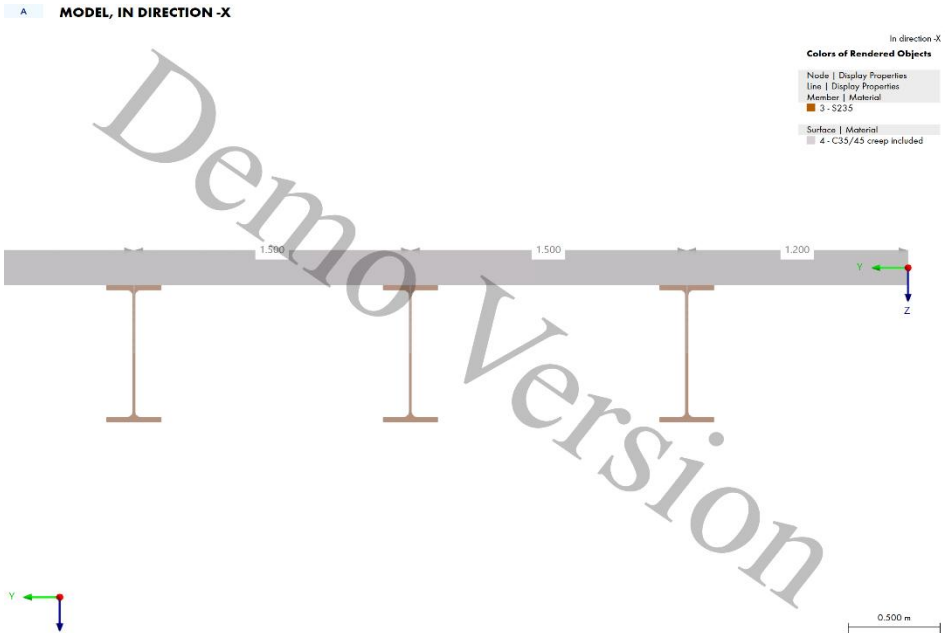

Figure 37 Visualization of right vertical alignment between the concrete surface and the steel beams by implementing an eccentricity.

1D line elements that transfer axial forces, shear forces, bending moments, and torsion along their longitudinal axis. These elements are defined along lines made in the concrete surface, that represent the beam's centerline and are assigned cross-sectional and material properties corresponding to the actual steel profiles.

This modelling approach ensures that the beams are fully connected to the concrete surface, which is the default behavior in RFEM. To accurately represent the real geometry, an eccentricity is introduced between the beam and the concrete surface so that the connection aligns correctly, as illustrated in Figure 37.
By modelling the beams as integrated elements within the concrete surface, nodes are automatically generated along the beam edges. At these nodes, nodal supports can be assigned according to the desired boundary conditions of the structure. Since the steel beams are supported by half-joint connections, these are the locations where the supports should be applied in the model.

4.10.3 Geometry and boundary conditions

The superstructure with the dimensions described in 4.9 will be removed and replaced by the composite weathering steel concrete superstructure. Therefore it has been chosen to make use of the same available length between the two abutments of 21.5 meters. The width is also to be assumed to be similar to the width of the original structure and therefore a width of 14.4 m will be assumed. The geometry of the superstructure are given in chapter 4.9.

The original superstructure has been placed on pot bearings which were placed on the abutments therefore in the schematization of this structure a simply supported connection could be assumed at the abutments. In the new modelled structure it will also be assumed that below each weathering steel beam a pot bearing will be placed which will connect the abutment and the weathering steel beams. Therefore it can be assumed that the weathering steel beams will be simply supported, as can be seen in Figure 38. The boundary conditions of the supports are given in Table 23. Figure 38 shows the geometry of the superstructure, with a total width of 14.4 m and a length of 21.5 m to be considered in the design.

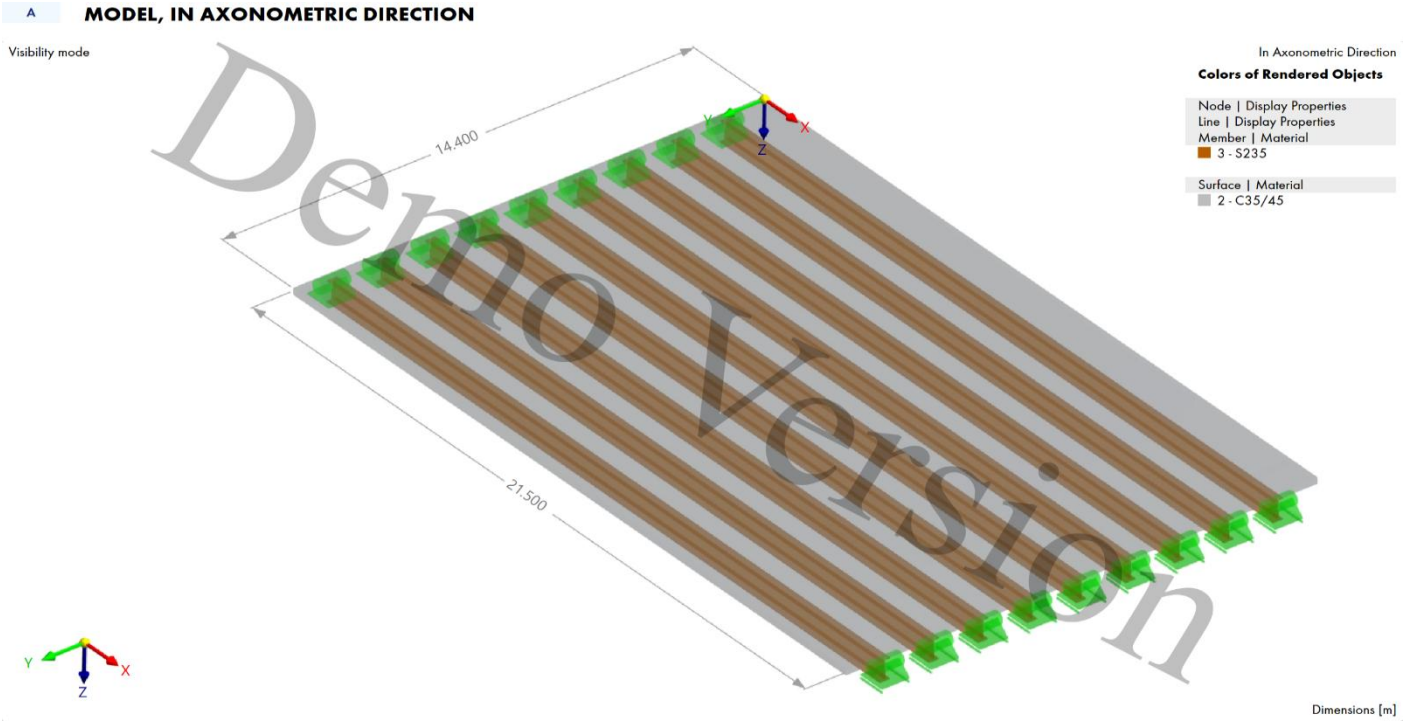

Figure 38 Geometry and boundary conditions.

Table 23 boundary conditions supports

Translation &rotation direction	Constraining at 0	Constraining at L
u_x	0	Free
u_y	0	0
u_z	0	0
ϕ_x	0	0
ϕ_y	Free	Free
ϕ_z	0	0

4.10.4 Material and geometrical properties

As mentioned before several variants will be considered for the design of the superstructure. Considering the concrete layer this will have a thickness of 200 mm and consist of concrete with a strength class of C35/45, see specifications in
Table 24. Considering the (weathering) steel elements 3 steel classes will be used for the different designs S235, S355 and S460, see Table 25 for the specifications. For the steel beams also three different profiles will be considered HEB600, HEB700 and HEB800, the geometrical properties can be found in Table 26. For the weathering steel elements, the sacrificial thickness should be reduced to determine the geometrical properties of these elements. From Figure 5 it can be observed that the Leenderheide junction is situated in the C3 area regarding the corrosion classification, from Table 4 it can be observed that for the ECCS recommendation a C3 area is linked to a recommended sacrificial thickness of 1 mm for a lifespan of 100 years, this results in the geometrical properties of the profiles as given in Table 27. In the design also the centre to centre distance between the beams will be varied, the following centre to centre distances will be considered: 1.5m, 2m and 2.5m. For each edge profile, the edge distance should be at least the height of the profile, due to the fixed centre to centre distances the edge distances in Table 30 are needeed.

Table 24 Concrete material properties compression layers (NBN EN 1992-1-1)

Strength class	$f_{cd,p}$[MPa]	$f_{ctk,0.05}$[MPa]	$f_{ctd,pl}$MPa]	$f_{cd,p}$[MPa]	$f_{c,lim}$[MPa]
C35/45	23.3	2.2	1.47	23.3	20

Table 25 Material properties (weathering) steel beams (EN1993-1-1 §3.2.6)

Strength class	f_y[MPa]	f_u[MPa]	E[MPa]	v	α [/°K]	ρ [kg/m3]	G[MPa]
S235	235	360	210000	0.3	$12*10^{-6}$	7850	81000
S355	355	510	210000	0.3	$12*10^{-6}$	7850	81000
S460	460	550	210000	0.3	$12*10^{-6}$	7850	81000

Table 26 geometrical properties of the conventional steel elements

Profile	Mass (kg/m)	Area (cm^2)	Height h (mm)	Width b (mm)	Web Thickness tw (mm)	Flange Thickness tf (mm)	Radius r (mm)	W_y (cm^3)	W_z (cm^3)
HEB600B	212	270	600	300	15.5	30.0	27.0	5701	902
HEB700B	241	306	700	300	17.0	32.0	27.0	7340	963
HEB800B	262	334	800	300	17.5	33.0	30.0	8977	994

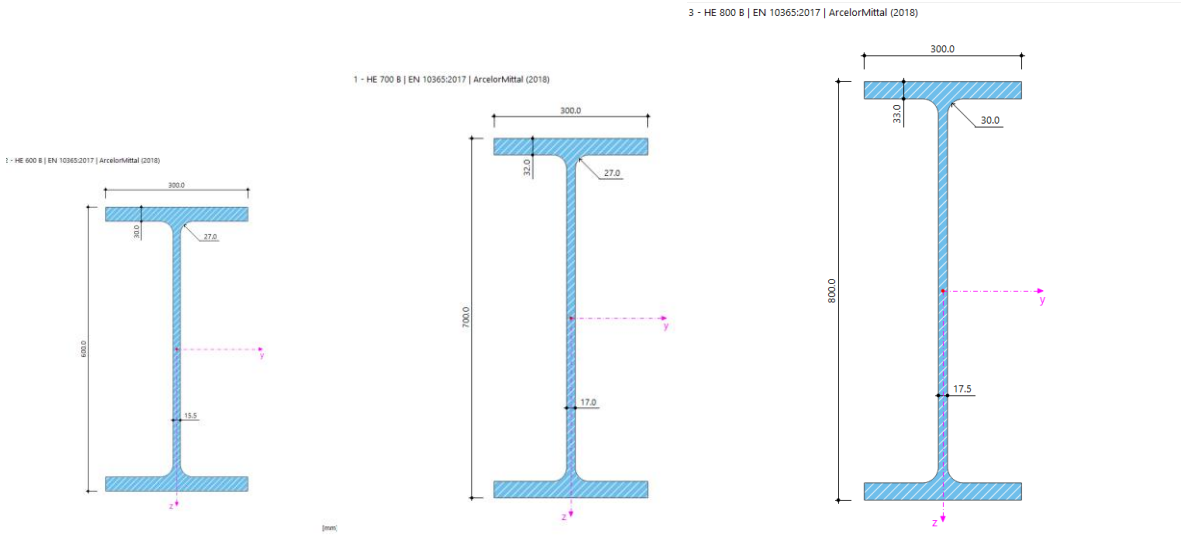

Figure 39 Visualization of profile dimensions and profiles used

Table 27 geometrical properties of the weathering steel elements including sacrificial thickness

Profile	Mass (kg/m)	Area (cm^2)	Height h (mm)	Width b (mm)	Web Thickness tw (mm)	Flange Thickness tf top (mm)	Flange Thickness tf bottom (mm)	Radius r (mm)	Wy (cm^3)	Wz (cm^3)	Sacrificial Thickness (mm)
HEB600B	194	247	599	298	13.5	29.0	28.0	27	5295	831	1.0
HEB700B	221	281	699	298	15.0	31.0	30.0	27	6838	890	1.0
HEB800B	241	307	799	298	15.5	32.0	31.0	30	8372	921	1.0
Reduction	–	–	**↓1**	**↓2**	**↓2**	**↓1**	**↓2**	–	–	–	–

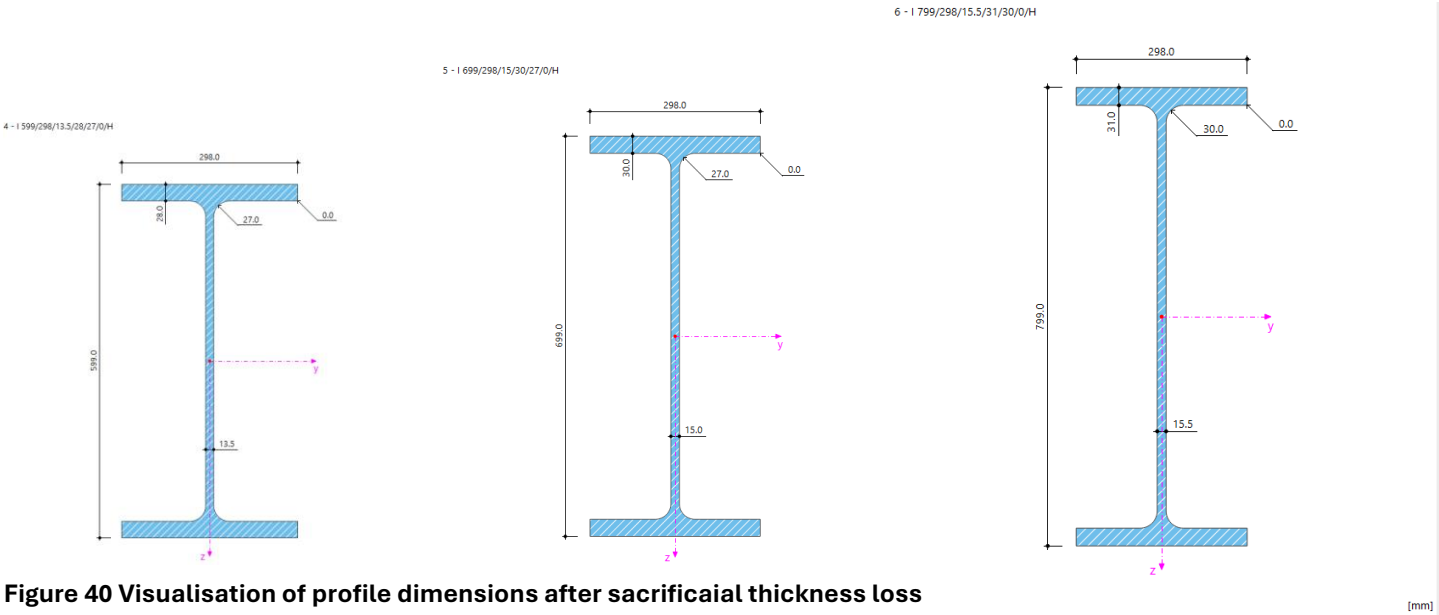

Figure 40 Visualisation of profile dimensions after sacrificaial thickness loss

Table 28 variants to be considered

Centre to centre distance	Edge distance HEB600B	Edge distance HEB700B	Edge distance HEB800B
1.5m	1.2 m	1.2 m	1.2 m
2m	1.2 m	1.2m	1.2 m
2.5m	0.95 m	0.95 m	0.95 m

4.10.5 Orientation of the local Axis system

To be sure that the results found after loading of the structure are correct, it is essential that the local axis system of the members and the surface used are performing as intended. To have easy comparable results it has been chosen to choose all the local axis systems similar to the global axis system as can be seen in Figure 41.

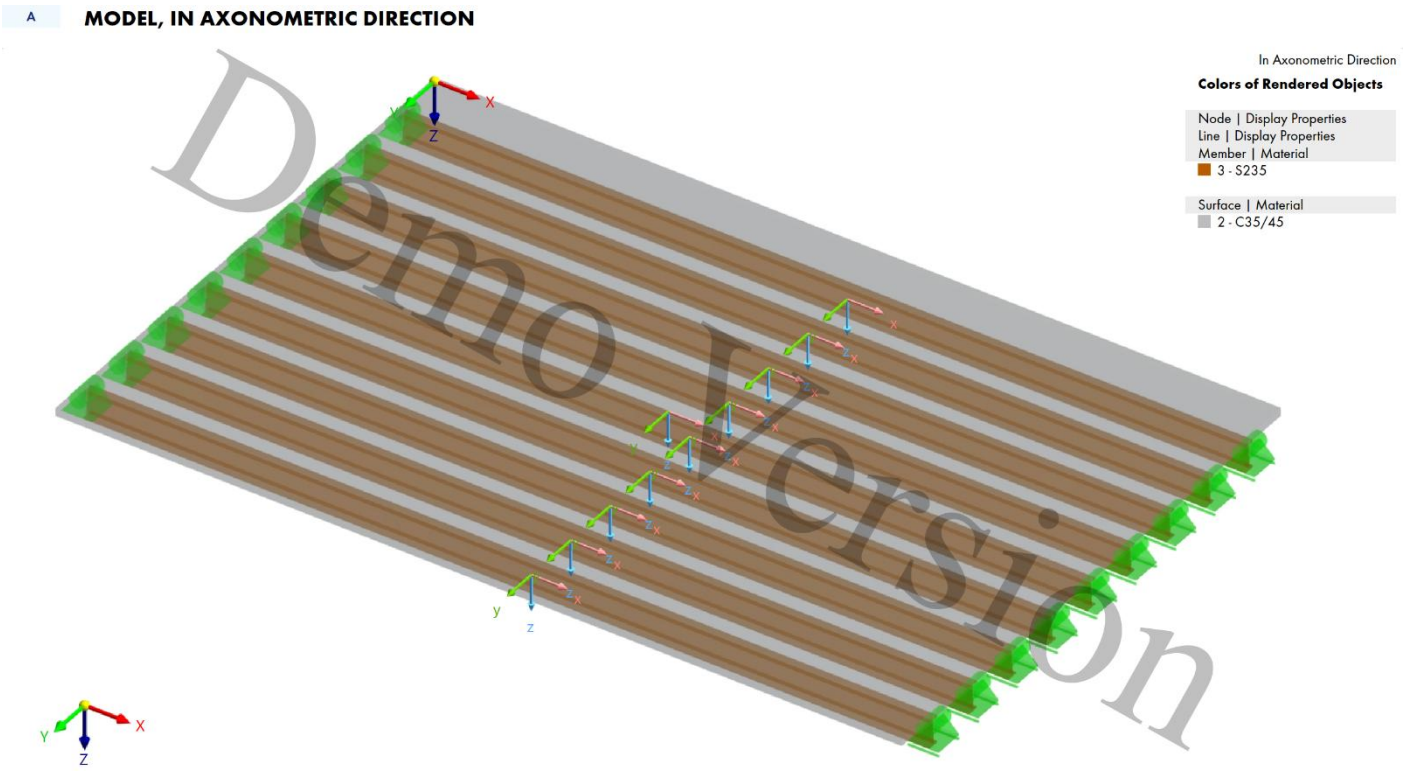

Figure 41 Visualization local and global axis systems.

4.10.6 Construction phasing

For the determination of the dimensions of the different elements of the superstructure it is essential to consider the different construction phases of the structure. This is due to the fact that in each phasing different load effect will be working which should be considered separately and accumulatively . For the displacement verification the vertical displacement of the bridge will be calculated accumulatively over the phasing, for bending moment verification, the shear force verification the governing phasing only will be considered. The following construction phases are considered:

- Phase 1: placing of the beam elements on the existing half joint
- Phase 2: the beam elements are loaded by the weight of wet concrete (non-composite situation)
- Phase 3: The composite action of the beam elements with the concrete deck, with the governing traffic load.

4.10.6.1 Phase 1 beam elements only

The beam elements will have a length of 21.5 m this is a transportable length due to conventional transport. First the pot bearing needs to be placed with precision on the right place on the existing half-joint. After this has been done the beam elements can be placed by making use of cranes. After the elements are placed the first loading phase has been started this is the case when the beam elements need to be able to withstand their self weight while being supported at the edges, this is seen as a simple supported beam as can be seen in Figure 42. The drawing also illustrates the shear studs that enable the composite interaction between the concrete slab and the (weathering) steel beams. These are shown indicatively, as they are required to ensure composite action between the materials. However, they are not considered in the design verification, since their dimensions have a negligible influence on the comparative analysis performed in this thesis.

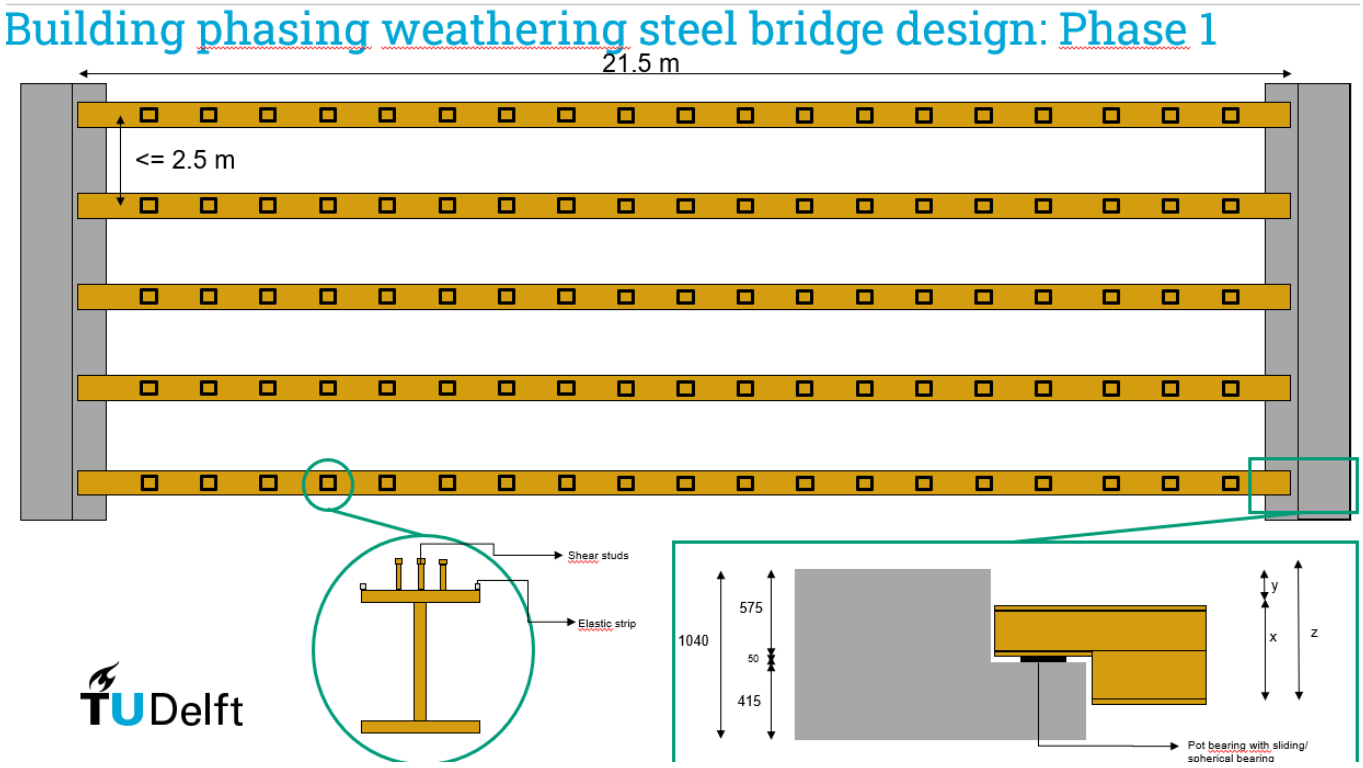

Figure 42 phase 1 simply supported beam elements

4.10.6.2 Phase 2 beam elements + wet weight of concrete

In this phase, semi-prefabricated slabs are placed between the beam elements to serve as formwork for the upper concrete layer. These slabs act as permanent (lost) formwork within the structure and contribute to the overall load-bearing capacity of the concrete deck. At the edges of the bridge it will still be necessary to make use of a temporary structure for the formwork to bear the load of the wet concrete. After this step is finished it is possible to place the reinforcement and the last step will be to pour the wet concrete on the bridge. This is seen as the loading of phase two when the beams need to be able to take the load of the wet concrete in a non composite action. These phasing are given in Figure 43 and Figure 44.

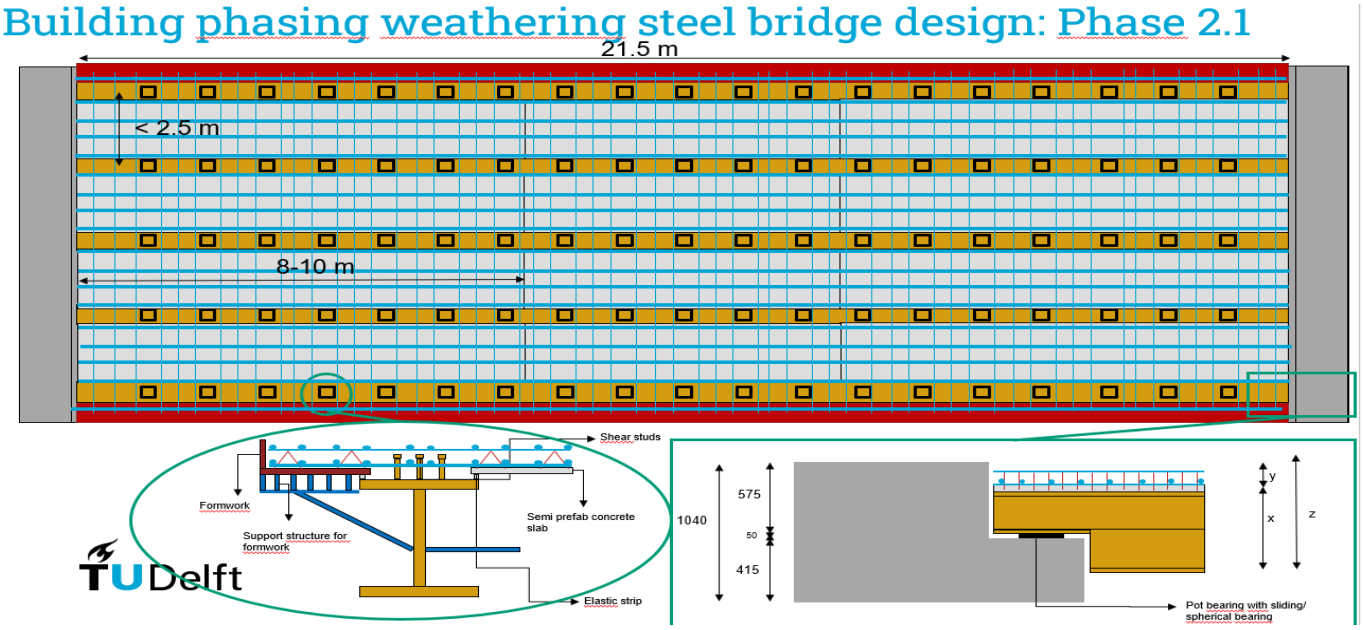

Figure 43 phase 2.1 placing of the formwork elements and the reinforcement

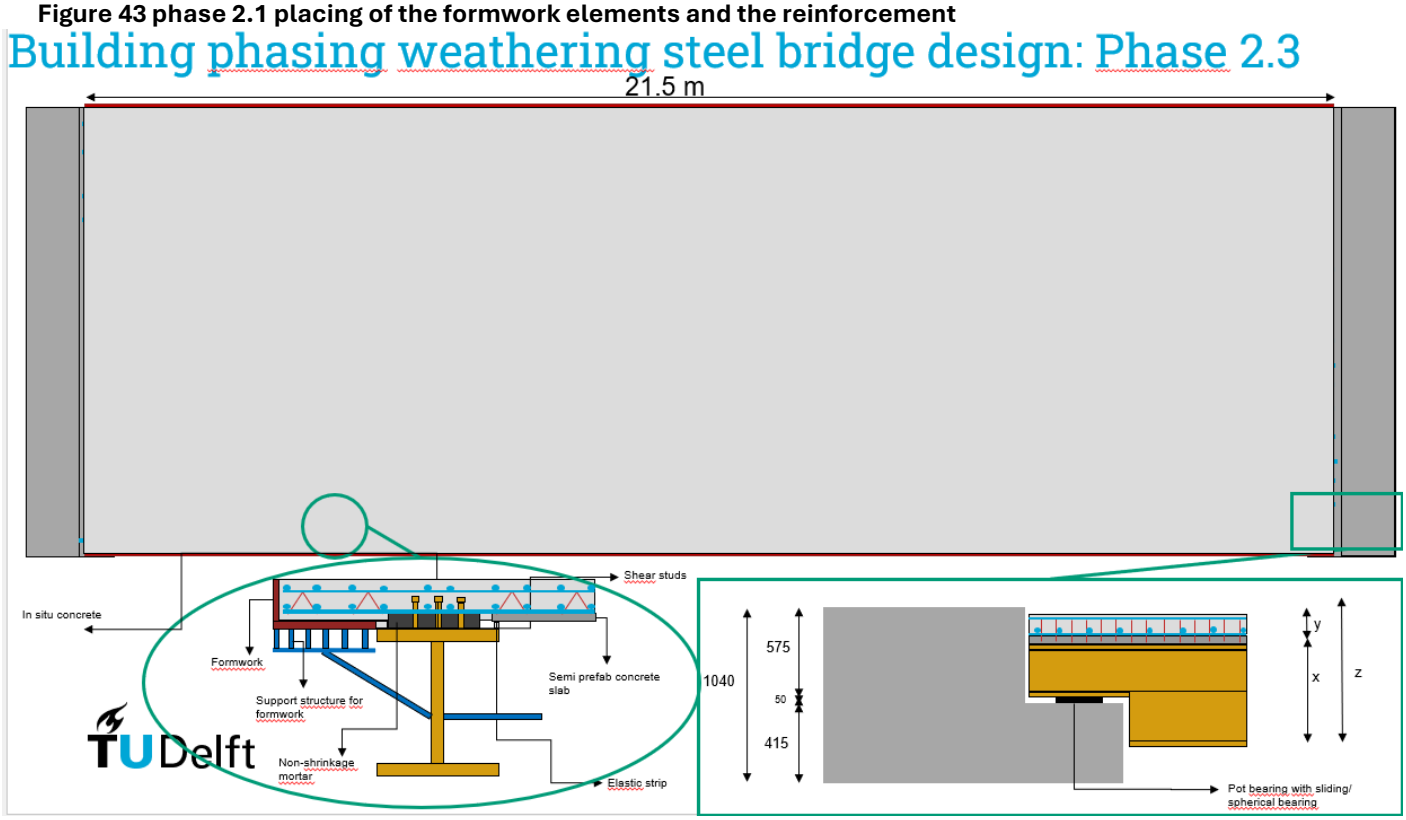

Figure 44 Phase 2.2 pouring of the wet concrete which gives the load case for the incomposite action between wet concrete and the beam elements.

4.10.6.3 Phase 3 composite action of beam elements and concrete under traffic load

The final stage will be after the composite action between the concrete and the beam elements has taken place. On the composite structure an asphalt layer will be placed and in the final stage the governing traffic loads need to be considered to determine the needed dimensions of the different elements according to the Eurocode verifications. In Figure 45 the final loading situation can be seen.

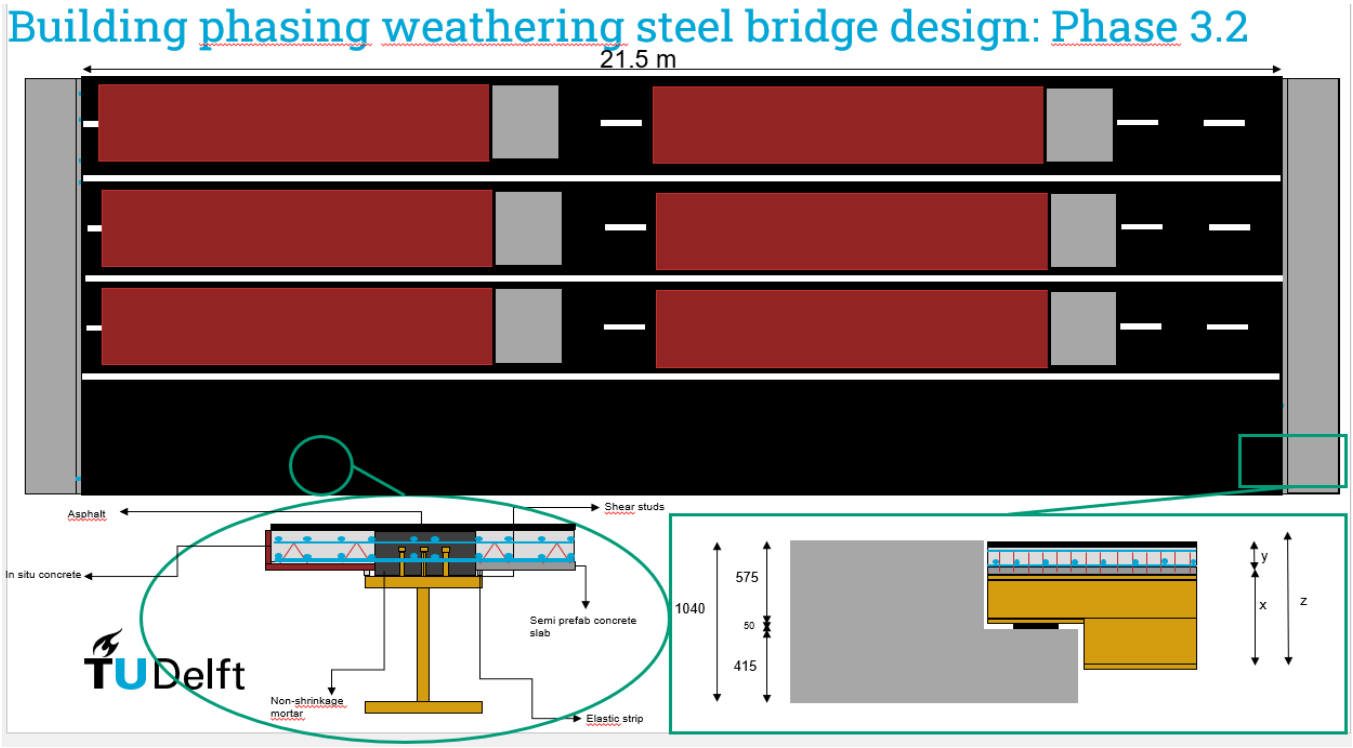

Figure 45 phase 3 composite action between beam elements and concrete deck under asphalt and traffic load

4.11 Loads & Load combinations

In this chapter the loads working on the structure will be given and the load combination which will be considered in the design calculation of the structure. These loads are categorized in three type of loads, the permanent loads, the variable loads and the special loads. The load combinations will be made according to the equations 6.10a and 6.10b given by the NEN-EN-1990+A1+A1/C2/NB:

Table 29 Design values according to equations 6.10a and 6.10b from the NEN-EN-1990+A1+A1/C2/NB

Blijvende en tijdelijke ontwerpsituaties	Blijvende belastingen		Overheersende veranderlijke belasting	Veranderlijke belastingen gelijktijdig met de overheersende	
	Ongunstig	Gunstig		Belangrijkste (indien aanwezig)	Andere
(Vgl. 6.10a)	1,35 $G_{k,j,sup}$ [a]	0,9 $G_{k,j,inf}$		1,5 $\psi_{0,1} Q_{k,1}$	1,5 $\psi_{0,i} Q_{k,i}$ $(i>1)$
(Vgl. 6.10b)	1,2 $G_{k,j,sup}$ [b]	0,9 $G_{k,j,inf}$	1,5 $Q_{k,1}$		1,5 $\psi_{0,i} Q_{k,i}$ $(i>1)$

[a] Bij vloeistofdrukken met een fysiek beperkte waarde mag zijn volstaan met 1,2 $G_{k,j,sup}$.

[b] Deze waarde is berekend met $\xi = 0{,}89$.

For the load combinations that will be made for this construction it is essential to make use of the combination factor according to table A2.1 from NEN-EN-1990+A1+A1/C2 as can be seen in Table 30.

Table 30 Recommended psi factors for traffic loads

Tabel A2.1 — Aanbevolen waarden voor de ψ-factoren voor bruggen voor wegverkeer

Belasting	Symbool		ψ_0	ψ_1	ψ_2
Verkeersbelastingen (zie EN 1991-2, tabel 4.4)	gr1a (LM1+voetgangers- of fietspadbelastingen) [1]	TS	0,75	0,75	0
		UDL	0,40	0,40	0
		Voetgangers- +fietspadbelastingen [2]	0,40	0,40	0
	gr1b (enkele as)		0	0,75	0
	gr2 (horizontale krachten)		0	0	0
	gr3 (voetgangersbelastingen)		0	0,40	0
	gr4 (LM4 – belasting door een menigte)		0	–	0
	gr5 (LM3 – speciale voertuigen)		0	–	0
Windkrachten	F_{wk} – blijvende ontwerpsituaties		0,6	0,2	0
	– uitvoering		0,8	–	0
	F_W^*		1,0	–	–
Thermische belastingen	T_k		0,6 [3]	0,6	0,5
Sneeuwbelastingen	$Q_{Sn,k}$ (tijdens de uitvoering)		0,8	–	0
Belastingen tijdens de bouw	Q_c		1,0	–	1,0

1) De aanbevolen waarden voor ψ_0, ψ_1, ψ_2 voor gr1a en gr1b zijn gegeven voor wegverkeer met de bijsturingsfactoren α_{Qi}, α_{qi}, α_{qr} en β_Q gelijk aan 1. Die met betrekking tot UDL komen overeen met gebruikelijke verkeersscenario's, waarin een zeldzame filevorming van vrachtwagens kan optreden. Andere waarden mogen zijn overwogen voor andere wegklassen, of voor te verwachten ander verkeer, gerelateerd aan de keuze van de corresponderende α-factoren. Bijvoorbeeld mag een waarde voor ψ_2 anders dan nul zijn overwogen voor alleen het UDL-systeem van LM1, voor bruggen die een continu zware verkeersstroom hebben te dragen. Zie ook EN 1998.

2) De combinatiewaarde van de voetgangers- en fietspadbelasting, vermeld in tabel 4.4a van EN 1991-2, is een "gereduceerde" waarde. ψ_0- en ψ_1-factoren zijn van toepassing op deze waarde.

3) De aanbevolen ψ_0-waarde voor thermische belastingen mag in de meeste gevallen voor de uiterste grenstoestanden EQU, STR en GEO tot 0 zijn verminderd. Zie ook de Eurocodes voor ontwerp en berekening.

4.11.1 Loads to be considered including partial factors

Table 31 loads and corresponding partial factors

Type of Load	Load	Partial factors (ULS)	Partial factors (SLS)	Combination factor ψo	Combination factor ψ1	Combination factor ψ2
Permanent						
Weight beams	See Table 26	1.35/0.9/1.2	1.0	-	-	-
Weight concrete Deck	25 [kN/m^3]	1.35/0.9/1.2	1.0	-	-	-
Weight asphalt	23 [kN/m^3]	1.35/0.9/1.2	1.0	-	-	-
Variable						
Traffic load LM 1 TS		1.5	1.0	0.75	0.75	0
Traffic load LM 1 UDL		1.5	1.0	0.40	0.40	0
Traffic load LM 2		1.5	1.0	0	0.75	0
Traffic load LM3		1.5	1.0	0	-	0
Traffic load LM4		1.5	1.0	0	-	0

4.11.2 Variable loads (traffic load)

Regarding the traffic load the traffic lane width should be used to divide the surface in traffic lanes. From Figure 35 It can be observed that the maximum net width is 14400-1305=13095 mm. therefore 3 theoretical traffic lanes can be placed on this surface with a width of 3 m and one remaining surface with a width of 4095 mm.

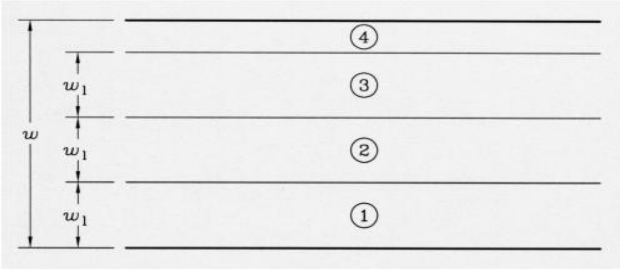

Verklaring

w	breedte van de rijweg
w_1	breedte van de theoretische rijstrook
1	theoretische rijstrook nr. 1
2	theoretische rijstrook nr. 2
3	theoretische rijstrook nr. 3
4	resterende oppervlakte

Figure 46 Traffic lane composition

4.11.2.1 Traffic load model 1 (LM1)

According to NEN-EN 1991-2 for 3 theoretical traffic lanes of 3 m and remaining surface of 4.095m the following loads should be considered for the Tandem system and the uniform distributed load, as can be seen in Figure 46. In a visualization of the distribution of these loads is given. For the correction factor α_Q, the maximum correction factor is assumed of α_Q= 1.0.

The wheel load for an axle load of 300 kN, will be 150 kN. This load can be distributed according to the Eurocode over a wheel print of 0.4m by 0.4m. In the calculation this has been used to determine the wheel load/m^2. Therefore the wheel load for an axle load of 300 kN is taken into account as 150 kN/ 0.16 m^2 = 937.5 kN/m^2.

However, according to the Eurocode, the load can be applied at the centroid of the concrete compression layer. This approach distributes the wheel load over a larger area, which is beneficial for reducing the overall effects on the structure.

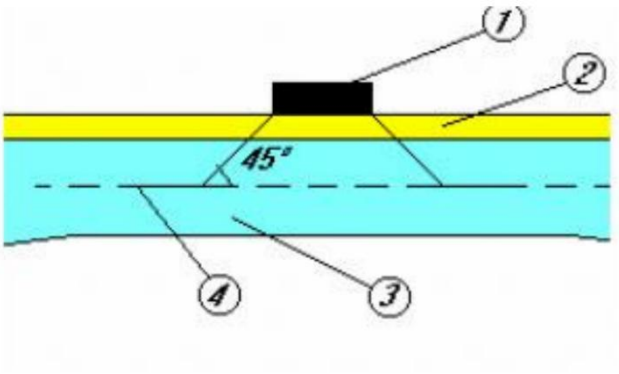

Figure 47 redistribution of the wheel load

For an asphalt layer of 70 mm and a concrete layer of 200 mm, it means the centre will be at 135 mm. Since the redistribution will be in an angle of 45 degree as can be seen in Figure 47 the total area the wheel load will be working on is:

$l_w = 0.4$ *m(wheel load length)*
$t_c = 0.135$ *m(distance from centroid of concrete layer)*
$P_w = 150$ *kN(wheel load)*

The contact area of the load on the concrete layer:

$$A = (l_w + 2 \cdot t_c) \cdot (l_w + 2 \cdot t_c)$$
$$A = (0.4 + 2 \cdot 0.135) \cdot (0.4 + 2 \cdot 0.135) = 0.67 \cdot 0.67 \approx 0.45\ m^2$$

The resulting surface load:

$$q = \frac{P_w}{A} = \frac{150\ kN}{0.45\ m^2} \approx 333\ kN/m^2$$

According to NEN-EN 1991-2/NB, Table NB.1, a correction factor of $\alpha_Q = 1.4$should be applied. Using this factor, the modeled surface load becomes:

$$q_{\text{mod}} = 333\ \text{kN/m}^2 \times 1.4 = 470\ \text{kN/m}^2.$$

In the current model, a conservative wheel load of 937.5 kN/m^2 has been used. This higher value is based solely on the actual wheel contact area and does not account for redistribution of the load over the concrete deck, which is not incorporated in this model. For future model optimization, the more realistic value of 470 kN/m^2, including redistribution effects, should be applied to better reflect actual traffic conditions.

Table 32 characteristic values load model 1

Positie	Tandemstelsel *TS*	Gelijkmatig verdeelde belasting (GVB)
	Aslast Q_{ik} (kN)	q_{ik} (of q_{rk}) (kN/m^2)
Rijstrook nummer 1	300	9
Rijstrook nummer 2	200	2,5
Rijstrook nummer 3	100	2,5
Overige rijstroken	0	2,5
Resterende oppervlakte (q_{rk})	0	2,5

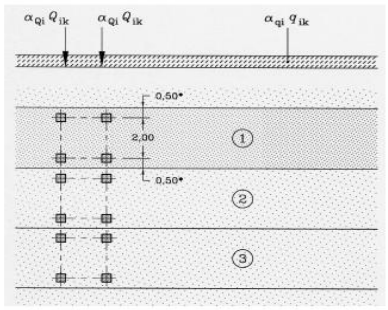

Verklaring

(1) rijstrook nummer 1 : Q_{1k} = 300 kN ; q_{1k} = 9 kN/m^2
(2) rijstrook nummer 2 : Q_{2k} = 200 kN ; q_{2k} = 2,5 kN/m^2
(3) rijstrook nummer 3 : Q_{3k} = 100 kN ; q_{3k} = 2,5 kN/m^2; tussenafstand assen in tandemstelsel = 1,2 m
* Voor w_l = 3,00 m

Figuur 4.2a – Toepassing van belastingsmodel 1

Figure 48 Distribution tandem axle loads

For load model 1 two situations are considered for two locations. The first location is placing the maximum load as much as possible to the edge so the governing situation can be simulated for the edge beam. As can be seen in Figure 49 the tandem axle is close to the edge of the structure, this is due to the fact that there are two superstructures next to each other in the Leenderheide bridge and only in one of the superstructures the guiding rail will be placed as can be seen in Figure 35. It is expected that the superstructure with the highest effective working load width will be the governing superstructure and therefore it has been chosen to model the situation where only one guiding rail is placed on the superstructure. For the edge beam it will be necessary to perform the verifications with a load at the midspan of the structure for the maximum bending moment and a load close to the support of the structure (0.5m) for the maximum shear force, as can be seen in Figure 50 and Figure 51.

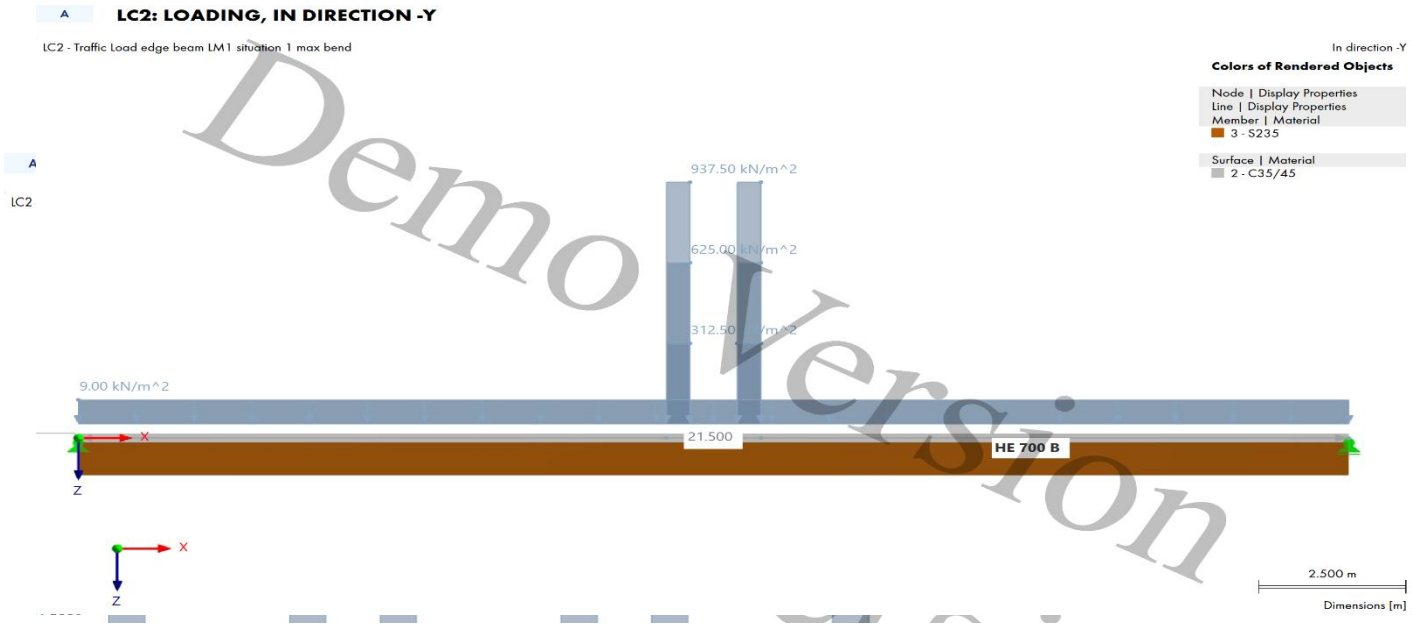

Figure 50 Max bending moment edge beam midspan of the structure side view.

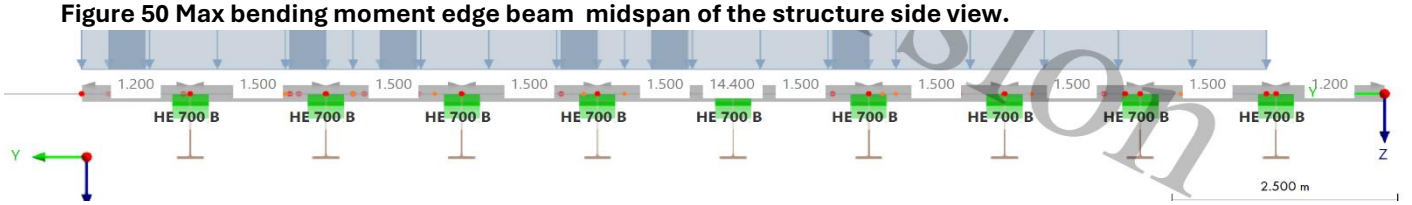

Figure 49 Max bending moment/shear force, edge beam, midspan/close to the support of the structure front view.

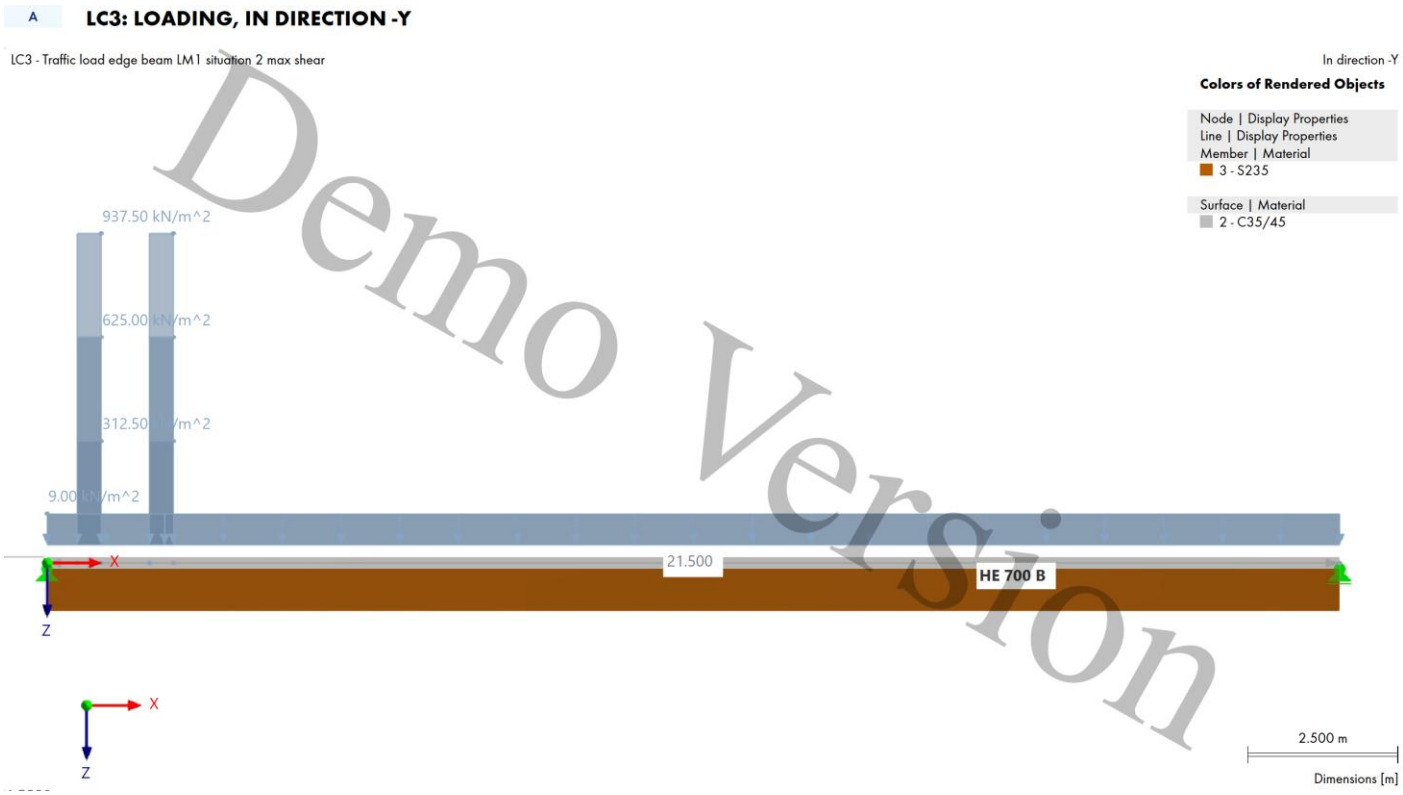

Figure 51 Max shear force edge beam close to the support side view.

Second location will be a maximum load configuration as close as possible to the middle beam, see Figure 53. For this beam another effective width needs to be considered and therefore the validity of this beam needs also to be verified. Also for this case the maximum load configuration will be placed at the midspan of the structure for the maximum bending moment verification and the maximum load configuration close to the support (0.5m) for the maximum shear force verification, see Figure 52 and Figure 54.

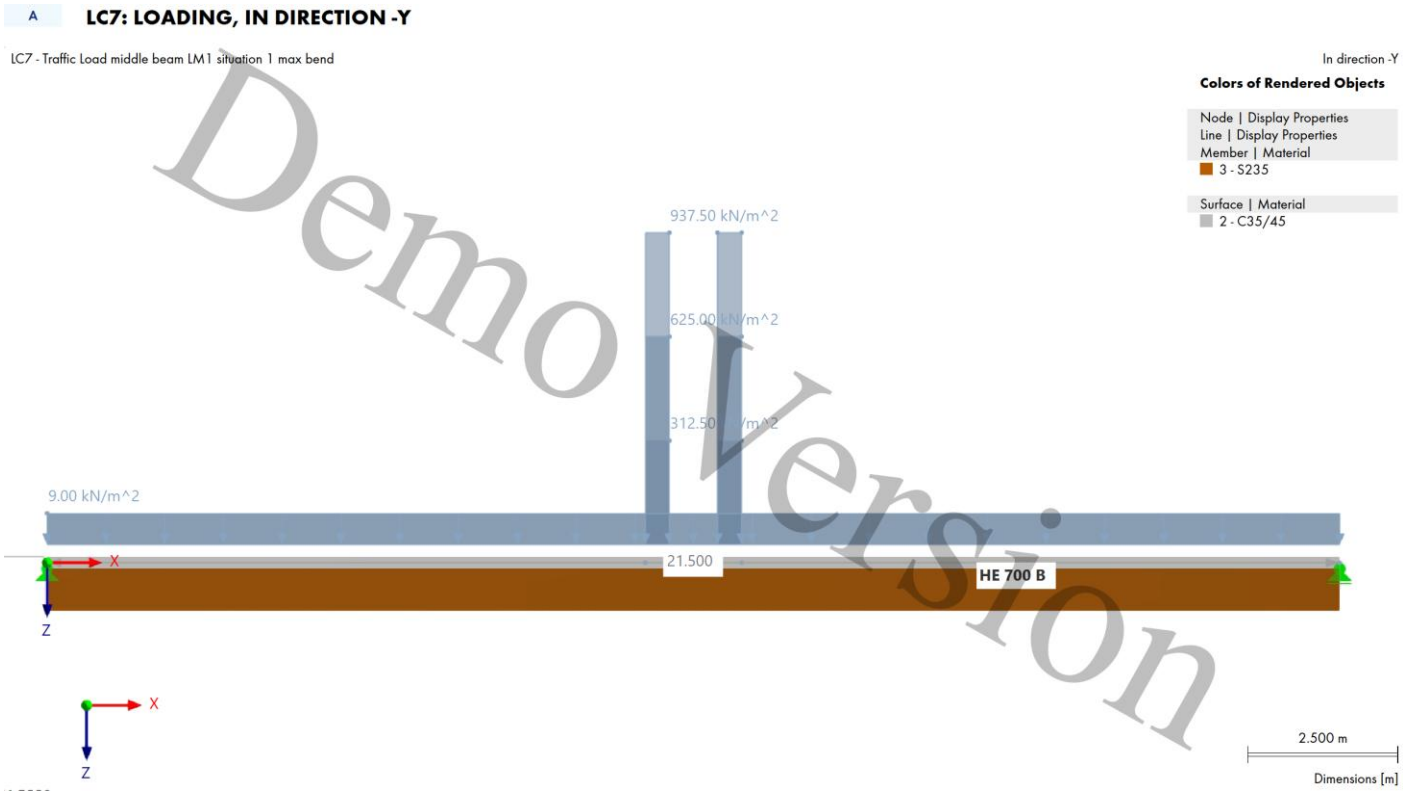

Figure 52 Max bending moment middle beam midspan of the structure side view.

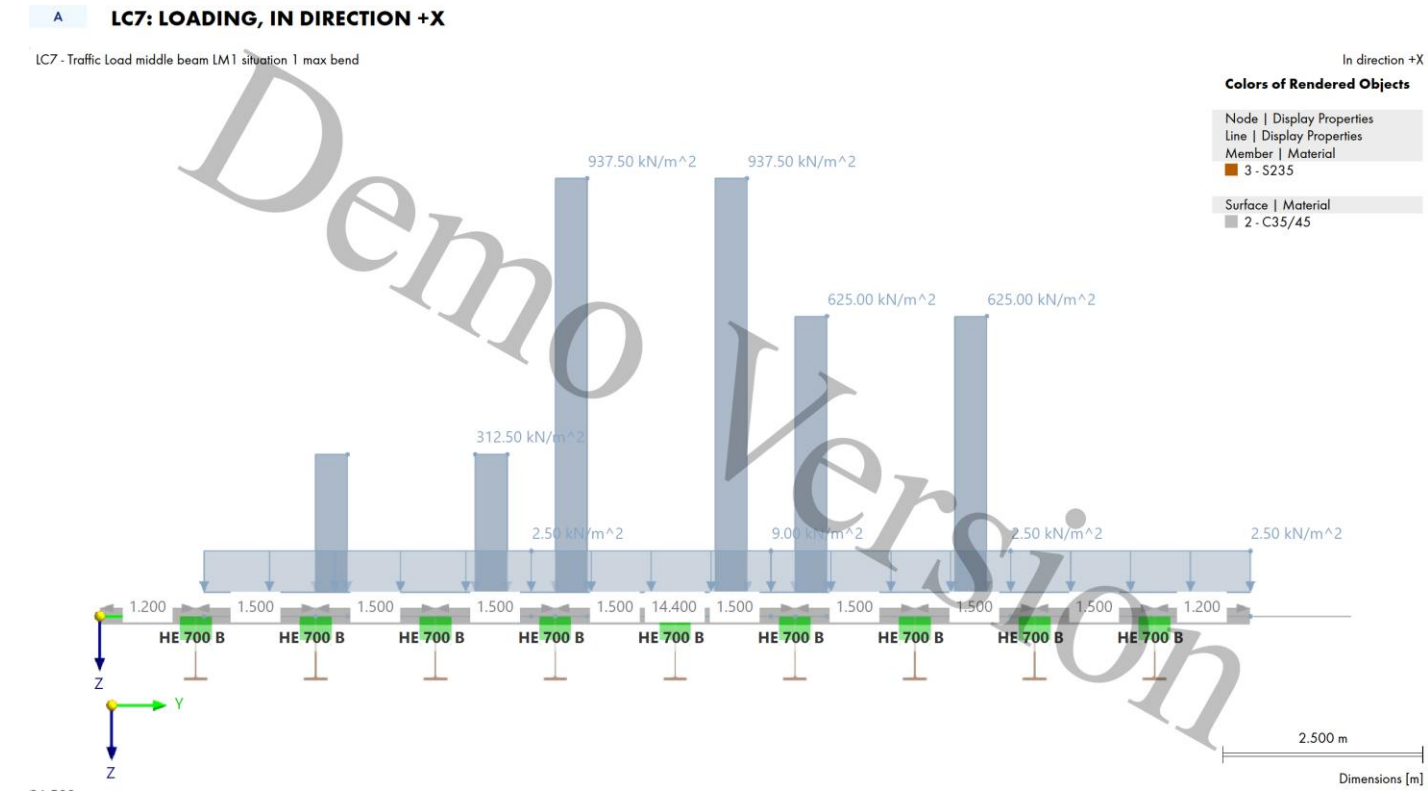

Figure 53 Max bending moment/shear force, middle beam, midspan/close to the support of the structure front view.

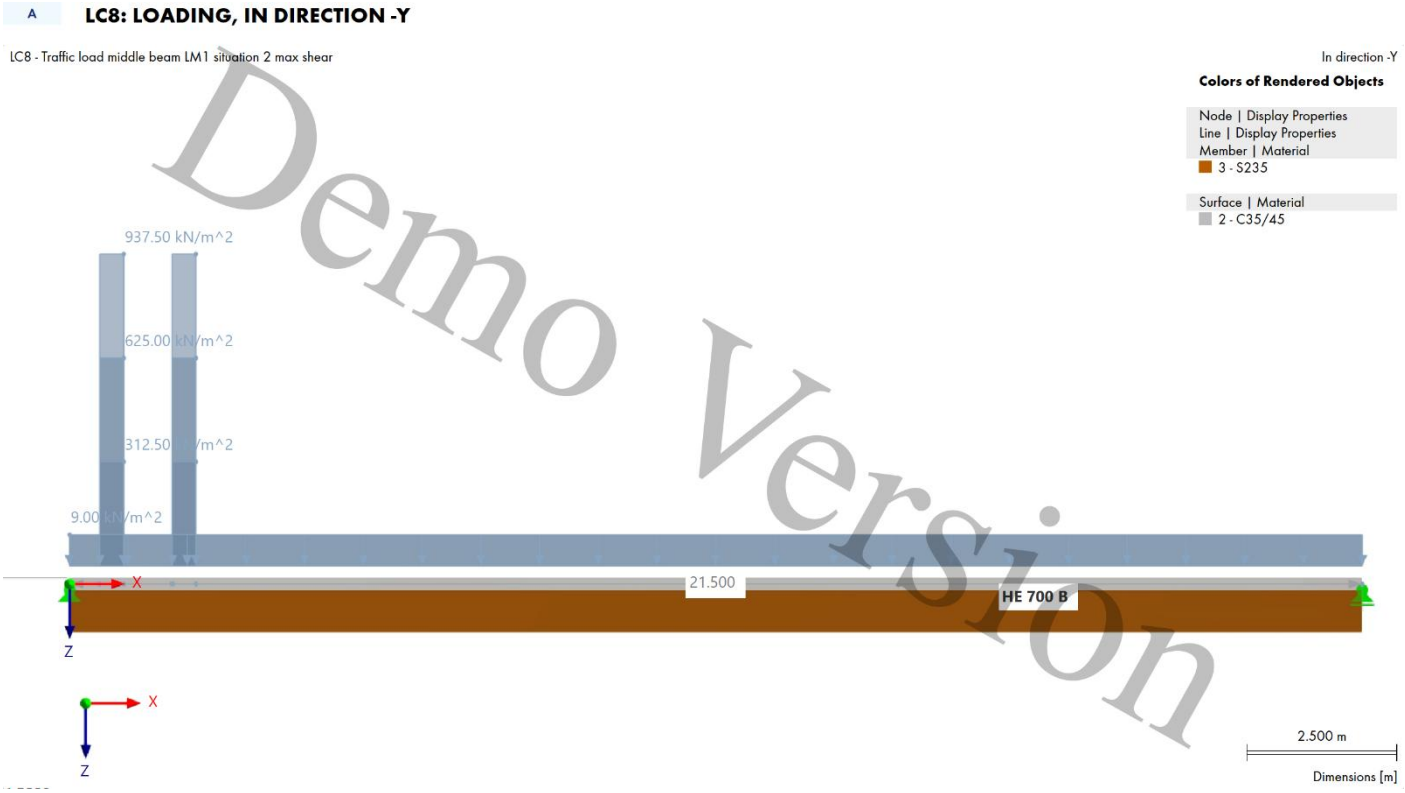

Figure 54 Max shear force edge beam close to the support side view.

4.11.2.2 Traffic load model 2 (LM2)

Traffic Load Model 2 (LM2) is not considered in the main calculations because, for a simply supported composite beam, LM1 is more critical in governing the bending moment and shear forces. LM1 accounts for multiple traffic lanes with tandem axle arrangements and uniform distributed loads, which generate the maximum longitudinal bending moments along the span and the highest shear at supports for edge and middle beams.
In contrast, LM2 represents a single axle load that can be placed anywhere along the bridge and is generally governing only for local effects, such as in the concrete deck itself between the steel beams. Since the focus of this study is on the overall composite superstructure (weathering steel beams + concrete deck), LM1 produces higher global effects and is therefore sufficient for determining the dimensions of the steel-concrete composite beams. LM2 would only influence the slab thickness or local punching shear, which is not part of the research questions. The geometry of this load can be seen in Figure 55 and Figure 56.

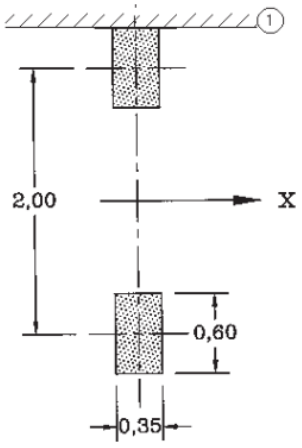

Verklaring

X Lengterichting van de brug
1 Stootrand

Figuur 4.3 – Belastingsmodel 2

Figure 55 Load model 2

Figure 56 Load model 2 max bending moment

4.11.2.3 Traffic load model 3 (LM3)

Traffic Load Model 3 (LM3) will not be considered because it is typically used for special heavy vehicle or abnormal loads, which do not produce higher bending or shear effects than LM1 for the simply supported composite beams. Including LM3 would not affect the design conclusions for the superstructure.

4.11.2.4 Traffic load model 4 (LM4)

Traffic Load Model 4 (LM4) represents crowd loading, for example pedestrians or runners during events. For this bridge, it is not expected that a crowd would use it for such activities (e.g., a marathon), so LM4 is not relevant for the design verification.

4.11.2.5 Fatigue load model 1 (FLM1)

Fatigue will not be considered, see 2.3.1.

4.11.3 Creep and shrinkage

The effects of creep will be taken into account by making use of the moduli ratio n_L for the concrete. The moduli ratio can be described as:

$$\boldsymbol{n_{L,long,creep} = n_0\,(1+\psi_L\phi_t) = \ 5.70(1+1.1*1.67) = \ 17.03} \quad (1)$$

$$\boldsymbol{n_{L,shrinkage} = n_0\,(1+\psi_L\phi_t) = \ 5.70(1+0.55*1.67) = \ 11.5} \quad (2)$$

The moduli for the short time load n_0 can be determined by:

$$\boldsymbol{n_0 = \frac{E_a}{E_{cm}} = \frac{210000}{37000} = 5.70} \quad (3)$$

For the creep multipliers factor $\boldsymbol{\psi_L}$, the value from ENV 19402:1997 table 4 is taken. By making use of the value for shrinkage: $\psi_L = 0.55$. To determine the different moduli the parameters in are used as assumptions based on the ENV 19402:1997.

Table 33 Assumed parameters for creep and shrinkage effects

description	symbol	value	unit
creep coefficient shrinkage	ψLs=	0.55	
creep coefficient permanent	ψLp=	1.1	
creep coefficient imposed def	ψLi=	1.5	
first time of loading	t0=	7	days
Relative humidity	RH=	80	%
design life structure (100y)	t=	36525	days

The creep coefficient factor ϕ_t can be determined by making use of the formula's below for the calculations:

$$\boldsymbol{\phi_t = \ \phi_0 * \beta_c(t-t_0) \ = 1.68*0.99 = 1.67} \quad (4)$$

$$\boldsymbol{\phi_0 = \phi RH * \beta(fcm) * \beta(t_0) \ = 1.68} \quad (5)$$

$$\boldsymbol{\phi RH = \ 1+\frac{1-\frac{RH}{100}}{0.1*h_0^{33}} \ = 1.034} \quad (6)$$

$$\boldsymbol{\beta(fcm) = \frac{16.8}{(f_{cm}^{0.5})} = \ 2.56} \quad (7)$$

$$\boldsymbol{\beta(t_0) = \frac{1}{(0.1+t_0^{0.2})} \ = \ 0.634} \quad (8)$$

Hereby the time of loading is estimated to be 7 days and the relative humidity is taken as 80%, while the theoretical height h_0 is determined by making use of the geometrical properties of the concrete, h_0 = 197 mm. The mean concrete compressive strength $f_{cm} = 8 + f_{ck}$ = 43 N/mm^2.

$$h_0 = 2 * \frac{A_{c,tot}}{u} = \frac{2880000}{29200} = 197\ mm, \quad with\ A_c\ the\ concrete\ area\ and\ u\ the\ circumference$$

The factor $\boldsymbol{\beta_c}$ depends on the first moment of loading (when removing the formwork) and the moment of considering the structure. The moment of removing the formwork will be assumed to be t_0= 7 days and the moment of consideration will be t= 100 years, since this is the design life of the structure. The formula that will be used for determining $\boldsymbol{\beta_c}$is:

$$\boldsymbol{\beta_c(t - t_0)} = \left[\frac{t-t_o}{\beta H + t - t_0}\right]^{0.3} = \boldsymbol{\beta_c(36500 - 7)} = \left[\frac{36500-7}{1010.27+36500-7}\right]^{0.3} = \mathbf{0.99} \quad (9)$$

$$\boldsymbol{\beta H = 1.5 * [1 + (0.012 * RH)^{18}] * h_0 + 250 = 1.5 * \left[1 + \left(0.12 * \frac{80}{100}\right)^{18}\right] * h_0 + 250 = 1010.27 \ < 1500} \quad (10)$$

4.11.3.1 Modelling of creep and shrinkage effect

Creep and shrinkage effects need to be considered in the RFEM model. Since construction phasing is not available in RFEM, the creep effect will be accounted for using the manual method. This method involves introducing a strain in each steel beam to represent the creep of the concrete, as illustrated in Figure 57. The formulas used for determining the strain on the steel beams due to the concrete shrinkage have been deduced from *Eurocode 2 – NEN-EN 1992-1-1: Design of Concrete Structures – Part 1-1: General Rules and Rules for Buildings*.

The effect is incorporated by determining the effective modulus of concrete as follows:

$$E_{eff} = \frac{E_{cm}}{1 + \phi_t} = \frac{37000}{1 + 1.67} = 13850\ MPa$$

For the shrinkage the total shrinkage strain needs to be determined, herby ε_{cs} = total shrinkage strain, ε_{cds}=drying shrinkage and ε_{cas}= autogenous shrinkage:

$$\boldsymbol{\varepsilon_{cs} = \varepsilon_{cds} + \varepsilon_{cas} = 0.0000825 + 0.0000158 = 0.0000983}$$

The autogenous shrinkage will be:

$$\boldsymbol{\varepsilon_{cas} = \varepsilon_{ca}(\infty) = 2.5 \cdot (f_{cm} - 10) \cdot 10^{-6} = 0.000825}$$

The drying shrinkage will be:

$$\boldsymbol{\varepsilon_{cds}(t) = \varepsilon_{cd,0} \cdot \beta_{ds}(t) = 0.0000983}$$

$$\boldsymbol{\varepsilon_{cd,0} = k_H \cdot \varepsilon_{cd,\infty} = 16.5 * 10^{-6}}$$

$$\boldsymbol{k_H = \frac{55}{h_0^{0.5}} = 0.110}$$

$$\boldsymbol{\varepsilon_{cd,\infty} = 150 * 10^{-6}, for\ f_{ck} = 35\ MPa}$$

$$\boldsymbol{\beta_{ds}(t) = \frac{t}{t + 0.04 \cdot h_0^2} = \frac{36525}{36525 + 0.04 \cdot 197^2} = 0.0000158}$$

To determine the imposed strain on each steel beam element due to the concrete shrinkage the following formula can be used:

$$\varepsilon_{shrinkage,eff} = \frac{\varepsilon_{cs}}{n_{L,shrinkage}} = \frac{0.0001}{11.5} = 8.7 * 10^{-6}$$

By creating a load case imposing a strain on the beams in longitudinal direction the shrinkage load will be taken into account, as can be seen in Figure 57.

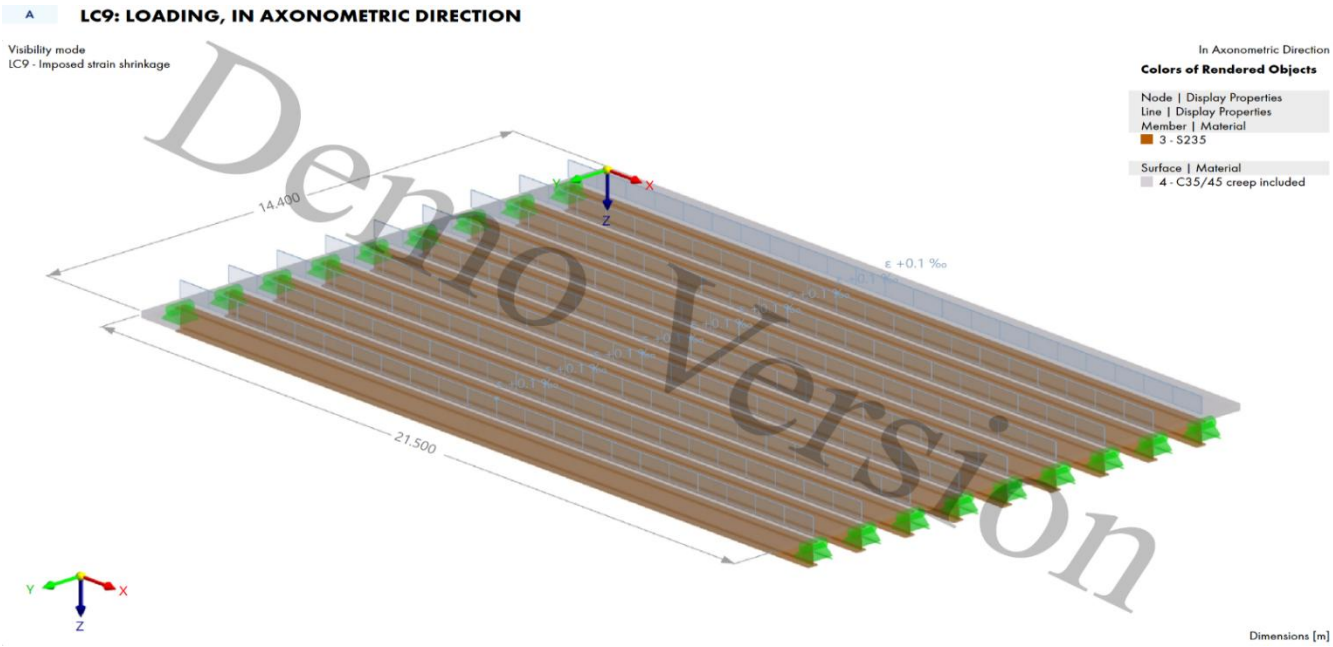

Figure 57 imposed strain due to shrinkage on the beam elements

4.11.4 Excluded load cases

Table 34 Excluded load cases in the design

Load Case	Description	Reason for Exclusion
Global temperature effects	Uniform temperature changes in the entire structure.	The bridge is statically determinate, which allows it to expand and contract freely without inducing internal forces. Therefore, global temperature variations have no influence on bending moments or stresses.
Local temperature differences	Temperature gradient over the height of the cross-section (e.g., top heated by sunlight).	Local gradients can cause minor bending moments. However, their impact is negligible compared to permanent and traffic loads. Moreover, these effects are typically relevant only for continuous or highly slender structures, not for this statically determinate bridge.
Braking and acceleration forces	Longitudinal horizontal forces caused by vehicle braking or acceleration.	These effects are small for this bridge type due to the short span length and stiff deck. The bearings and abutments are designed to accommodate such horizontal loads without inducing significant internal moments. Therefore, they are not governing for the design.
Impact and accidental loads	Loads resulting from vehicle impact, explosion, or seismic events.	These are considered exceptional load cases and fall outside the scope of this analysis, which focuses on normal operating conditions and ultimate limit states under standard Eurocode 1 Part 2 load models. In a further design stage this should be included.
Wind loads	Wind pressure acting on the structure.	Wind loads are minor compared to traffic and dead loads for low-level bridges. Since the bridge is not a tall or flexible structure, wind effects are not critical for bending or deflection verifications. In a further design stage this should be included.
Thermal restraint effects	Secondary stresses due to restrained thermal expansion.	Since the structure is simply supported, there is no restraint to thermal movement; therefore, these stresses do not develop.

4.12 Verification of the model

To verify the constructed RFEM model, it is necessary to compare the results obtained by the RFEM calculations with hand calculations. For a meaningful comparison, the edge portion of the composite slab, with an effective width of 1.425 m, has been selected, as can be seen in Figure 58. This approach simplifies the model to a fully connected composite beam with a concrete slab, providing a more accurate basis for comparison with the hand calculation. The hand calculation is based on the assumption of a composite beam element, ensuring consistency between both methods.

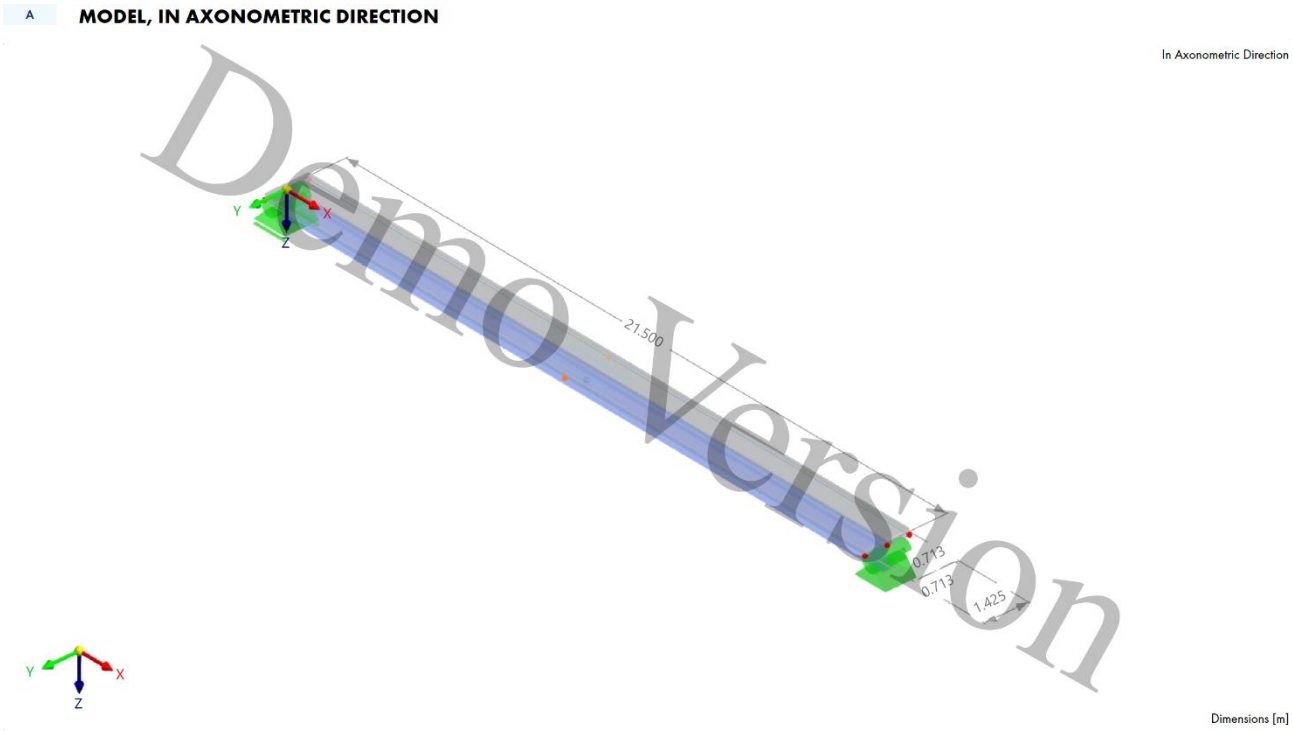

Figure 58 Verification model

Three type of verifications will be performed to check the quality of the model. The verifications will be based on hand calculations. The selfweight of the structure will be used to perform the verification checks. The following verifications will be performed:

- Displacement of the edge beam in the midspan of the structure
- Vertical shear force of the edge beam
- Bending moment at the midspan of the structure

4.12.1 Boundary conditions

For the boundary conditions two cases will be considered to check the influence of the set boundary conditions. Case 1 represents a realistic idealization of a simply supported beam, allowing certain degrees of freedom such as horizontal displacement and rotation in one direction to reflect the movement permitted by pot bearings and half-joint connections. Case 2 represents a more conservative scenario, where the supports are partially constrained and allow only rotation in the vertical plane (y-direction), providing a way to examine the sensitivity of the structural response to different boundary condition assumptions.

Case 1: For a simple supported beam structure displacements and rotations are constrained in one side except the rotation in y direction and the other side the displacements and rotations are constrained except the displacement in x and the rotation in y, as can be seen in Table 35.

Table 35 Boundary conditions case 1

Translation &rotation direction	Constraining at x= 0	Constraining at x = L
u_x	0	Free
u_y	0	0
u_z	0	0
ϕ_x	0	0
ϕ_y	Free	Free
ϕ_z	0	0

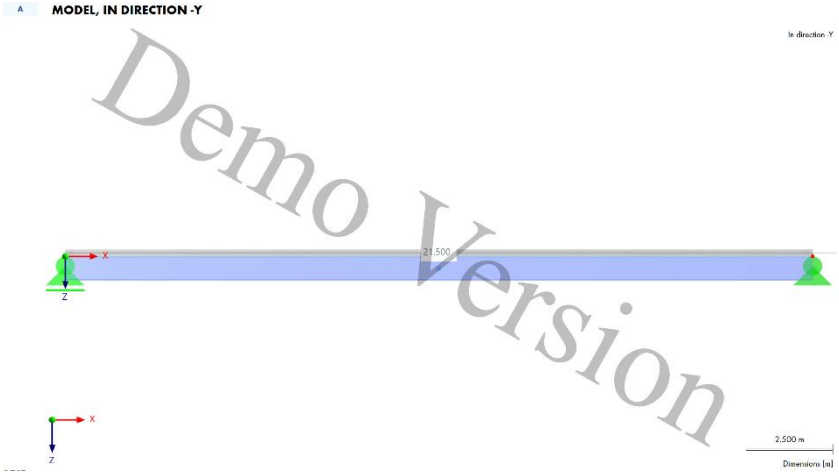

Figure 59 Schematization of boundary conditions of case 1

Case 2 will be to check the influence of this assumption by comparing it to fully constraining the displacements on both sides and the rotations while only allowing rotation in y direction, as can be seen in Table 36.

Table 36 Boundary conditions case 2

Translation &rotation direction	Constraining at x= 0	Constraining at x = L
u_x	0	0
u_y	0	0
u_z	0	0
ϕ_x	0	0
ϕ_y	Free	Free
ϕ_z	0	0

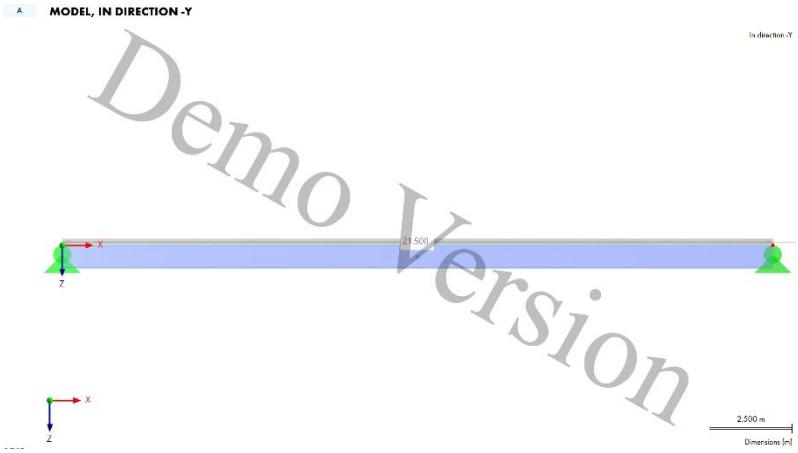

Figure 60 Schematization of boundary conditions of case 2

4.12.2 Displacement of the edge beam at midspan

The first verification of the model is to check whether the composite action between the concrete deck and the weathering steel beams is correctly represented. If the elements behave compositely, the displacements along the length of the structure should match. By plotting the displacement of the steel beam element and taking a section of the concrete surface element, it is possible to compare the displacements of the two elements along the length of the structure. In Figure 61 the displacement distribution of the beam member and the concrete surface element are given. It can be observed that both elements have the same displacement distribution over the length of the structure and also have the same maximum displacement of 19.9 mm at the midspan of the structure. From this observation it can be assumed that the two modeled elements are behaving as a fully connected composite beam element.

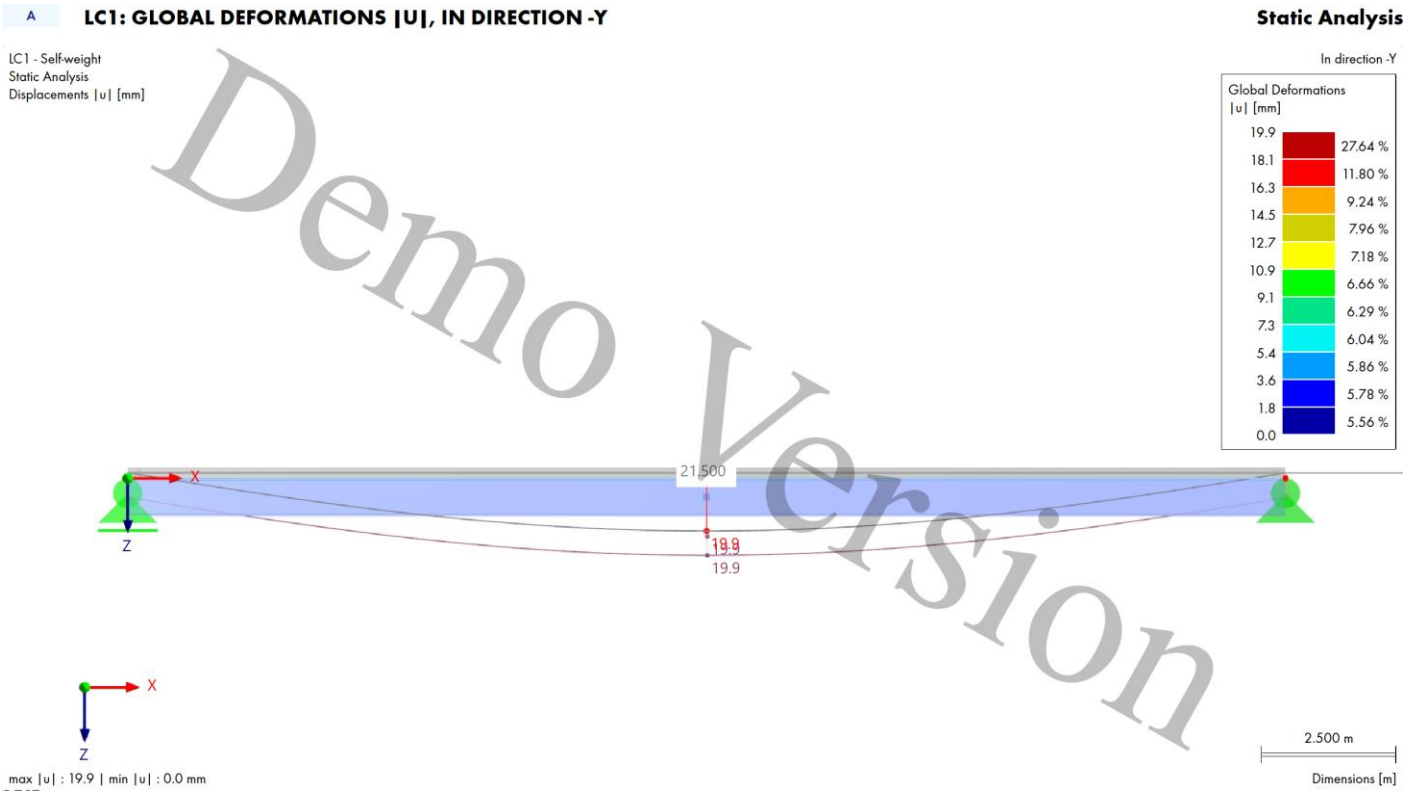

Figure 61 displacement behavior of the concrete surface element & the weathering steel member plotted together

Second, the maximum displacement should be compared with the displacement calculated from hand calculations. For the performance of the hand calculation the data in . is used. Hereby the moment of inertia, different q-loads are taken from the material properties of the modelled elements in RFEM to have a proper comparison. It is assumed that the elastic behavior of the steel will be the governing situation for the maximum displacement calculation of the structure. For the hand calculation the formula for the maximum displacement for a simply supported beam is taken. This is $w_{max} = \frac{5}{384} * \frac{ql^4}{EI}$. In table the comparison between the hand calculation and the outcome of RFEM is given Table 37. It can be observed that a difference in outcome of 2.8 % can be observed. This accuracy is smaller than 5% which is in line with the expectations. Therefore it can be stated that the displacement comparison of the model satisfies the expectations.

Table 37 Outcome wmax comparison betweent RFEM model and hand calculations

	Case 1 (ux free)	Case 2 (disp, constr)
$W_{max,RFem}$	**19.9 [mm]**	**18.9 [mm]**
$W_{max,HC}$	**19.4 [mm]**	**19.4 [mm]**
Difference between the outcomes	2.4%	2.3%

Below the full calculation will be given for the hand calculation performed for the determination of the deflection of the composite steel concrete beam and in case the steel concrete beams work as an non composite system to showcase the difference between these two and to confirm that the RFEM model works as a composite system. In the data used for performing the hand calculation is given, this is also the data taken into account in the RFEM Model.

Table 38 Data used for hand calculations

Parameter	Symbol	Value
Span	L	21.5 m = 21 500 mm
Steel modulus	E_s	210 GPa = 2.1 × 10^5 N/mm^2
Concrete modulus	E_c	35 GPa = 3.5 × 10^4 N/mm^2
Modular ratio	n= E_s/ E_c	6.0
Steel section area	A_s	30 640 mm^2
Steel section inertia	I_s	2.569 × 10^9 mm^4
Concrete slab width	b_c	1.425 m = 1425 mm
Concrete slab thickness	t_c	200 mm
Uniform load (self-weight)	q_{sf}	9.5 kN/m = 9.5 N/mm

4.12.2.1 Determination midspan deflection of composite beam

First it is needed to determine the neutral axis location of the elements separately where the top of the concrete slab will be taken as y = 0, where the positive axis points downwards. The results are given in Table 39.

Table 39 location of the neutral axis of the components relative to the top fiber of the concrete

Component	Limits [mm]	Centroid (y_i) [mm]
Concrete slab	0 → 200	100
Steel beam	200 → 900	550

For the composite action the concrete area needs to be transformed to an effective area for the composite action:

$$A_c' = \frac{b_c t_c}{n} = \frac{1425 * 200}{6} = 47500\ mm^2$$

The neutral axis location from the top will be:

$$y_{NA} = \frac{A_c' y_c + A_s y_s}{A_c' + A_s} = \frac{47500*100+30640*550}{47500+30640} = 277\ \text{mm}$$

Now the neutral axis location is clear it is possible to transform the concrete slab moment of inertia to the effective moment of inertia and determine the composite moment of inertia:

$$I_c' = \frac{b_c * t_c^3}{12 * n} = \frac{1425 * 200^3}{12 * 6} = 1.58 * 10^8\ mm^4$$

$$I_{comp} = I_c' + A_c'(y_c - y_{na})^2 + I_s + A_s(y_s - y_{na})^2$$

$$I_{comp} = 1.58 * 10^8 + 47500 * (100 - 277)^2 + 2.569 \times 10^9 + 30640(550 - 277)^2 = 6.50 * 10^9\ mm^4$$

Now the moment of inertia of the composite beam is determined it is possible to determine the deflection of the composite section:

$$w_{max} = \frac{5}{384} * \frac{q_{tot} * l^4}{EI_{comp}} = \frac{5}{384} * \frac{9.5 * 21500^4}{210000 * 6.50 * 10^9} = 19.4\ mm$$

4.12.2.2 Determination midspan deflection of non-composite beam

For the non-composite situation only the stiffness of the steel beams will contribute to the deflection resistance :

$$w_{max} = \frac{5}{384} * \frac{q_{tot} * l^4}{EI} = \frac{5}{384} * \frac{9.5 * 21500^4}{210000 * 2.569 * 10^9} = 49.2\ mm$$

4.12.2.3 Conclusion of the deflection verification

The deflection verification confirms that the RFEM model accurately represents the intended composite action between the concrete deck and the weathering steel beams. The displacement curves of the steel beam element and the concrete surface element are identical along the span, both reaching a maximum deflection at midspan of approximately 19.9 mm, demonstrating that the two components act together as a fully connected composite section.

When comparing RFEM results with the independent hand calculations, very good agreement is observed. In Case 1 (u_x free), the RFEM model produced a maximum deflection of 19.9 mm, while the hand calculation gave 19.4 mm, resulting in a difference of 2.4%. In Case 2 (displacement constrained), the RFEM deflection was 18.9 mm compared to the same 19.4 mm from the hand calculation, giving a difference of 2.3%.

These deviations are well below the acceptable tolerance of 5%, confirming that both model setups realistically capture the composite behavior and stiffness of the structure. Additionally, comparison with the non-composite steel-only scenario (49.2 mm deflection) shows a significant reduction in deflection about 60% lower when composite action is fully developed.

Therefore, it can be concluded that the RFEM model accurately reproduces the structural performance of a fully composite steel–concrete system, and both Case 1 and Case 2 satisfy the verification requirements.

4.12.3 Bending moment (Mxd+) verification

The bending moment verification of the structure is a more complex verification. This is due to the fact that the bending moment consists of several moments which should be accumulated to get the total bending moment at a certain cross-section. The bending moment in the midspan of the structure consists of the following components:

- Bending moment in the concrete layer
- Bending moment in the steel cross-section
- Bending moment due to the normal force in the concrete
- Bending moment due to the normal force in the steel cross-section

4.12.3.1 Bending moment in the concrete section

The concrete element is modelled as a surface element, therefore to determine the bending moment at a certain cross-section it is needed to integrate the observed bending moment over the effective width. In this structure it means the bending moment needs to be integrated over the total width of the concrete which is 1.425 m. At the midspan of the structure this results in a bending moment of 13.56 kNm as can be observed in Figure 62 and Figure 63.

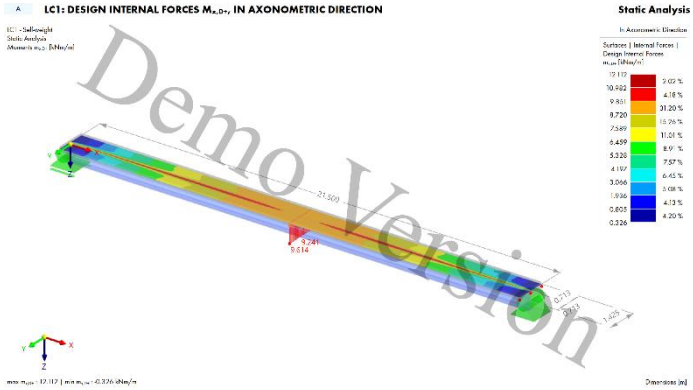

Figure 63 Moment distribution in the concrete layer due to self-weight of the structure

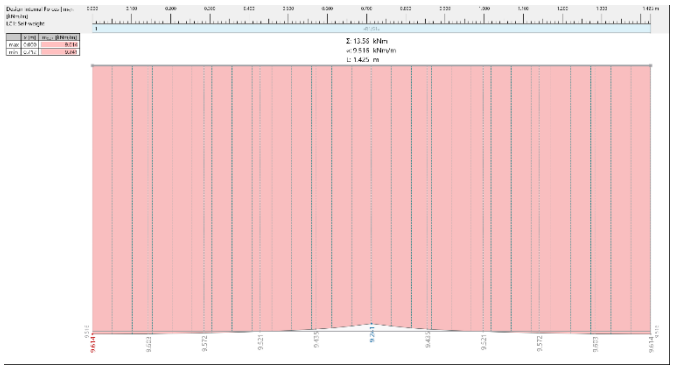

Figure 62 integration of the section in the concrete layer midspan of the structure

4.12.3.2 Bending moment in the steel section

The steel section is modeled as a member element therefore the observed bending moment at midspan of the structure is sufficient to have the effect bending moment. As can be observed in Figure 64, due to the self-weight of the structure a bending moment of 218 kNm can be observed.

Figure 64 Bending moment in the steel section due to the selfweight of the structure

4.12.3.3 Determination of the neutral axis

Before it will be possible to determine the bending moment due to the normal forces it is essential to determine the neutral axis of the structure due to the working internal normal forces in the structure, This is essential since the bending moments due to the internal forces is dependent of the location of the neutral axis. Different internal force distributions can be observed if the neutral axis is in the concrete layer, the upper flange of the steel section or the web of the steel section.

To determine the location of the neutral axis the internal forces should be determined. From RFEM the internal forces can be obtained. In the concrete section it is needed to integrate the normal force at the middle of the section over the width of the section to get the total internal normal force at the middle of the section. As can be observed in Figure 65 and Figure 66 a normal force can be observed of 710 kN.

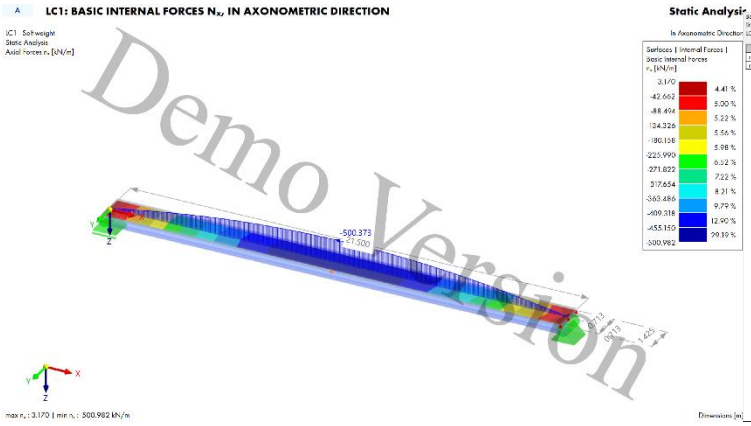

Figure 66 Normal force distribution due to selfweight in the concrete section

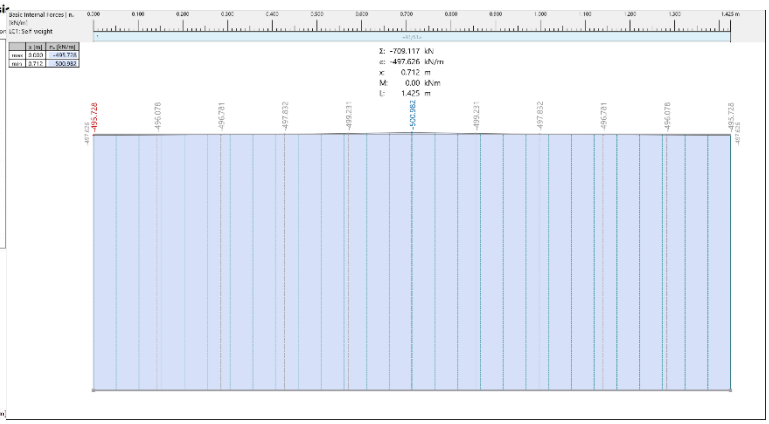

Figure 65 Integration of the normal force over the width of the sconcrete section

Regarding the steel section as it is modeled as a member the normal force at the middle of the section can be directly observed from RFem as can be seen in Figure 67, this results in a normal force of 710 kNm.

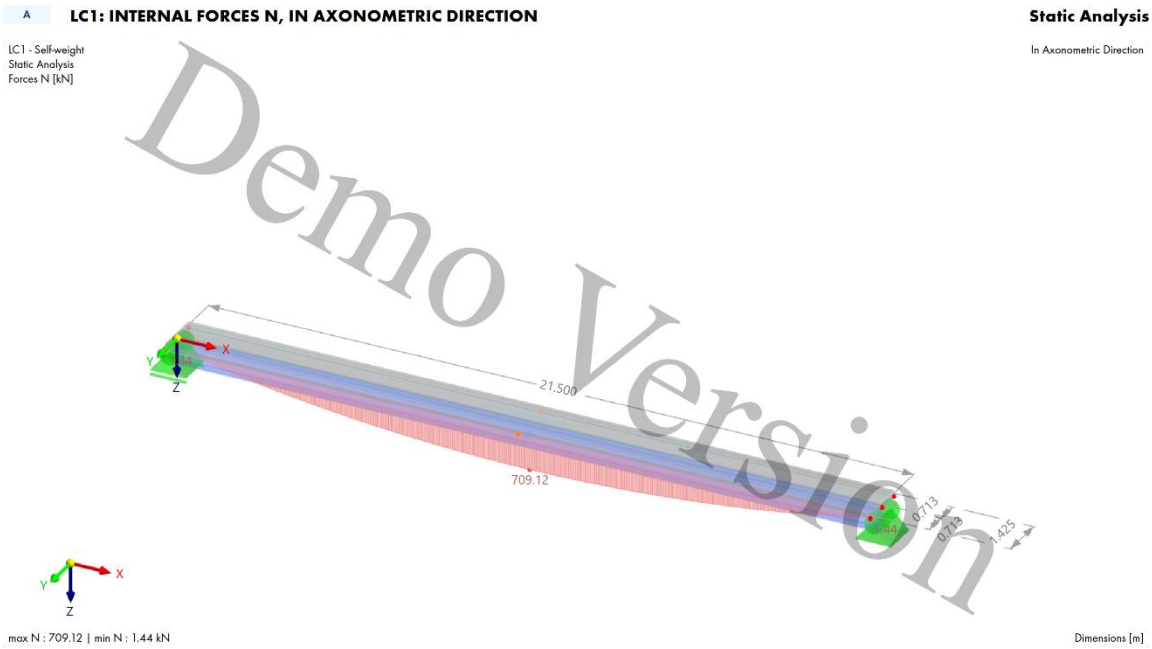

Figure 67 Normal force distribution of the steel section

The neutral axis can be determined by computing the normal force contribution of each component and by ensuring horizontal equilibrium the neutral axis can be determined as can be observed in and Figure 68:

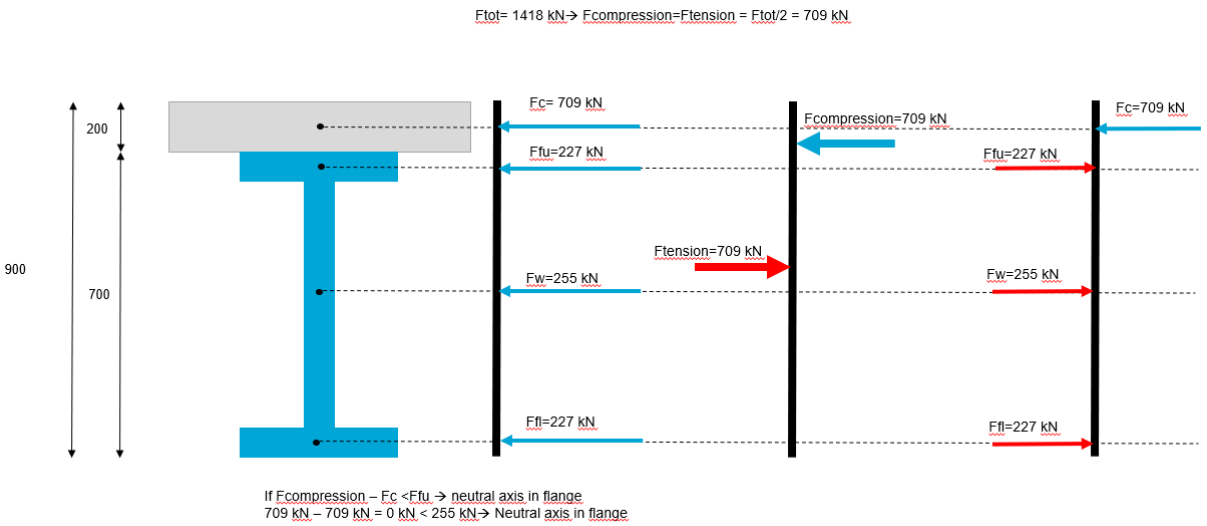

Figure 68 visualization of internal force equillibrium

Table 40 Internal force equillibrium

Force type	Force [kN] case 1	Force [kN] case 2
Normal force concrete section	709	504
Normal force in upper steel flange	227	254
Normal force in steel web	255	286
Normal force in lower steel flange	227	254
Total internal force	1418	1298
Total force in compression needed for horizontal equillibrium	709	649
Normal force upper flange in compression	0	145
Normal force upper flange in tension	227	109

Since the stress distribution is assumed to be constant over the thickness of the flange the force proportion can be used to determine the location of the neutral axis in the flange, so

$$\frac{F_{comp,flange}}{F_{total,flange}} * t_f = n.a._{flange} = \quad \frac{0}{227} * 25 = 0\ mm$$

which means that the neutral axis is exactly at the transition zone between the concrete and the upper steel flange.

4.12.3.4 Bending moment due to internal normal forces

Since the neutral axis of the composite system is in the upper flange, the stress distribution and the formulas in in Figure 70 can be used to determine the internal moment due to the internal normal forces. The used formulas are deduced from the internal stresses decomposition as can be seen in Figure 69.

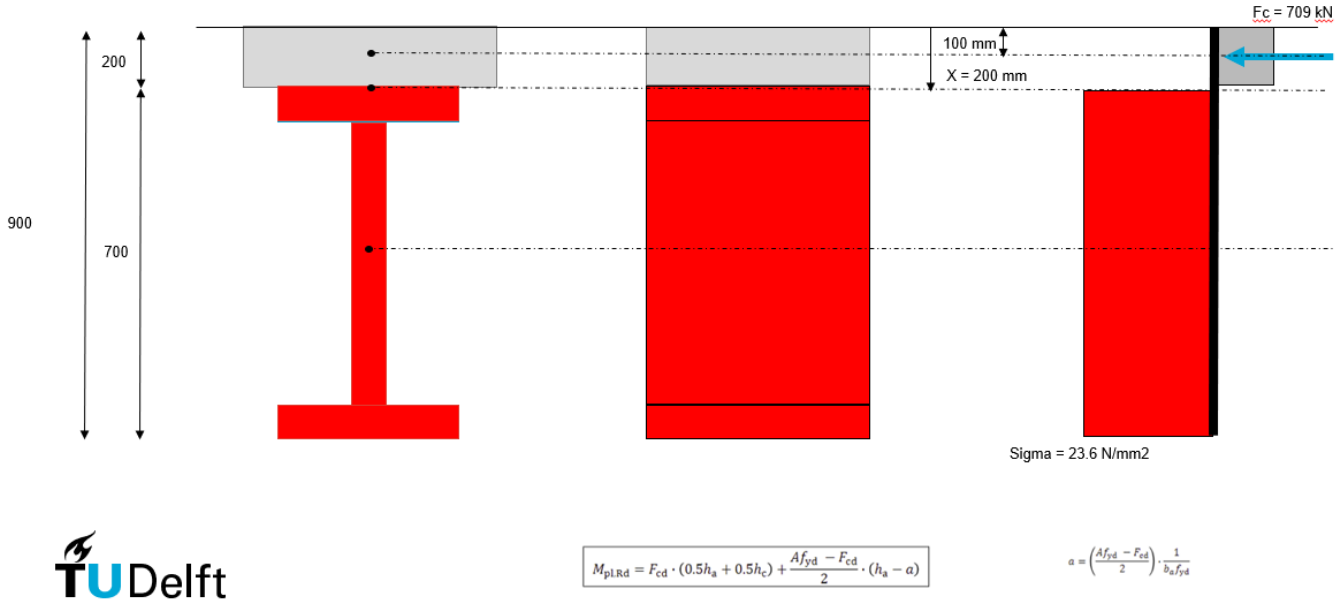

Figure 70 Stress distribution of cross-section at midspan of the structure

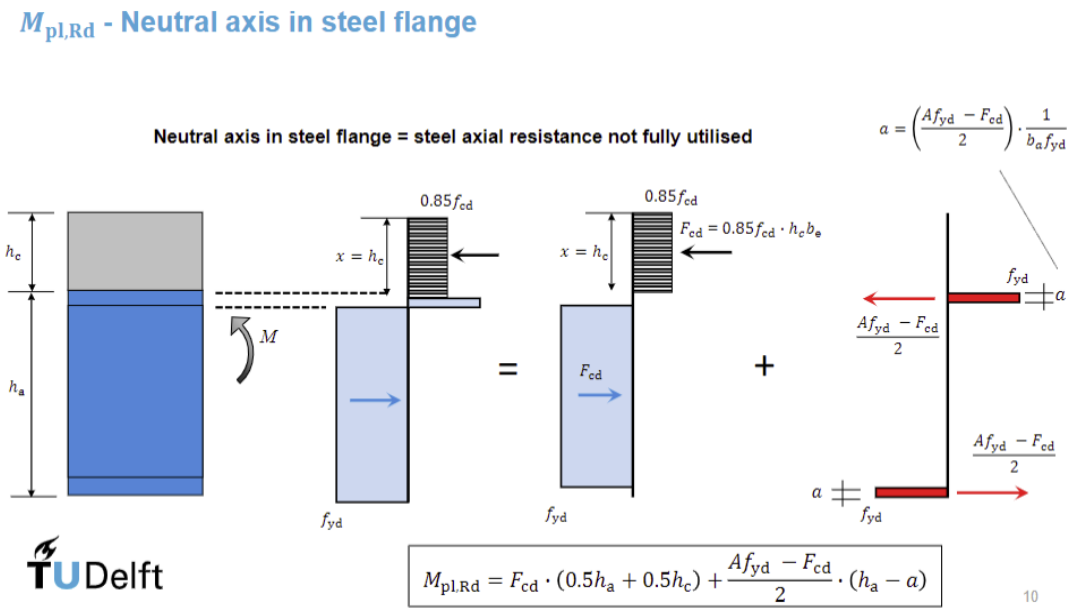

Figure 69 Internal stress decomposition (Kavoura, 2023)

In the total internal moment due to the internal normal forces at the midspan of the structure is determined. This results in a bending moment of $M_{pl,Ed} = 319\ kNm$ for case 1 and $M_{pl,Ed} = 321\ kNm$for case 2, herefore the parameters in Table 41 have been used, to fill in the formula below determined from Figure 69 and Figure 70.

$$\mathbf{M_{pl,Rd}} = \mathbf{F_{cd}} * (\mathbf{0.5h_a} + \mathbf{0.5h_c}) + (\frac{\mathbf{A_s f_{yd}} - \mathbf{F_{cd}}}{\mathbf{2}}) * (\mathbf{h_a} - \mathbf{a})$$

Table 41 determination in moment due to internal forces

	Case 1	Case 2
Stress in steel section due to normal force f_s	23.62 [N/mm²]	26.5 [N/mm²]
Area of steel section A	30012 [mm²]	30012 [mm²]
Normal compression force concrete F_c	709 [kN]	504 [kN]
Width of upper flange b_f	300 [mm]	300 [mm]
Height of steel part h_a	700 [mm]	700 [mm]
Height of concrete section	200 [mm]	200 [mm]
a	50 [mm]	50 [mm]
Internal moment due to internal forces	319 [kNm]	321 [kNm]

Bending moment verification

The bending moment verification can be performed by determining first the total bending moment due to the internal forces and the external working bending moments. This should be compared with the bending moment due to the self-weight of the structure at midspan of the structure, which can be determined by making use of the formula.

$$M_{hc} = \frac{1}{8} * q_{sf,tot} * l^2 = \frac{1}{8} * 9.53 * 21.5^2 = 550\ kNm.$$

This verification has been done in Table 42 from this verification it can be concluded that the model is behaving as expected regarding the bending moment distribution, since the verification made clear that there is a negligible difference between the outcome from the RFEM model and the outcome of the hand calculation by 0.017%.

Table 42 bending moment verification

	Case 1	Case 2
$M_{external,\ concrete}$	13.7 [kNm]	13 [kNm]
$M_{external,\ steel}$	218 [kNm]	209 [kNm]
$M_{internal,total}$	319 [kNm]	321 [kNm]
$M_{Total,rfem}$	**550,75 [kNm]**	**543 [kNm]**
M_{hc}	**550 [kNm]**	**550 [kNm]**
Difference between the outcomes	-0.017%	1.4%

4.12.4 Vertical shear force verification in longitudinal direction

The vertical shear force verification can be performed by comparing the reaction forces at the support of the structure with the force determined by the formula $V_{Ed} = 0.5 * q_{tot} * L = 0.5 * 9.53 * 21.5 = 102.45\ kN$. The reaction forces in the RFEM model can be observed in Figure 71. This comparison has been done in Table 43, which shows that the outcomes are identical, which means that the regarding the vertical shear force the model is behaving as expected.

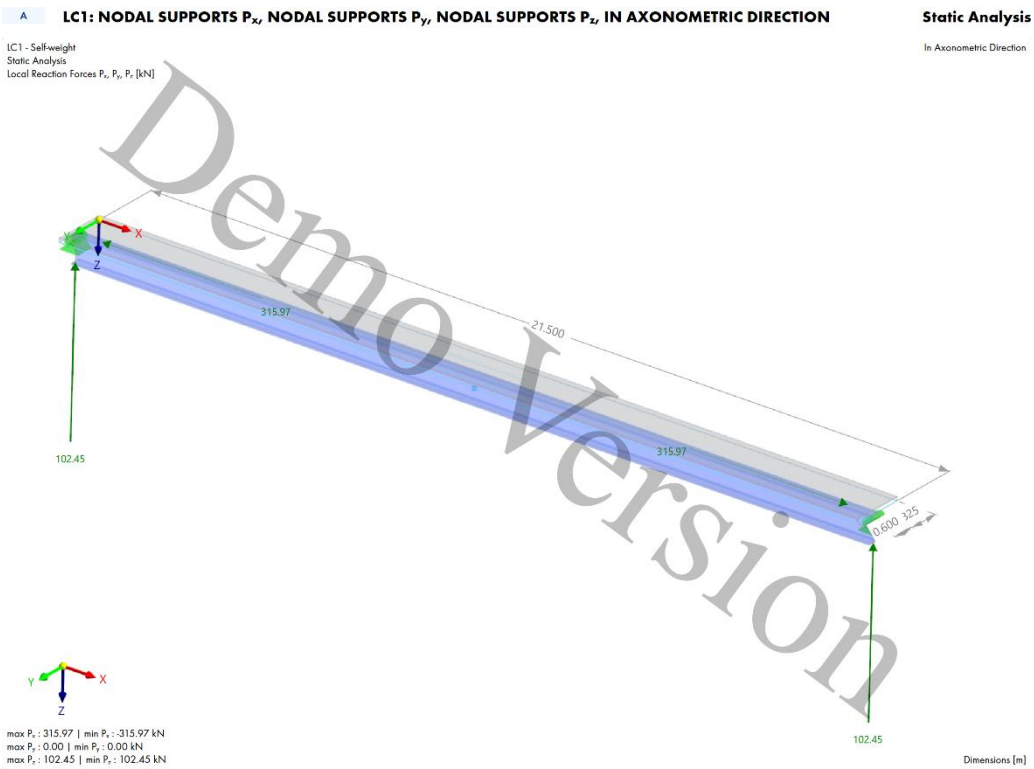

Figure 71 Reaction forces at the support

Table 43 Vertical shear force verification

	Case 1	Case 2
Reaction force RFEM	**102.45 [kN]**	**102.45 [kN]**
V_{ED} hand calculation	**102.45 [kN]**	**102.45 [kN]**
Difference between the outcomes	0.0024%	0.0024%

4.12.5 Overall conclusion of the verification of the model

After verifying the model's displacement, bending moment, and vertical shear force, it can be concluded that the results closely match those obtained from hand calculations. The differences are minimal, indicating that the model behaves as expected and is therefore suitable for subsequent calculations aimed at optimizing the structure's cross-sectional properties.

When comparing Case 1 and Case 2, it is evident that over-constraining the structure in Case 2 leads to an underestimation of deflection. However, the deviation remains within the acceptable range defined for deflection verification. In contrast, allowing displacement in the x-direction at one boundary in Case 1 results in a slight overestimation of deflection, which also stays within the admissible limits.

In terms of bending moment comparison, Case 1 shows a significant improvement, with only a 0.017% difference from the hand-calculated result. Case 2, due to the over-constraining, slightly underestimates the bending moment, yet this result is still within the accepted tolerance.

For vertical shear force verification, both Case 1 and Case 2 demonstrate a high level of accuracy, with only a 0.0024% deviation from the hand calculations.
The up following structural analysis will work with the boundary conditions of Case 1, since these boundary conditions simulate the reality the best.

5 Design calculations

5.1 Method

In this chapter the determined modelling considerations will be used to calculate the different effect and resistance of the structure. As mentioned in the modelling sequences different variants will be considered and different parameters will be varied to come up with the optimal design of the superstructure. In Table 44 the different modelling variants that will be considered are summarized, within these variants there will also be varied in the steel strength parameters, S235, S355 and S460 will be considered. In this chapter the full design calculation will be done for one variant namely the superstructure with a center to center distance of 1.5m and an HEB700 profile for the steel class S235. This will be done so the performed steps are clear for understanding. In another paragraph all the results of the different variants will be given and discussed.

Table 44 modelling variants

Centre to centre distance	S235/S355/S460 Edge distance HEB600B	Edge distance HEB700B	Edge distance HEB800B
1.5m	1.2 m	1.2 m	1.2 m
2m	1.2 m	1.2m	1.2 m
2.5m	0.95 m	0.95 m	0.95 m

5.2 Cross-sectional properties HEB 600B/700B/800B and concrete layer

Table 45 cross-sectional properties HEB 600B and concrete layer

Properties steel beam		
Material properties		
Steel class	-	*S235/S355/S460*
Elastic modulus	E_s	*210000 [N/mm²]*
Dimensional properties steel beam		
Part 1 (lower flange)		
Width lower flance	b_1	*300 [mm]*
Thickness lower flance	d_1	*32 [mm]*
Area part 1	A_1	*8344 [mm²]*
Neutral axis part 1	zw_1	*16 [mm]*
Part 2 (Web)		
Height web	h_2	*582 [mm]*
Thickness web	d_2	*17 [mm]*
Area part 2	A_2	*8019[mm²]*
Neutral axis part 2	Zw_2	*350 [mm]*
Part 3 (upper flange)		
Width upper flance	b_3	*300 [mm]*
Thickness upper flance	d_3	*32 [mm]*
Area part 3	A_3	*8344 [mm²]*
Neutral axis part 3	Zw_3	*684 [mm]*
Total area steel	A_s	*30640 [mm²]*
Moment of Inertia steel	I_s	*2569000000 [mm³]*
Dimensional properties concrete		
Thickness concrete	t	*200 [mm]*
Total area concrete	A_s	*2880000 [mm²]*
Moment of Inertia concrete	I_c	*9.6*10⁶ [mm³]*

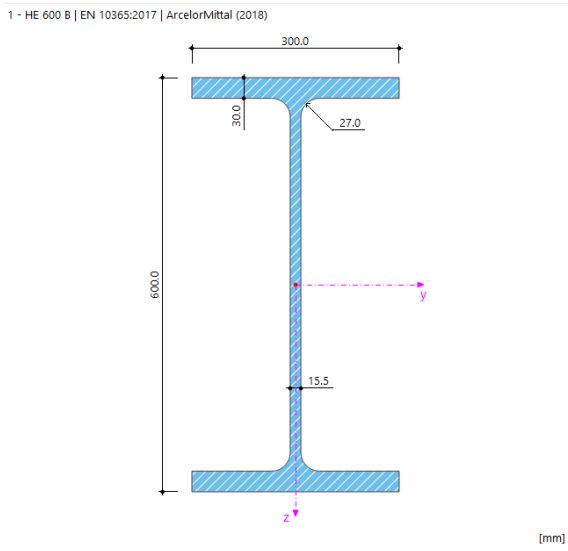

Figure 72 Cross-section HEB600B

Table 46 cross-sectional properties HEB 700B and concrete layer

Properties steel beam		
Material properties		
Steel class	**-**	*S235/S355/S460*
Elastic modulus	E_s	*210000 [N/mm²]*
Dimensional properties steel beam		
Part 1 (lower flange)		
Width lower flance	b_1	*300 [mm]*
Thickness lower flance	d_1	*30 [mm]*
Area part 1	A_1	*9600 [mm²]*
Neutral axis part 1	zw_1	*15 [mm]*
Part 2 (Web)		
Height web	h_2	*486 [mm]*
Thickness web	d_2	*15.5 [mm]*
Area part 2	A_2	*11352 [mm²]*
Neutral axis part 2	Zw_2	*273 [mm]*
Part 3 (upper flange)		
Width upper flance	b_3	*300 [mm]*
Thickness upper flance	d_3	*30 [mm]*
Area part 3	A_3	*9600 [mm²]*
Neutral axis part 3	Zw_3	*531 [mm]*
Total area steel	A_s	*27000 [mm²]*
Moment of Inertia steel	I_s	*1710000000 [mm⁴]*
Dimensional properties concrete		
Thickness concrete	**t**	*200 [mm]*
Total area concrete	A_s	*2880000 [mm²]*
Moment of Inertia concrete	I_c	*9.6*10⁶ [mm³]*

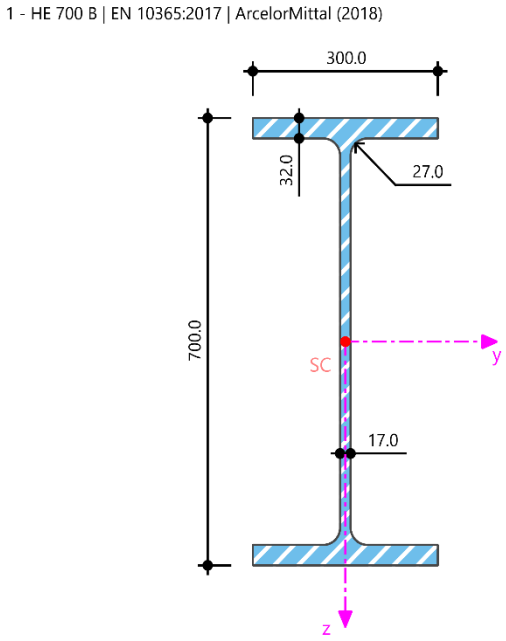

Figure 73 Cross-section HEB700B

Table 47 cross-sectional properties HEB 800B and concrete layer

Properties steel beam		
Material properties		
Steel class	**-**	*S235/S355/S460*
Elastic modulus	E_s	*210000 [N/mm²]*
Dimensional properties steel beam		
Part 1 (lower flange)		
Width lower flance	b_1	*300 [mm]*
Thickness lower flance	d_1	*33 [mm]*
Area part 1	A_1	*9900 [mm²]*
Neutral axis part 1	zw_1	*16.5 [mm]*
Part 2 (Web)		
Height web	h_2	*674 [mm]*
Thickness web	d_2	*17.5 [mm]*
Area part 2	A_2	*13620[mm²]*
Neutral axis part 2	Zw_2	*370 [mm]*
Part 3 (upper flange)		
Width upper flance	b_3	*300 [mm]*
Thickness upper flance	d_3	*33 [mm]*
Area part 3	A_3	*9900 [mm²]*
Neutral axis part 3	Zw_3	*723.5 [mm]*
Total area steel	A_s	*33420 [mm²]*
Moment of Inertia steel	I_s	*3591000000 [mm³]*
Dimensional properties concrete		
Thickness concrete	**t**	*200 [mm]*
Total area concrete	A_s	*2880000 [mm²]*
Moment of Inertia concrete	I_c	*9.6*10⁶ [mm³]*

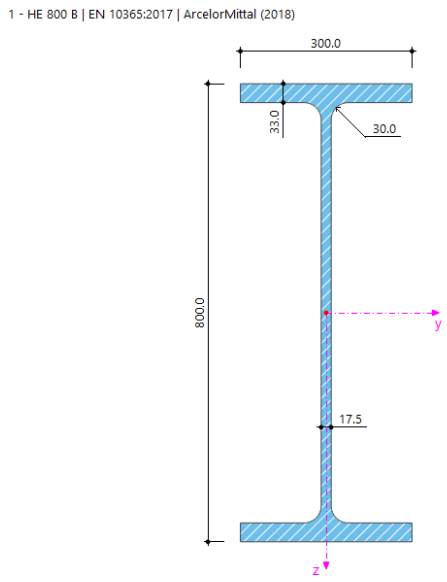

Figure 74 Cross-section HEB800B

5.3 *Effective width as consequence of the shear lag*

In composite steel-concrete beams, the effective width of the concrete flange must be considered in the design to account for shear lag. Shear lag reduces the contribution of the concrete flange in transferring longitudinal stresses, particularly in wide flanges. According to Eurocode 4 (EN 1994-1-1), the effective width depends on span, spacing between beams, and the location of the section (midspan or support, edge or interior beam). The formulas below are used to determine the effective widths for different beam configurations.

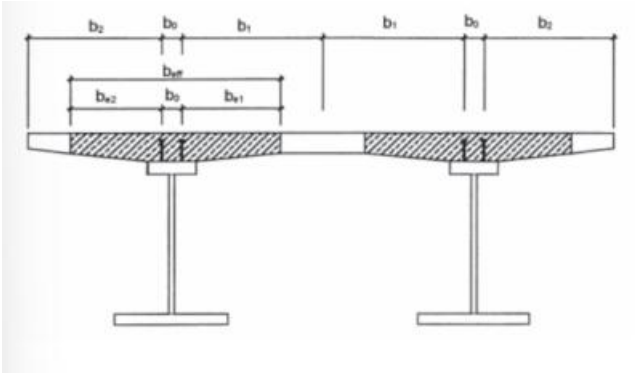

Figure 75 Effective width determination shear leg

Table 48 General parameters for shear leg determination

description	symbol	value	unit
Width of top flange	b0=	300	mm
Total span	L=	21.5	m
Effective length = 0.85*L	Le=	18.275	m
spacing	s=	1.5	m
available concrete width per side ($b_i = \frac{s}{2} - \frac{b_0}{2}$)	bi=	0.6	m
theoretical max effective width ($bei = min(\frac{L_e}{8}, b_i)$)	bei=	0.6	m

Table 49 effective width at midspan of the edge beam

description	symbol	value	unit
distance from centre beam to edge at least 1:1	e=	1200	mm
from outer flange to edge $b_{ei,outer} = e - \frac{b_0}{2}$	bei,outer=	1.05	m
from inner side to next beam $b_{ei,inner} = \frac{s}{2} - \frac{b_0}{2}$	bei,inner=	0.6	m
eff width midspan edge $b_{eff,mid,edge} = b_0 + b_{ei,outer} + b_{ei,inner}$	beff,mid,edge=	**1.95**	m

Table 50 effective width interior beam at midspan

description	symbol	value	unit
Effective widt interior beam $b_{eff,mid,int} = b_o + 2 * b_{ei}$	$b_{eff,mid,int}$	**1.5**	**m**

Table 51 effective width edge beam at endsupport

description	symbol	value	unit
$\beta_i = 0.55 + 0.025 * \frac{L_e}{b_{ei}}$	β_i=	1	m
Effective widt at end support $b_{eff,sup,edge} = b_0 + \sum \beta_i * b_{ei}$	$b_{eff,sup,edge} =$	**1.95**	**m**

Table 52 effective width interior beam at endsupport

description	symbol	value	unit
$\beta_i = 0.55 + 0.025 * \frac{L_e}{b_{ei}}$	β_i=	1	m
Effective widt at end support $b_{eff,sup,int} = b_0 + \sum \beta_i * b_{ei}$	$b_{eff,sup,int} =$	**1.5**	**m**

In Table 49 to Table 52 the effective widths have been determined of the edge beam and the interior beams at midspan and at the support. These results can be used to determine the composite moments of inertia at this location for the composite structure. With this moment of inertia the bending moment resistances can be determined of the structure while including the shear leg effect. As can be seen in Table 48 the effective width has only be determined for the variant with a centre to centre distance of 1.5 m. In the upcoming calculations the different variants will be considered, therefore in Table 53 the effective widths due to the shear leg effect are given for a spacing of 1.5m, 2m and 2.5m.

Table 53 Effective widths due to shear leg effect for the spacing of 1.5m, 2m and 2.5 m

description	symbol	Spacing = 1.5 m	Spacing = 2 m	Spacing = 2.5 m	unit
eff width midspan edge $b_{eff,mid,edge} = b_0 + b_{ei,outer} + b_{ei,inner}$	beff,mid,edge=	1.95	2.2	2.2	m
Effective widt interior beam $b_{eff,mid,int} = b_o + 2 * b_{ei}$	$b_{eff,mid,int}$	1.5	2	2.5	m
Effective widt at end support $b_{eff,sup,edge} = b_0 + \sum \beta_i * b_{ei}$	$b_{eff,sup,edge} =$	1.95	2.2	2.2	m
Effective widt at end support $b_{eff,sup,int} = b_0 + \sum \beta_i * b_{ei}$	$b_{eff,sup,int} =$	1.5	2	2.4	m

5.4 Classification of cross section

To determine the appropriate type of analysis, the cross-section must first be classified. This classification is carried out in accordance with Table 5.2 of NEN-EN 1993-1-1+C2+A1:2016. Below, the classification calculation is demonstrated for a HEB700B beam made of S235 steel, to illustrate the procedure.

Table 54 according to table 5.2 of NEN-EN 1993-1-1+C2+A1:2016

Tabel 5.2 (blad 2 van 3) — Maximale breedte-dikteverhoudingen voor op druk belaste onderdelen

Uitkragende flenzen			
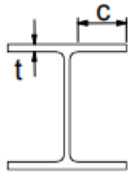	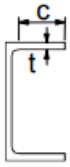	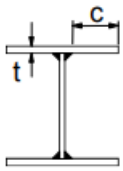	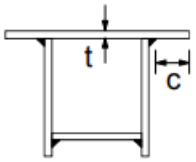
Gewalste profielen		Gelaste profielen	

Klasse	Onderdeel belast op druk	Onderdeel belast op druk en buiging	
		Uiterste vezel onder druk	Uiterste vezel onder trek
Spannings-verdeling in de onderdelen (druk is positief)	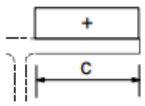	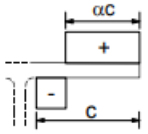	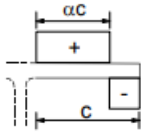
1	$c/t \le 9\varepsilon$	$c/t \le \frac{9\varepsilon}{\alpha}$	$c/t \le \frac{9\varepsilon}{\alpha\sqrt{\alpha}}$
2	$c/t \le 10\varepsilon$	$c/t \le \frac{10\varepsilon}{\alpha}$	$c/t \le \frac{10\varepsilon}{\alpha\sqrt{\alpha}}$
Spannings-verdeling in de onderdelen (druk is positief)	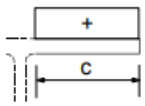	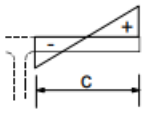	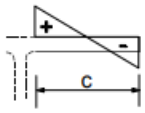
3	$c/t \le 14\varepsilon$	$c/t \le 21\varepsilon\sqrt{k_\sigma}$ Voor k_σ zie EN 1993-1-5	

$\varepsilon = \sqrt{235/f_y}$	f_y	235	275	355	420	460
	ε	1,00	0,92	0,81	0,75	0,71

Hereby it is assumed that the top flange will be fully in compression. By making use of the classification properties determined in chapter 5.2 The cross section can be classified.

Regarding the flange of the structure with an assumed throat thickness of a = 5 mm the formula for c will be:

$$\boldsymbol{c = \frac{b - 2 * t_w - 2 * a * \sqrt{2}}{2} = \frac{300 - 2 * 17 - 2 * 5 * \sqrt{2}}{2} = 134.4\ mm}$$

With $\frac{c}{t} = 4.2 < 9\varepsilon = 9 * 0.81 = 7.3$ the flange can be classified as a <u>class 1 section.</u>

Regarding the web of the structure with an assumed throat thickness of a = 5 mm the formula for c will be:

$$\boldsymbol{c = h_a - 2 * t_f - 2 * a * \sqrt{2} = 700 - 2 * 32 - 2 * 5 * \sqrt{2} = 621.86\ mm}\ (11)$$

With $\frac{c}{t_w} = 36.58 < 72\varepsilon = 72 * 0.81 = 58.32$ the cross section can be classified as a <u>class 1 section</u>.

Since both the flanges as the web can be classified as class 1 the total cross-section will be classified as class 1. Above the calculation is given for the HEB700B profile, in this study also the HEB 600B and HEB 800B will be considered for the steel classes S235, S355 and S460. The results of the classification of these profiles are given in Table 55.

Table 55 Result of the classification of the different profiles for the different steel grades

Profile	S235	S355	S460
HEB600B	Class 1	Class 1	Class 1
HEB700B	Class 1	Class 1	Class 1
HEB800B	Class 1	Class 1	Class 1

5.5 Elastic design

For the elastic design several verifications need to be performed, first the phase 1 and Phase 2 need to be considered for the elastic design. These are the cases when no composite action is taken into account and the beams are loaded due to self weight and or the weight of wet reinforced concrete. In the elastic verification the following verification will be performed:

- Bending moment verification
- Shear force verification
- Displacement verification

5.5.1 Elastic Bending moment verification

The elastic bending moment resistance of the cross-section can be calculated by making use of the following formula:

$$M_{el,Rd} = \frac{W_{el} * f_{yd}}{\gamma_{M0}}$$

$$f_{yd} = yield\ strength\ of\ the\ steel$$

$$W_{el} = \frac{I_y}{y_{max}}\ Elastic\ section\ modulus$$

$$\gamma_{M0} = Partial\ safety\ factor\ for\ resistance\ of\ cross-sections\ , \gamma_{M0} = 1.0$$

Table 56 Elastic moment resistances of the different steel profiles for the different yield strengths

Profile	S235	S355	S460	unit
HEB600B	1340	2025	2620	kNm
HEB700B	1725	2605	3375	kNm
HEB800B	2110	3185	4130	kNm

For the elastic design Phase 2 will be the governing situation where the beams are working as incomposite beams with a load on the beams due to the wet reinforced concrete. The governing situation will be when the effective width of the wet reinforcement concrete is at its maximum. For the different variants this has been determined in Table 53. In Table 57 the bending moment verifications have been performed for the incomposite action of the steel beams. The formula used to determine the bending moment effect on the steel beams is given by:

$$M_{el,Ed} = \frac{1}{8} * (q_c + q_s) * L^2$$

$$q_c = line\ load\ of\ reinforced\ wet\ concrete\ for\ the\ maximum\ b_{eff}$$

$$q_s = Line\ load\ of\ the\ steel\ beam$$

$$L = length\ of\ the\ steel\ beam$$

Table 57 Bending moment verifications incomposite action steel beams for c.t.c. of 1.5m ($b_{eff,max}$ = 1.95 m)

Profile	S235			S355			S460		
	$M_{el,Ed}$ [kNm]	$M_{el,Rd}$ [kNm]	U.C [-]	$M_{el,Ed}$ [kNm]	$M_{el,Rd}$ [kNm]	U.C [-]	$M_{el,Ed}$ [kNm]	$M_{el,Rd}$ [kNm]	U.C [-]
HEB600B	685	1340	0.51	685	2025	0.34	685	2620	0.26
HEB700B	702	1725	0.41	702	2605	0.27	702	3375	0.21
HEB800B	715	2110	0.34	715	3185	0.22	715	4130	0.17

Table 58 Bending moment verifications incomposite action steel beams for c.t.c. of 2.0 m ($b_{eff,max}$ = 2.2 m)

Profile	S235			S355			S460		
	$M_{el,Ed}$ [kNm]	$M_{el,Rd}$ [kNm]	U.C [-]	$M_{el,Ed}$ [kNm]	$M_{el,Rd}$ [kNm]	U.C [-]	$M_{el,Ed}$ [kNm]	$M_{el,Rd}$ [kNm]	U.C [-]
HEB600B	758	1340	0.57	758	2025	0.37	758	2620	0.29
HEB700B	775	1725	0.45	775	2605	0.30	775	3375	0.23
HEB800B	787	2110	0.37	787	3185	0.24	787	4130	0.19

Table 59 Bending moment verifications incomposite action steel beams for c.t.c. of 2.5m ($b_{eff,max}$ = 2.5 m)

Profile	S235			S355			S460		
	$M_{el,Ed}$ [kNm]	$M_{el,Rd}$ [kNm]	U.C [-]	$M_{el,Ed}$ [kNm]	$M_{el,Rd}$ [kNm]	U.C [-]	$M_{el,Ed}$ [kNm]	$M_{el,Rd}$ [kNm]	U.C [-]
HEB600B	845	1340	0.63	845	2025	0.42	845	2620	0.32
HEB700B	861	1725	0.50	861	2605	0.33	861	3375	0.26
HEB800B	874	2110	0.41	874	3185	0.27	874	4130	0.21

5.5.2 Vertical shear force resistance

The vertical shear force resistance for the different cross sections can be determined by the formula:

$$\tau_{Rd} = \frac{f_{yd}}{\sqrt{3} * \gamma_{M0}}$$

$$f_{yd} = yield\ strength\ of\ the\ steel$$

$$\gamma_{M0} = Partial\ safety\ factor\ for\ resistance\ of\ cross - sections\ , \gamma_{M0} = 1.25$$

Table 60 Elastic vertical shear resistance of the different steel profiles for the different yield strengths

Profile	S235	S355	S460	unit
HEB600B	119	164	212	N/mm²
HEB700B	119	164	212	N/mm²
HEB800B	119	164	212	N/mm²

The shear force effect will be deduced from the RFEM models hereby the maximum governing load in the ULS from the different load combinations will be used. This force needs to be converted to a shear stress, this can be done by the following formula:

$$\tau_{Ed} = \frac{V_{ED}}{A_w}$$

$$V_{Ed} = Maximum\ shear\ force\ due\ to\ the\ governing\ load\ combination\ in\ ULS$$

$$A_w = Area\ of\ the\ web$$

For the vertical shear it has been chosen to check only the governing situation for all the variants if this situation satisfies the verification it means all the other variants will satisfy. The governing situation will be for the smallest steel profile with the biggest maximum effective width. This will be for the HEB600B profile with a c.t.c. of 2.5 m which also results in a $b_{eff,max}$ =2.5 m. As can be seen in Table 61, this variant satisfies the verification criteria therefore automatically all the other variants satisfy the verification criteria.

Table 61 Verification of vertical shear force of governing beam for a centre to centre distance of 2.5 m ($b_{eff,max}$ = 2.5 m)

Profile	S235				S355				S460			
	V_{Ed} [kNm]	τ_{Ed} [N/mm²]	τ_{Rd} [N/mm²]	U.C [-]	V_{Ed} [kNm]	τ_{Ed} [N/mm²]	τ_{Rd} [N/mm²]	U.C [-]	V_{Ed} [kNm]	τ_{Ed} [N/mm²]	τ_{Rd} [N/mm²]	U.C [-]
HEB600B	155	21	109	0.19	155	21	164	0.12	155	21	212	0.1

5.5.3 Deflection verification

According to the NEN-EN 1990+A1+A1/C2:2019/NB:2019 nl the deflection restrictions are mentioned for bridge decks. Hereby in A2.4.4.3 the maximum total vertical deflection should be taken as L/500. For the maximum allowable deflection due to traffic load only it is stated that maximum deflection is permitted of L/250.
To satisfy these criteria it is necessary to make use of precambering of the steel beams. The steel beams will be precambered such that the deflection to the loading of phase 2 (reinforced wet concrete + steel beams) will be neutralized. To determine the needed precambering the deflection due to this loading needs to be determined. This has been done in Table 62 to Table 64. These precambering will be used for the SLS deflection verification of phase 3.

$$u_{tot} = \frac{5}{384} * \frac{(q_c + q_s) * L^4}{EI}$$
$$q_c = line\ load\ of\ reinforced\ wet\ concrete\ for\ the\ maximum\ b_{eff}$$
$$q_s = Line\ load\ of\ the\ steel\ beam$$
$$L = length\ of\ the\ steel\ beam$$
$$E = 210000 \frac{N}{mm^2}\ Elasticity\ modulus$$
$$I = moment\ of\ inertia\ steel\ beams$$

Table 62 Verification of the deflection phase to for a ctc distance of 1.5m ($b_{eff,max}$ = 1.95 m)

Profile	S235/S355/S460				
	$u_{tot,P2}$ [mm]	$u_{precamb}$ [mm]	u_{net} [mm]	u_{max} [mm]	U.C [-]
HEB600B	**92**	**92**	**0**	**43**	**0**
HEB700B	**63**	**63**	**0**	**43**	**0**
HEB800B	**46**	**46**	**0**	**43**	**0**

Table 63 Verification of the deflection phase to for a ctc distance of 2.0 m ($b_{eff,max}$ = 2.2 m)

Profile	S235/S355/S460				
	$u_{tot,P2}$ [mm]	$u_{precamb}$ [mm]	u_{net} [mm]	u_{max} [mm]	U.C [-]
HEB600B	**101**	**101**	**0**	**43**	**0**
HEB700B	**69**	**69**	**0**	**43**	**0**
HEB800B	**50**	**50**	**0**	**43**	**0**

Table 64 Verification of the deflection phase to for a ctc distance of 2.5m ($b_{eff,max}$ = 2.5 m)

Profile	S235/S355/S460				
	$u_{tot,P2}$ [mm]	$u_{precamb}$ [mm]	u_{net} [mm]	u_{max} [mm]	U.C [-]
HEB600B	**113**	**113**	**0**	**43**	**0**
HEB700B	**77**	**77**	**0**	**43**	**0**
HEB800B	**56**	**56**	**0**	**43**	**0**

5.5.4 Conclusion Elastic design

The elastic design was carried out for the governing conditions of Phase 1 and Phase 2, when composite action between the concrete and steel beams has not yet been achieved. The analysis focused solely on the steel beams, as these are the elements relevant to the experimental part of this research. The results of the elastic design show that the steel beams meet all verification requirements. For the displacement verification, precambering was required to ensure that the (weathering) steel elements satisfy the criteria. It should be noted that this verification is identical for weathering steel and conventional steel beams, since during Phase 1 and Phase 2 no thickness reduction occurs in the weathering steel beams.

5.6 Plastic design

For the plastic design of the composite working cross-section the plastic bending moment verification the plastic vertical shear verification, the deflection verification and the fatigue verification will be performed. The plastic bending moment resistance of the structure is dependent on the position of the neutral axis of the structure. Therefore first the neutral axes will be determined for the different variants that will be considered. To determine the neutral axis of the different variants it is essential to know the governing internal forces and bending moments on the structure due to the governing load case.

Considering the variant consisting of weathering steel a reduction of the thickness should be considered due to degradation of the steel. Due to this reduction of the steel the location of the neutral axis will change of the structure which also influences effects and the resistances of the structure. By considering Table 4 Allowance for the loss of thickness for a design life of 100 years and the reassessment of the Avenhornbrug a sacrificial thickness loss of 1 mm will be a sustained assumption. This will be taken into account for the upcomping calculations for the weathering steel variant.

Table 65 Allowed thickness loss according to the differen guidelines.

Country/guidelines	Allowance for the loss of thickness related to corrosion classification in EN ISO 9223				
	C1	C2	C3	C4	C5
Belgium	-	0.11-0.8	0.53-1.2	1.05-1.5	Not allowed
ECCS recommendation for bridges	Not applicable	0.8	1.0	1.5	Not allowed

5.6.1 Effects on structure due to governing situations for bending moment verification

In this paragraph the effects on the structure will be determined due to the governing loading on the structure. This will be done on the following locations of the structure:

- Midspan of the edge beam
- Close to the support of the edge beam
- Midspan of the middle beam
- Close to the support of the middle beam

First the performed steps will be shown for the structure consisting of HEB700B conventional steel beams of S235, with a centre to centre distance of 1.5m. The calculations will be shown for the edge beam in the upcoming paragraphs. For the middle beam the same steps will be considered and therefore only the results will be given.

5.6.1.1 Governing load combination edge beam

In Table 66 the load cases which are included in the governing load combination are shown for the maximum bending moment midspan of the edge beam of the structure. In Figure 77 the corresponding model with the Load combination are given including the corresponding load factors.

In Table 67 the load cases which are included in the governing load combination are shown for the maximum shear force close to the support . In Figure 78 the corresponding model with the Load combination are given including the corresponding load factors.

Table 66 Load cases including in load combination for governing bending moment midspan of the edge beam

Load cases	description
LC1	Self weight of the structure
LC2	Traffic load LM1 edge beam max bending moment
LC6	Asphalt load
LC9	Imposed load shrinkage

Table 67 Load cases including in load combination for governing shear force of the edge beam

Load cases	description
LC1	Self weight of the structure
LC3	Traffic load LM1 edge beam max shear force
LC6	Asphalt load

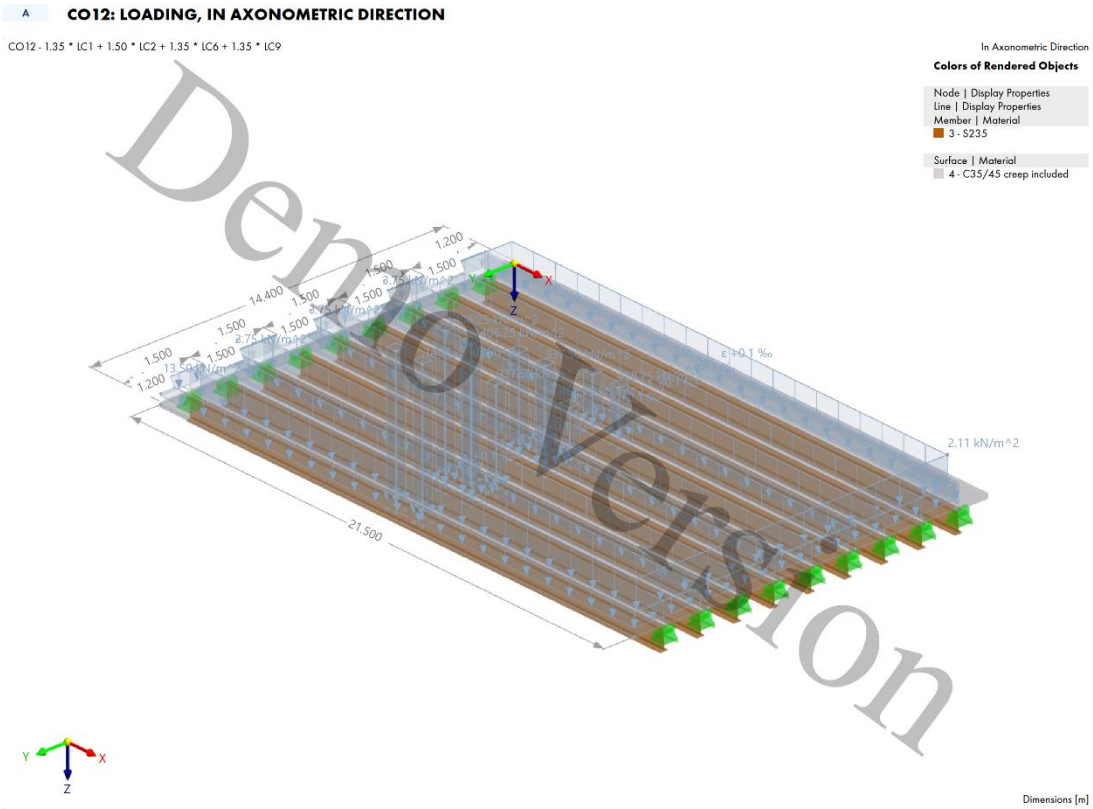

Figure 77 Governing Load combination for maximum bending moment midspan of the edge beam

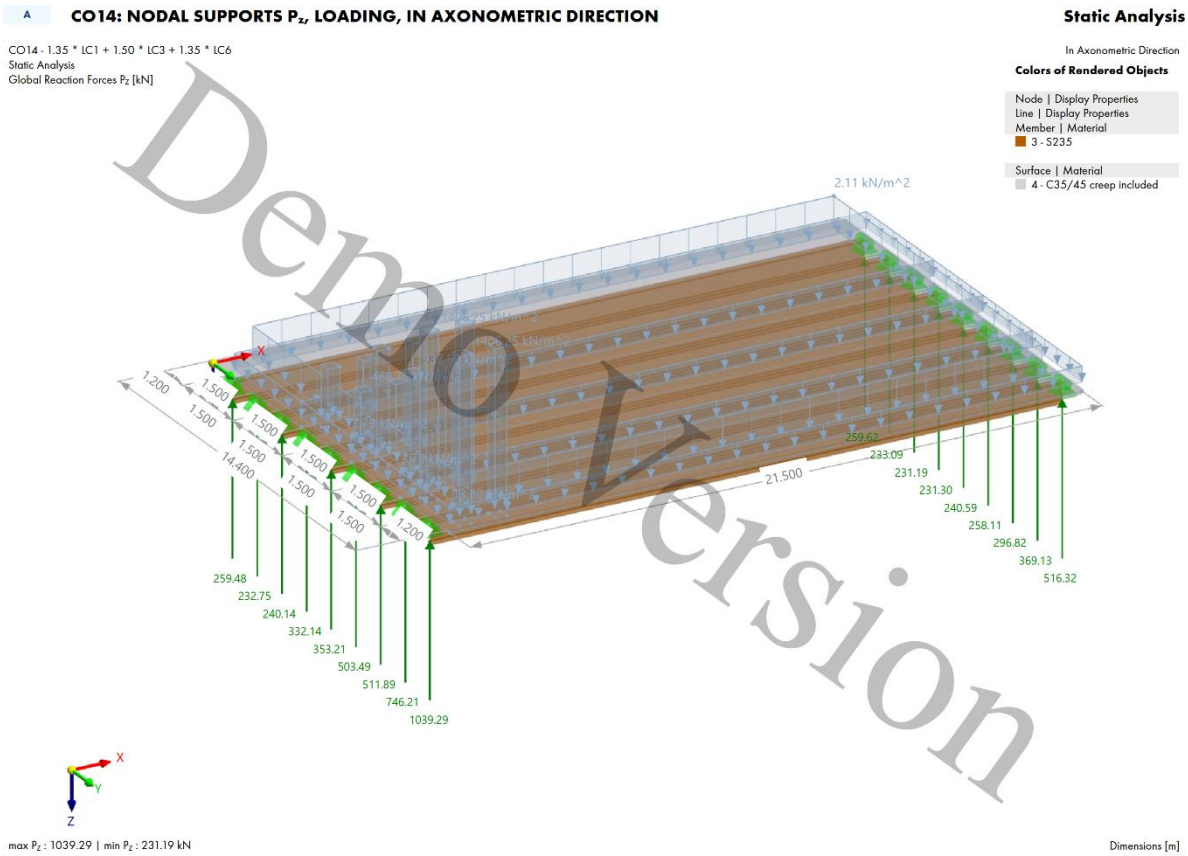

Figure 76 Governing Load combination for maximum shear force edge beam

5.6.1.2 Determination of external bending moment Edge composite beam

The external bending moments on the edge beam should be deduced from the model. The External bending moment in the steel member and in the concrete part should be considered. The steel member is modelled as a member type therefore the effect bending moment can be directly found as can be seen in Figure 78, 2400 [kN] for the edge beam.

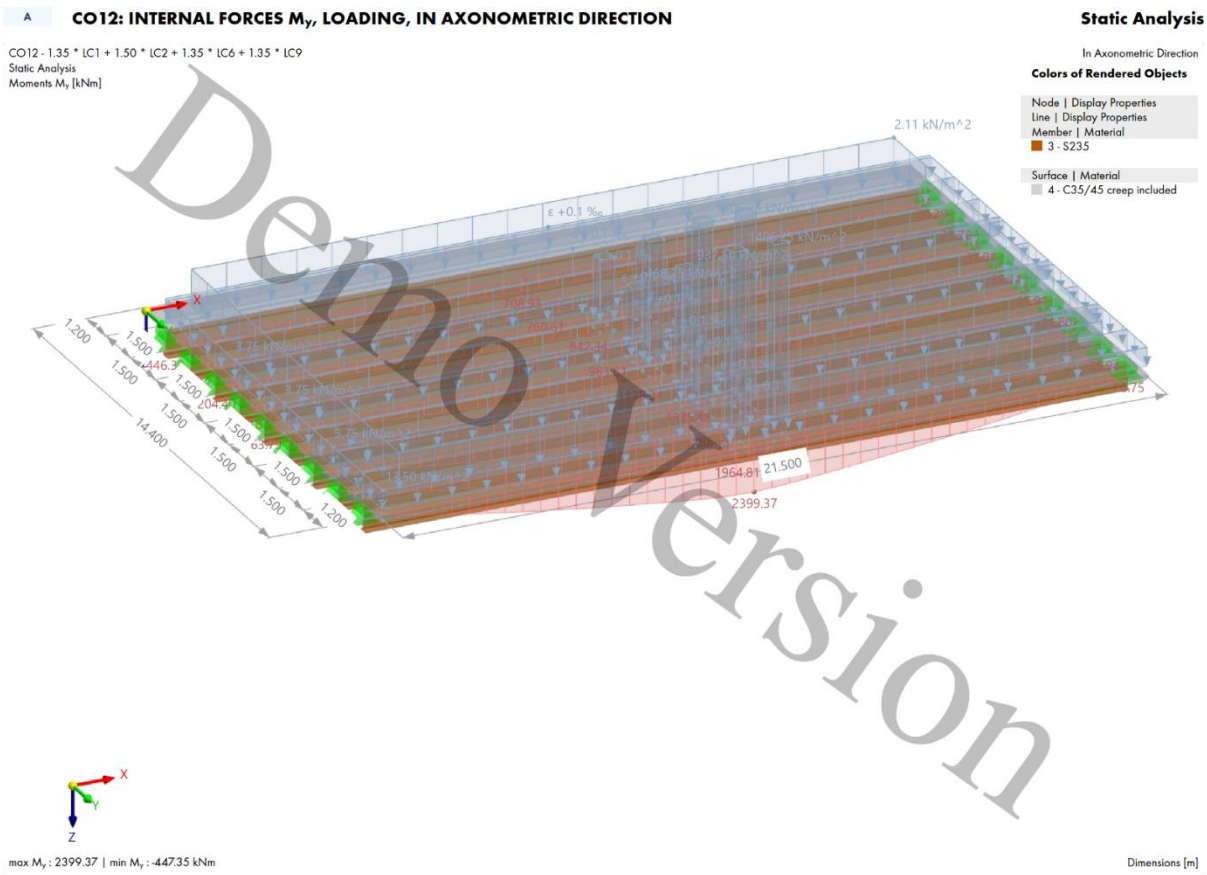

Figure 78 Maximum bending moment in edge beam

The bending moment in the concrete layer should be considered by integrating the bending moment of the cross section over the width where the load of the structure is applicable. These are the effective widths determined in Table 53. For the edge beam of the structure at the midspan of the beam an effective width of 1.95m is considered to integrate the bending moment. In Figure 79 Bending moment distribution due to the governing load combination is shown. Hereby section 1 shows the axes where the integration of the bending moment should be performed. In Figure 80 the result of the integration over the effective width is given. Considering the external bending moment effect on the structure, the results are given in Table 68.

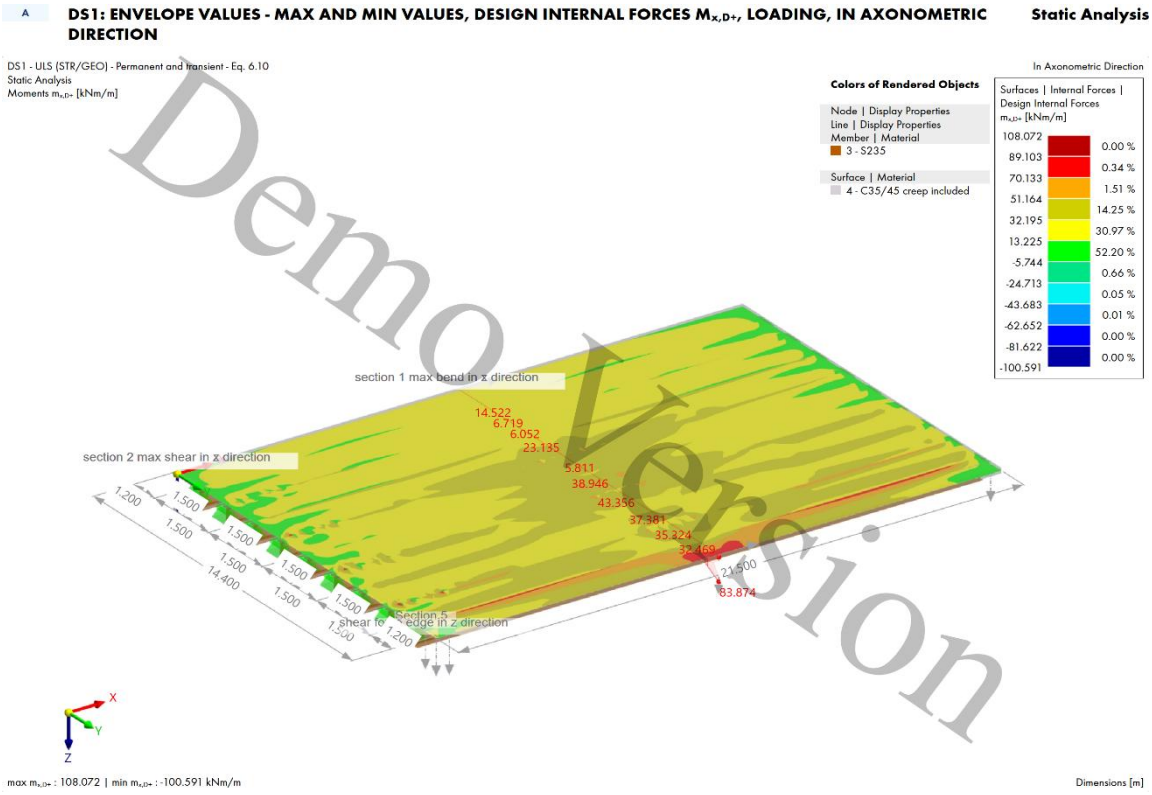

Figure 79 Maximum bending moment in edge beam concrete layer (Result section 1)

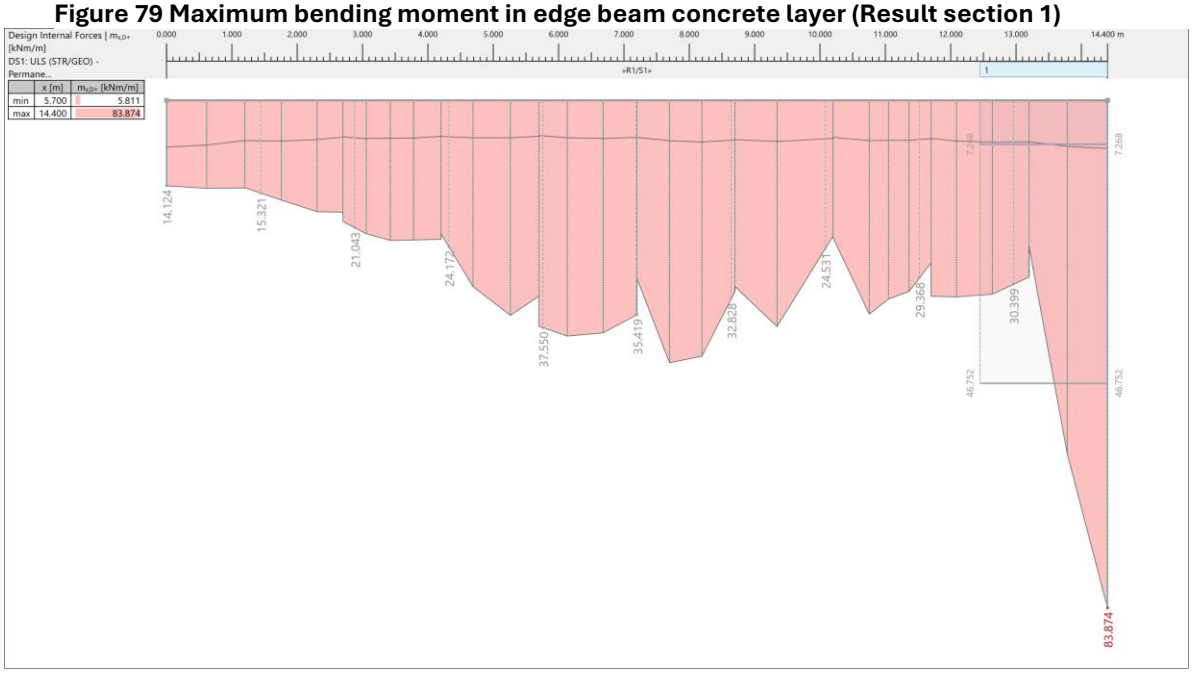

Figure 80 Integration of the bending moment in section 1 over an effective width of 1.95m.

Table 68 results bending moment effect midspan of the edge beam.

description	Symbol	Value [kNm]
Effect bending moment edge beam	$M_{ED,\ beam}$	2400
Effect bending moment concrete layer edge beam	$M_{ED,concrete}$	90

5.6.1.3 *Determination of internal forces edge composite beam*

In composite structures the internal forces in the elements also contribute to the total bending moment of the composite structure. Therefore the internal forces should be deduced from the model to determine the bending moment effects due to internal forces.

The internal force in the edge beam can be directly deduced from the models results since this is modelled as a member type. This result can be seen in Figure 81, where the edge beam to be considered is the beam where an internal force of 6393 [kN] can be observed.

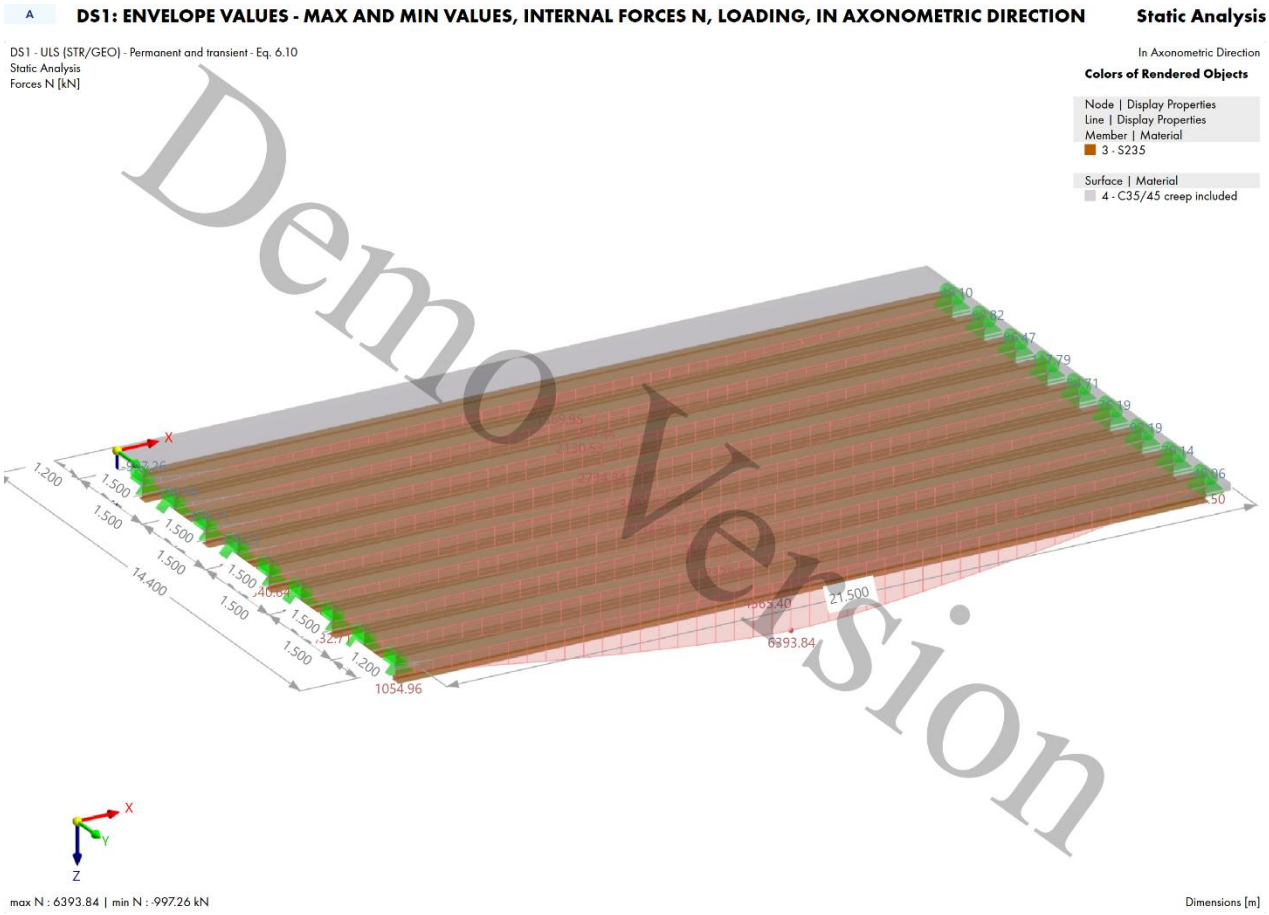

Figure 81 Internal normal force in the edge beam due to the governing load combination

In Figure 82, the internal force N_x [kN/m] in the concrete layer is shown and the governing load combination for the internal force of the concrete layer. The force over the made section 1, as can be seen in Figure 82, should be integrated over the effective width as determined in Table 53 to get the resulting internal force in the concrete layer in [kN]. In Figure 82 the normal force distribution in the concrete layer is shown and the location of section 1 is shown. In Figure 83 the integrated section is shown for the determination of the internal axial force in the concrete layer. The resulting internal forces in the concrete layer and in the edge beam are given in Table 69.

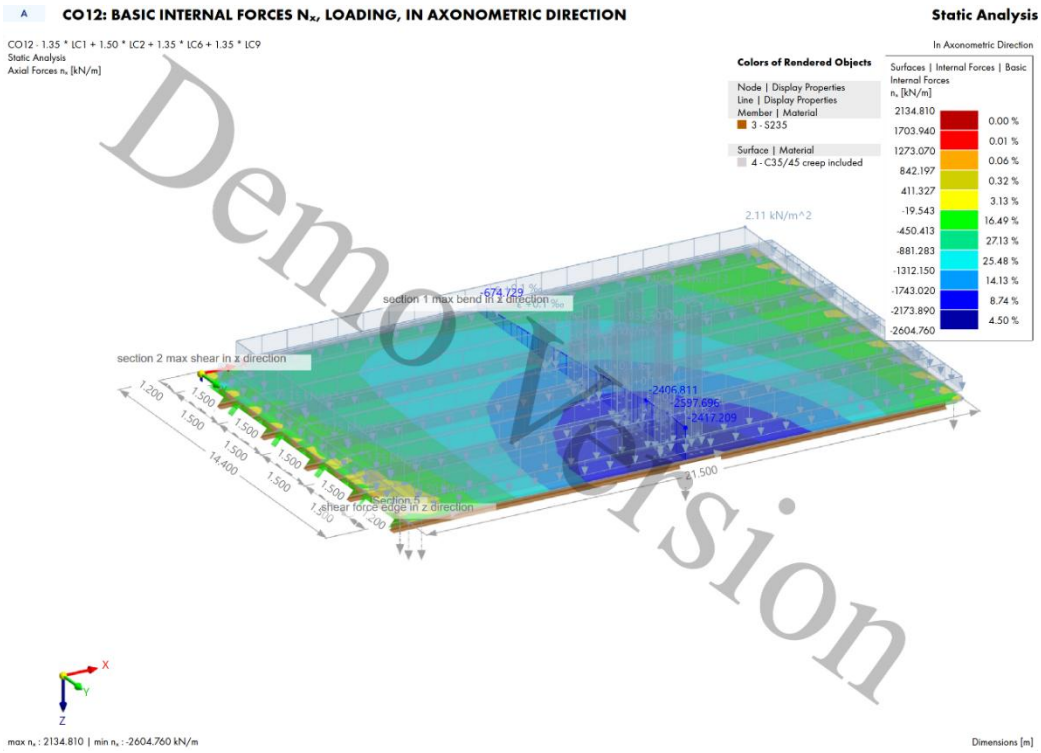

Figure 82 internal force in concrete layer due to governing load combination

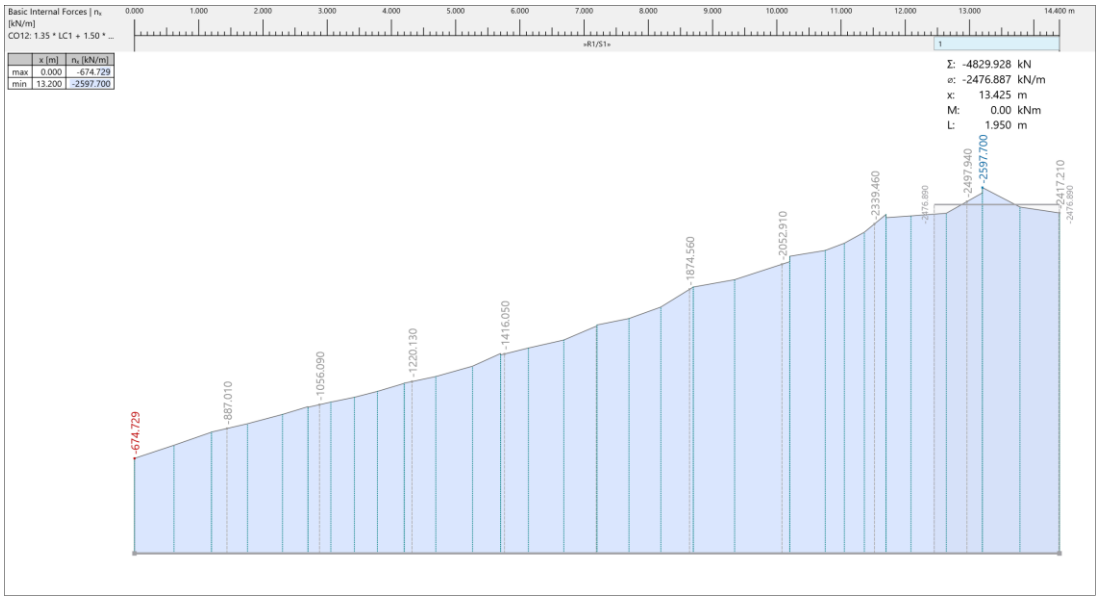

Figure 83 Integration of the internal normal force in the concrete layer over an effective width of 1.95 m.

Table 69 results bending moment effect in midspan of the edge beam.

description	Symbol	Value [kN]
Effect internal axial force edge beam	$N_{ED,\ beam}$	6395
Effect internal axial force concrete layer edge beam	$N_{ED,concrete}$	4830

5.6.1.4 *Determination of shear force edge composite beam*

For the edge beam also the governing situation should be determined for the maximum shear force of the structure. The result of the governing load combination is given in Figure 76 and in Table 70.

Table 70 Result maximum shear force effect close to the support of the edge beam

description	Symbol	Value [kN]
Effect shear force	V_{ED}	1040

5.6.1.5 *Neutral axis determination*

In this paragraph the neutral axes positions will be determined for the different variants. First the calculation will be shown for the variant with the HEB700B profile of S235, with a centre to centre distance of 1.5 and for the edge beam of the structure, then the neutral axis positions will be shown for all the different variants. To determine the neutral axes the effects on the edge beam due to the governing load combinations are needed, which were determined in paragraph 5.6.1. The overall results from the performed example are given in Table 71. For the other variants the overall results can be found in Anex B.

Table 71 Overall results effects edge composite bean for governing load combination for HEB700B and ctc=1.5m

description	Symbol	Value	unit
Effect bending moment edge beam	$M_{ED,\ beam}$	2400	kNm
Effect bending moment concrete layer edge beam	$M_{ED,concrete}$	90	kNm
Effect internal axial force edge beam	$N_{ED,\ beam}$	6395	kNm
Effect internal axial force concrete layer edge beam	$N_{ED,concrete}$	4830	kNm
Effect shear force	V_{ED}	1040	kN

By determining the internal force equilibrium of the structure as has been done in the paragraph Verification of the model and sub paragraph Determination of the neutral axis, it is possible to determine the location of the neutral axis. In the results are given for the determination of the location of the neutral axis, hereby the location is determined relative to the upper concrete fiber of the structure.

Table 72 Neutral axis determination for the different variants at the edge beam conventional steel

Profile	Neutral axis location for the differen centre to centre distance of the beams [mm]		
	1.5m	2m	2.5m
HEB600B	209 (F)	209 (F)	209 (F)
HEB700B	212 (F)	211 (F)	211 (F)
HEB800B	214 (F)	213 (F)	212 (F)

(F) = Neutral axis in upper flange.
(W) = Neutral axis in web.

Table 73 Neutral axis determination for the different variants at the edge beam Weathering steel

Profile	Neutral axis location for the differen centre to centre distance of the beams [mm]		
	1.5m	2m	2.5m
HEB600B	209 (F)	209 (F)	209 (F)
HEB700B	212 (F)	211 (F)	211 (F)
HEB800B	214 (F)	213 (F)	212 (F)

(F) = Neutral axis in upper flange.
(W) = Neutral axis in web.

Table 74 Neutral axis determination for the different variants at the middle beam convention steel

Profile	Neutral axis location for the differen centre to centre distance of the beams [mm]		
	1.5m	2m	2.5m
HEB600B	208 (F)	208 (F)	207 (F)
HEB700B	210 (F)	210 (F)	209 (F)
HEB800B	213 (F)	213 (F)	211 (F)

(F) = Neutral axis in upper flange.
(W) = Neutral axis in web.

Table 75 Neutral axis determination for the different variants at the middle beam weathering steel

Profile	Neutral axis location for the differen centre to centre distance of the beams [mm]		
	1.5m	2m	2.5m
HEB600B	208 (F)	208 (F)	208 (F)
HEB700B	212 (F)	210 (F)	210 (F)
HEB800B	213 (F)	212 (F)	211 (F)

(F) = Neutral axis in upper flange.
(W) = Neutral axis in web.

5.6.2 Bending moment verification composite structure

For the bending moment verification of the composite structure the effects on the structure are needed for determining the total bending moment and the bending moment resistance is needed. These two are both dependent of the location of the neutral axis. For the different variants these verifications will be performed, as an example these calculations will be performed for the HEB700B of S235 variant with a c.t.c. of 1.5m and only for the edge beam. As discussed before the method to determine the bending moment effect and bending moment resistance is dependent of the location of the neutral axis. The different methods are shown in Figure 84 to

Figure 86.

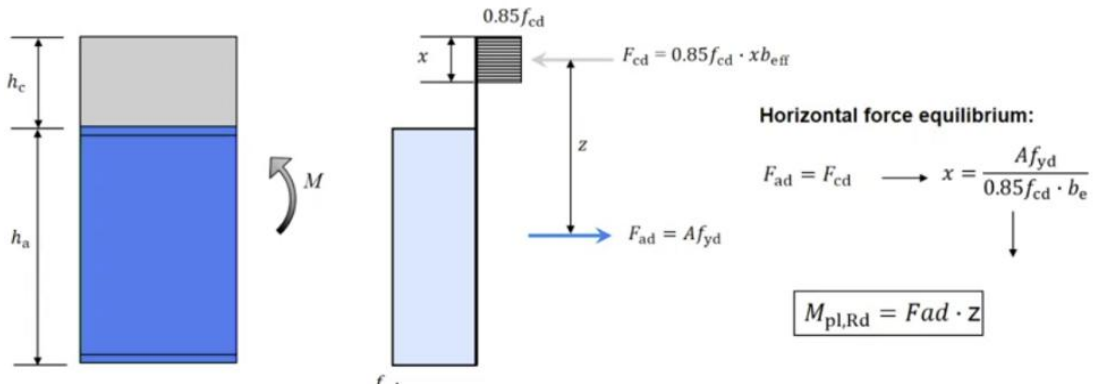

Figure 84 Stress distribution if the n.a is in the concrete layer

Table 76 Parameters for determining bending moment resistance of edge beam

parameters	values
Yield stress steel f_{YD}	235 [N/mm^2]
Area of steel section A	30552 [mm^2]
Maximumormal compression force concrete F_c	7735 [kN]
Width of upper flange b_f	300 [mm]
Height of steel part h_a	700 [mm]
Height of concrete section	200 [mm]
a	50.86 [mm]
Internal moment due to internal forces	3310 [kNm]

Figure 85 Stress distribution if the n.a. is in the steel flange (Kavoura, 2023)

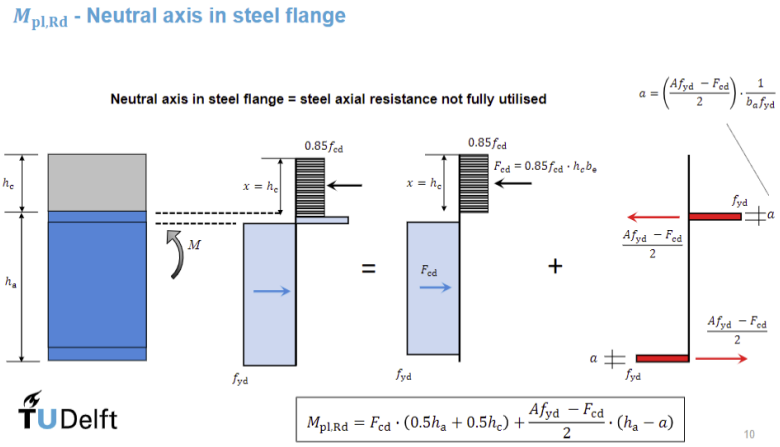

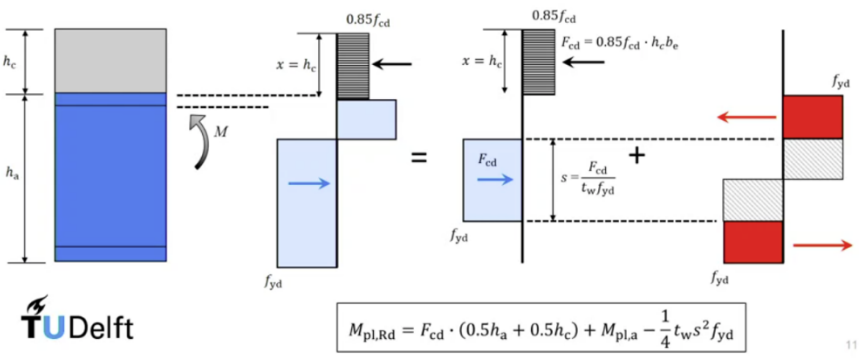

Figure 86 Stress distrubution if the n.a is in the steel web (Kavoura, 2023)

The conversion of the effect loads to the governing bending moment on the composite structure has been worked out in the chapter 4.12, the same method will be performed to convert the parameters in Table 71 to a bending moment due to the governing load combination M_{Ed}.

For the bending moment resistance, the parameters used in Table 76 and the formulas in Figure 85 are used to determine the bending moment resistance at the edge beam M_{Rd}.

Table 77 Verification of bending moment of edge beam for a centre to centre distance of 1.5m

Profile	S235			S355			S460		
	M_{Ed} [kNm]	M_{Rd} [kNm]	U.C [-]	M_{Ed} [kNm]	M_{Rd} [kNm]	U.C [-]	M_{Ed} [kNm]	M_{Rd} [kNm]	U.C [-]
HEB600B	4975	2710	1.84	4975	3605	1.38	4975	4395	1.13
HEB700B	5170	3310	1.56	5170	4500	1.15	5170	5544	0.93
HEB800B	5275	3910	1.35	5275	5405	0.98	5275	6710	0.79

Table 78 Verification of bending moment of edge beam for a centre to centre distance of 2.0m

Profile	S235			S355			S460		
	M_{Ed} [kNm]	M_{Rd} [kNm]	U.C [-]	M_{Ed} [kNm]	M_{Rd} [kNm]	U.C [-]	M_{Ed} [kNm]	M_{Rd} [kNm]	U.C [-]
HEB600B	5745	2830	2.03	5745	3730	1.54	5745	4515	1.27
HEB700B	5915	3430	1.72	5915	4625	1.28	5915	5670	1.04
HEB800B	6045	4040	1.5	6045	5530	1.09	6045	6835	0.88

Table 79 Verification of bending moment of edge beam for a centre to centre distance of 2.5m

Profile	S235			S355			S460		
	M_{Ed} [kNm]	M_{Rd} [kNm]	U.C [-]	M_{Ed} [kNm]	M_{Rd} [kNm]	U.C [-]	M_{Ed} [kNm]	M_{Rd} [kNm]	U.C [-]
HEB600B	5920	2830	2.09	5920	3730	1.59	5920	4515	1.3
HEB700B	6030	3430	1.76	6030	4625	1.30	6030	5670	1.06
HEB800B	6105	4040	1.51	6105	5530	1.10	6105	6835	0.89

Table 80 Verification of bending moment of edge weathering steel beam for a centre to centre distance of 1.5m

Profile	S235			S355			S460		
	M_{Ed} [kNm]	M_{Rd} [kNm]	U.C [-]	M_{Ed} [kNm]	M_{Rd} [kNm]	U.C [-]	M_{Ed} [kNm]	M_{Rd} [kNm]	U.C [-]
HEB600B	4970	2570	1.93	4970	3410	1.46	4970	4140	1.20
HEB700B	5170	3130	1.65	5170	4235	1.22	5170	5205	0.99
HEB800B	5275	3775	1.40	5275	5205	1.01	5205	6450	0.82

Table 81 Verification of bending moment of edge weathering steel beam for a centre to centre distance of 2.0m

Profile	S235			S355			S460		
	M_{Ed} [kNm]	M_{Rd} [kNm]	U.C [-]	M_{Ed} [kNm]	M_{Rd} [kNm]	U.C [-]	M_{Ed} [kNm]	M_{Rd} [kNm]	U.C [-]
HEB600B	5745	2595	2.21	5745	3430	1.67	5745	4165	1.38
HEB700B	5915	3251	1.81	5915	4360	1.36	5915	5330	1.11
HEB800B	6040	3900	1.55	6040	5330	1.14	6040	6580	0.92

Table 82 Verification of bending moment of edge weathering steel beam for a centre to centre distance of 2.5m

Profile	S235			S355			S460		
	M_{Ed} [kNm]	M_{Rd} [kNm]	U.C [-]	M_{Ed} [kNm]	M_{Rd} [kNm]	U.C [-]	M_{Ed} [kNm]	M_{Rd} [kNm]	U.C [-]
HEB600B	5920	2690	2.20	5920	3530	1.68	5920	4259	1.39
HEB700B	6030	3250	1.85	6030	4360	1.38	6030	5330	1.13
HEB800B	6100	3900	1.56	6100	5330	1.14	6100	6580	0.93

In Figure 87 and Figure 88, the result of the bending moment verification of the edge beam are presented for both the conventional steel variant and the weathering steel variant. The results have been extrapolated to provide a clear 3D plot showing all variants that satisfy the bending moment verification. As can be seen. Variations were made in the profile type, centre-to-centre distance, and the steel grade. This results in three distinct layers in the plot, each corresponding to a different steel grade with the lowest layer representing S460 and the highest representing S460.

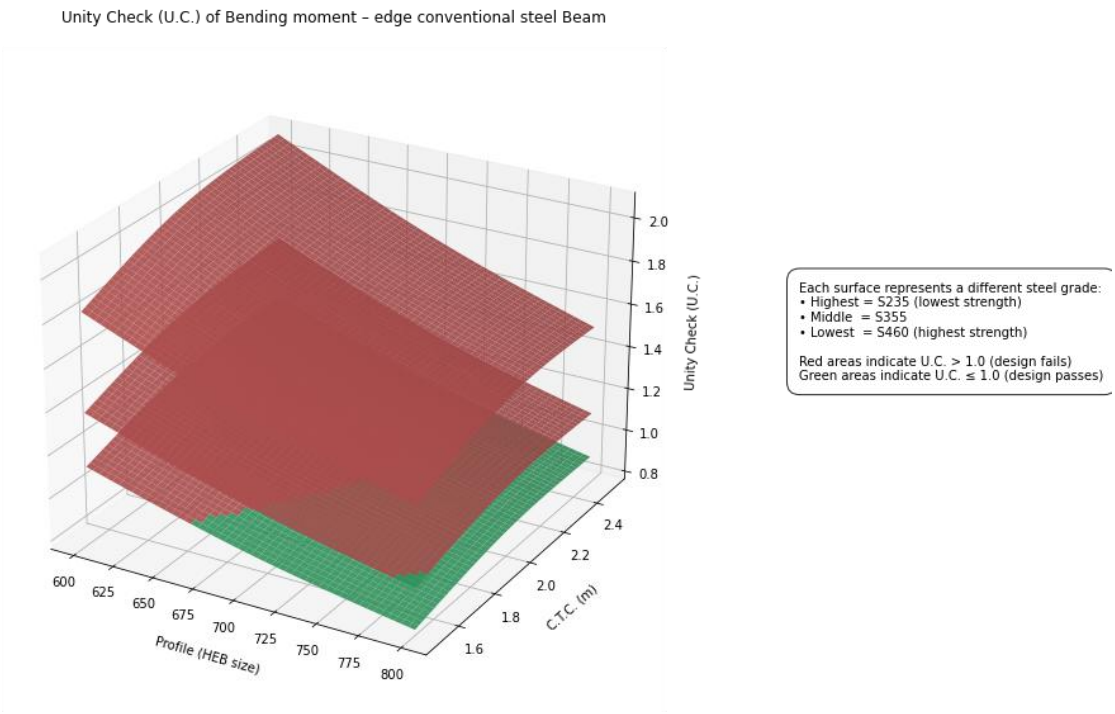

Figure 87 visualization of the performed bending moment verification for the edge conventional steel beam by interpolating the c.t.c. distance and the HEB profiles.

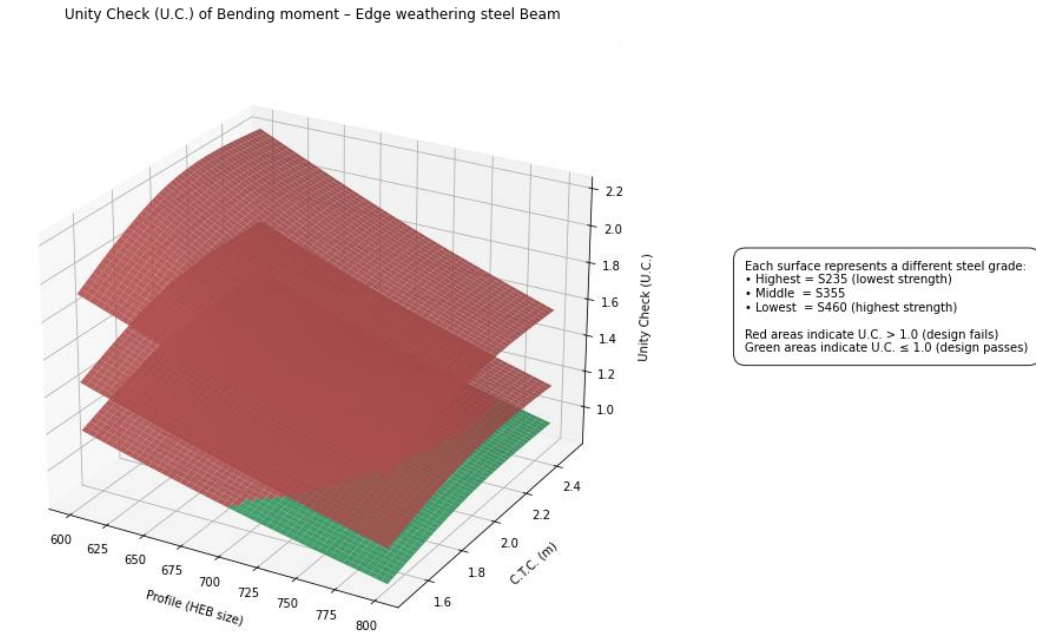

Figure 88 visualization of the performed bending moment verification for the edge weathering steel beam by interpolating the c.t.c. distance and the HEB profiles.

Table 83 Verification of bending moment of middle conventional steel beam for a centre to centre distance of 1.5m

Profile	S235			S355			S460		
	M_{Ed} [kNm]	M_{Rd} [kNm]	U.C [-]	M_{Ed} [kNm]	M_{Rd} [kNm]	U.C [-]	M_{Ed} [kNm]	M_{Rd} [kNm]	U.C [-]
HEB600B	3070	2490	1.23	3070	3390	0.91	3070	4175	0.735
HEB700B	3185	3085	1.03	3185	4275	0.75	3185	5320	0.60
HEB800B	3280	3685	0.89	3280	5175	0.63	3280	6480	0.51

Table 84 Verification of bending moment of middle conventional steel beam for a centre to centre distance of 2.0m

Profile	S235			S355			S460		
	M_{Ed} [kNm]	M_{Rd} [kNm]	U.C [-]	M_{Ed} [kNm]	M_{Rd} [kNm]	U.C [-]	M_{Ed} [kNm]	M_{Rd} [kNm]	U.C [-]
HEB600B	3990	2735	1.46	3990	3630	1.10	3990	4420	0.90
HEB700B	4150	3330	1.25	4150	4525	0.92	4150	5570	0.75
HEB800B	4275	3935	1.09	4275	5430	0.78	4275	6735	0.63

Table 85 Verification of bending moment of middle conventional steel beam for a centre to centre distance of 2.5m

Profile	S235			S355			S460		
	M_{Ed} [kNm]	M_{Rd} [kNm]	U.C [-]	M_{Ed} [kNm]	M_{Rd} [kNm]	U.C [-]	M_{Ed} [kNm]	M_{Rd} [kNm]	U.C [-]
HEB600B	4785	2975	1.60	4785	3875	1.23	4785	4660	1.03
HEB700B	4965	3580	1.39	4965	4775	1.04	4965	5820	0.85
HEB800B	5110	4190	1.21	5110	5685	0.90	5110	6990	0.73

Table 86 Verification of bending moment of middle weathering steel beam for a centre to centre distance of 1.5m

Profile	S235			S355			S460		
	M_{Ed} [kNm]	M_{Rd} [kNm]	U.C [-]	M_{Ed} [kNm]	M_{Rd} [kNm]	U.C [-]	M_{Ed} [kNm]	M_{Rd} [kNm]	U.C [-]
HEB600B	3070	2355	1.30	3070	3190	0.96	3070	3925	0.78
HEB700B	3180	2905	1.10	31880	4015	0.79	3180	4985	0.64
HEB800B	3280	3550	0.92	3280	4975	0.65	3280	6225	0.53

Table 87 Verification of bending moment of middle weathering steel beam for a centre to centre distance of 2.0m

Profile	S235			S355			S460		
	M_{Ed} [kNm]	M_{Rd} [kNm]	U.C [-]	M_{Ed} [kNm]	M_{Rd} [kNm]	U.C [-]	M_{Ed} [kNm]	M_{Rd} [kNm]	U.C [-]
HEB600B	3990	2595	1.54	3990	3430	1.16	3990	4165	0.96
HEB700B	4150	3155	1.32	4150	4260	0.97	4150	5230	0.79
HEB800B	4275	3800	1.12	4275	5230	0.82	4275	6475	0.66

Table 88 Verification of bending moment of middle weathering steel beam for a centre to centre distance of 2.5m

Profile	S235			S355			S460		
	M_{Ed} [kNm]	M_{Rd} [kNm]	U.C [-]	M_{Ed} [kNm]	M_{Rd} [kNm]	U.C [-]	M_{Ed} [kNm]	M_{Rd} [kNm]	U.C [-]
HEB600B	4780	2835	1.69	4780	3670	1.30	4780	4405	1.08
HEB700B	4960	3400	1.46	4960	4505	1.10	4960	5475	0.91
HEB800B	5110	4050	1.26	5110	5480	0.93	5110	6730	0.76

In Figure 90 and Figure 89, the result of the bending moment verification of the middle beam are presented for both the conventional steel variant and the weathering steel variant. The results have been extrapolated to provide a clear 3D plot showing all variants that satisfy the bending moment verification. As can be seen. Variations were made in the profile type, centre-to-centre distance, and the steel grade. This results in three distinct layers in the plot, each corresponding to a different steel grade with the lowest layer representing S460 and the highest representing S460.

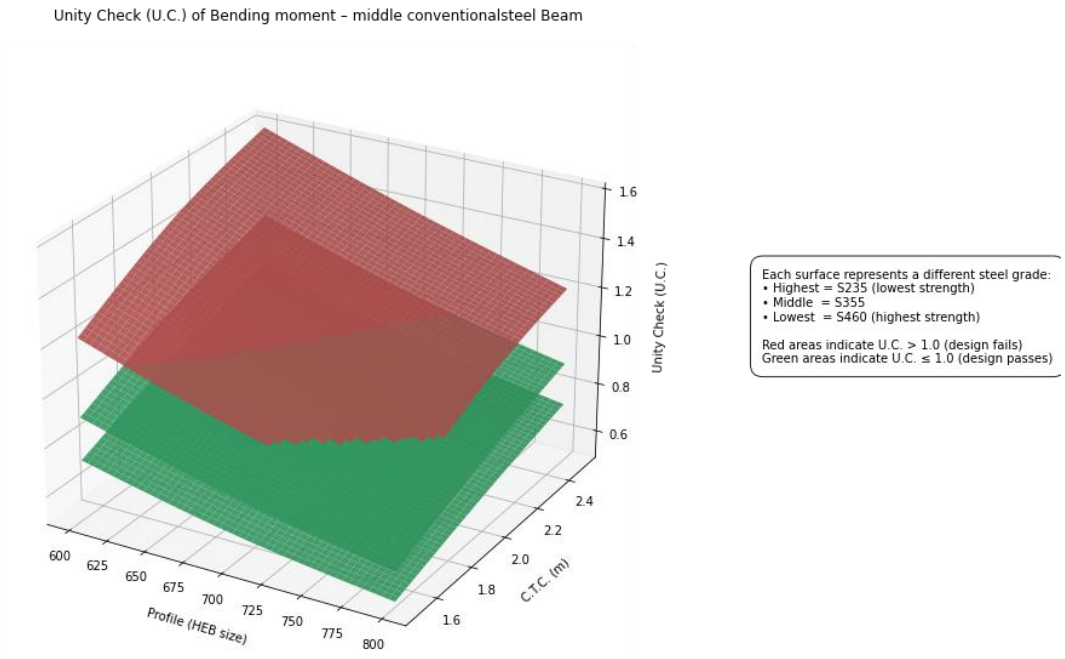

Figure 89 visualization of the performed bending moment verification for the middle conventional steel beam by interpolating the c.t.c. distance and the HEB profiles.

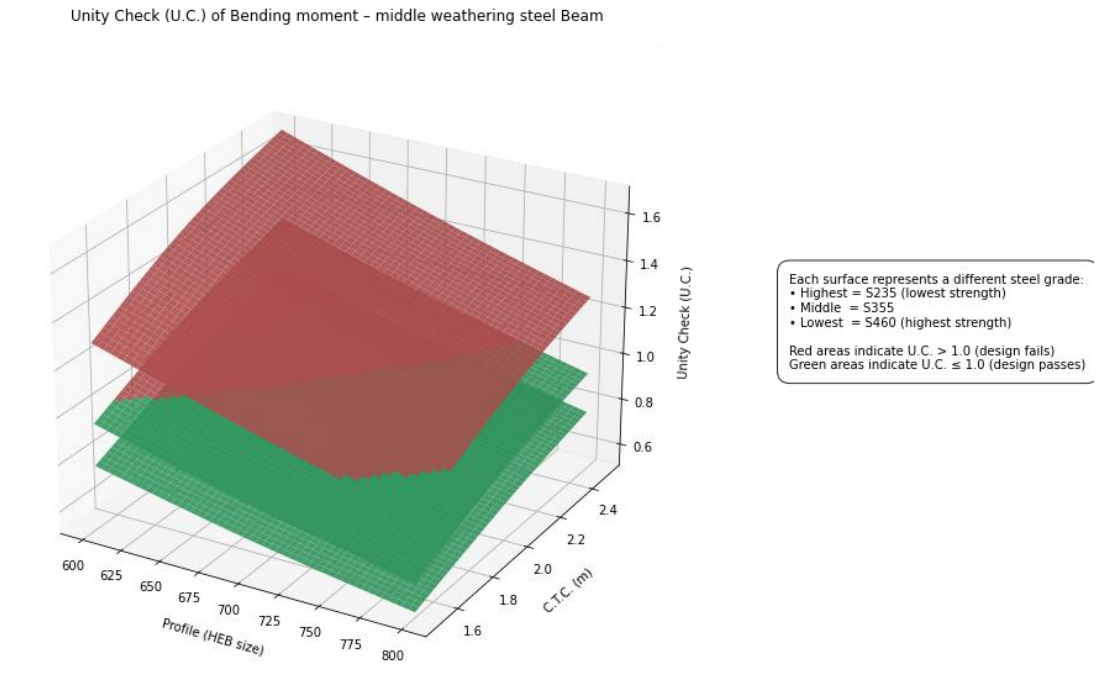

Figure 90 visualization of the performed bending moment verification for the middle weathering steel beam by interpolating the c.t.c. distance and the HEB profiles.

5.6.3 Vertical shear verification

For the vertical shear verification, it was first checked if the full cross-section as can be seen in Figure 91 satisfies the verification. This was done to check what the capacity of the beams are, however, it was clearly mentioned in the boundary conditions that the superstructure should align with the existing abutments therefore this situation will not be the one to be considered. The full verification of the full cross-section can be found in ANNEX C. From this verification it could be concluded that overall the full cross-section can handle the governing shear loads on the structure.

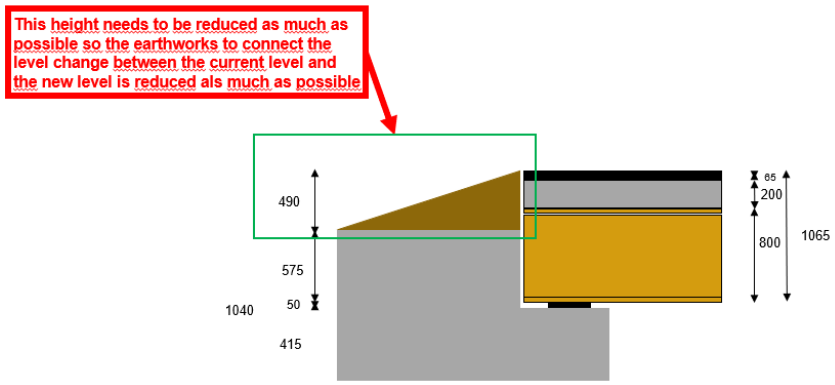

Figure 91 Unreduced cross-section at the edges of the structure

Regarding the reduced cross section as can be seen in Figure 112 Without adding any shear force capacity to the beams also the verification has been performed. From this verification it was clear that for all variants the shear force verification was not met and therefore the shear force capacity should be increased. The full verification has been performed in ANNEX C.

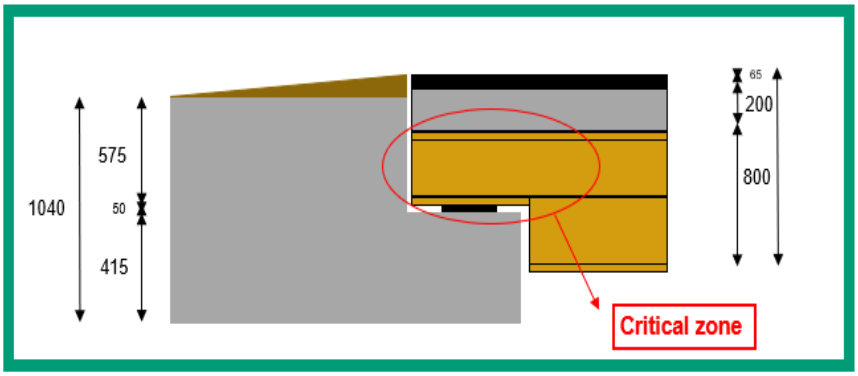

Figure 92 Local cross-section reduction to align with the level of the road.

As can be seen from the results in ANNEX C for the local reduced cross-section extra measures need to be taken to have a structure which satisfies the shear force verification. To get this extra shear force resistance it is needed to locally increase the web thickness. Therefore 2 options are considered to increase the web thickness. Option 1 will be by making use of a bolted connection, by connecting extra plates to the web, as can be seen in Figure 93. Option 2 will be by welding an extra plate to the web to also increase the web thickness as can be seen in Figure 94.

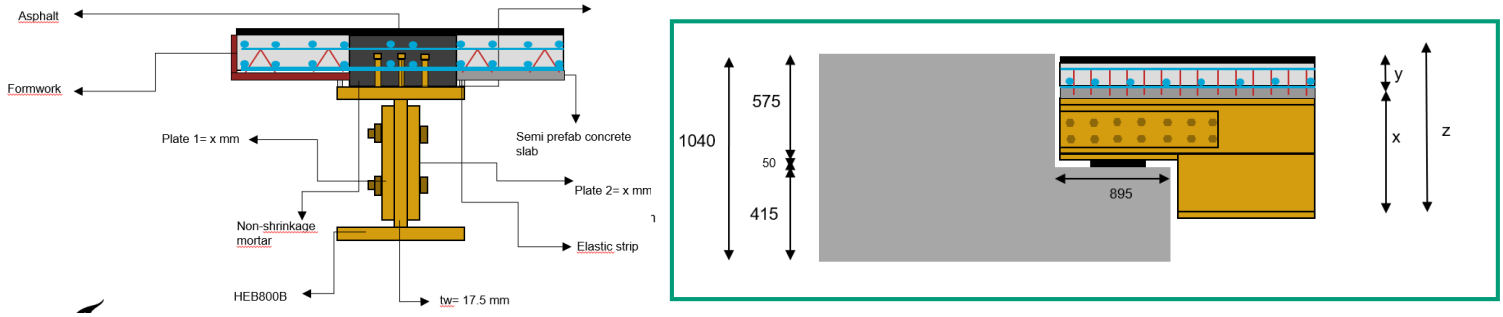

Figure 93 Option 1 bolted plate conection for increasing the web thickness

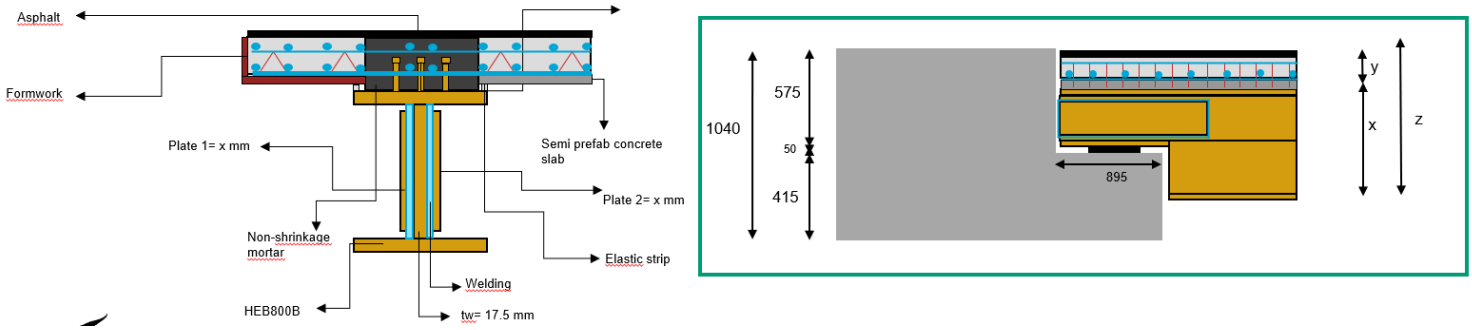

Figure 94 Option 2 welded plate connection for increasing the web thickness

For the determination of the shear resistance, only the increased thickness will be considered. The shear capacity of the bolts and welds is not taken into account, as these connections are designed in such a way that they do not govern the overall resistance. An additional plate thickness of 20 mm × 10 mm will be applied on each side. In Table 89 and Table 90 the changed cross-section properties are given. In Table 91 to Table 96 the results are given for the verification of the shear force at the edge support, with Figure 95 visualizing these results. For the shear force verification of the middle beam the results are given in Table 97 to Table 102 and these results are visualized in Figure 97.

Table 89 determination of the reduced heights and areas of the web of the different profiles of conventional steel, with two connected plates of each 10 mm.

	$h_{web}[mm]$	$t_{web,tot}[mm]$	$A_{web}[mm^2]$
HEB600B	**250**	**35.5**	**8875**
HEB700B	**246**	**37**	**9102**
HEB800B	**244**	**37.5**	**9150**

Table 90 determination of the reduced heights and areas of the web of the different profiles of weathering steel , with two connected plates of each 10 mm, including a total thickness loss of 2 mm.

	$h_{web}[mm]$	$t_{web,tot}[mm]$	$A_{web}[mm^2]$
HEB600B	**250**	**33.5**	**8375**
HEB700B	**246**	**35**	**8610**
HEB800B	**244**	**35.5**	**8662**

Table 91 Verification of vertical shear force of edge conventional steel beam for a centre to centre distance of 1.5m for the increased web thickness.

Profile	**S235**				**S355**				**S460**			
	V_{Ed} [kNm]	τ_{Ed} [N/mm²]	τ_{Rd} [N/mm²]	U.C [-]	V_{Ed} [kNm]	τ_{Ed} [N/mm²]	τ_{Rd} [N/mm²]	U.C [-]	V_{Ed} [kNm]	τ_{Ed} [N/mm²]	τ_{Rd} [N/mm²]	U.C [-]
HEB600B	**1030**	**116**	**109**	**1.06**	**1030**	**116**	**164**	**0.71**	**1030**	**116**	**212**	**0.55**
HEB700B	**1040**	**114**	**109**	**1.05**	**1040**	**114**	**164**	**0.70**	**1040**	**114**	**212**	**0.54**
HEB800B	**1045**	**114**	**109**	**1.05**	**1045**	**114**	**164**	**0.70**	**1045**	**114**	**212**	**0.54**

Table 92 Verification of vertical shear force of edge conventional steel beam for a centre to centre distance of 2.0 m for the increased web thickness.

Profile	S235				S355				S460			
	V_{Ed} [kNm]	τ_{Ed} [N/mm²]	τ_{Rd} [N/mm²]	U.C [-]	V_{Ed} [kNm]	τ_{Ed} [N/mm²]	τ_{Rd} [N/mm²]	U.C [-]	V_{Ed} [kNm]	τ_{Ed} [N/mm²]	τ_{Rd} [N/mm²]	U.C [-]
HEB600B	1165	131	109	1.20	1165	131	164	0.80	1165	131	212	0.62
HEB700B	1170	129	109	1.18	1170	129	164	0.78	1170	129	212	0.61
HEB800B	1180	129	109	1.18	1180	129	164	0.79	1180	129	212	0.61

Table 93 Verification of vertical shear force of edge conventional steel beam for a centre to centre distance of 2.5 m for the increased web thickness.

Profile	S235				S355				S460			
	V_{Ed} [kNm]	τ_{Ed} [N/mm²]	τ_{Rd} [N/mm²]	U.C [-]	V_{Ed} [kNm]	τ_{Ed} [N/mm²]	τ_{Rd} [N/mm²]	U.C [-]	V_{Ed} [kNm]	τ_{Ed} [N/mm²]	τ_{Rd} [N/mm²]	U.C [-]
HEB600B	1160	131	109	1.20	1160	131	164	0.80	1160	131	212	0.62
HEB700B	1160	127	109	1.17	1160	127	164	0.78	1160	127	212	0.60
HEB800B	1165	127	109	1.17	1165	127	164	0.78	1165	127	212	0.60

Table 94 Verification of vertical shear force of edge weatherin steel beam for a centre to centre distance of 1.5m for the increased web thickness.

Profile	S235				S355				S460			
	V_{Ed} [kNm]	τ_{Ed} [N/mm²]	τ_{Rd} [N/mm²]	U.C [-]	V_{Ed} [kNm]	τ_{Ed} [N/mm²]	τ_{Rd} [N/mm²]	U.C [-]	V_{Ed} [kNm]	τ_{Ed} [N/mm²]	τ_{Rd} [N/mm²]	U.C [-]
HEB600B	1030	123	109	1.13	1030	123	164	0.75	1030	123	212	0.58
HEB700B	1040	121	109	1.11	1040	121	164	0.74	1040	121	212	0.57
HEB800B	1045	121	109	1.11	1045	121	164	0.74	1045	121	212	0.57

Table 95 Verification of vertical shear force of edge weathering steel beam for a centre to centre distance of 2.0 m for the increased web thickness.

Profile	S235				S355				S460			
	V_{Ed} [kNm]	τ_{Ed} [N/mm²]	τ_{Rd} [N/mm²]	U.C [-]	V_{Ed} [kNm]	τ_{Ed} [N/mm²]	τ_{Rd} [N/mm²]	U.C [-]	V_{Ed} [kNm]	τ_{Ed} [N/mm²]	τ_{Rd} [N/mm²]	U.C [-]
HEB600B	1165	139	109	1.28	1165	139	164	0.85	1165	139	212	0.66
HEB700B	1170	136	109	1.25	1170	136	164	0.83	1170	136	212	0.64
HEB800B	1180	136	109	1.25	1180	136	164	0.83	1180	136	212	0.64

Table 96 Verification of vertical shear force of edge weathering steel beam for a centre to centre distance of 2.5 m for the increased web thickness.

Profile	S235				S355				S460			
	V_{Ed} [kNm]	τ_{Ed} [N/mm²]	τ_{Rd} [N/mm²]	U.C [-]	V_{Ed} [kNm]	τ_{Ed} [N/mm²]	τ_{Rd} [N/mm²]	U.C [-]	V_{Ed} [kNm]	τ_{Ed} [N/mm²]	τ_{Rd} [N/mm²]	U.C [-]
HEB600B	1160	139	109	1.27	1160	139	164	0.84	1160	139	212	0.65
HEB700B	1160	135	109	1.24	1160	135	164	0.82	1160	135	212	0.64
HEB800B	1165	134	109	1.23	1165	134	164	0.82	1165	134	212	0.63

In Figure 96 and Figure 95, the result of the vertical shear verification of the edge beam are presented for both the conventional steel variant and the weathering steel variant. The results have been extrapolated to provide a clear 3D plot showing all variants that satisfy the vertical shear verification. As can be seen. Variations were made in the profile type, centre-to-centre distance, and the steel grade. This results in three distinct layers in the plot, each corresponding to a different steel grade with the lowest layer representing S460 and the highest representing S460.

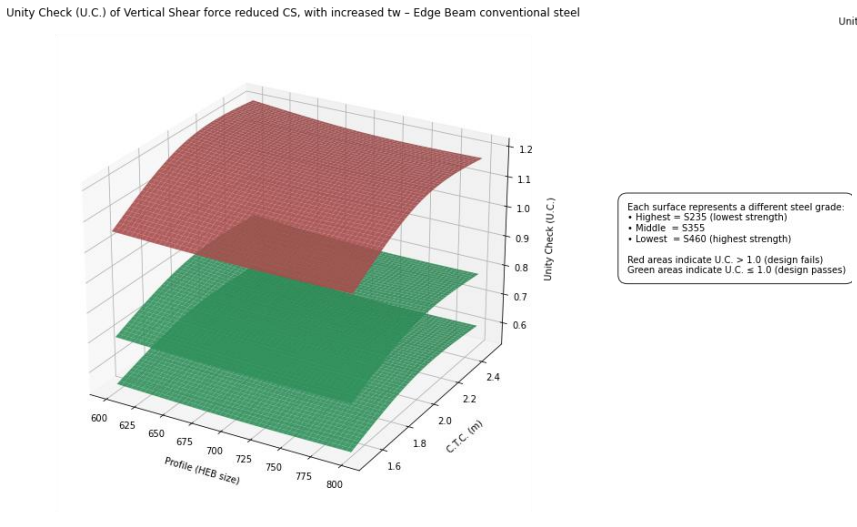

Figure 96 visualization of the performed Vertical shear verification for the edge beam by interpolating the c.t.c. distance and the HEB profiles of the conventional steel beams, for the reduced web height, and an increased web thickness.

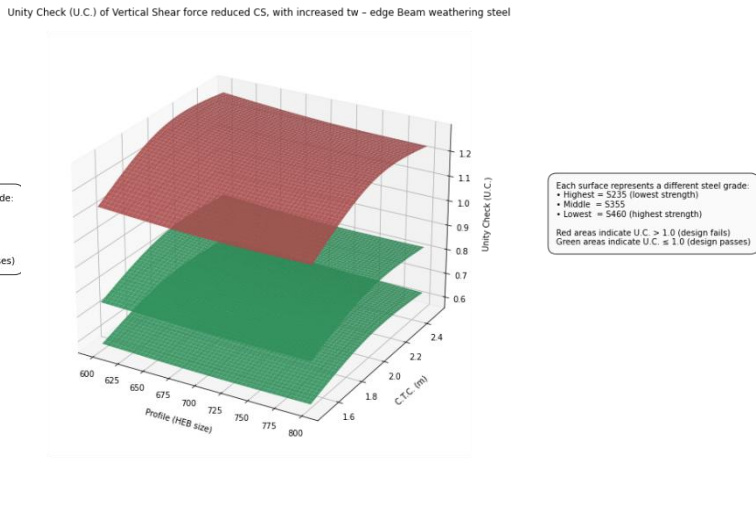

Figure 95 visualization of the performed Vertical shear verification for the edge beam by interpolating the c.t.c. distance and the HEB profiles of the weathering steel beams, for the reduced web height, and an increased web thickness.

Table 97 Verification of vertical shear force of middle conventional steel beam for a centre to centre distance of 1.5m for the increased web thickness.

Profile	S235				S355				S460			
	V_{Ed} [kNm]	τ_{Ed} [N/mm²]	τ_{Rd} [N/mm²]	U.C [-]	V_{Ed} [kNm]	τ_{Ed} [N/mm²]	τ_{Rd} [N/mm²]	U.C [-]	V_{Ed} [kNm]	τ_{Ed} [N/mm²]	τ_{Rd} [N/mm²]	U.C [-]
HEB600B	635	72	109	0.66	635	72	164	0.44	635	72	212	0.34
HEB700B	640	70	109	0.65	640	70	164	0.43	640	70	212	0.33
HEB800B	645	70	109	0.65	645	70	164	0.43	645	70	212	0.33

Table 98 Verification of vertical shear force of middle conventional steel beam for a centre to centre distance of 2.0m for the increased web thickness.

Profile	S235				S355				S460			
	V_{Ed} [kNm]	τ_{Ed} [N/mm²]	τ_{Rd} [N/mm²]	U.C [-]	V_{Ed} [kNm]	τ_{Ed} [N/mm²]	τ_{Rd} [N/mm²]	U.C [-]	V_{Ed} [kNm]	τ_{Ed} [N/mm²]	τ_{Rd} [N/mm²]	U.C [-]
HEB600B	880	99	109	0.91	880	99	164	0.60	880	99	212	0.47
HEB700B	890	98	109	0.90	890	98	164	0.60	890	98	212	0.46
HEB800B	900	98	109	0.90	900	98	164	0.60	900	98	212	0.46

Table 99 Verification of vertical shear force of middle conventional steel beam for a centre to centre distance of 2.5 m for the increased web thickness.

Profile	S235				S355				S460			
	V_{Ed} [kNm]	τ_{Ed} [N/mm²]	τ_{Rd} [N/mm²]	U.C [-]	V_{Ed} [kNm]	τ_{Ed} [N/mm²]	τ_{Rd} [N/mm²]	U.C [-]	V_{Ed} [kNm]	τ_{Ed} [N/mm²]	τ_{Rd} [N/mm²]	U.C [-]
HEB600B	1060	119	109	1.10	1060	119	164	0.73	1060	119	212	0.56
HEB700B	1075	118	109	1.08	1075	118	164	0.72	1075	118	212	0.56
HEB800B	1090	119	109	1.09	1090	119	164	0.73	1090	119	212	0.56

Table 100 Verification of vertical shear force of middle weathering steel beam for a centre to centre distance of 1.5m for the increased web thickness.

Profile	S235				S355				S460			
	V_{Ed} [kNm]	τ_{Ed} [N/mm²]	τ_{Rd} [N/mm²]	U.C [-]	V_{Ed} [kNm]	τ_{Ed} [N/mm²]	τ_{Rd} [N/mm²]	U.C [-]	V_{Ed} [kNm]	τ_{Ed} [N/mm²]	τ_{Rd} [N/mm²]	U.C [-]
HEB600B	635	76	109	0.70	635	76	164	0.46	635	76	212	0.36
HEB700B	640	74	109	0.68	640	74	164	0.45	640	74	212	0.35
HEB800B	645	74	109	0.68	645	74	164	0.45	645	74	212	0.35

Table 101 Verification of vertical shear force of middle weathering steel beam for a centre to centre distance of 2.0m for the increased web thickness.

Profile	S235				S355				S460			
	V_{Ed} [kNm]	τ_{Ed} [N/mm²]	τ_{Rd} [N/mm²]	U.C [-]	V_{Ed} [kNm]	τ_{Ed} [N/mm²]	τ_{Rd} [N/mm²]	U.C [-]	V_{Ed} [kNm]	τ_{Ed} [N/mm²]	τ_{Rd} [N/mm²]	U.C [-]
HEB600B	880	105	109	0.96	880	105	164	0.64	880	105	212	0.50
HEB700B	890	103	109	0.95	890	103	164	0.63	890	103	212	0.49
HEB800B	900	104	109	0.95	900	104	164	0.63	900	104	212	0.49

Table 102 Verification of vertical shear force of middle weathering steel beam for a centre to centre distance of 2.5 m for the increased web thickness.

Profile	S235				S355				S460			
	V_{Ed} [kNm]	τ_{Ed} [N/mm²]	τ_{Rd} [N/mm²]	U.C [-]	V_{Ed} [kNm]	τ_{Ed} [N/mm²]	τ_{Rd} [N/mm²]	U.C [-]	V_{Ed} [kNm]	τ_{Ed} [N/mm²]	τ_{Rd} [N/mm²]	U.C [-]
HEB600B	1060	127	109	1.16	1060	127	164	0.77	1060	127	212	0.60
HEB700B	1075	125	109	1.15	1075	125	164	0.76	1075	125	212	0.59
HEB800B	1090	126	109	1.15	1090	126	164	0.77	1090	126	212	0.59

In Figure 98 and Figure 97, the result of the vertical shear verification of the middle beam are presented for both the conventional steel variant and the weathering steel variant. The results have been extrapolated to provide a clear 3D plot showing all variants that satisfy the vertical shear verification. As can be seen. Variations were made in the profile type, centre-to-centre distance, and the steel grade. This results in three distinct layers in the plot, each corresponding to a different steel grade with the lowest layer representing S460 and the highest representing S460.

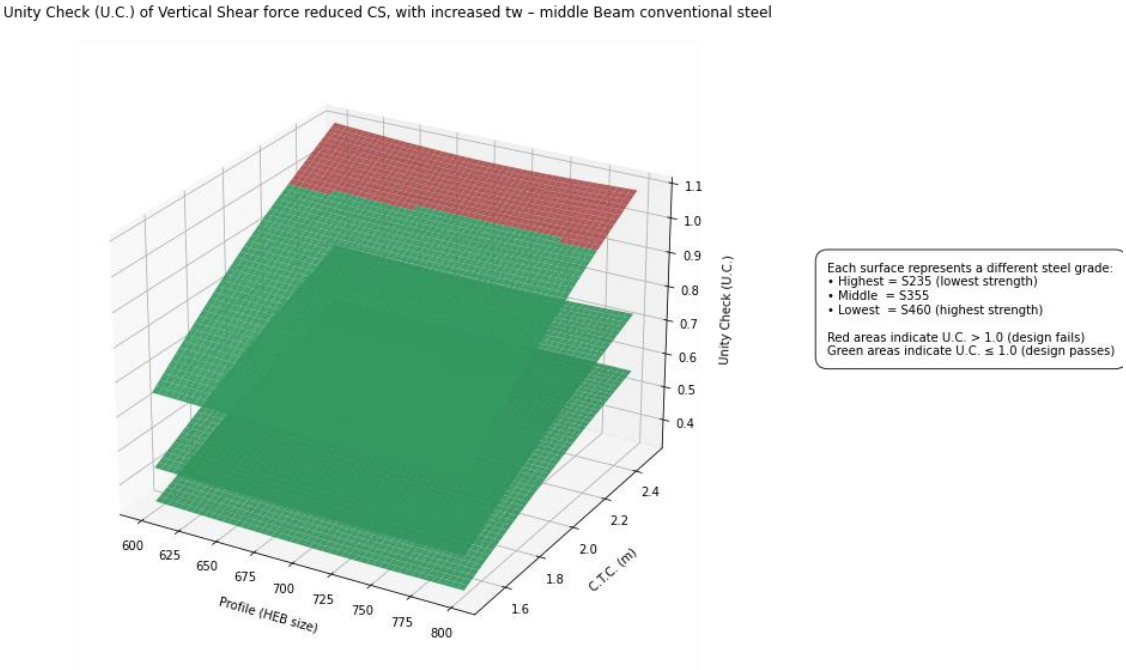

Figure 97 visualization of the performed Vertical shear verification for the middle beam by interpolating the c.t.c. distance and the HEB profiles for conventional steel beams, for the reduced web height, and an increased web thickness.

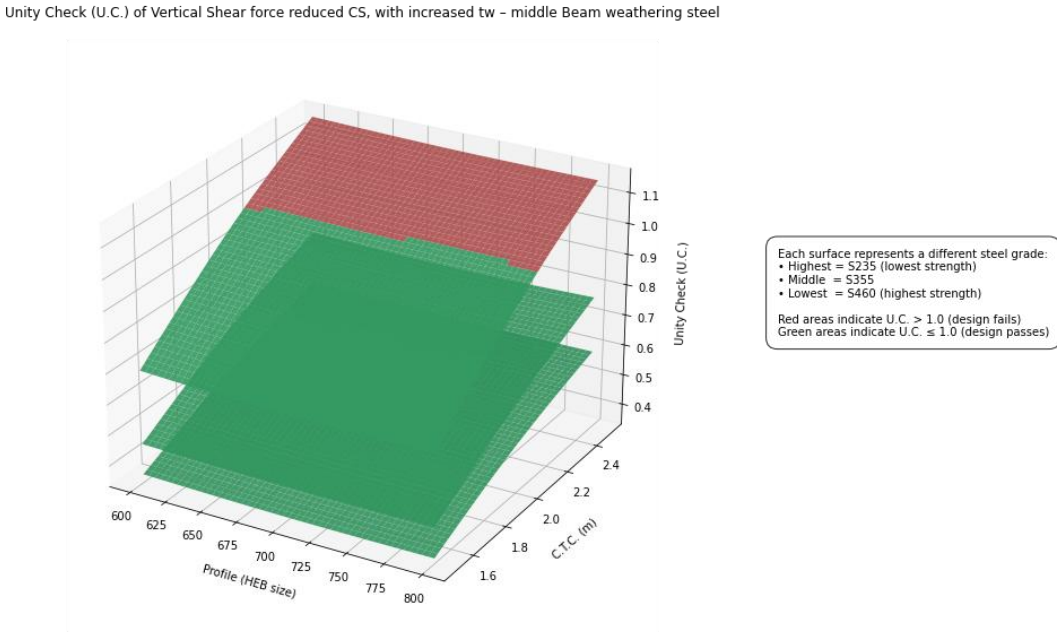

Figure 98 visualization of the performed Vertical shear verification for the middle beam by interpolating the c.t.c. distance and the HEB profiles for weathering steel beams, for the reduced web height, and an increased web thickness.

5.6.4 Deflection verification

According to the NEN-EN 1990+A1+A1/C2:2019/NB:2019 nl the deflection restrictions are mentioned for bridgedecks. Hereby in A2.4.4.3 the maximum total vertical deflection should be taken as L/500. For the maximum allowable deflection due to traffic load only it is stated that maximum deflection is permitted of L/250.

To satisfy the stringent restrictions for the SLS deflection it is needed to make use of precambering of the steel beams. The precambering will be done to neutralize the self weight of the structure in phase 2. The results of the precambering are given in Table 62 to Table 64. The total governing deflection due to the different load cases will be determined by the RFEM model. The governing load combination will be for all the variants the same it will be as given in the tables below. Herby the characteristic load combination will be taken into account.

SLS_{char} : LC1 +LC2 +LC6+LC9 (midspan of the edge beam)

SLS_{char} : LC1 +LC7 +LC6+LC9 (midspan of the middle beam)

Table 103 Load cases including in load combination for governing vertical deflection midspan of the edge beam

Load cases	description
LC1	Self weight of the structure
LC2	Traffic load LM1 edge beam max bending moment
LC6	Asphalt load
LC9	Imposed load shrinkage

Table 104 Load cases including in load combination for governing vertical deflection midspan of the middle beam

Load cases	description
LC1	Self weight of the structure
LC7	Traffic load LM1 middle beam max bending moment
LC6	Asphalt load
LC9	Imposed load shrinkage

In paragraph 5.5.3, the required precambering is determined to ensure that the beam profile is neutralized under the loading conditions of Phase 2, which includes the self-weight of the beams as well as the wet weight of the reinforced concrete. The required precambering is presented in the second column of the tables below. The first column shows the deflection resulting from the governing load combinations, as specified in Table 103 and Table 104. These combinations include deflection due to the self-weight of the structure. To calculate the net deflection in Phase 3, the deflection due to self-weight must be subtracted from the total deflection. This resulting net deflection is referred to as u_{net} and is shown in the fourth column.

This net deflection is then divided by the maximum allowable deflection according to Eurocode standards, resulting in the initial utilization check (U.C.), which includes only the precambering due to self-weight. As seen in all the tables, this alone is not sufficient; additional precambering is required to achieve satisfactory results. Therefore, an additive precambering is calculated so that the U.C. reaches approximately 0.8.For certain variants, this means that even an additional precambering of up to 130 mm is required, resulting in a total precambering of 202 mm, to comply with Eurocode deflection limits.

Additionally, the deflection due to traffic loads must also remain below specific thresholds as defined by the Eurocode. This verification is shown in the column u_{traf}, where the deflection due to traffic loading is isolated by subtracting the additive precambering from the total deflection. As shown, with the inclusion of the additive precambering, all deflection verifications for traffic loads are satisfied. In Figure 99 to Figure 101, the result of the deflection verification of the edge/middle beam are presented for both the conventional steel variant and the weathering steel variant. The results have been extrapolated to provide a clear 3D plot showing all variants that satisfy the deflection verification. As can be seen. Variations were made in the profile type, centre-to-centre distance. Hereby the steel class is independent of for the deflection verification.

Table 105 Verification of the deflection phase 3 to for a ctc distance of 1.5m for the conventional steel edge beam

Profile	S235/S355/S460												
	$u_{tot,P3}$ [mm]	$u_{precamb}$ [mm]	u_{sw} [mm]	u_{net} [mm]	u_{max} [mm]	U.C [-]	$u_{precam,add}$ [mm]	u_{net} [mm]	U.C [-]	u_{traf} [mm]	u_{net} [mm]	u_{max} [mm]	U.C [-]
HEB600B	**184**	**92**	**40**	**144**	**43**	**3.35**	**110**	**34**	**0.79**	130	**20**	**86**	**0.23**
HEB700B	**135**	**63**	**29**	**106**	**43**	**2.5**	**70**	**36**	**0.84**	95	**25**	**86**	**0.29**
HEB800B	**104**	**46**	**23**	**81**	**43**	**1.9**	**45**	**36**	**0.84**	73	**28**	**86**	**0.33**

Table 106 Verification of the deflection phase 3 to for a ctc distance of 2.0 m for the conventional steel edge beam

Profile	S235/S355/S460												
	$u_{tot,P3}$ [mm]	$u_{precamb}$ [mm]	u_{sw} [mm]	u_{net} [mm]	u_{max} [mm]	U.C [-]	$u_{precam,add}$ [mm]	u_{net} [mm]	U.C [-]	u_{traf} [mm]	u_{net} [mm]	u_{max} [mm]	U.C [-]
HEB600B	**206**	**92**	**44**	**162**	**43**	**3.8**	**125**	**37**	**0.86**	147	**22**	**86**	**0.26**
HEB700B	**151**	**63**	**32**	**119**	**43**	**2.8**	**85**	**34**	**0.79**	106	**21**	**86**	**0.24**
HEB800B	**116**	**46**	**25**	**91**	**43**	**2.1**	**55**	**36**	**0.84**	82	**27**	**86**	**0.31**

Table 107 Verification of the deflection phase 3 to for a ctc distance of 2.5 m for the conventional steel edge beam

Profile	S235/S355/S460												
	$u_{tot,P3}$ [mm]	$u_{precamb}$ [mm]	u_{sw} [mm]	u_{net} [mm]	u_{max} [mm]	U.C [-]	$u_{precam,add}$ [mm]	u_{net} [mm]	U.C [-]	u_{traf} [mm]	u_{net} [mm]	u_{max} [mm]	U.C [-]
HEB600B	**207**	**92**	**45**	**162**	**43**	**3.77**	**130**	**32**	**0.74**	153	**18**	**86**	**0.21**
HEB700B	**151**	**63**	**33**	**118**	**43**	**2.74**	**85**	**33**	**0.77**	110	**20**	**86**	**0.23**
HEB800B	**116**	**46**	**25**	**91**	**43**	**2.12**	**55**	**36**	**0.84**	84	**24**	**86**	**0.28**

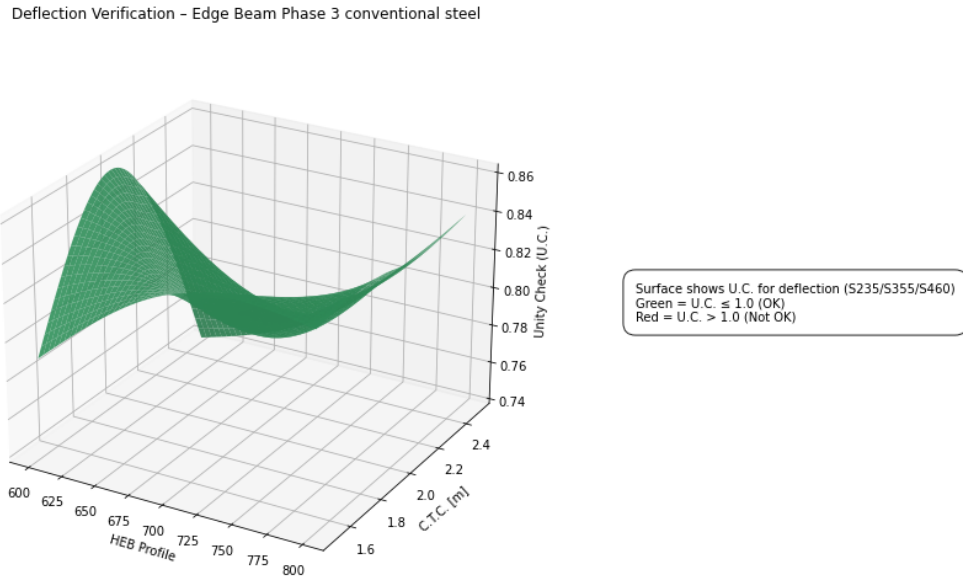

Figure 99 For a satisfying verification for the deflection U.C. is plotted against the Profile type and the c.t.c. distance for the conventional steel edge beam.

Table 108 Verification of the deflection phase 3 to for a ctc distance of 1.5m for the conventional steel middle beam

Profile	S235/S355/S460												
	$u_{tot,P3}$ [mm]	$u_{precamb}$ [mm]	u_{sw} [mm]	u_{net} [mm]	u_{max} [mm]	U.C [-]	$u_{precam,add}$ [mm]	u_{net} [mm]	U.C [-]	u_{traf} [mm]	u_{net} [mm]	u_{max} [mm]	U.C [-]
HEB600B	125	92	36	89	43	2.07	55	34	0.79	77	62	86	0.72
HEB700B	93	63	26	67	43	1.56	30	37	0.86	57	52	86	0.60
HEB800B	71	46	20	51	43	1.19	15	36	0.84	44	44	86	0.51

Table 109 Verification of the deflection phase 3 to for a ctc distance of 2.0 m for the conventional steel middle beam

Profile	S235/S355/S460												
	$u_{tot,P3}$ [mm]	$u_{precamb}$ [mm]	u_{sw} [mm]	u_{net} [mm]	u_{max} [mm]	U.C [-]	$u_{precam,add}$ [mm]	u_{net} [mm]	U.C [-]	u_{traf} [mm]	u_{net} [mm]	u_{max} [mm]	U.C [-]
HEB600B	149	92	41	108	43	2.51	75	33	0.77	93	68	86	0.79
HEB700B	110	63	30	80	43	1.86	45	35	0.81	69	59	86	0.69
HEB800B	79	46	23	56	43	1.30	20	36	0.84	59	59	86	0.69

Table 110 Verification of the deflection phase 3 to for a ctc distance of 2.5 m for the conventional steel middle beam

Profile	S235/S355/S460												
	$u_{tot,P3}$ [mm]	$u_{precamb}$ [mm]	u_{sw} [mm]	u_{net} [mm]	u_{max} [mm]	U.C [-]	$u_{precam,add}$ [mm]	u_{net} [mm]	U.C [-]	u_{traf} [mm]	u_{net} [mm]	u_{max} [mm]	U.C [-]
HEB600B	149	92	47	102	43	2.37	65	37	0.86	104	74	86	0.86
HEB700B	110	63	34	76	43	1.77	40	36	0.84	77	62	86	0.72
HEB800B	85	46	26	59	43	1.37	25	34	0.79	60	60	86	0.70

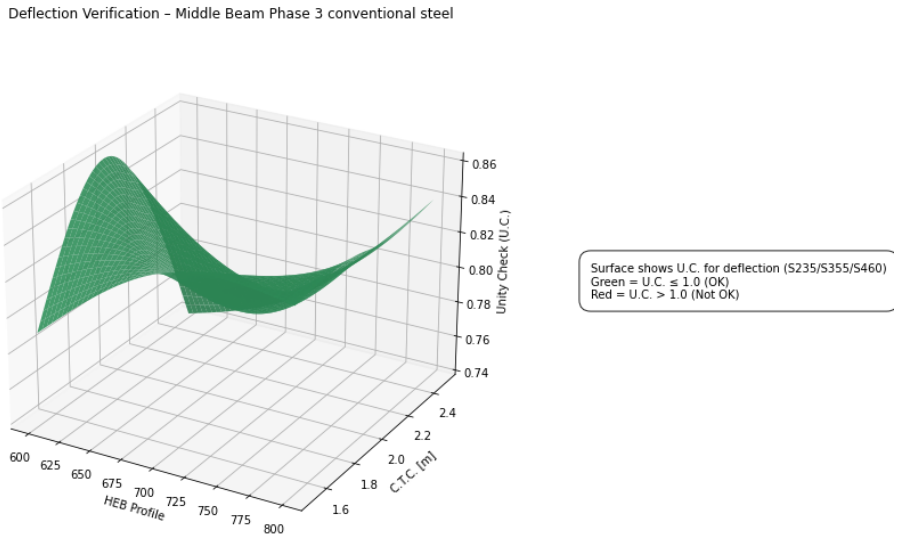

Figure 100 For a satisfying verification for the deflection U.C. is plotted against the Profile type and the c.t.c. distance for the conventional steel middle beam.

Table 111 Verification of the deflection phase 3 to for a ctc distance of 1.5m for the edge beam (reduced cross-section)

Profile	S235/S355/S460												
	$u_{tot,P3}$ [mm]	$u_{precamb}$ [mm]	u_{sw} [mm]	u_{net} [mm]	u_{max} [mm]	U.C [-]	$u_{precam,add}$ [mm]	u_{net} [mm]	U.C [-]	u_{traf} [mm]	u_{net} [mm]	u_{max} [mm]	U.C [-]
HEB600B	**194**	**92**	**40**	**154**	**43**	**3.58**	**120**	**34**	**0.79**	130	**20**	**86**	**0.23**
HEB700B	**142**	**63**	**29**	**113**	**43**	**2.63**	**80**	**33**	**0.77**	95	**25**	**86**	**0.29**
HEB800B	**110**	**46**	**23**	**87**	**43**	**2.02**	**50**	**37**	**0.86**	73	**28**	**86**	**0.33**

Table 112 Verification of the deflection phase 3 to for a ctc distance of 2.0 m for the edge beam (reduced cross-section)

Profile	S235/S355/S460												
	$u_{tot,P3}$ [mm]	$u_{precamb}$ [mm]	u_{sw} [mm]	u_{net} [mm]	u_{max} [mm]	U.C [-]	$u_{precam,add}$ [mm]	u_{net} [mm]	U.C [-]	u_{traf} [mm]	u_{net} [mm]	u_{max} [mm]	U.C [-]
HEB600B	**218**	**92**	**44**	**174**	**43**	**4.05**	**140**	**34**	**0.79**	147	**22**	**86**	**0.26**
HEB700B	**159**	**63**	**32**	**127**	**43**	**2.95**	**90**	**37**	**0.86**	106	**21**	**86**	**0.24**
HEB800B	**123**	**46**	**25**	**98**	**43**	**2.28**	**65**	**33**	**0.77**	82	**27**	**86**	**0.31**

Table 113 Verification of the deflection phase 3 to for a ctc distance of 2.5 m for the edge beam (reduced cross-section)

Profile	S235/S355/S460												
	$u_{tot,P3}$ [mm]	$u_{precamb}$ [mm]	u_{sw} [mm]	u_{net} [mm]	u_{max} [mm]	U.C [-]	$u_{precam,add}$ [mm]	u_{net} [mm]	U.C [-]	u_{traf} [mm]	u_{net} [mm]	u_{max} [mm]	U.C [-]
HEB600B	**218**	**92**	**45**	**173**	**43**	**4.02**	**135**	**38**	**0.88**	153	**18**	**86**	**0.21**
HEB700B	**160**	**63**	**33**	**127**	**43**	**2.95**	**90**	**37**	**0.86**	110	**20**	**86**	**0.23**
HEB800B	**122**	**46**	**25**	**97**	**43**	**2.26**	**60**	**37**	**0.86**	84	**24**	**86**	**0.28**

Table 114 Verification of the deflection phase 3 to for a ctc distance of 1.5m for the middle beam (reduced cross-section)

Profile	S235/S355/S460												
	$u_{tot,P3}$ [mm]	$u_{precamb}$ [mm]	u_{sw} [mm]	u_{net} [mm]	u_{max} [mm]	U.C [-]	$u_{precam,add}$ [mm]	u_{net} [mm]	U.C [-]	u_{traf} [mm]	u_{net} [mm]	u_{max} [mm]	U.C [-]
HEB600B	**131**	**92**	**36**	**95**	**43**	**2.21**	**60**	**35**	**0.81**	**77**	**62**	**86**	**0.72**
HEB700B	**97**	**63**	**26**	**71**	**43**	**1.65**	**35**	**36**	**0.84**	**57**	**52**	**86**	**0.60**
HEB800B	**75**	**46**	**20**	**55**	**43**	**1.28**	**20**	**35**	**0.81**	**44**	**44**	**86**	**0.51**

Table 115 Verification of the deflection phase 3 to for a ctc distance of 2.0 m for the middle beam (reduced cross-section)

Profile	S235/S355/S460												
	$u_{tot,P3}$ [mm]	$u_{precamb}$ [mm]	u_{sw} [mm]	u_{net} [mm]	u_{max} [mm]	U.C [-]	$u_{precam,add}$ [mm]	u_{net} [mm]	U.C [-]	u_{traf} [mm]	u_{net} [mm]	u_{max} [mm]	U.C [-]
HEB600B	**156**	**92**	**41**	**115**	**43**	**2.67**	**85**	**30**	**0.70**	**93**	**68**	**86**	**0.79**
HEB700B	**115**	**63**	**30**	**85**	**43**	**1.98**	**50**	**35**	**0.81**	**69**	**59**	**86**	**0.69**
HEB800B	**83**	**46**	**23**	**60**	**43**	**1.40**	**25**	**35**	**0.81**	**59**	**59**	**86**	**0.69**

Table 116 Verification of the deflection phase 3 to for a ctc distance of 2.5 m for the middle beam (reduced cross-section)

Profile	S235/S355/S460												
	$u_{tot,P3}$ [mm]	$u_{precamb}$ [mm]	u_{sw} [mm]	u_{net} [mm]	u_{max} [mm]	U.C [-]	$u_{precam,add}$ [mm]	u_{net} [mm]	U.C [-]	u_{traf} [mm]	u_{net} [mm]	u_{max} [mm]	U.C [-]
HEB600B	**156**	**92**	**47**	**109**	**43**	**2.53**	**75**	**34**	**0.79**	**104**	**74**	**86**	**0.86**
HEB700B	**115**	**63**	**34**	**81**	**43**	**1.88**	**45**	**36**	**0.84**	**77**	**62**	**86**	**0.72**
HEB800B	**89**	**46**	**26**	**63**	**43**	**1.47**	**30**	**33**	**0.77**	**60**	**60**	**86**	**0.70**

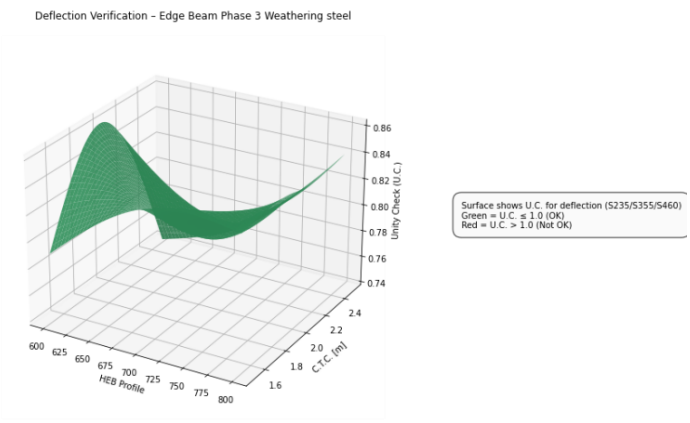

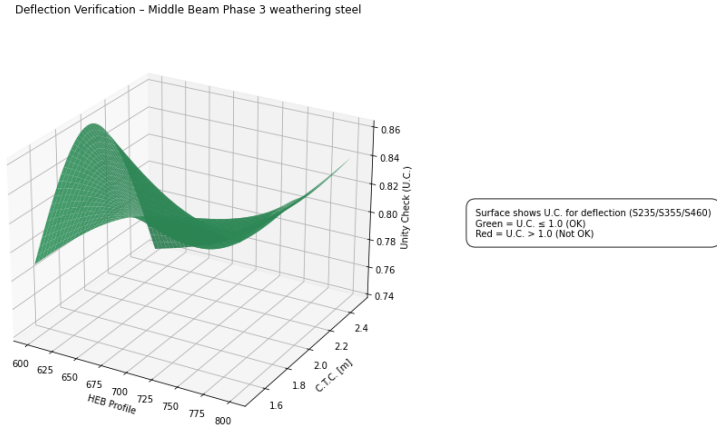

Figure 101 For a satisfying verification for the deflection U.C. is plotted against the Profile type and the c.t.c. distance for the weathering steel edge beam (left) and middle beam (right).

IV Sustainability impact analysis

In this chapter the determined sustainability impact of the different used components for the different variants which are determined in paragraph 2.5 will be used in combination with the determined dimensions of the variants in chapter 5 to determine the sustainability impact of each variant. The variants that will be considered are as follow:

- **Variant 1** full reinforced concrete superstructure
- **Variant 2** Composite conventional steel concrete superstructure
- **Variant 3** Composite weathering steel concrete superstructure

For variant 2 and 3 it has also been chosen to variate the centre to centre distance between the profiles, the profile section (HEB600B,HEB700B andHEB800B) and the steel class used (S235, S355 and S460). According to the performed verifications of the structural analyses, only a few of all subvariants satisfy all the verifications, and only these few are considered in the sustainability analysis. In Table 117 and Table 118 an overview is given of the satisfying variants for the edge beam of the structure and the in between beams of the structure.

Table 117 Overview of which variants satisfy the verification for the edge beam made of conventional steel (left table) and weathering steel (right table)

Centre to centre distance	Steel class	HEB600	HEB700	HEB800
1.5m (2 profiles)	S235			
	S355			
	S460			
2m (2 profiles)	S235			
	S355			
	S460			
2.5m (2 profiles)	S235			
	S355			
	S460			

Centre to centre distance	Steel class	HEB600	HEB700	HEB800
1.5m (2 profiles)	S235			
	S355			
	S460			
2m (2 profiles)	S235			
	S355			
	S460			
2.5m (2 profiles)	S235			
	S355			
	S460			

Table 118 Overview of which variants satisfy the verification for the in between beams made of conventional steel (left table) and weathering steel (rightn table)

Centre to centre distance	Steel class	HEB600	HEB700	HEB800
1.5m (7 profiles)	S235			
	S355			
	S460			
2m (5 profiles)	S235			
	S355			
	S460			
2.5m (4 profiles)	S235			
	S355			
	S460			

Centre to centre distance	Steel class	HEB600	HEB700	HEB800
1.5m (7 profiles)	S235			
	S355			
	S460			
2m (5 profiles)	S235			
	S355			
	S460			
2.5m (4 profiles)	S235			
	S355			
	S460			

For both variant 2 and variant 3 the most optimal combination will be used for the sustainability analysis for the different centre to centre distance.

Table 119 Overview of optimal combination of steel profiles to be used for the conventional steel variant

Centre to centre distance	Optimal composition of steel profiles
1.5m (9x profile)	2x HEB800 (S355) and 7x HEB600 (S460)
2m (7x profile)	2x HEB800 (S460) and 5x HEB700 (S355)
2.5m (6x profile)	2x HEB800 (S460) and 4x HEB700 (S460)

Table 120 Overview of optimal combination of steel profiles to be used for the weathering steel variant

Centre to centre distance	Optimal composition of steel profiles
1.5m (9x profile)	2x HEB800 (S460) and 7x HEB600 (S460)
2m (7x profile)	2x HEB800 (S460) and 5x HEB700 (S460)
2.5m (6x profile)	2x HEB800 (S460) and 4x HEB700 (S460)

Variant 2 and 3 concise also of a concrete component this concrete component is the same for both structures it is a 200 mm thick concrete layer with al length of 21.5m and a width of 14.4 m.

The analysis of the structural variants , as can be seen in Table 121 shows a clear difference in total mass between the full concrete variant and the composite steel-concrete variants. The full concrete variant 1 is significantly heavier, with a total mass of 400 t and a mass per unit area of 1,292 kg/m^2. In contrast, the composite (weathering) steel-concrete variants 2 and 3 have much lower total masses, ranging from 187t to 198t and mass per unit area between 603 kg/m^2 and 639 kg/m^2.

Among the composite variants, the difference is more modest: the 1.5 m centre-to-centre distance variant (variant 2) is slightly heavier at 198 t compared to the 2.5 m variant (variant 3) at 187 t, reflecting the reduced amount of steel used as the spacing between steel profiles increases.

This highlights that while moving from a full reinforced concrete superstructure to a composite system significantly reduces structural weight, variations in steel spacing within the composite system produce only moderate changes in mass.

Table 121 total mass calculation of the different variants

steel component	Centre to centre distance	Optimal composition of steel profiles	mass [tonne]	Dimensions concrete deck	mass [tonne]	Total mass [tonne]	Mass/area [kg/m2]
Full concrete variant 1	**-**	**-**	**-**	-	-	400	1292
composite (weathering) steel concrete variants 2 and 3	**1.5m (9x profile)**	2x HEB800 (S355) and 7x HEB600 (S460)	43.172	14,4m * 21,5m *0.2m	154.8	198	639
composite (weathering) steel concrete variants 2 and 3	**2m (7x profile)**	2x HEB800 (S460) and 5x HEB700 (S355)	37.1735	14,4m * 21,5m *0.2m	154.8	192	620
composite (weathering) steel concrete variants 2 and 3	**2.5m (6x profile)**	2x HEB800 (S460) and 4x HEB700 (S460)	31.992	14,4m * 21,5m *0.2m	154.8	187	603

6 Sustainability impact calculation per variant

6.1 *Variant 1 full concrete structure*

For Variant 1, the existing concrete girder superstructure is considered, based on the Rijkswaterstaat case study. The environmental cost is determined from literature correlating bridge type and span length, distinguishing between concrete girder and plated superstructures. According to Figure 102, the MKI for a girder superstructure with a 21.5 m span is approximately €39.00/m^2. From this, the total environmental cost of the full concrete variant is calculated as €12,074.40 (Table 122).

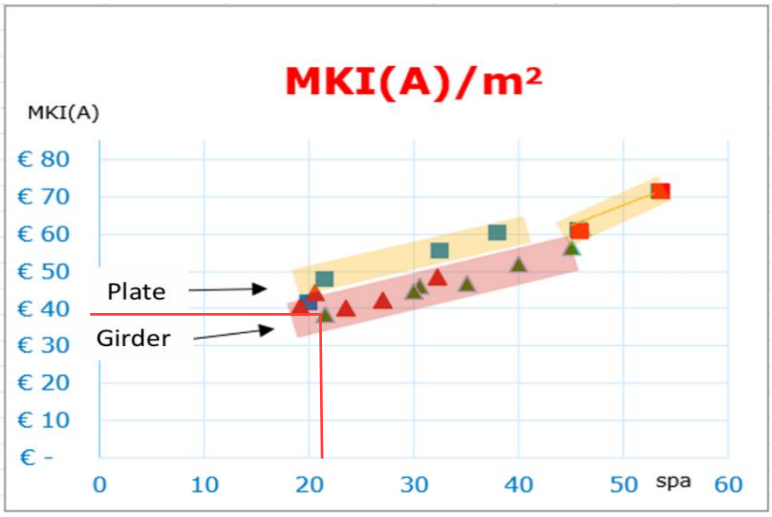

Figure 102 MKI of a concrete superstructure according to indicator A1, phase A1-A5

To ensure a consistent and comparable assessment, only the upfront life-cycle stages A1–A5 are considered in Figure 102 . These stages cover raw material extraction, production, transport, and construction, which account for 80–90% of the total impact for small concrete bridges. Use and maintenance (B-modules) and End-of-Life (C-modules) are excluded, as their contribution is limited and highly project-specific. This A1–A5 focus ensures comparability with the other variants while capturing the dominant environmental impacts (Thie, 2025).

Table 122 Total MKI of variant 1, phase A1-A5

Length [m]	width [m]	Area [m2]	MKI/m2	Total MKI
21.5	14.40	309.60	39	€ 12,074.40

6.2 *Variant 2 conventional composite steel concrete superstructure*

6.2.1 reinforced concrete component

For the reinforced concrete component, both the concrete and the reinforcement steel must be considered. For the concrete, the assessment is based on the NMD Environmental Product Declaration #nmd_201627 for Betonmortel C35/45 (CEM IIIB), reporting an MKI of €27.66/m^3 for a 100-year service life. The NMD dataset is methodologically complete, covering all relevant impact categories and the full production and construction phases (A1–A5), with production dominating the environmental burden (€24.34/m^3). Use, end-of-life (C-modules), and Module D contributions are minor, with a small net credit from Module D (–€1.34/m^3).

For the reinforcement steel, two datasets are available: the company-specific Holterman B500B steel and the NMD dataset #nmd_45791. Holterman steel focuses mainly on production phases (A1–A3), with limited coverage of A4–A5 and no Module D credits, making it less comparable to other materials assessed over all life-cycle stages.

In contrast, the NMD dataset includes A1–A5, use and end-of-life phases, and Module D, providing a fully comparable, methodologically complete assessment. The total environmental cost of NMD reinforcement steel is €163.03 per tonne for A1–A5, with Module D offering a small credit for material recovery.

It is assumed that for a composite superstructure, the upper concrete layer contains 110 kg/m^3 of reinforcement (ONE click LCA, 2025) . Using the NMD datasets for both concrete and reinforcement ensures that the environmental assessment of Variant 1 is fully consistent with A1–A5 across all materials, enabling robust comparisons with other variants. Table 123 summarizes the MKI/unit values for the reinforced concrete components based on NMD data for A1-A5.

Table 123 MKI/unit of the different components of reinforced concrete

component	MKI	unit	remarks
Betonmortel C35/45 (o.b.v. CEM IIIB), 2438,7 kg/m3[NMD]	24.34	€/m3	All impact categories, phase A1-A5 (NO supplement taken into accoant for comparebility)
holterman reinforcement	114.20	€/tonne	All impact categories, phase A1-A3 (NO supplement taken into accoant for comparebility)
Reinforcement LCA from [NMD]	163.03	€/tonne	All impact categories, phase A1-A5 (NO supplement taken into accoant for comparebility)

In Table 124 the total environmental costs are given of the reinforced concrete. A total environmental costs of **€ 2,617.46** should be taken into account for the concrete part.

Table 124 total environmental costs of reinforced concrete according to indicator A1, phase A1-A5

component	Quantity	unit	MKI	unit2	Total MKI [€]
Betonmortel C35/45 (o.b.v. CEM IIIB), 2438,7 kg/m3[NMD]	61.92	m3	24.34	€/m3	€ 1,507.13
Reinforcement NMD (110kg/m3)	6.81	tonne	163.03	€/tonne	€ 1,110.43
Total costs of reinforced concrete					**€ 2,617.56**

6.2.2 Painted steel component

The first component to be considered is the steel elements. Table 125 shows the MKI per unit for different steel suppliers based on the EPDs presented in Chapter 2.5. There is considerable variation between suppliers, primarily for two reasons. First, some suppliers, such as ArcelorMittal (conventional plated steel) and SSAB, report only 6 of the 11 EN 15804+A1 impact categories and cover only part of the lifecycle (mainly A1–A3), whereas the National Environmental Database (NMD) and the Xcrarb profiles include all 11 impact categories and covers the complete A1–A5 stages.

Table 125 MKI/unit of the different found suppliers of steel profiles for bridging solutions phase A

component	MKI	unit	remarks
Steel plates Arcellor Mittal	153.34	€/tonne	6/11 impactcategories considered, phase A1-A3, (NO supplement taken into accoant for comparebility)
XCarb™ structural steel sections Arcelor Mittal	58.44	€/tonne	11/11 impactcategories considered, phase A1-A5, (NO supplement taken into accoant for comparebility)
Conventional steel plates SSAB	167.48	€/tonne	6/11 impactcategories considered , phase A1-A3,(NO supplement taken into accoant for comparebility)
Staal constructieprofielen (HEA/HEB/HEM/IPE/UNP) [NMD]	163.37	€/tonne	11/11 impactcategories considered, phase A1-A5, (NO supplement taken into accoant for comparebility)

Second, the ArcelorMittal XCarb® steel, produced via a 100% electric arc furnace (EAF) using renewable electricity and 100% scrap, shows the lowest environmental impact. Other suppliers, including conventional ArcelorMittal plated steel and SSAB, rely on blast furnace processes, which result in higher production-related impacts.

For Variant 2, two MKI values will be used to provide a realistic range for comparison: the environmentally favorable XCarb® steel and the fully methodologically complete NMD steel. Both datasets include all relevant A1–A5 lifecycle stages and all impact categories, making them fully comparable with Variant 1, which also considers all 11 impact categories over A1–A5. Using these two extremes gives a representative range for the potential environmental impact of steel in the superstructure.

Table 126 MKI/unit of the different found suppliers of steel profiles for bridging solutions phase D

component	MKI	unit	remarks
Steel plates Arcellor Mittal	-110.18	€/tonne	6/11 impactcategories considered, phase D, (NO supplement taken into accoant for comparebility)
XCarb™ structural steel sections Arcelor Mittal	20.68	€/tonne	11/11 impactcategories considered, phase D, (NO supplement taken into accoant for comparebility)
Conventional steel plates SSAB	-89.05	€/tonne	6/11 impactcategories considered , phase D,(NO supplement taken into accoant for comparebility)
Staal constructieprofielen (HEA/HEB/HEM/IPE/UNP) [NMD]	-5.10	€/tonne	11/11 impactcategories considered, phase D, (NO supplement taken into accoant for comparebility)

It is important to note that Phase D (beyond-life-cycle benefits) can significantly influence the total MKI values. As shown in Table 125, steel products that contribute most heavily to Phase A impacts, such as the conventional ArcelorMittal and SSAB plates, also receive the largest reductions in Phase D (–€110.18/tonne and –€89.05/tonne, respectively). In contrast, the XCarb® structural steel sections and NMD profiles, which already have lower Phase A impacts, receive smaller Phase D credits (20.68 €/tonne and –5.10 €/tonne). This difference highlights that looking solely at the total environmental costs can give a skewed view of the relative sustainability performance, as high production impacts can be partially offset by end-of-life recycling benefits. For a more accurate understanding of the total environmental cost, it is therefore advisable to examine both the production phase (A1–A5) and the Phase D contributions individually for each material, rather than relying only on the net MKI.

The results as shown in Table 127, show a substantial difference between the two options. For example, with a centre-to-centre distance of 1.5 m, the difference in total environmental cost can reach nearly €4,500, illustrating the significant sustainability benefits of using XCarb® steel while also providing a conservative upper bound using the NMD dataset.

Table 127 Environmental impact of the steel component for the different compositions of variant 2 (phase A1-A5)

steel component	Centre to centre distance	Optimal composit	Quantity	unit	MKI	unit2	Total MKI [€]
XCarb™ structural steel sections Arcelor Mittal	**1.5m (9x profile)**	2x HEB800	43.172	tonne	58.44	€/tonne	**€ 2,522.97**
XCarb™ structural steel sections Arcelor Mittal	**2m (7x profile)**	2x HEB800	37.1735	tonne	58.44	€/tonne	**€ 2,172.42**
XCarb™ structural steel sections Arcelor Mittal	**2.5m (6x profile)**	2x HEB800	31.992	tonne	58.44	€/tonne	**€ 1,869.61**
Staal constructieprofielen (HEA/HEB/HEM/IPE/UNP) [NMD]	**1.5m (9x profile)**	2x HEB800	43.172	tonne	163.37	€/tonne	**€ 7,053.01**
Staal constructieprofielen (HEA/HEB/HEM/IPE/UNP) [NMD]	**2m (7x profile)**	2x HEB800	37.1735	tonne	163.37	€/tonne	**€ 6,073.03**
Staal constructieprofielen (HEA/HEB/HEM/IPE/UNP) [NMD]	**2.5m (6x profile)**	2x HEB800	31.992	tonne	163.37	€/tonne	**€ 5,226.53**

These steel components require protective coating to prevent corrosion in harsh atmospheric environments. For the MKI calculation, two sources are available: the Rijkswaterstaat (RWS) painting matrix and the NMD environmental declaration (#nmd_94250) for zinc-coated steel construction profiles, as can be seen in Table 128.

The NMD value represents a steel profile with a zinc coating suitable for civil engineering applications, with a standard thickness of 314 µm, corresponding to approximately 1.8 kg of zinc per m^2 of steel surface.

The NMD dataset is based on a detailed lifecycle assessment covering all 11 EN 15804 impact categories and all relevant phases (A1–A5, B, C, and D). It provides a clear breakdown of the contributions from production, use, end-of-life, and recycling, making it methodologically complete and highly transparent.

In contrast, the RWS matrix is more generic, and while it considers the lifespan and scheduled maintenance, it does not provide the same level of detail across all phases.

Because of its completeness and detailed breakdown, the NMD value is preferred for the MKI calculation, ensuring a more accurate and consistent assessment of the environmental impact of corrosion protection. The total MKI per m^2 for the zinc coating, based on the NMD, is therefore used in the overall calculation for the steel components. The total environmental costs for the phase A1-A5 for the painting can be viewed in Table 129.

Table 128 MKI/unit of the different found painting of the steel structure

component	MKI	unit	remarks
Zinq conservation according to the NMD 100y	2.03	€/m2	11/11 impactcategories considered, Phase A1-A5, (NO supplement taken into accoant for comparebility)
Zinq conservation according to the RWS report 100y	5.51	€/m2	11/11 impactcategories considered, total MKI, (NO supplement taken into accoant for comparebility)

Table 129 Environmental costs of painting of the steel elements per variant phase A1-A5

Centre to centre distance	Optimal composition of steel profiles	Quantity	unit	MKI	unit	Total MKI A1-A5 [€]
1.5m (9x profile)	2x HEB800 (S355) and 7x HEB600 (S460)	466	m2	2.03	€/m2	**€ 946.53**
2m (7x profile)	2x HEB800 (S460) and 5x HEB700 (S355)	388	m2	2.03	€/m2	**€ 786.74**
2.5m (6x profile)	2x HEB800 (S460) and 4x HEB700 (S460)	333	m2	2.03	€/m2	**€ 676.76**
1.5m (9x profile)	2x HEB800 (S355) and 7x HEB600 (S460)	466	m2	2.03	€/m2	**€ 946.53**
2m (7x profile)	2x HEB800 (S460) and 5x HEB700 (S355)	388	m2	2.03	€/m2	**€ 786.74**
2.5m (6x profile)	2x HEB800 (S460) and 4x HEB700 (S460)	333	m2	2.03	€/m2	**€ 676.76**

6.2.3 Total environmental costs variant 2

Table 130 presents the total environmental costs for Variant 2, including the different subvariants based on varying centre-to-centre distances and the two calculation methods used for the steel beam production. It can be observed that both the spacing between the beams and the chosen calculation method have a significant impact on the total environmental costs of Variant 2.

Table 130 total environmental costs of variant 2 phase A1-A5

steel component	Centre to centre distance	Optimal composition of steel profiles	Quantity beams	unit	MKI beams	unit 1	total costs beam [€]	Quantity painting	unit3	MKI painting	unit4	Total MKI painting [€]	MKI reinforced concrete	Total MKI variant 2
XCarb™ structural steel sections Arcelor Mittal	**1.5m (9x profile)**	2x HEB800 (S355) and 7x HEB600 (S460)	43.172	tonne	58.44	€/tonne	**€ 2,522.97**	466	m2	2.03	€/m2	**€ 946.53**	**€ 2,617.50**	**€ 6,087.00**
XCarb™ structural steel sections Arcelor Mittal	**2m (7x profile)**	2x HEB800 (S460) and 5x HEB700 (S355)	37.1735	tonne	58.44	€/tonne	**€ 2,172.42**	388	m2	2.03	€/m2	**€ 786.74**	**€ 2,617.50**	**€ 5,576.66**
XCarb™ structural steel sections Arcelor Mittal	**2.5m (6x profile)**	2x HEB800 (S460) and 4x HEB700 (S460)	31.992	tonne	58.44	€/tonne	**€ 1,869.61**	333	m2	2.03	€/m2	**€ 676.76**	**€ 2,617.50**	**€ 5,163.87**
Staal constructieprofielen (HEA/HEB/HEM/IPE/UNP) [NMD]	**1.5m (9x profile)**	2x HEB800 (S355) and 7x HEB600 (S460)	43.172	tonne	163.37	€/tonne	**€ 7,053.01**	466	m2	2.03	€/m2	**€ 946.53**	**€ 2,617.50**	**€ 10,617.04**
Staal constructieprofielen (HEA/HEB/HEM/IPE/UNP) [NMD]	**2m (7x profile)**	2x HEB800 (S460) and 5x HEB700 (S355)	37.1735	tonne	163.37	€/tonne	**€ 6,073.03**	388	m2	2.03	€/m2	**€ 786.74**	**€ 2,617.50**	**€ 9,477.28**
Staal constructieprofielen (HEA/HEB/HEM/IPE/UNP) [NMD]	**2.5m (6x profile)**	2x HEB800 (S460) and 4x HEB700 (S460)	31.992	tonne	163.37	€/tonne	**€ 5,226.53**	333	m2	2.03	€/m2	**€ 676.76**	**€ 2,617.50**	**€ 8,520.79**

6.3 *Variant 3 composite weathering steel concrete superstructure*

The process for calculating the environmental costs of variant 3 is the same as for variant 2, except for the fact that variant 3 does not have to be painted. As can be seen in Table 131 by excluding the painting of the beams and reduction of the costs can be realized between variant 3 and variant 2 of 9% for a centre to centre distance of 1.5m.

Table 131 total environmental costs of variant 3

steel component	Centre to centre distance	Optimal composition of steel profiles	Quantity beams	unit	MKI beams	unit 1	total costs beam [€]	Quantity painting	unit3	MKI painting	unit4	Total MKI painting [€]	MKI reinforced concrete	Total MKI variant 2
XCarb™ structural steel sections Arcelor Mittal	1.5m (9x profile)	2x HEB800 (S355) and 7x HEB600 (S460)	43.172	tonne	58.44	€/tonne	€ 2,522.97	0	m2	2.03	€/m2	€ -	€ 2,617.50	€ 5,140.47
XCarb™ structural steel sections Arcelor Mittal	2m (7x profile)	2x HEB800 (S460) and 5x HEB700 (S355)	37.1735	tonne	58.44	€/tonne	€ 2,172.42	0	m2	2.03	€/m2	€ -	€ 2,617.50	€ 4,789.92
XCarb™ structural steel sections Arcelor Mittal	2.5m (6x profile)	2x HEB800 (S460) and 4x HEB700 (S460)	31.992	tonne	58.44	€/tonne	€ 1,869.61	0	m2	2.03	€/m2	€ -	€ 2,617.50	€ 4,487.11
Staal constructieprofielen (HEA/HEB/HEM/IPE/UNP) [NMD]	1.5m (9x profile)	2x HEB800 (S355) and 7x HEB600 (S460)	43.172	tonne	163.37	€/tonne	€ 7,053.01	0	m2	2.03	€/m2	€ -	€ 2,617.50	€ 9,670.51
Staal constructieprofielen (HEA/HEB/HEM/IPE/UNP) [NMD]	2m (7x profile)	2x HEB800 (S460) and 5x HEB700 (S355)	37.1735	tonne	163.37	€/tonne	€ 6,073.03	0	m2	2.03	€/m2	€ -	€ 2,617.50	€ 8,690.53
Staal constructieprofielen (HEA/HEB/HEM/IPE/UNP) [NMD]	2.5m (6x profile)	2x HEB800 (S460) and 4x HEB700 (S460)	31.992	tonne	163.37	€/tonne	€ 5,226.53	0	m2	2.03	€/m2	€ -	€ 2,617.50	€ 7,844.03

6.4 *Conclusion sustainability impact*

Table 122 highlights the mass differences between the variants: the full concrete superstructure (Variant 1) is much heavier at 400 t (1,292 kg/m^2), while the composite steel–concrete variants (Variants 2 and 3) are lighter, ranging from 187 t to 198 t (603–639 kg/m^2). Within the composites, the 1.5 m spacing variant (198 t) is slightly heavier than the 2.5 m variant (187 t), showing that moving to a composite system greatly reduces weight, whereas changes in steel spacing have only a moderate effect.

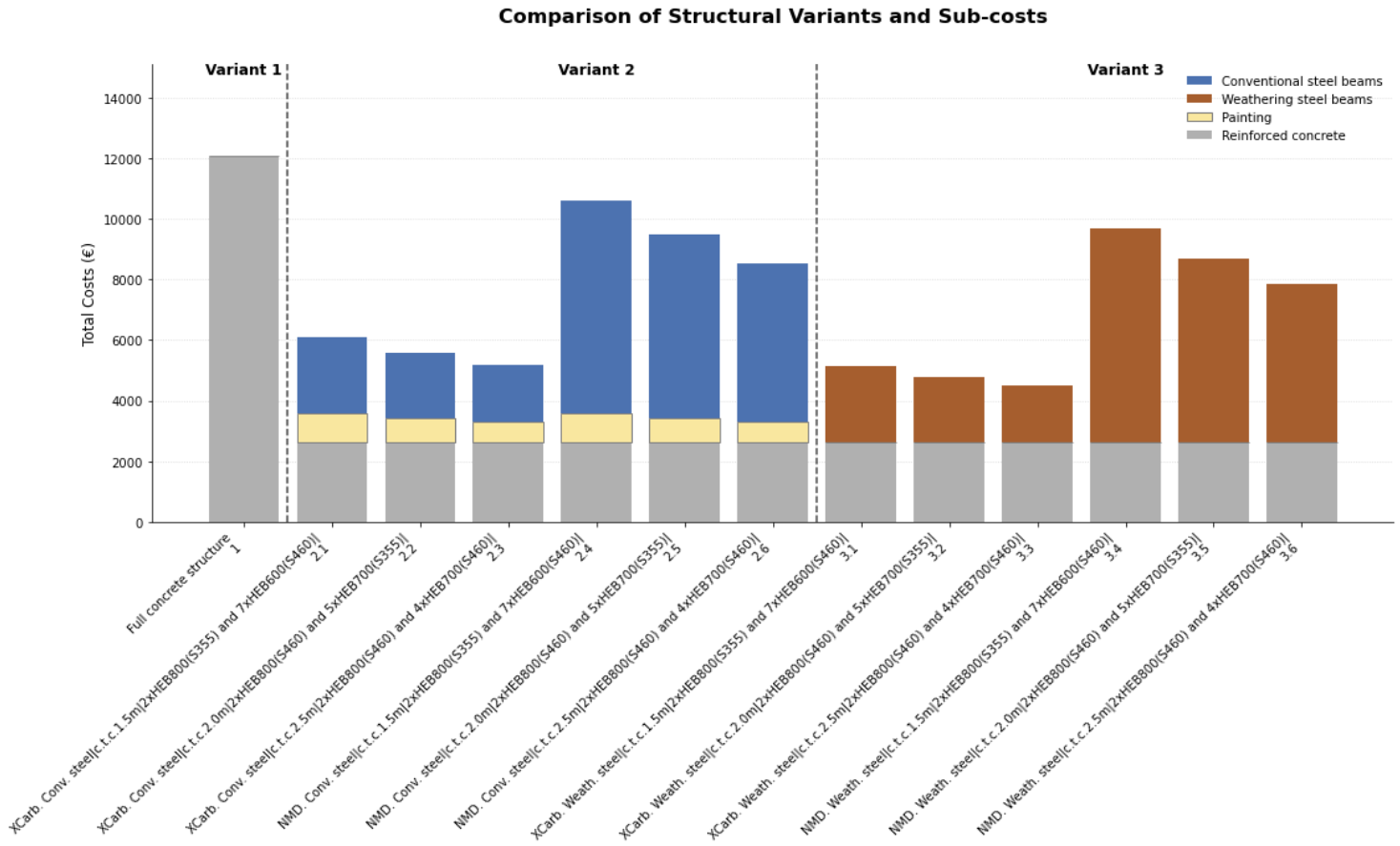

Figure 103 Total environmental impact (MKI) per bridge variant (phases A1-A5).

Figure 103 shows clear differences in environmental impact between the three superstructure variants. The full reinforced concrete structure (Variant 1) has the highest environmental cost at €12,074, mainly due to its large concrete volume.

Both composite variants perform substantially better. The composite weathering steel superstructure (Variant 3) consistently shows the lowest environmental impact, with total MKI values ranging from €4,488 to €9,671, depending on the dataset (XCarb vs. NMD) and beam spacing. The conventional composite variant (Variant 2) falls in between, with impacts ranging from €5,164 to €10,617.

Using the low-carbon XCarb® steel instead of the conservative NMD dataset results in large reductions for both composite variants:

- Variant 2 (1.5 m spacing): XCarb = €5,087 vs. NMD = €10,617 (difference: €5,530)
- Variant 3 (1.5 m spacing): XCarb = €4,488 vs. NMD = €9,671 (difference: €5,183)

Across all configurations, XCarb reduces the total MKI of composite structures by 50–55% compared to NMD steel. Weathering steel (Variant 3) performs better than conventional steel (Variant 2) because no painting is required, resulting in a ~9% reduction at 1.5 m spacing and similar reductions at 2.0 m and 2.5 m.

Because Variant 1 is assessed only for phases A1–A5, the same boundary conditions are applied to the composite superstructures. Module D (recycling benefits) is therefore excluded from comparison. Including Module D would disproportionately favour high-impact blast-furnace steels, as they receive much larger credits (e.g., –€110/t), whereas low-impact steels such as XCarb® receive costs. Excluding Module D ensures a fair and transparent comparison focused on upfront impacts.

Overall ranking (lowest to highest environmental cost):

1. Variant 3 (weathering steel–concrete composite): from €4,488
2. Variant 2 (conventional steel–concrete composite): from €5,087
3. Variant 1 (full concrete superstructure): €12,074

Thus, the weathering steel composite superstructure provides the most sustainable solution, with the full concrete alternative performing worst and conventional composite variants in between.

VI Results and final remarks

This chapter synthesizes the findings from the literature review, structural analysis, sustainability assessment, and cost evaluation to determine the overall feasibility and competitiveness of weathering steel–concrete composite bridges within the Dutch market.

7 Results and Final remarks

7.1 Insights from Literature

The literature review highlighted that weathering steel bridges are widely applied internationally, especially in the UK, USA, and Japan, due to their proven durability and low maintenance requirements. The protective oxide layer (patina) formed on the steel surface eliminates the need for painting, leading to reduced life-cycle costs and reduced sustainability impact.

However, the Dutch macro-environment poses challenges for uncoated weathering steel. The country experiences high relative humidity (≥76%) for more than eight months a year and frequent use of de-icing salts on highways. These conditions place nearly all Dutch bridge sites within corrosion classes C3 to C5, as defined by EN ISO 9223. As such, the application of weathering steel must be approached with caution and accompanied by detailed design measures that minimize prolonged wetness, ensure adequate drainage, and provide sufficient ventilation.

A critical constraint identified is the vertical clearance requirement. According to international guidelines, a minimum clearance of 6.1 m is recommended to prevent chloride-laden spray from reaching uncoated steel members. In the Netherlands, the standard vertical clearance is approximately 4.5 m, particularly for highway overpasses. This means that the American guidelines and ECCS clearance criteria cannot be met under Dutch design conditions. Consequently, the use of sacrificial thicknesses, targeted protective detailing, or hybrid coating strategies becomes essential to safeguard durability in such chloride-rich micro-environments.

The reassessment of the Avenhornbrug indicates that its location, approximately 8 km from the coastline, subjects the structure to a highly corrosive marine environment. Recorded general thickness losses of up to 1.5 mm and local losses reaching 2.5 mm (at the supports) after only 50 years are already approaching or even exceeding the code-based expectations for a 100-year service life (1.05–1.5 mm). These findings highlight the need for continued monitoring to better understand the long-term corrosion behavior.

7.2 Structural Performance

The structural verification confirmed that all governing limit states bending moment, shear, and deflection were satisfied for both conventional and weathering steel variants across several configurations of profile type, steel grade, and centre-to-centre distance. In Table 132 and Table 133 the optimal variants are given per centre to centre distance considered.

Table 132 Overview of optimal combination of steel profiles to be used for the conventional steel variant

Centre to centre distance	Optimal composition of steel profiles
1.5m (9x profile)	2x HEB800 (S355) and 7x HEB600 (S460)
2m (7x profile)	2x HEB800 (S460) and 5x HEB700 (S355)
2.5m (6x profile)	2x HEB800 (S460) and 4x HEB700 (S460)

Table 133 Overview of optimal combination of steel profiles to be used for the weathering steel variant

Centre to centre distance	Optimal composition of steel profiles
1.5m (9x profile)	2x HEB800 (S460) and 7x HEB600 (S460)
2m (7x profile)	2x HEB800 (S460) and 5x HEB700 (S460)
2.5m (6x profile)	2x HEB800 (S460) and 4x HEB700 (S460)

The sacrificial thickness applied in the weathering steel design had a negligible influence on global stiffness, bending moment resistance, vertical shear force resistance and deflection indicating that durability allowances do not compromise structural performance.

Overall, the mechanical behavior of weathering steel was virtually identical to that of conventional painted steel, confirming its structural equivalence under Eurocode-based design.

7.3 Sustainability Performance

The sustainability assessment, based on Life Cycle Assessment (LCA) and Environmental Cost Indicator (MKI) values for phases A1–A5, showed that the weathering steel–concrete composite variant (Variant 3) achieved the best environmental performance. The absence of coating systems and reduced maintenance requirements resulted in lower total MKI values compared to the conventional painted steel composite (Variant 2).

The use of ArcelorMittal XCarb® data, reflecting low-carbon electric-arc-furnace production, further reduced environmental impacts compared to the conservative National Environmental Database (NMD) baseline. Module D recycling credits were excluded, as including them can skew the total MKI by giving disproportionately high benefits to conventional high-impact steels, while low-impact steels like XCarb® receive minimal credit. This ensures a fair comparison for the A1–A5 stages, which account for 80–90% of the total impact (Thie, 2025). In Figure 104 the total environmental impact per variant is shown.

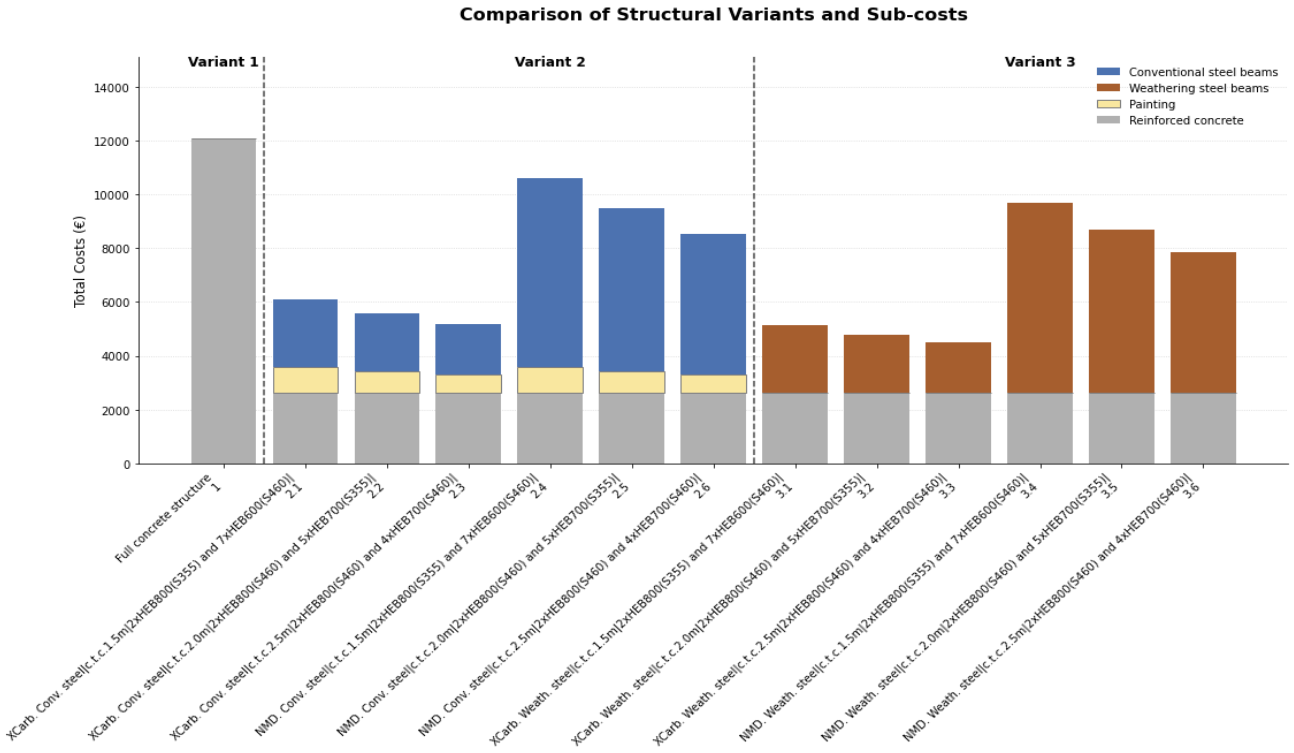

Figure 104 Total environmental impact (MKI) per bridge variant (phases A1-A5).

7.4 Economic Evaluation

From an economic perspective, the weathering steel option has slightly higher initial costs but offers up to 30% lower total lifecycle costs over 100 years due to the elimination of painting, simplified fabrication, and reduced maintenance interventions (Ungermann & Hatke, 2021). These savings are enhanced by minimized traffic disruptions during maintenance, aligning well with Rijkswaterstaat's focus on Total Cost of Ownership and sustainable asset management.

7.5 Overall Evaluation and Final Remarks

Integrating literature, structural, sustainability, and economic analyses, this study shows that weathering steel–concrete composite bridges (Variant 3) are feasible, sustainable, and cost-competitive for medium-span bridges in the Netherlands.

Structural verification confirmed that all bending, shear, and deflection limits are satisfied across multiple profile configurations. Accounting for a 1 mm thickness loss in weathering steel results in a 3.5–6% reduction in bending moment resistance, showing a small but not negligible impact on structural capacity. Mechanically, weathering steel behaves comparably to conventional painted steel. Further studies could investigate increasing the concrete slab thickness, currently 200 mm, to evaluate the potential benefits for stiffness and load distribution.

Life Cycle Assessment results highlight the sustainability advantage of Variant 3. MKI values range from €4,488 to €9,671, compared to €5,087–€10,617 for conventional painted steel composites (Variant 2) and €12,074 for the full concrete superstructure (Variant 1). Using low-carbon XCarb® steel reduces environmental costs by 50–55% relative to NMD steel, while eliminating coating in Variant 3 provides an additional ~9% reduction. Future studies could assess sustainability using the extended A2 category, which better captures upstream impacts from raw material extraction and production, providing a more complete picture than A1.

Mass analysis shows Variant 1 is much heavier (400 t, 1,292 kg/m^2) than the composite variants (187–198 t, 603–639 kg/m^2), representing a 53–56% reduction in total mass. This significant weight reduction not only decreases material use but also substantially reduces the load on existing abutments, improving feasibility for bridge replacements or upgrades. Within the composites, increasing steel profile spacing from 1.5 m (198 t) to 2.5 m (187 t) yields only moderate weight savings.

Economically, Variant 3 offers up to 30% lifecycle cost savings over 100 years due to the elimination of painting, simplified fabrication, reduced maintenance, and minimized traffic disruptions. For a more accurate cost assessment, further studies should obtain detailed quotations for constructing each variant to determine the realistic cost implications.

Despite Dutch clearance limits (≈4.5 m), which are lower than the 6.1 m recommended in American ACTS and ECCS guidelines, appropriate mitigation strategies, including sacrificial thickness, optimized drainage, and preventive maintenance, can ensure long-term performance. Future research should investigate the effect of these lower clearances on the corrosion behavior of weathering steel bridges in the Netherlands to provide a clearer understanding of their long-term durability under local conditions.

In summary, the weathering steel–concrete composite variant provides the best combination of environmental performance, structural efficiency, and lifecycle economy:

- Bending moment resistance: 3.5–6% for weathering steel accounting for 1 mm sacrificial thickness
- MKI (A1–A5): €4,488–€9,671 (Variant 3) vs €5,087–€10,617 (Variant 2) and €12,074 (Variant 1)
- Structural mass: 187–198 t (Variants 2 & 3) vs 400 t (Variant 1), a 53–56% reduction
- Lifecycle cost savings: up to 30%

When properly designed, weathering steel–concrete composite bridges potentially offer the Dutch infrastructure sector a robust pathway toward low-maintenance, low-impact, and long-lasting bridge solutions, particularly for replacing aged concrete superstructures while preserving the existing substructure.

Bibliography

American Institute of steel construction. (2022). *Uncoated weathering steel reference guide*. United states of America: AISC. Retrieved April 03, 2024

ArcellorMittal. (2023). *EPD XCarb® Recycled and renewably produced structural steel sections and merchant bars*. stichting MRPI.

ArcelorMittal. (2020). *Wirkowice composite bridge*. Retrieved October 11, 2024, from ArcelorMittal.com: https://sections.arcelormittal.com/Projects/5306/EN

ArcelorMittal. (2023). *Environmental prduct declaration according to ISO 14026 and EN 15804*. luxembourg: Milieu relevante product informatie. Retrieved October 11, 2024

ArcelorMittal Europe. (2025). *EPD Heavy steel plates*. Institute Bauen und Umwelt.

Arcorox. (2021). *Arcorox® Weathering steel sections*. Retrieved February 26, 2024, from ArcelorMittal: https://constructalia.arcelormittal.com/en/products/arcorox

betonakkoord. (2023). *Productblad * circulariteit % / € MKI*. Standaardbestek.

Center of advanced infrastructure and transportation. (n.d.). *Fatigue and Fracture of Steel Bridges*. Retrieved from https://cait.rutgers.edu/: https://cait.rutgers.edu/event/fatigue-and-fracture-of-steel-bridges/

Du, G. (2015). *Life cycle assessment of bridges, model*. Stockholm, Sweden: KTH Vetenskap och Konst.

Hicks, S. J., El Sarraf, R., & Mandeno, W. (2017). *Weathering Steel - Design Guide for Bridges in Australia*. Aukland City, New Zealand: Hera House. Retrieved March 26, 2024

Highways England. (2019). *Weathering steel for highway structures*. Highways England. Retrieved February 26, 2024, from https://www.standardsforhighways.co.uk/

Jong, J. d. (2024). *Herberekening 2 staal-betonbruggen en Molenbrug Kampen*. ARUP & NEBEST. Retrieved october 09, 2024

Joostdevree. (n.d.). *Corrosieklasse*. Retrieved november 2, 2024, from joostdevree: https://www.joostdevree.nl/shtmls/corrosieklasse.shtml

Kavoura, F. (2023). Lectures Composite steel-concrete structures.

NationaalMilieudatabase. (n.d.). *De Nationale Milieudatabase*. Retrieved from Milieudatabase: https://milieudatabase.nl/nl/database/nationale-milieudatabase/

National Institute for public health and the Environment. (2012). *Assessment of the level of sea salt inPM10*. The Netherlands: RIVM. Retrieved May 06, 2024

NEN-EN 15804+A2. (2019). *Sustainability of construction works -Environmental product declarations - Core rules for the product category of construction products* . Delft: Koninklijk Nederlands Normalisatie-instituut.

NEN-EN-ISO 14040:2006. (2006). *NEN-EN-ISO 14040 Environmental management - Life cycle assesment Principles and frameworks*. Delft: Nederlands Normalisatie-instituut.

NSC. (2024, February 06). *Atmospheric corrosivity classification for weathering steel*. (NSC, Producer) Retrieved February 26, 2024, from NewSteelConstructions: https://www.newsteelconstruction.com/wp/atmospheric-corrosivity-classifications-for-weathering-steel/

ONE click LCA. (2025, march 01). *Average Quantities of Reinforcement in Concrete*. Retrieved from ONECLICKLCA: https://help.oneclicklca.com/en/articles/275888-average-quantities-of-reinforcement-in-concrete?utm_source=chatgpt.com

Rademacher, D. (2019). Composite bridge in Luxemburg over railway line with hot-rolled sections in weathering steel grade. *Maintenance free corrosion protection for composite bridges with hot-rolled*. ArcelorMittal Europe, Luxemburg. Retrieved March 26, 2024

Rijkswaterstaat. (2022). *Handreiking duurzaamheid staal convservering*. Utrecht: Steunpunt conserveringskennis. Retrieved October 09, 2024

Rijkswaterstaat. (n.d.). *Vernieuwen van bruggen, tunnels, sluizen en viaducten*. Retrieved March 26, 2024, from Rijkswaterstaat.nl: https://www.rijkswaterstaat.nl/over-ons/onze-organisatie/vervanging-en-renovatie

shutterstock. (2021, juli 19). *Corrosion damage on a concrete bridge on a busy thoroughfare in Frankfurt With an age of about 50 years, it has its best days behind it*. Retrieved from https://www.shutterstock.com/:

https://www.shutterstock.com/nl/image-photo/corrosion-damage-on-concrete-bridge-busy-2010846272
SSAB. (2020). *EPD Hot rolled steel plates*. SSAB.
Sullivan, K., & Olson, G. (2022). *Laying the Foundation of Cement and Concrete Decarbonization*. World resources institute.
Thie, E. (2025). *Circular performance of small road bridges* . Utrecht: Rijkswaterstaat.
Ungermann, D., & Hatke, P. (2021). *ECCS-Design-Guide-Weathering-Steel-Bridges*. ECCS AC3 Bridge comittee. Retrieved February 26, 2024
Verhoef, G. (2021). *Viaduct Beemsteruitweg A7*. Geldermalsen: Antea groep. Retrieved october 09, 2024
Weerplaza. (2023, January 1). *Klimaat Nederland*. Retrieved May 6, 2024, from Weerplaza: https://www.weerplaza.nl/nederland/klimaat/vochtigheid/?maand=dec
Yu Zhang, K. Z. (2019). *Corrosion-Fatigue Evaluation of Uncoated*. Chengdu: Department of Bridge Engineering, School of Civil Engineering, Southwest Jiaotong University,. Retrieved November 2, 2024

ANNEX A Acrobi calculations

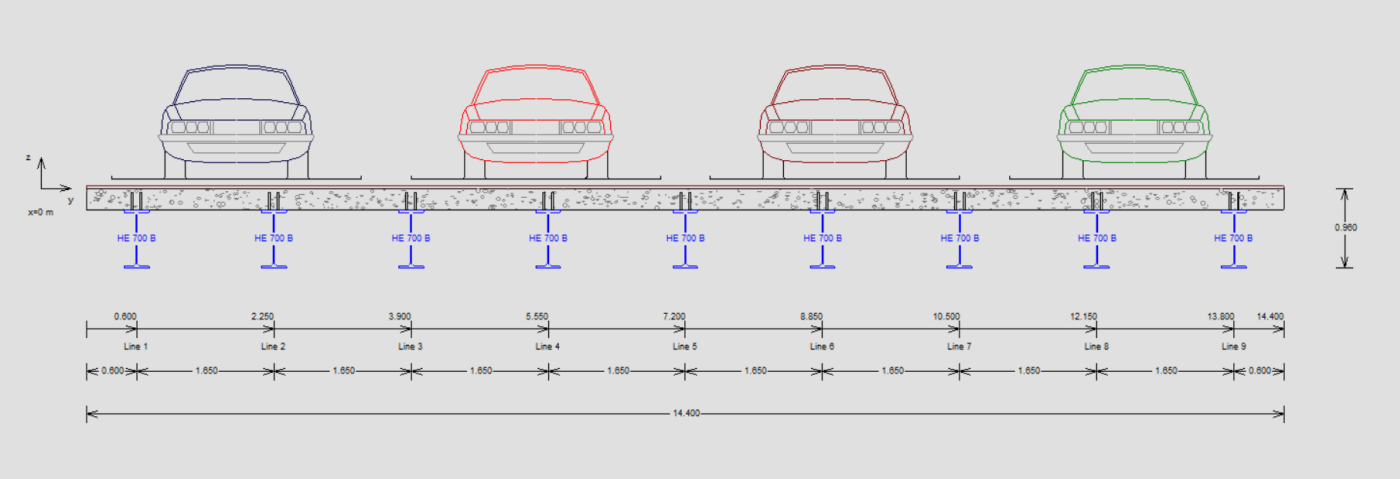

Figure 106 Satisfying design performed by Acrobi software

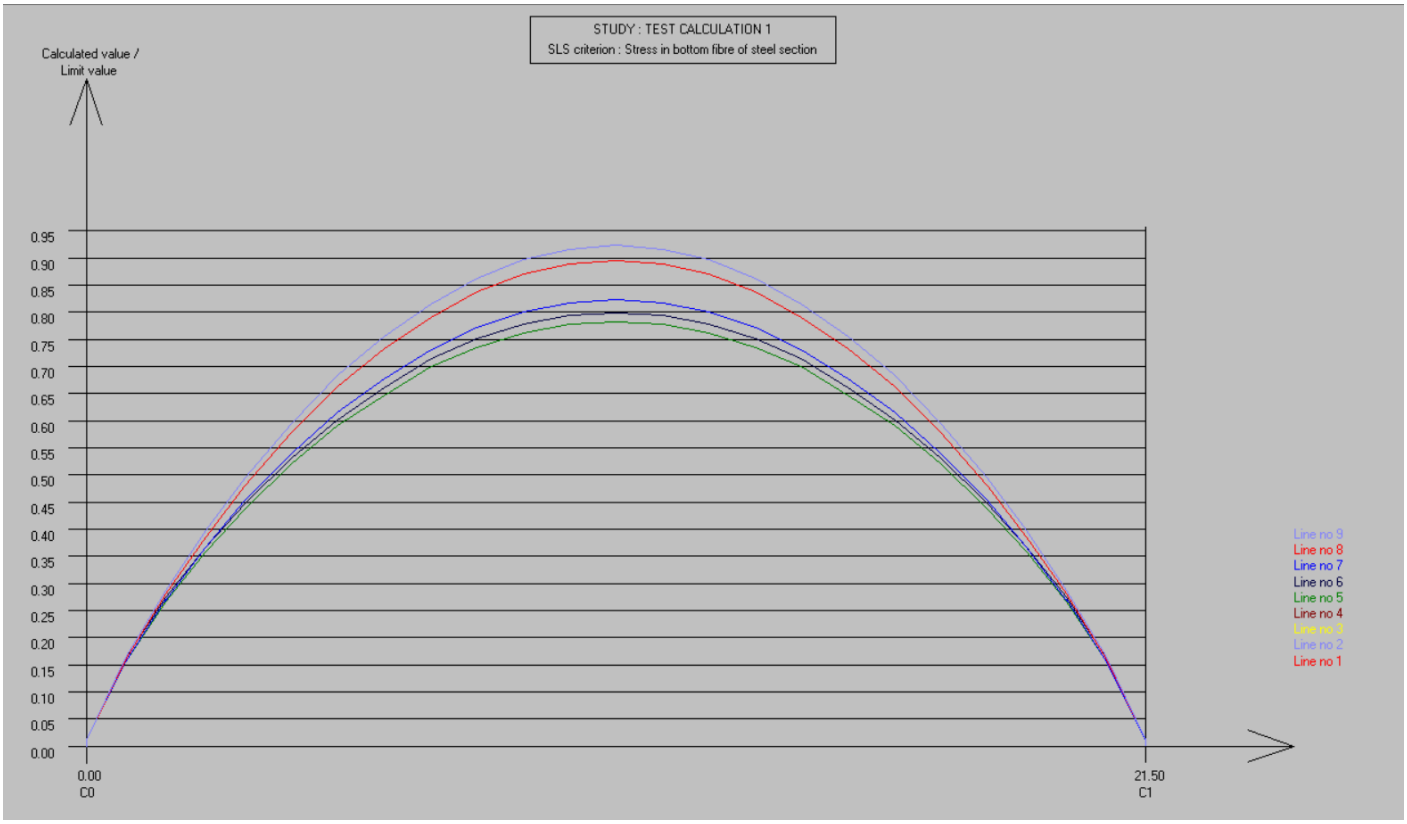

Figure 105 SLS unity check stress bottom fibre Acrobi software

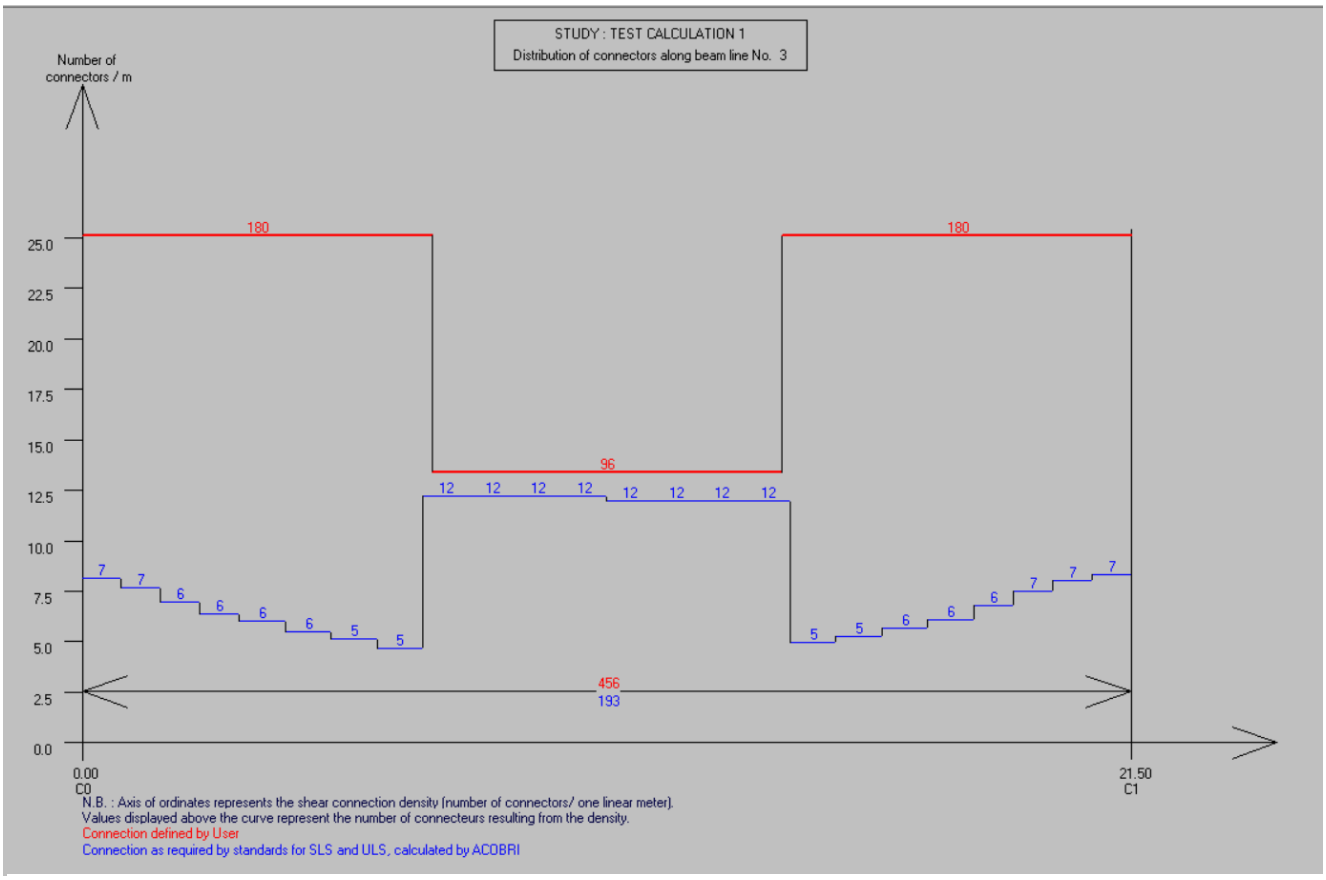

Figure 108 Shear force verification shear studs Acrobi software

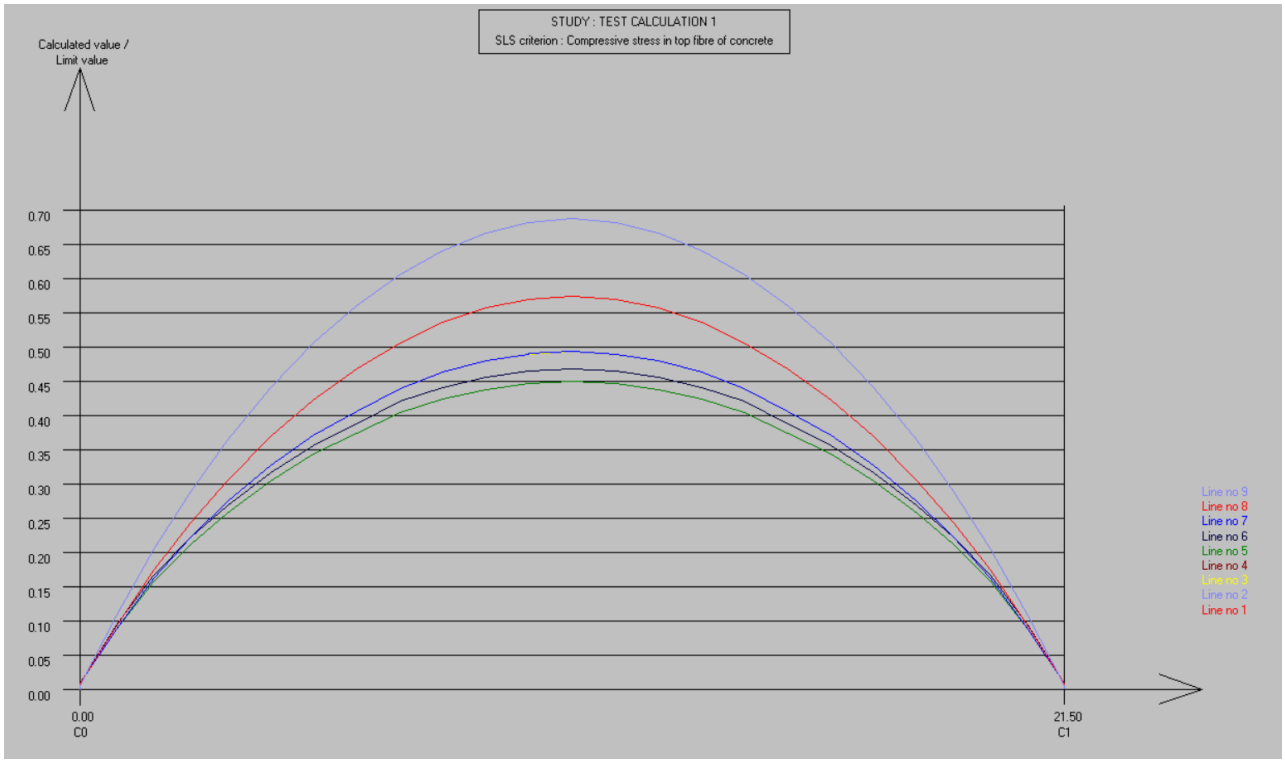

Figure 107 SLS verification Concrete compressive strenth Acrobi software

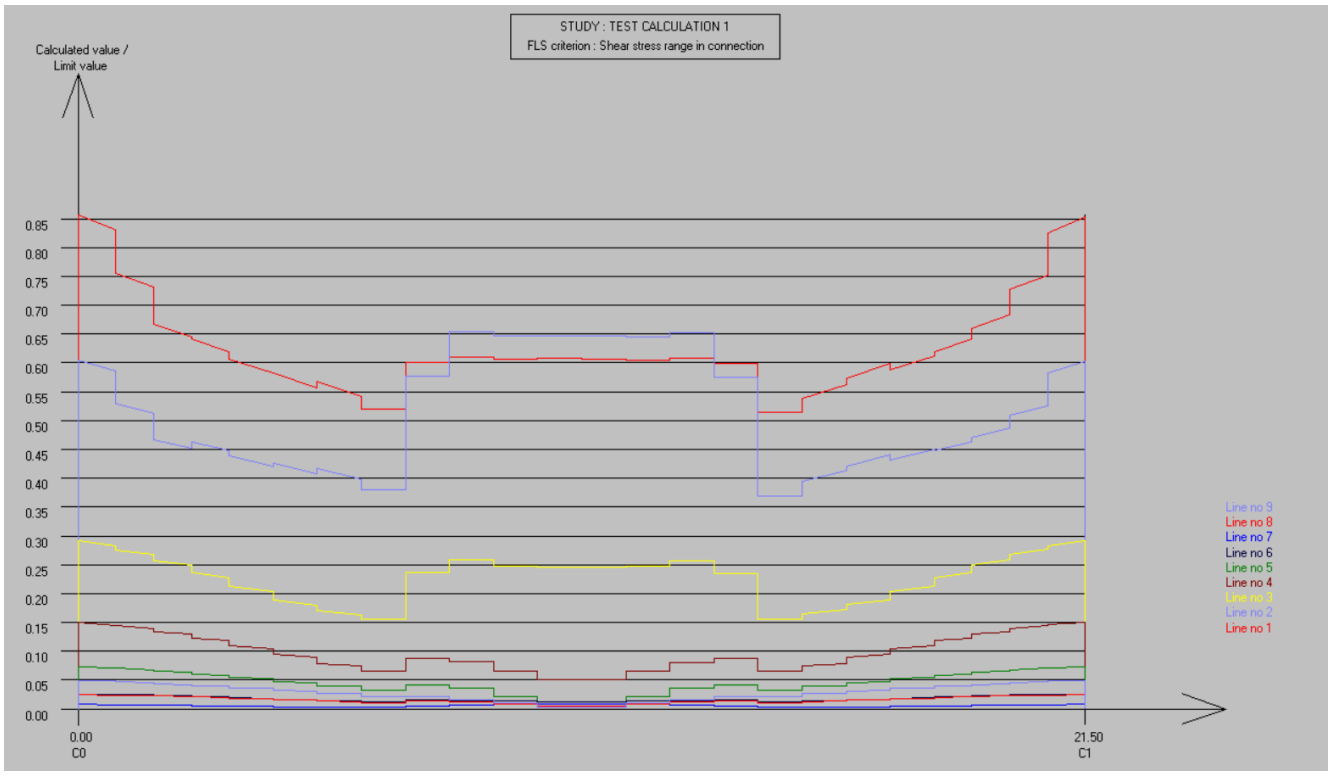

Figure 109 Fatigue limit state verifcation Acrobi software

ANNEX B Overall effect results for bending moment verification

Results edge beam

Table 134 Overall results effects edge composite bean for governing load combination for HEB700B and ctc=1.5m

description	Symbol	Value	unit
Effect bending moment edge beam	$M_{ED,\ beam}$	2400	kNm
Effect bending moment concrete layer edge beam	$M_{ED,concrete}$	90	kNm
Effect internal axial force edge beam	$N_{ED,\ beam}$	6395	kNm
Effect internal axial force concrete layer edge beam	$N_{ED,concrete}$	4830	kNm
Effect shear force	$V_{ED,}$	1040	kN

Table 135 Overall results effects edge composite bean for governing load combination for HEB600B and ctc=1.5m

description	Symbol	Value	unit
Effect bending moment edge beam	$M_{ED,\ beam}$	2185	kNm
Effect bending moment concrete layer edge beam	$M_{ED,concrete}$	125	kNm
Effect internal axial force edge beam	$N_{ED,\ beam}$	7110	kNm
Effect internal axial force concrete layer edge beam	$N_{ED,concrete}$	5635	kNm
Effect shear force	$V_{ED,}$	1030	kN

Table 136 Overall results effects edge composite bean for governing load combination for HEB800B and ctc=1.5m

description	Symbol	Value	unit
Effect bending moment edge beam	$M_{ED,\ beam}$	2570	kNm
Effect bending moment concrete layer edge beam	$M_{ED,concrete}$	70	kNm
Effect internal axial force edge beam	$N_{ED,\ beam}$	5635	kNm
Effect internal axial force concrete layer edge beam	$N_{ED,concrete}$	4205	kNm
Effect shear force	$V_{ED,}$	1045	kN

Table 137 Overall results effects edge composite bean for governing load combination for HEB600B and ctc=2 m

description	Symbol	Value	unit
Effect bending moment edge beam	$M_{ED,\ beam}$	2445	kNm
Effect bending moment concrete layer edge beam	$M_{ED,concrete}$	155	kNm
Effect internal axial force edge beam	$N_{ED,\ beam}$	8395	kNm
Effect internal axial force concrete layer edge beam	$N_{ED,concrete}$	6655	kNm
Effect shear force	$V_{ED,}$	1165	kN

Table 138 Overall results effects edge composite bean for governing load combination for HEB700B and ctc=2 m

description	Symbol	Value	unit
Effect bending moment edge beam	$M_{ED,\ beam}$	2680	kNm
Effect bending moment concrete layer edge beam	$M_{ED,concrete}$	115	kNm
Effect internal axial force edge beam	$N_{ED,\ beam}$	7400	kNm
Effect internal axial force concrete layer edge beam	$N_{ED,concrete}$	5745	kNm
Effect shear force	$V_{ED,}$	1170	kN

Table 139 Overall results effects edge composite bean for governing load combination for HEB800B and ctc=2 m

description	Symbol	Value	unit
Effect bending moment edge beam	$M_{ED,\ beam}$	2860	kNm
Effect bending moment concrete layer edge beam	$M_{ED,concrete}$	85	kNm
Effect internal axial force edge beam	$N_{ED,\ beam}$	6595	kNm
Effect internal axial force concrete layer edge beam	$N_{ED,concrete}$	5035	kNm
Effect shear force	$V_{ED,}$	1180	kN

Table 140 Overall results effects edge composite bean for governing load combination for HEB600B and ctc=2.5 m

description	Symbol	Value	unit
Effect bending moment edge beam	$M_{ED,\ beam}$	2525	kNm
Effect bending moment concrete layer edge beam	$M_{ED,concrete}$	155	kNm
Effect internal axial force edge beam	$N_{ED,\ beam}$	8660	kNm
Effect internal axial force concrete layer edge beam	$N_{ED,concrete}$	6850	kNm
Effect shear force	$V_{ED,}$	1160	kN

Table 141 Overall results effects edge composite bean for governing load combination for HEB700B and ctc=2.5 m

description	Symbol	Value	unit
Effect bending moment edge beam	$M_{ED,\ beam}$	2740	kNm
Effect bending moment concrete layer edge beam	$M_{ED,concrete}$	115	kNm
Effect internal axial force edge beam	$N_{ED,\ beam}$	7500	kNm
Effect internal axial force concrete layer edge beam	$N_{ED,concrete}$	5915	kNm
Effect shear force	$V_{ED,}$	1160	kN

Table 142 Overall results effects edge composite bean for governing load combination for HEB800B and ctc=2.5 m

description	Symbol	Value	unit
Effect bending moment edge beam	$M_{ED,\ beam}$	2905	kNm
Effect bending moment concrete layer edge beam	$M_{ED,concrete}$	85	kNm
Effect internal axial force edge beam	$N_{ED,\ beam}$	6585	kNm
Effect internal axial force concrete layer edge beam	$N_{ED,concrete}$	5185	kNm
Effect shear force	$V_{ED,}$	1165	kN

Table 143 Neutral axis determination for the different variants at the edge beam conventional steel

Profile	Neutral axis location for the differen centre to centre distance of the beams [mm]		
	1.5m	2m	2.5m
HEB600B	209 (F)	209 (F)	209 (F)
HEB700B	212 (F)	211 (F)	211 (F)
HEB800B	214 (F)	213 (F)	212 (F)

(F) = Neutral axis in upper flange.
(W) = Neutral axis in web.

Table 144 Neutral axis determination for the different variants at the edge beam weathering steel

Profile	Neutral axis location for the differen centre to centre distance of the beams [mm]		
	1.5m	2m	2.5m
HEB600B	208 (F)	208 (F)	208 (F)
HEB700B	212 (F)	210 (F)	210 (F)
HEB800B	213 (F)	212 (F)	211 (F)

(F) = Neutral axis in upper flange.
(W) = Neutral axis in web.

Table 145 Verification of bending moment of edge beam for a centre to centre distance of 1.5m

Profile	S235			S355			S460		
	M_{Ed} [kNm]	M_{Rd} [kNm]	U.C [-]	M_{Ed} [kNm]	M_{Rd} [kNm]	U.C [-]	M_{Ed} [kNm]	M_{Rd} [kNm]	U.C [-]
HEB600B	**4975**	**2710**	**1.84**	**4975**	**3605**	**1.38**	**4975**	**4395**	**1.13**
HEB700B	**5170**	**3310**	**1.56**	**5170**	**4500**	**1.15**	**5170**	**5544**	**0.93**
HEB800B	**5275**	**3910**	**1.35**	**5275**	**5405**	**0.98**	**5275**	**6710**	**0.79**

Table 146 Verification of bending moment of edge beam for a centre to centre distance of 2.0m

Profile	S235			S355			S460		
	M_{Ed} [kNm]	M_{Rd} [kNm]	U.C [-]	M_{Ed} [kNm]	M_{Rd} [kNm]	U.C [-]	M_{Ed} [kNm]	M_{Rd} [kNm]	U.C [-]
HEB600B	**5745**	**2830**	**2.03**	**5745**	**3730**	**1.54**	**5745**	**4515**	**1.27**
HEB700B	**5915**	**3430**	**1.72**	**5915**	**4625**	**1.28**	**5915**	**5670**	**1.04**
HEB800B	**6045**	**4040**	**1.5**	**6045**	**5530**	**1.09**	**6045**	**6835**	**0.88**

Table 147 Verification of bending moment of edge beam for a centre to centre distance of 2.5m

Profile	S235			S355			S460		
	M_{Ed} [kNm]	M_{Rd} [kNm]	U.C [-]	M_{Ed} [kNm]	M_{Rd} [kNm]	U.C [-]	M_{Ed} [kNm]	M_{Rd} [kNm]	U.C [-]
HEB600B	5920	2830	2.09	5920	3730	1.59	5920	4515	1.3
HEB700B	6030	3430	1.76	6030	4625	1.30	6030	5670	1.06
HEB800B	6105	4040	1.51	6105	5530	1.10	6105	6835	0.89

Table 148 Verification of bending moment of edge weathering steel beam for a centre to centre distance of 1.5m

Profile	S235			S355			S460		
	M_{Ed} [kNm]	M_{Rd} [kNm]	U.C [-]	M_{Ed} [kNm]	M_{Rd} [kNm]	U.C [-]	M_{Ed} [kNm]	M_{Rd} [kNm]	U.C [-]
HEB600B	4970	2570	1.93	4970	3410	1.46	4970	4140	1.20
HEB700B	5170	3130	1.65	5170	4235	1.22	5170	5205	0.99
HEB800B	5275	3775	1.40	5275	5205	1.01	5205	6450	0.82

Table 149 Verification of bending moment of edge weathering steel beam for a centre to centre distance of 2.0m

Profile	S235			S355			S460		
	M_{Ed} [kNm]	M_{Rd} [kNm]	U.C [-]	M_{Ed} [kNm]	M_{Rd} [kNm]	U.C [-]	M_{Ed} [kNm]	M_{Rd} [kNm]	U.C [-]
HEB600B	5745	2595	2.21	5745	3430	1.67	5745	4165	1.38
HEB700B	5915	3251	1.81	5915	4360	1.36	5915	5330	1.11
HEB800B	6040	3900	1.55	6040	5330	1.14	6040	6580	0.92

Table 150 Verification of bending moment of edge weathering steel beam for a centre to centre distance of 2.5m

Profile	S235			S355			S460		
	M_{Ed} [kNm]	M_{Rd} [kNm]	U.C [-]	M_{Ed} [kNm]	M_{Rd} [kNm]	U.C [-]	M_{Ed} [kNm]	M_{Rd} [kNm]	U.C [-]
HEB600B	5920	2690	2.20	5920	3530	1.68	5920	4259	1.39
HEB700B	6030	3250	1.85	6030	4360	1.38	6030	5330	1.13
HEB800B	6100	3900	1.56	6100	5330	1.14	6100	6580	0.93

Results middle beam

Table 151 Overall results effects middle composite bean for governing load combination for HEB600B and ctc=1.5m

description	Symbol	Value	unit
Effect bending moment edge beam	$M_{ED,\ beam}$	1460	kNm
Effect bending moment concrete layer edge beam	$M_{ED,concrete}$	75	kNm
Effect internal axial force edge beam	$N_{ED,\ beam}$	4055	kNm
Effect internal axial force concrete layer edge beam	$N_{ED,concrete}$	3350	kNm
Effect shear force	$V_{ED,}$	635	kN

Table 152 Overal results effects middle composite bean for governing load combination for HEB700B and ctc=1.5m

description	Symbol	Value	unit
Effect bending moment edge beam	$M_{ED,\ beam}$	1610	kNm
Effect bending moment concrete layer edge beam	$M_{ED,concrete}$	55	kNm
Effect internal axial force edge beam	$N_{ED,\ beam}$	3575	kNm
Effect internal axial force concrete layer edge beam	$N_{ED,concrete}$	2855	kNm
Effect shear force	$V_{ED,}$	640	kN

Table 153 Overall results effects middle composite bean for governing load combination for HEB800B and ctc=1.5m

description	Symbol	Value	unit
Effect bending moment edge beam	$M_{ED,\ beam}$	1730	kNm
Effect bending moment concrete layer edge beam	$M_{ED,concrete}$	45	kNm
Effect internal axial force edge beam	$N_{ED,\ beam}$	3195	kNm
Effect internal axial force concrete layer edge beam	$N_{ED,concrete}$	2475	kNm
Effect shear force	$V_{ED,}$	645	kN

Table 154 Overall results effects middle composite bean for governing load combination for HEB600B and ctc=2 m

description	Symbol	Value	unit
Effect bending moment edge beam	$M_{ED,\ beam}$	1715	kNm
Effect bending moment concrete layer edge beam	$M_{ED,concrete}$	120	kNm
Effect internal axial force edge beam	$N_{ED,\ beam}$	5695	kNm
Effect internal axial force concrete layer edge beam	$N_{ED,concrete}$	4705	kNm
Effect shear force	$V_{ED,}$	880	kN

Table 155 Overall results effects middle composite bean for governing load combination for HEB700B and ctc=2 m

description	Symbol	Value	unit
Effect bending moment edge beam	$M_{ED,\ beam}$	1890	kNm
Effect bending moment concrete layer edge beam	$M_{ED,concrete}$	95	kNm
Effect internal axial force edge beam	$N_{ED,\ beam}$	5100	kNm
Effect internal axial force concrete layer edge beam	$N_{ED,concrete}$	4065	kNm
Effect shear force	$V_{ED,}$	890	kN

Table 156 Overall results effects middle composite bean for governing load combination for HEB800B and ctc=2 m

description	Symbol	Value	unit
Effect bending moment edge beam	$M_{ED,\ beam}$	2030	kNm
Effect bending moment concrete layer edge beam	$M_{ED,concrete}$	75	kNm
Effect internal axial force edge beam	$N_{ED,\ beam}$	4610	kNm
Effect internal axial force concrete layer edge beam	$N_{ED,concrete}$	3565	kNm
Effect shear force	$V_{ED,}$	900	kN

Table 157 Overall results effects middle composite bean for governing load combination for HEB600B and ctc=2.5 m

description	Symbol	Value	unit
Effect bending moment edge beam	$M_{ED,\ beam}$	1950	kNm
Effect bending moment concrete layer edge beam	$M_{ED,concrete}$	170	kNm
Effect internal axial force edge beam	$N_{ED,\ beam}$	6970	kNm
Effect internal axial force concrete layer edge beam	$N_{ED,concrete}$	5950	kNm
Effect shear force	$V_{ED,}$	1060	kN

Table 158 Overall results effects middle composite bean for governing load combination for HEB700B and ctc=2.5 m

description	Symbol	Value	unit
Effect bending moment edge beam	$M_{ED,\ beam}$	2150	kNm
Effect bending moment concrete layer edge beam	$M_{ED,concrete}$	130	kNm
Effect internal axial force edge beam	$N_{ED,\ beam}$	6270	kNm
Effect internal axial force concrete layer edge beam	$N_{ED,concrete}$	5175	kNm
Effect shear force	$V_{ED,}$	1075	kN

Table 159 Overall results effects middle composite bean for governing load combination for HEB800B and ctc=2.5 m

description	Symbol	Value	unit
Effect bending moment edge beam	$M_{ED,\ beam}$	2315	kNm
Effect bending moment concrete layer edge beam	$M_{ED,concrete}$	100	kNm
Effect internal axial force edge beam	$N_{ED,\ beam}$	5675	kNm
Effect internal axial force concrete layer edge beam	$N_{ED,concrete}$	4565	kNm
Effect shear force	$V_{ED,}$	1090	kN

Table 160 Neutral axis determination for the different variants at the middle conventional steel beam

Profile	Neutral axis location for the differen centre to centre distance of the beams [mm]		
	1.5m	2m	2.5m
HEB600B	208 (F)	208 (F)	207 (F)
HEB700B	210 (F)	210 (F)	209 (F)
HEB800B	213 (F)	213 (F)	211 (F)

(F) = Neutral axis in upper flange.
(W) = Neutral axis in web.

Table 161 Neutral axis determination for the different variants at the middle weathering steel beam

Profile	Neutral axis location for the differen centre to centre distance of the beams [mm]		
	1.5m	2m	2.5m
HEB600B	207 (F)	207 (F)	206 (F)
HEB700B	209 (F)	209 (F)	208 (F)
HEB800B	212 (F)	212 (F)	210 (F)

(F) = Neutral axis in upper flange.
(W) = Neutral axis in web.

Table 162 Verification of bending moment of middle conventional steel beam for a centre to centre distance of 1.5m

Profile	S235			S355			S460		
	M_{Ed} [kNm]	M_{Rd} [kNm]	U.C [-]	M_{Ed} [kNm]	M_{Rd} [kNm]	U.C [-]	M_{Ed} [kNm]	M_{Rd} [kNm]	U.C [-]
HEB600B	**3070**	**2490**	**1.23**	**3070**	**3390**	**0.91**	**3070**	**4175**	**0.735**
HEB700B	**3185**	**3085**	**1.03**	**3185**	**4275**	**0.75**	**3185**	**5320**	**0.60**
HEB800B	**3280**	**3685**	**0.89**	**3280**	**5175**	**0.63**	**3280**	**6480**	**0.51**

Table 163 Verification of bending moment of middle conventional steel beam for a centre to centre distance of 2.0m

Profile	S235			S355			S460		
	M_{Ed} [kNm]	M_{Rd} [kNm]	U.C [-]	M_{Ed} [kNm]	M_{Rd} [kNm]	U.C [-]	M_{Ed} [kNm]	M_{Rd} [kNm]	U.C [-]
HEB600B	**3990**	**2735**	**1.46**	**3990**	**3630**	**1.10**	**3990**	**4420**	**0.90**
HEB700B	**4150**	**3330**	**1.25**	**4150**	**4525**	**0.92**	**4150**	**5570**	**0.75**
HEB800B	**4275**	**3935**	**1.09**	**4275**	**5430**	**0.78**	**4275**	**6735**	**0.63**

Table 164 Verification of bending moment of middle conventional steel beam for a centre to centre distance of 2.5m

Profile	S235			S355			S460		
	M_{Ed} [kNm]	M_{Rd} [kNm]	U.C [-]	M_{Ed} [kNm]	M_{Rd} [kNm]	U.C [-]	M_{Ed} [kNm]	M_{Rd} [kNm]	U.C [-]
HEB600B	4785	2975	1.60	4785	3875	1.23	4785	4660	1.03
HEB700B	4965	3580	1.39	4965	4775	1.04	4965	5820	0.85
HEB800B	5110	4190	1.21	5110	5685	0.90	5110	6990	0.73

Table 165 Verification of bending moment of middle weathering steel beam for a centre to centre distance of 1.5m

Profile	S235			S355			S460		
	M_{Ed} [kNm]	M_{Rd} [kNm]	U.C [-]	M_{Ed} [kNm]	M_{Rd} [kNm]	U.C [-]	M_{Ed} [kNm]	M_{Rd} [kNm]	U.C [-]
HEB600B	3070	2355	1.30	3070	3190	0.96	3070	3925	0.78
HEB700B	3180	2905	1.10	31880	4015	0.79	3180	4985	0.64
HEB800B	3280	3550	0.92	3280	4975	0.65	3280	6225	0.53

Table 166 Verification of bending moment of middle weathering steel beam for a centre to centre distance of 2.0m

Profile	S235			S355			S460		
	M_{Ed} [kNm]	M_{Rd} [kNm]	U.C [-]	M_{Ed} [kNm]	M_{Rd} [kNm]	U.C [-]	M_{Ed} [kNm]	M_{Rd} [kNm]	U.C [-]
HEB600B	3990	2595	1.54	3990	3430	1.16	3990	4165	0.96
HEB700B	4150	3155	1.32	4150	4260	0.97	4150	5230	0.79
HEB800B	4275	3800	1.12	4275	5230	0.82	4275	6475	0.66

Table 167 Verification of bending moment of middle weathering steel beam for a centre to centre distance of 2.5m

Profile	S235			S355			S460		
	M_{Ed} [kNm]	M_{Rd} [kNm]	U.C [-]	M_{Ed} [kNm]	M_{Rd} [kNm]	U.C [-]	M_{Ed} [kNm]	M_{Rd} [kNm]	U.C [-]
HEB600B	4780	2835	1.69	4780	3670	1.30	4780	4405	1.08
HEB700B	4960	3400	1.46	4960	4505	1.10	4960	5475	0.91
HEB800B	5110	4050	1.26	5110	5480	0.93	5110	6730	0.76

ANNEX C Vertical Shear verifications

In case the cross section is not reduced the edges it will be possible to make use of the full cross-section for the shear force resistance calculation. However this means that it is needed to elevate the whole upcoming road to the bridge as ca be seen in Figure 91. This is a time consuming operation and economical unattractive solution. Therefore it is opted to make use of a reduced cross-section at the edge so that the level of the existing road is respected. To show the influence of the cross-section reduction both calculations will be performed for the original cross-section and for the reduced cross-section. The calculations for the original cross section can be found in the tables below and the overall visualization of the results can be found in Figure 110 and Figure 111.

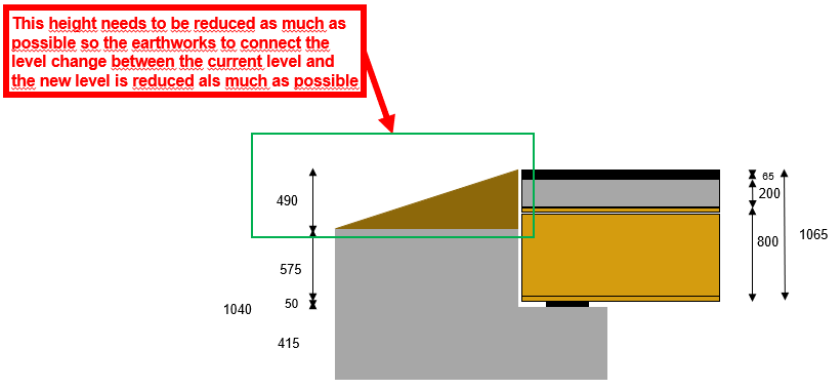

Table 168 Verification of vertical shear force of edge beam for a centre to centre distance of 1.5m

Profile	S235				S355				S460			
	V_{Ed} [kNm]	τ_{Ed} [N/mm²]	τ_{Rd} [N/mm²]	U.C [-]	V_{Ed} [kNm]	τ_{Ed} [N/mm²]	τ_{Rd} [N/mm²]	U.C [-]	V_{Ed} [kNm]	τ_{Ed} [N/mm²]	τ_{Rd} [N/mm²]	U.C [-]
HEB600B	**1030**	**137**	**109**	**1.26**	**1030**	**137**	**164**	**0.83**	**1030**	**137**	**212**	**0.64**
HEB700B	**1040**	**105**	**109**	**0.97**	**1040**	**105**	**164**	**0.64**	**1040**	**105**	**212**	**0.49**
HEB800B	**1045**	**89**	**109**	**0.81**	**1045**	**89**	**164**	**0.54**	**1045**	**89**	**212**	**0.41**

Table 169 Verification of vertical shear force of edge beam for a centre to centre distance of 2.0 m

Profile	S235				S355				S460			
	V_{Ed} [kNm]	τ_{Ed} [N/mm²]	τ_{Rd} [N/mm²]	U.C [-]	V_{Ed} [kNm]	τ_{Ed} [N/mm²]	τ_{Rd} [N/mm²]	U.C [-]	V_{Ed} [kNm]	τ_{Ed} [N/mm²]	τ_{Rd} [N/mm²]	U.C [-]
HEB600B	**1165**	**154**	**109**	**1.42**	**1165**	**154**	**164**	**0.94**	**1165**	**154**	**212**	**0.72**
HEB700B	**1170**	**118**	**109**	**1.09**	**1170**	**118**	**164**	**0.72**	**1170**	**118**	**212**	**0.56**
HEB800B	**1180**	**100**	**109**	**0.92**	**1180**	**100**	**164**	**0.61**	**1180**	**100**	**212**	**0.47**

Table 170 Verification of vertical shear force of edge beam for a centre to centre distance of 2.5 m

Profile	S235				S355				S460			
	V_{Ed} [kNm]	τ_{Ed} [N/mm²]	τ_{Rd} [N/mm²]	U.C [-]	V_{Ed} [kNm]	τ_{Ed} [N/mm²]	τ_{Rd} [N/mm²]	U.C [-]	V_{Ed} [kNm]	τ_{Ed} [N/mm²]	τ_{Rd} [N/mm²]	U.C [-]
HEB600B	**1160**	**154**	**109**	**1.42**	**1160**	**154**	**164**	**0.93**	**1160**	**154**	**212**	**0.72**
HEB700B	**1160**	**117**	**109**	**1.08**	**1160**	**117**	**164**	**0.72**	**1160**	**117**	**212**	**0.55**
HEB800B	**1165**	**99**	**109**	**0.91**	**1165**	**99**	**164**	**0.60**	**1165**	**99**	**212**	**0.46**

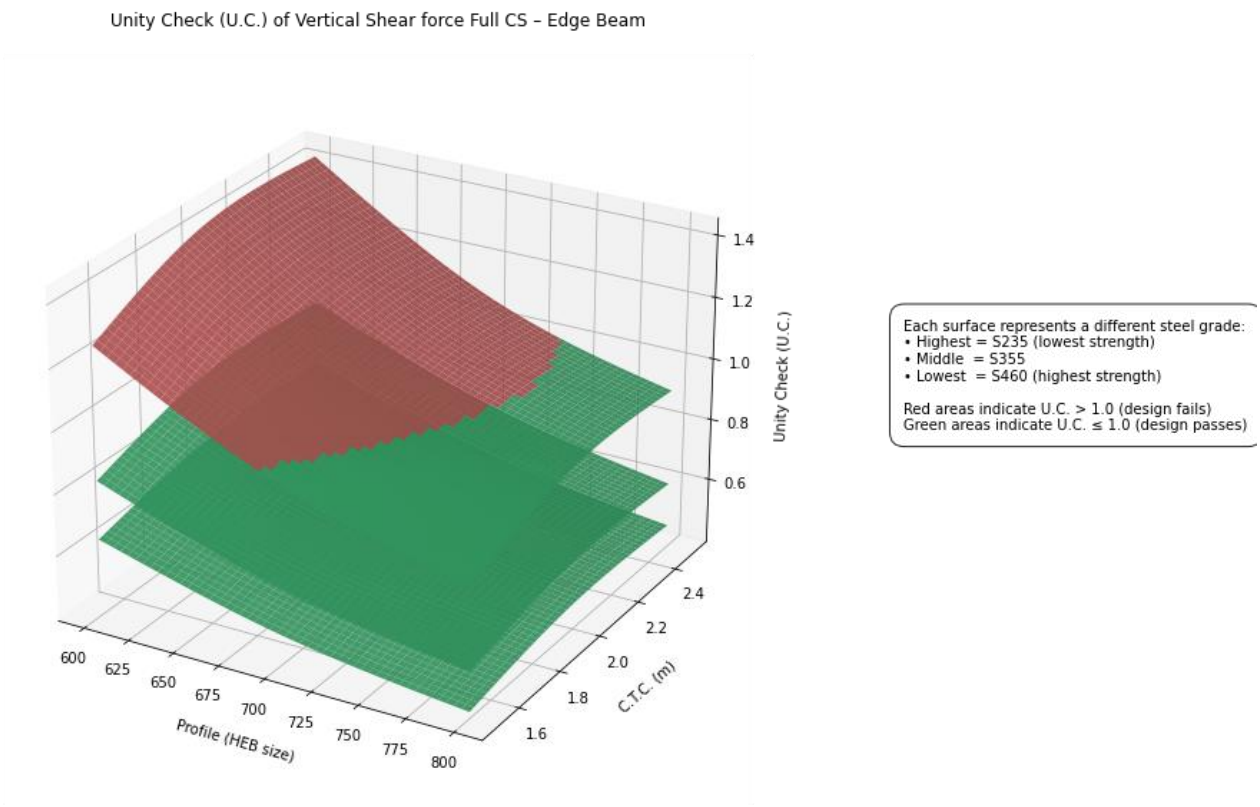

Figure 110 visualization of the performed Vertical shear verification for the edge beam by interpolating the c.t.c. distance and the HEB profiles.

Table 171 Verification of vertical shear force of middle beam for a centre to centre distance of 1.5m

Profile	S235				S355				S460			
	V_{Ed} [kNm]	τ_{Ed} [N/mm²]	τ_{Rd} [N/mm²]	U.C [-]	V_{Ed} [kNm]	τ_{Ed} [N/mm²]	τ_{Rd} [N/mm²]	U.C [-]	V_{Ed} [kNm]	τ_{Ed} [N/mm²]	τ_{Rd} [N/mm²]	U.C [-]
HEB600B	635	84	109	0.78	635	84	164	0.51	635	84	212	0.40
HEB700B	640	65	109	0.60	640	65	164	0.39	640	65	212	0.30
HEB800B	645	55	109	0.50	645	55	164	0.33	645	55	212	0.26

Table 172 Verification of vertical shear force of middle beam for a centre to centre distance of 2.0m

Profile	S235				S355				S460			
	V_{Ed} [kNm]	τ_{Ed} [N/mm²]	τ_{Rd} [N/mm²]	U.C [-]	V_{Ed} [kNm]	τ_{Ed} [N/mm²]	τ_{Rd} [N/mm²]	U.C [-]	V_{Ed} [kNm]	τ_{Ed} [N/mm²]	τ_{Rd} [N/mm²]	U.C [-]
HEB600B	880	117	109	1.08	880	117	164	0.71	880	117	212	0.55
HEB700B	890	90	109	0.83	890	90	164	0.55	890	90	212	0.42
HEB800B	900	766	109	0.70	900	76	164	0.47	900	76	212	0.36

Table 173 Verification of vertical shear force of middle beam for a centre to centre distance of 2.5 m

Profile	S235				S355				S460			
	V_{Ed} [kNm]	τ_{Ed} [N/mm²]	τ_{Rd} [N/mm²]	U.C [-]	V_{Ed} [kNm]	τ_{Ed} [N/mm²]	τ_{Rd} [N/mm²]	U.C [-]	V_{Ed} [kNm]	τ_{Ed} [N/mm²]	τ_{Rd} [N/mm²]	U.C [-]
HEB600B	1060	141	109	1.30	1060	141	164	0.85	1060	141	212	0.66
HEB700B	1075	109	109	1.00	1075	108	164	0.662	1075	108	212	0.51
HEB800B	1090	92	109	0.85	1090	92	164	0.56	1090	92	212	0.43

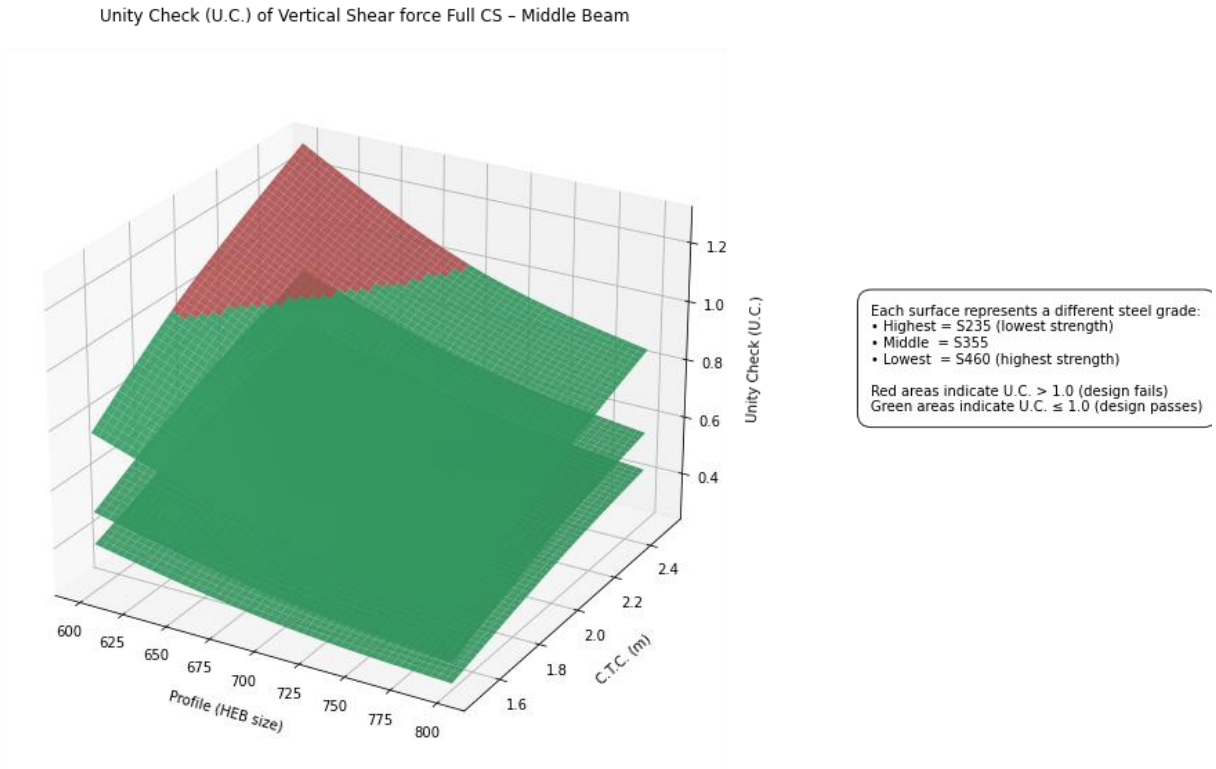

Figure 111 visualization of the performed Vertical shear verification for the middle beam by interpolating the c.t.c. distance and the HEB profiles.

As mentioned before the preferred solution is when the road is directly aligning with the level of the bridge here fore it is needed to reduce the cross section locally. In Figure 112 it is shown how the preferred solution should look like. As can be seen there will be a reduced web height at the edge, this will cause a critical zone for the shear force ressistalce calculations, since it will be significantly smaller compared to the original solution, the web heights of the reduced profiles are given in Table 174. By performing the calculation for the reduced web it will be possible to determine if any extra measures should be taken to satisfy the shearforce verification. In the tables below the results are given of the calculation and in Figure 113 and Figure 114 these results are visualized.

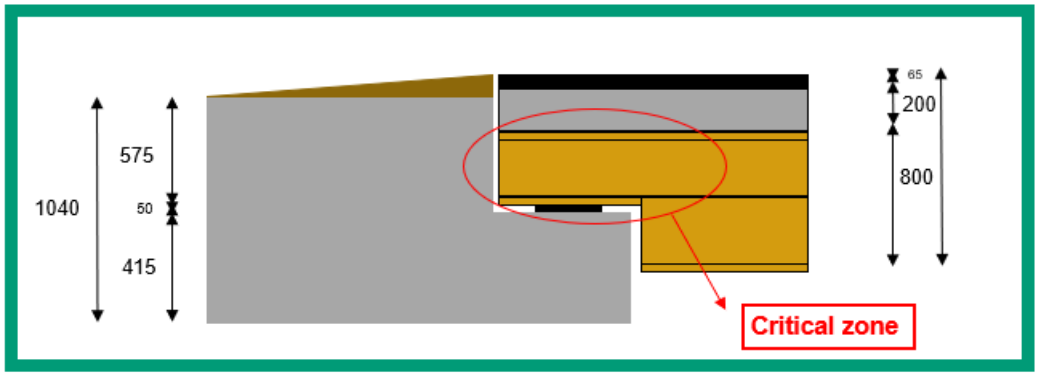

Figure 112 Local cross-section reduction to align with the level of the road.

Table 174 determination of the reduced heights and areas of the web of the differen profiles.

	$h_{web}[mm]$	$A_{web}[mm^2]$
HEB600B	**250**	**3875**
HEB700B	**246**	**4182**
HEB800B	**244**	**4270**

Table 175 Verification of vertical shear force of edge beam for a centre to centre distance of 1.5m

Profile	S235				S355				S460			
	V_{Ed} [kNm]	τ_{Ed} [N/mm²]	τ_{Rd} [N/mm²]	U.C [-]	V_{Ed} [kNm]	τ_{Ed} [N/mm²]	τ_{Rd} [N/mm²]	U.C [-]	V_{Ed} [kNm]	τ_{Ed} [N/mm²]	τ_{Rd} [N/mm²]	U.C [-]
HEB600B	**1030**	**266**	**109**	**2.4**	**1030**	**266**	**164**	**1.6**	**1030**	**266**	**212**	**1.3**
HEB700B	**1040**	**249**	**109**	**2.3**	**1040**	**249**	**164**	**1.5**	**1040**	**249**	**212**	**1.2**
HEB800B	**1045**	**245**	**109**	**2.2**	**1045**	**245**	**164**	**1.5**	**1045**	**245**	**212**	**1.2**

Table 176 Verification of vertical shear force of edge beam for a centre to centre distance of 2.0 m

Profile	S235				S355				S460			
	V_{Ed} [kNm]	τ_{Ed} [N/mm²]	τ_{Rd} [N/mm²]	U.C [-]	V_{Ed} [kNm]	τ_{Ed} [N/mm²]	τ_{Rd} [N/mm²]	U.C [-]	V_{Ed} [kNm]	τ_{Ed} [N/mm²]	τ_{Rd} [N/mm²]	U.C [-]
HEB600B	**1165**	**301**	**109**	**2.8**	**1165**	**301**	**164**	**1.8**	**1165**	**301**	**212**	**1.4**
HEB700B	**1170**	**280**	**109**	**2.6**	**1170**	**280**	**164**	**1.7**	**1170**	**280**	**212**	**1.3**
HEB800B	**1180**	**276**	**109**	**2.5**	**1180**	**276**	**164**	**1.7**	**1180**	**276**	**212**	**1.3**

Table 177 Verification of vertical shear force of edge beam for a centre to centre distance of 2.5 m

Profile	S235				S355				S460			
	V_{Ed} [kNm]	τ_{Ed} [N/mm²]	τ_{Rd} [N/mm²]	U.C [-]	V_{Ed} [kNm]	τ_{Ed} [N/mm²]	τ_{Rd} [N/mm²]	U.C [-]	V_{Ed} [kNm]	τ_{Ed} [N/mm²]	τ_{Rd} [N/mm²]	U.C [-]
HEB600B	**1160**	**299**	**109**	**2.7**	**1160**	**299**	**164**	**1.8**	**1160**	**299**	**212**	**1.4**
HEB700B	**1160**	**277**	**109**	**2.5**	**1160**	**277**	**164**	**1.7**	**1160**	**277**	**212**	**1.3**
HEB800B	**1165**	**273**	**109**	**2.5**	**1165**	**273**	**164**	**1.7**	**1165**	**273**	**212**	**1.3**

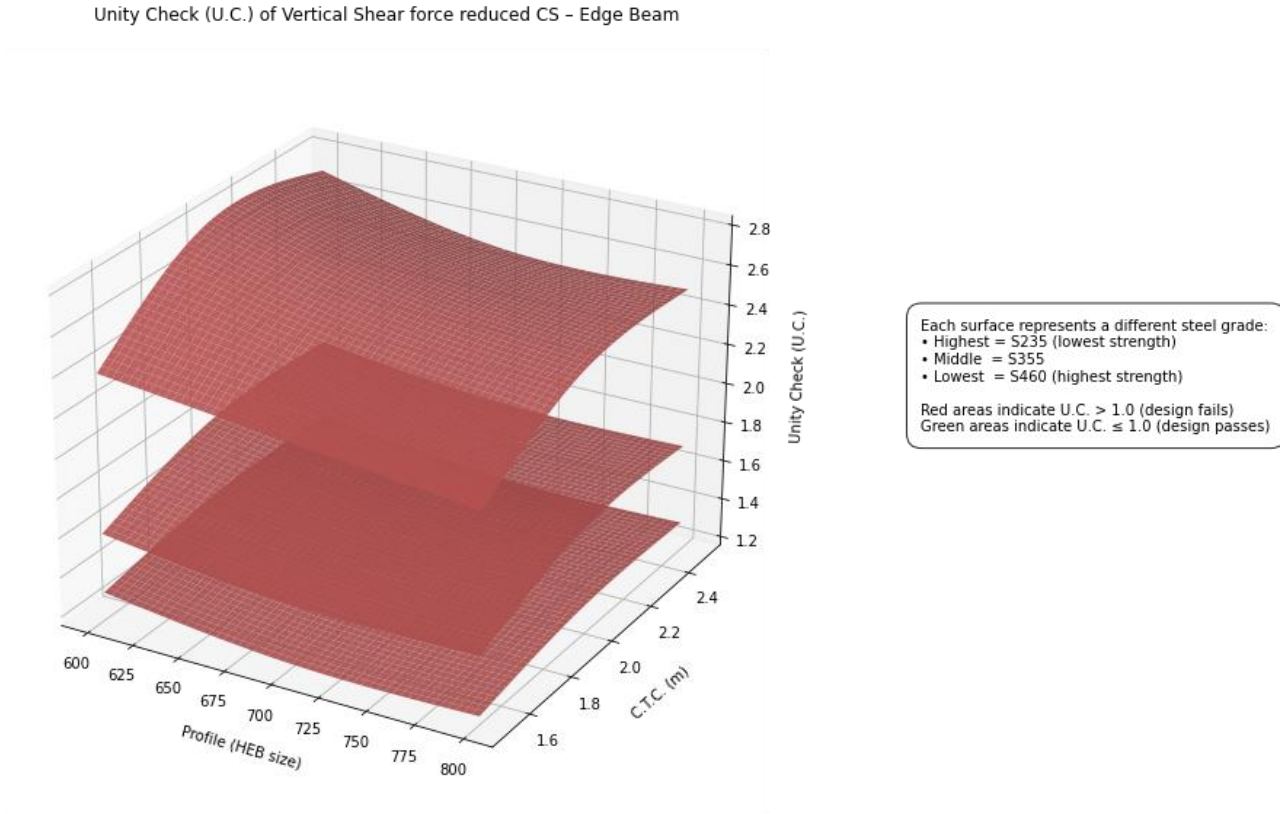

Figure 113 visualization of the performed Vertical shear verification for the edge beam by interpolating the c.t.c. distance and the HEB profiles, for the reduced web height.

Table 178 Verification of vertical shear force of middle beam for a centre to centre distance of 1.5m

Profile	S235				S355				S460			
	V_{Ed} [kNm]	τ_{Ed} [N/mm²]	τ_{Rd} [N/mm²]	U.C [-]	V_{Ed} [kNm]	τ_{Ed} [N/mm²]	τ_{Rd} [N/mm²]	U.C [-]	V_{Ed} [kNm]	τ_{Ed} [N/mm²]	τ_{Rd} [N/mm²]	U.C [-]
HEB600B	635	164	109	1.5	635	164	164	1.0	635	164	212	0.8
HEB700B	640	153	109	1.4	640	153	164	0.9	640	153	212	0.7
HEB800B	645	151	109	1.4	645	151	164	0.9	645	151	212	0.7

Table 179 Verification of vertical shear force of middle beam for a centre to centre distance of 2.0m

Profile	S235				S355				S460			
	V_{Ed} [kNm]	τ_{Ed} [N/mm²]	τ_{Rd} [N/mm²]	U.C [-]	V_{Ed} [kNm]	τ_{Ed} [N/mm²]	τ_{Rd} [N/mm²]	U.C [-]	V_{Ed} [kNm]	τ_{Ed} [N/mm²]	τ_{Rd} [N/mm²]	U.C [-]
HEB600B	880	227	109	2.1	880	227	164	1.4	880	227	212	1.1
HEB700B	890	213	109	2.0	890	213	164	1.3	890	213	212	1.0
HEB800B	900	211	109	1.9	900	211	164	1.3	900	211	212	1.0

Table 180 Verification of vertical shear force of middle beam for a centre to centre distance of 2.5 m

Profile	S235				S355				S460			
	V_{Ed} [kNm]	τ_{Ed} [N/mm²]	τ_{Rd} [N/mm²]	U.C [-]	V_{Ed} [kNm]	τ_{Ed} [N/mm²]	τ_{Rd} [N/mm²]	U.C [-]	V_{Ed} [kNm]	τ_{Ed} [N/mm²]	τ_{Rd} [N/mm²]	U.C [-]
HEB600B	1060	274	109	2.5	1060	274	164	1.7	1060	274	212	1.3
HEB700B	1075	257	109	2.4	1075	257	164	1.6	1075	257	212	1.2
HEB800B	1090	255	109	2.3	1090	255	164	1.6	1090	255	212	1.2

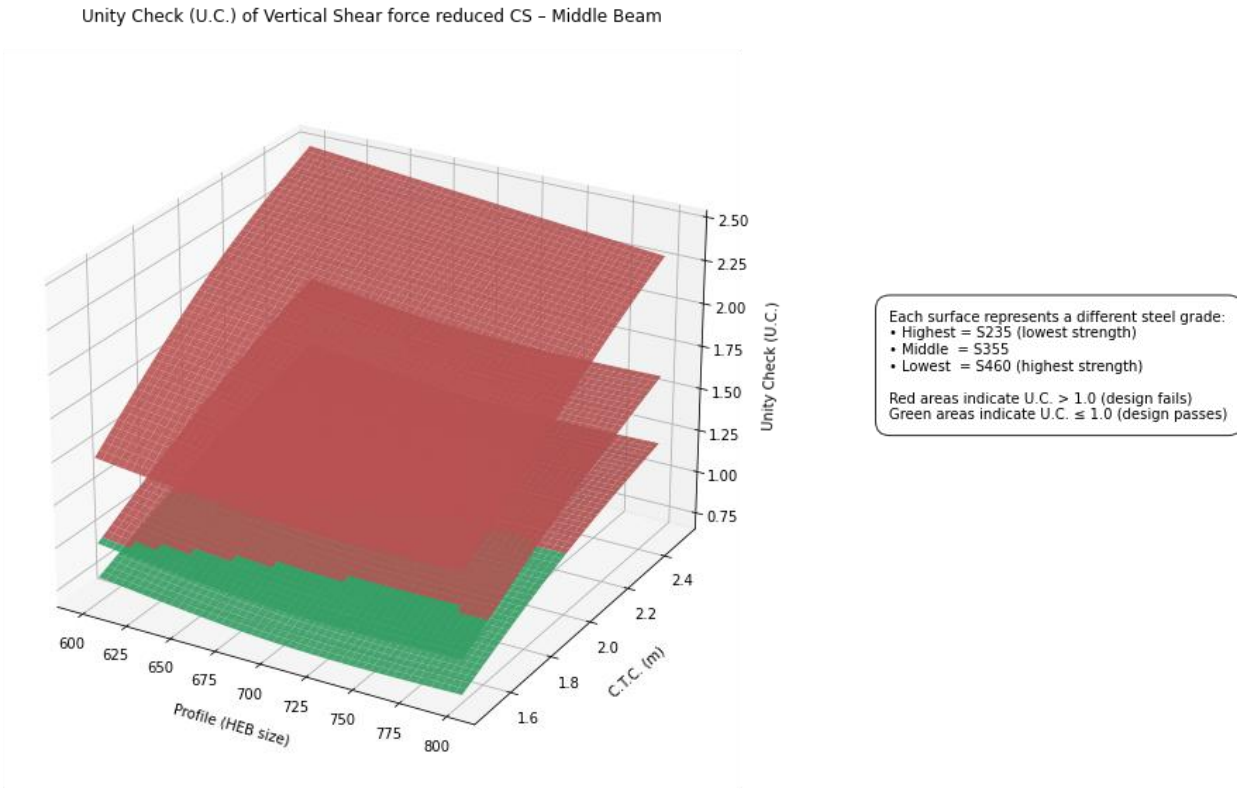

Figure 114 visualization of the performed Vertical shear verification for the middle beam by interpolating the c.t.c. distance and the HEB profiles , for the reduced web height.